

**Correlations Between Molecular Architecture, Morphology and
Deformation Behaviour of Styrene/Butadiene
Block Copolymers and Blends**



Dissertation

zur Erlangung des Akademischen Grades

Doktor-Ingenieur (Dr.-Ing.)

genehmigt durch

Mathematisch-Naturwissenschaftlich-Technischen Fakultät
(Ingenieurwissenschaftlicher Bereich)
der Martin-Luther-Universität Halle-Wittenberg

von Herrn M. Sc. Chem. Rameshwar Adhikari
geb. am 03.09.1963 in Nuwakot/Nepal

Gutachter

1. Prof. Dr. rer. nat. G. H. Michler
2. Prof. Dr. F. J. Baltá Calleja
3. Prof. Dr.-Ing. V. Altstädt

Merseburg, den 30.11.2001

urn:nbn:de:gbv:3-000003100

[<http://nbn-resolving.de/urn/resolver.pl?urn=nbn%3Ade%3Agbv%3A3-000003100>]

ACKNOWLEDGEMENTS

For many helpful suggestions, discussions, supports and inspirations; and providing me an opportunity to work in his prosperous group 'Morphologie und Mikromechanik' and write this thesis on one of the most fascinating scientific topics of nanostructured polymeric materials under his intensive guidance, I sincerely extend my thanks to Prof. G.H. Michler.

Many sincere thanks go to Dr. R. Godehardt for teaching me AFM techniques, for his fatherly support in every respects and helps during the clarification of several bureaucratic issues. Thanks are due to W. Lebek for his untiring helps in many aspects like software, computer problematic, AFM experiments etc.

I would like to thank S. Goerlitz (TEM), C. Becker and S. Henning (SEM) and Dr. E. Ivankova (HVEM) for beautiful electron micrographs which form the soul of this thesis. Many thanks are due to C. Hatscher for helping design many nice schemes. Dr. T.A. Huy is thanked for carrying out DMA as well as DSC experiments. Many helpful discussions, suggestions and helps from Dr. R. Weidisch are acknowledged. Special thanks go to Dr. R. Lach for many scientific discussions and helps in fracture mechanics investigations. Intensive helps from C. Becker, S. Goerlitz, S. Henning, J. Laatsch and V. Seydewitz are simply unforgettable.

I extend my sincere thanks to Doz. Dr. K. Schmutzler, C. Wittig, E. Kühnberger and H. Otto for their co-operation. Diverse helps from groups of Prof. Grellmann, Prof. Kreßler, Prof. Radosch, Prof. Arnold and Doz. Dr. Höring are earnestly acknowledged. Co-operation with P. Simon (Dresden), M. Buschnakowski, M. Schoßig, S. Dunger and S. Großstück are hearty acknowledged.

I would like to acknowledge the BASF AG, especially Dr. K. Knoll, for the fruitful co-operation and providing the samples and characterisation data. Co-operation with Dr. K. Geiger (Universität Stuttgart) and M. Langela (MPI-P, Mainz) in the frame of the BASF-Project-'Styrol/Butadien-Blockcopolymer' is sincerely acknowledged. I am indebted to the Land Sachsen-Anhalt and the Max-Buchner-Forschungstiftung for financial support.

I am greatly indebted to the members of our group for their warm affection. Everyday before I started to work (often during coffee hour), the people around the table (whom I feel as my family) frequently asked me if I need help; if I have any kinds of troubles; whether my family is ok etc.; and they helped me from the depth of their hearts. These were the most important things that always inspired me and enhanced my works. I would like to thank once again the whole group for this family environment.

I thank my wife Pooja for her unlimited patient and moral support; it would have been impossible to successfully terminate this mission without her understanding and help. Finally, I acknowledge the efforts of my parents to make me able stand on my foot; and dedicate this work to my children *PariPurak* who think that polymers are the things to play with.

Warm reception from many Merseburger and Hallenser have also contributed indirectly to make our stay in Germany a pleasant experience and make this work a success.

CONTENTS

1.	INTRODUCTION	1
1.1	Significance of Block Copolymers	1
1.2	Aims and Overview of Thesis	2
1.3	Sample Preparation and Investigation Methods	3
2.	STRUCTURE-PROPERTY-CORRELATIONS OF BLOCK COPOLYMERS	4
2.1	Microphase Separation and Morphology	4
2.2	Morphology Control via Architectural Modification	9
2.2.1	<i>Variation of Chain Topology</i>	9
2.2.2	<i>Asymmetric Block Structure</i>	12
2.2.3	<i>Interfacial Modification</i>	14
2.3	Blends Containing Block Copolymers	16
2.3.1	<i>Block Copolymer/Homopolymer Blends</i>	16
2.3.2	<i>Binary Block Copolymer Blends</i>	19
2.4	Mechanical Properties and Deformation Behaviour	21
2.4.1	<i>Thermomechanical Properties</i>	21
2.4.2	<i>Mechanical Behaviour of Polymers</i>	22
2.4.3	<i>Micromechanical Construction of Polymers</i>	24
2.4.4	<i>Deformation Behaviour of Styrenic Block Copolymers</i>	26
2.4.5	<i>Molecular Architecture vs. Micromechanics</i>	37
3.	EXPERIMENTAL PART	39
3.1	Materials	39
3.1.1	<i>Pure Block Copolymers</i>	39
3.1.2	<i>Block Copolymer/Homopolystyrene (hPS) Blends</i>	39
3.1.3	<i>Binary Block Copolymer Blends</i>	39
3.1.4	<i>Synthesis of Block Copolymers</i>	39
3.2	Sample Preparation	42
3.3	Mechanical Properties	42
3.3.1	<i>Tensile Testing</i>	43
3.3.2	<i>Fracture Mechanics</i>	43
3.4	Microscopic Techniques	45
3.4.1	<i>Electron Microscopy</i>	45
3.4.2	<i>Scanning Force Microscopy</i>	46
3.5	Additional Characterisation Methods	46

3.5.1	<i>Thermomechanical Properties and Glass Transitions</i>	46
3.5.2	<i>Molecular Weight and Composition</i>	46
4.	STRUCTURE-PROPERTY-CORRELATIONS IN DIFFERENT BLOCK COPOLYMER ARCHITECTURES	47
4.1	Phase Behaviour and Morphology	47
4.1.1	<i>Correlation Between Molecular Architecture and Phase Behaviour</i>	47
4.1.2	<i>Equilibrium Morphologies</i>	50
4.1.3	<i>Effects of Sample Preparation Methods</i>	57
4.2	Mechanical Properties	59
4.2.1	<i>Tensile Behaviour</i>	59
4.2.2	<i>Mechanical Anisotropy in Oriented Samples</i>	62
4.3	Micromechanical Behaviour	63
4.3.1	<i>Influence of Microphase Morphology</i>	63
4.3.2	<i>Influence of Molecular Structure</i>	70
4.3.3	<i>Thin Layer Yielding Mechanism in Lamellar Star Block Copolymers</i>	74
4.3.4	<i>Additional Evidences of Thin Layer Yielding Mechanism</i>	78
4.4	Fracture Toughness of the Block Copolymers	80
4.5	Conclusions	82
5.	STRUCTURE-PROPERTY-CORRELATIONS IN BLOCK COPOLYMER/PS BLENDS	84
5.1	Phase Behaviour and Morphology	84
5.1.1	<i>Dynamic Mechanical Properties</i>	84
5.1.2	<i>Influence of hPS Molecular Weight on Morphology</i>	85
5.1.3	<i>Morphology of Injection Moulds</i>	88
5.2	Mechanical Properties	92
5.2.1	<i>Tensile Behaviour</i>	92
5.2.2	<i>Fracture Mechanics</i>	95
5.3	Micromechanical Deformation Behaviour	97
5.3.1	<i>Solution Cast Blends</i>	97
5.3.2	<i>Injection Moulded Blends</i>	102
5.4	Conclusions	108

6.	STRUCTURE-PROPERTY-CORRELATIONS IN BINARY BLOCK COPOLYMER BLENDS	110
6.1	Motivation Why Binary Block Copolymer Blends?	110
6.2	Phase Behaviour and Morphology	111
6.2.1	<i>Phase Behaviour and Equilibrium Morphologies</i>	111
6.2.2	<i>Morphology of Injection Moulded Samples</i>	116
6.3	Mechanical Properties and Micromechanical Behaviour	117
6.3.1	<i>Tensile Properties</i>	117
6.3.2	<i>Toughness Characterisation by Fracture Mechanics Approach</i>	121
6.4	Conclusions	128
7.	SUMMARY AND PERSPECTIVES	130
8.	ZUSAMMENFASSUNG UND PERSPEKTIVE	134
9.	REFERENCES	139
10.	APPENDICES	150

LIST OF ABBREVIATIONS AND SYMBOLS

a	distance between two adjacent chemical junctions along an interface/statistical segment length (Kuhn length)
a/a ₀	relative distance between the adjacent chemical junction points
Δa	stable crack growth
α	degree of polymerisation of homopolystyrene relative to that of corresponding block of the block copolymer (N _{hPS} / N _{PS-block})
bcc	body centred cubic
<i>sec</i> -BuLi	secondary butyllithium
CTOD	crack tip opening displacement (δ)
χ	Flory-Huggins interaction parameter
D	domain thickness
D _{crit}	critical thickness of lamellae
DG	double gyroid
DMA	dynamic mechanical analysis
DSC	differential scanning calorimetry
EB	ethylene/butylene copolymer
E _d	Young's modulus determined in impact test
ESIS TC4	European structural integrity society, technical committee 4: polymers and composites
ε	strain, (also mol. Asymmetry parameter used by Milner, ref. [36])
F	impact load
f	composition of block copolymer (also represented by Φ)/deflection of the specimen during impact testing
f _c	composition of block copolymer at which the continuous transition from disordered to lamellar phase occurs
FTIR	Fourier transform infra-red spectroscopy
G'	dynamic storage shear modulus
G''	dynamic loss modulus
GPC	gel permeation chromatography
ΔG	Gibbs's free energy
hex	hexagonal phase (also hpc)
HML	hexagonal modulated layers
hpc	hexagonal packed cylinders
HPL	hexagonal perforated lamellae
hPS	polystyrene homopolymer
HVEM	high voltage electron microscope
ΔH	enthalpy change
ISR	intermediate segregation regime
J	J-integral
J _{0.1}	J-integral value determined at a stable crack growth of 0.1 mm at the point of technical crack initiation
J _i	J-integral value as resistance against stable crack initiation called physical crack initiation
J _{Id}	J-integral value as resistance against unstable crack initiation for crack opening mode I, geometry independent parameter
k	Boltzmann's constant
L	long period of domains
lam	lamellar phase
λ	extension ratio, λ _{max} maximum extension ratio
MEK	methyl ethyl ketone
M _n	number average molecular weight

MSS	microphase separated structures
M_w	weight average molecular weight
N	total degree of polymerisation
N_{hPS}	degree of polymerisation of polystyrene homopolymer
$N_{PS-block}$	degree of polymerisation of polystyrene block of a block copolymer
OBDD	ordered bicontinuous double diamond
ODT	order-disorder transition
OOT	order-order transition
OsO_4	osmium tetroxide
PB	polybutadiene
PE	polyethylene
PEO	polyethylene oxide
PI	polyisoprene
PMMA	polymethyl methacrylate
P2VP	polyvinyl pyridine
PP	polypropylene
PPO	polyphenylene oxide
PS	polystyrene
PVC	polyvinyl chloride
R-curves	crack resistance curves
R_g	radius of gyration
SAXS	small angle X-ray scattering
SB	block copolymer consisting of polystyrene and polybutadiene
S/B	a statistical copolymer of styrene and butadiene (styrene-co-butadiene)
SBS	styrene-b-butadiene-b-styrene triblock copolymer
SBR	styrene/butadiene rubber
SCFT	self consistent field theory
SEM	scanning electron microscopy
SFM	scanning force microscopy
SIS	styrene-b-isoprene-b-styrene triblock copolymer
SSL	strong segregation limit
ΔS	entropy change
σ	stress
σ_y	yield stress
σ_Y^{lam}	yield stress of PS lamellae
$\tan\delta$	dynamic loss tangent (G''/G')
TEM	transmission electron microscopy
T_g	glass transition temperature
THF	tetrahydrofurane
TPE	thermoplastic elastomer
τ	asymmetry parameter as introduced by de la Cruz, ref. [50]
WSL	weak segregation limit

1. INTRODUCTION

1.1 Significance of Block Copolymers

Polymeric materials offer a wide range of application relevant properties. Therefore, these materials find growing applications in various fields of everyday life. Since their ultimate properties are determined by their chemical microstructures, control of chemical structure (macromolecular designing) is the first step of creating materials of desired properties profile. In practice, different properties are simultaneously desirable, e.g. a combination of stiffness and drawability, or strength and toughness etc. A technological way of achieving these combinations is the heterogenisation of existing polymers. Polymer blends represent this strategy of designing polymeric materials [1-3].

Blending may often lead to the deterioration of the mechanical properties due to insufficient phase adhesion resulting from the incompatibility of the blend components; hence these blends need compatibilisation. One of the strategy being practiced for about 50 years to get rid of this problem is to join the desired polymer chains with a primary covalent bond which has given rise to today's fascinating world of block copolymers [2-4].

All block copolymers belong to a broad category of condensed matter sometimes referred collectively as soft materials, which, in contrast to crystalline solids, are characterised by fluid-like disorder on the molecular scale and a high degree of order at longer length scales. Combining the incompatible polymer chains in a single macromolecule leads to intra-molecular phase separation whereby the problem of inadequate phase adhesion will be eliminated. This, in turn, leads to the formation of highly ordered self-assembled "crystalline-like" phase separated structures in melt as well as solid state whose periodicity lies in the range of radius of gyration (R_g) of the constituent molecules. The nature and size of these structures can be controlled by various methods including interfacial and architectural modification [4].

The block copolymers find application in diverse fields: as thermoplastic elastomers, pressure sensitive adhesives, impact modifiers, compatibilisers etc. In solutions, their surfactant properties are exploited in foams, oil additives, solubilisers, thickeners and dispersion agents. The block copolymers may have potential applications in medicines, nanotemplating and nanotechnology [2]. An annual growth rate of 9-10% of thermoplastic elastomers (compared to 2-4% growth rate of other polymers) in the last 20 years reflects the significance of these materials in polymer market [5].

Recently, synthesis of several block copolymer architectures including ABC triblock copolymers has triggered the discovery of novel morphologies and opened new potential of controlling mechanical properties [2]. Especially, the block copolymers with complex molecular characteristics are being paid special attention.

1.2 Aims and Overview of Thesis

Styrene/butadiene block copolymers find applications as thermoplastic elastomers, moulding products, toughness modifiers and films. They are, generally, not used commercially as pure materials but compounded with other polymers, fillers etc. to achieve the particular requirements for each end-use. In many applications, mechanical properties are of prime interest. In spite of a detailed knowledge of phase behaviour of simple linear block copolymers, correlation between their morphology, mechanical properties and micromechanical mechanisms, very important for technical applications, is not well understood. Hence, it is of prime importance from materials scientific stand point that this correlation is intensively investigated.

The primary goal of this work is to investigate experimentally correlations between phase behaviour, morphology and micromechanical deformation behaviour of block copolymers (and blends) as a function of their molecular architecture.

The work is limited to amorphous styrene/butadiene block copolymers in a narrow composition range ($\Phi_{\text{styrene}} \sim 0.70$) with an special emphasis on few selected asymmetric architectures. Detailed discussion of morphology development in a wide composition range and their synthetic and rheological aspects are outside the scope of this thesis. The thesis has been organised in the following way:

A short review of thermodynamics, morphology and deformation behaviour of amorphous block copolymers is given in chapter 2. Chapter 3 deals with experimental techniques and general methods of synthesising block copolymers of the types used in this study. Experimental results are discussed in chapters 4, 5 and 6. A brief summary of the research works and future perspective are given in chapter 7.

First, influence of block copolymer architecture on microphase morphology and ultimate mechanical properties of styrene/butadiene block copolymers, which is the main issue of this work, is discussed in chapter 4. For this purpose, phase behaviour, morphology, mechanical properties and micromechanical deformation mechanisms of linear and star shaped block copolymers having different interfacial structures are comparatively analysed.

Styrene/butadiene block copolymers are often used in combination with polystyrene homopolymer (hPS) which find applications in injection moulded parts, food packaging films and beakers for soft and warm drinks. In such applications, a balance between transparency and toughness lies in the centre of interest. Hence, another objective is to study the morphology and micromechanical as well as mechanical behaviour of binary star block copolymer/hPS blends in chapter 5.

Finally, binary block copolymer blends offer new possibilities of tailoring mechanical properties. Despite a few works on phase behaviour and morphology of block copolymer blends, no systematic works about their mechanical behaviour are reported. Structure-property correlations of binary block copolymer blends (star block and triblock) shall be discussed in chapter 6 especially using several concepts of elastic-plastic fracture mechanics.

1.3 Sample Preparation and Investigation Methods

Block copolymers samples synthesised via living anionic polymerisation and provided by the BASF were prepared by different methods: solution casting, extrusion, injection and compression moulding. Polystyrene homopolymers used to blend with selected block copolymers were synthesised by radical polymerisation.

Electron microscopy (TEM, SEM and HVEM) and scanning force microscopy (SFM) were used as principal experimental tools. Mechanical properties are characterised by tensile and impact testing. Dynamic mechanical analysis (DMA) and differential scanning calorimetry (DSC) were employed to determine the glass transition temperature and gain insight into the phase behaviour of the materials. Samples were prepared by solution casting and common processing techniques (injection moulding, press moulding and extrusion).

2. STRUCTURE-PROPERTY-CORRELATIONS OF BLOCK COPOLYMERS

2.1 Microphase Separation and Morphology

If two polymers are mixed, the most frequent result is a system that exhibits a complete phase separation due to the repulsive interaction between the components (i.e. the chemical incompatibility between the polymers) [6-8]. Complete miscibility in a mixture of two polymers requires that the following conditions be fulfilled.

$$\Delta G_m = \Delta H_m - T\Delta S_m < 0 \quad \text{i.e., } \Delta G_m = -ve, \quad (2.1)$$

where ΔG_m , ΔH_m , and ΔS_m stand for Gibb's free energy, enthalpy and entropy of mixing at temperature T, respectively. Generally, ΔH_m and $T\Delta S_m$ are both positive for polymer pairs. The value of $T\Delta S_m$ is always positive since there is an increase in the entropy on mixing. Therefore the sign of ΔG_m always depends on the value of the enthalpy of mixing ΔH_m . Surprisingly the heat of mixing is usually positive which does not favour mixing. Hence, the polymer pairs mix to form a single phase only if the entropic contribution to free energy exceeds enthalpic contribution, i.e.,

$$\Delta H_m < T\Delta S_m \quad (2.2)$$

The lattice theory for the enthalpy of mixing in polymer solutions, developed by Flory and Huggins, can be formally applied to polymer mixtures, which provides a rough estimation of the miscibility of the polymers. The entropy and enthalpy of mixing of two polymers are given by [7,8]:

$$\Delta S_m = -k[n_1 \ln \Phi_1 + n_2 \ln \Phi_2] \quad (2.3)$$

$$\Delta H_m = kT\chi_{12}N\Phi_1\Phi_2 \quad (2.4)$$

where ϕ_i is the volume fraction of the polymer i and $N = n_1 + n_2$ is the total number of polymer molecules in the mixture. χ is called Flory-Huggin's interaction parameter. Hence, enthalpic and entropic contribution to free energy of mixing can be parameterised in terms of Flory-Huggins segmental interaction parameter χ and the degree of polymerisation N, respectively.

The fundamental thermodynamics of phase separation in polymer blends is applicable to block copolymers as well. The phase behaviour of a bulk two-component block copolymer AB is determined by three experimentally controllable factors [2,4,9-11]:

- i. the overall degree of polymerisation N,
- ii. architectural constrains (diblock, triblock, star block etc.) and composition f (overall volume fraction of component A),
- iii. the A-B segment-segment interaction parameter χ

The first two factors are regulated through the polymerisation stoichiometry and affect the translational and configurational entropy, while the magnitude of (the largely enthalpic) χ is determined by selection of A-B monomer pairs, and has a temperature dependence given by:

$$c = \frac{a}{T} + b \quad (2.5)$$

where α and β are constant depending on composition and architectural constraints of the block copolymer.

At equilibrium, the block copolymer chains assume the lowest free energy configuration. Increasing the energy parameter χ (i.e., lowering the temperature) favours a reduction in A-B monomer contacts. If the value of N is sufficiently large, it is accomplished with some loss of translational and configurational entropy by local compositional ordering [2]. Such local segregation is referred to as *microphase separation* in the block copolymer. Alternatively, if χ or N is decreased enough, the entropic factor will dominate, leading to a compositionally disordered phase. Since the entropic and enthalpic contribution to free energy density scale respectively as N^{-1} and χ , it is the product χN that dictates the block copolymer phase state, and it is called the reduced interaction parameter or lumped interaction parameter [9-11]. When the value of this parameter exceeds a certain value specific for the system under consideration, the microphase-separated structures evolve below which the system is in the disordered state. This phenomenon is called *microphase separation transition* (MST) or *order-disorder transition* (ODT) [9]. For a symmetric diblock copolymer (i.e., composition $f = 0.5$) the transition occurs when $\chi N \approx 10.5$ [10-14]. At sufficiently large values of χN , different ordered structures are formed in the melt as well as in the solid state. These structures, also termed as *microphase separated structures* (MSS), are best represented in the form of phase diagrams (Appendix 2.1) which are generally constructed by plotting the lumped parameter (χN) as a function of composition. Two limiting regimes have been postulated in the block copolymer phase diagrams, as illustrated in figure 2.1. For $\chi N \ll 1$, a copolymer melt is disordered and the A-B interaction is sufficiently low that the individual chains assume unperturbed Gaussian statistics. The composition profile is almost sinusoidal (fig 2.1a), and the domain periodicity L scales as [11]:

$$L \propto R_g \propto aN^{1/2}, \quad (2.6)$$

where a is the characteristic segment length; R_g and N stand for gyration radius of copolymer molecule and polymerisation index, respectively.

This regime is called *weak segregation limit* and the copolymers showing this behaviour are characterised by a widened interface due to enhanced phase mixing. Approaching this regime, thermotropic order-order transitions are predicted. A thermoreversible morphology transition at the upper portion of the phase diagrams is allowed.

As the value of χN is greater than 10, nearly pure A and B domains are formed. The chain conformation is, in this case, no longer Gaussian one but rather perturbed (stretched chain conformation). This regime is termed as *strong segregation limit*^{*}. The interface between the constituent microdomains in strongly segregated systems is quite narrow (in the order of about 1 nm) with the monomer composition profile resembling a sharp step (fig 2.1b). In this regime the thermotropic order-order transitions (OOT) are not expected. The boundaries delineating the different microphases are expected to be vertical. The interaction energy associated with the A-B contacts is localised in the interfacial regions; the system would like to minimise the total area of such an interface by decreasing the energetically unfavourable contacts, but must do so under the constraint of incompressibility and entropic penalty of extended chain conformations. These opposing forces lead to perturbed chain configurations, and the periodicity L can be scaled as [11,14]:

$$L \propto R_g \propto aN^{2/3} c^{1/6} \quad (2.7)$$

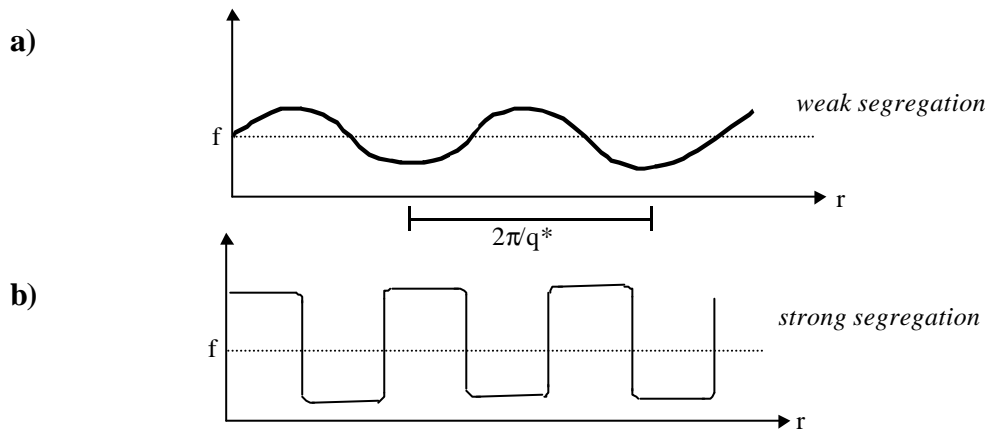


Figure 2.1: Comparison of the one-dimensional composition profiles characterising a) WSL and b) SSL [14].

A wide variety of microstructure develops in block copolymer systems upon microphase separation (MS). The process of MS is a result of two competing effects. Firstly, dissimilar blocks prefer to segregate due to their inherent chemical incompatibility. The spatial extent of phase separation is, however, limited by the connectivity of the blocks imposed by the architecture of the molecules. As a compromise of both the effects, periodic microstructures evolve. The geometry of the microphase separated structure is, therefore, very sensitive to the chemical nature and molecular structure of the copolymer as well as its total composition. Unlike microphase separated block copolymers, the domain diameter in phase separated polymer blends are typically several hundred nanometers, and the morphology is independent of detailed features of the molecules [6].

^{*} Intermediate segregation regime (ISR) has also been reported in various block copolymers for $10.5 < \chi N < 29$, where the domain periodicity scales as $L \propto N^{0.83}$ e.g., for SB diblock, C. M. Papadakis, K. Almdal, K. Mortensen, D. Posselt: Identification of ISR in diblock copolymer systems, *Europhys. Lett.* 36, 289-294, (1996).

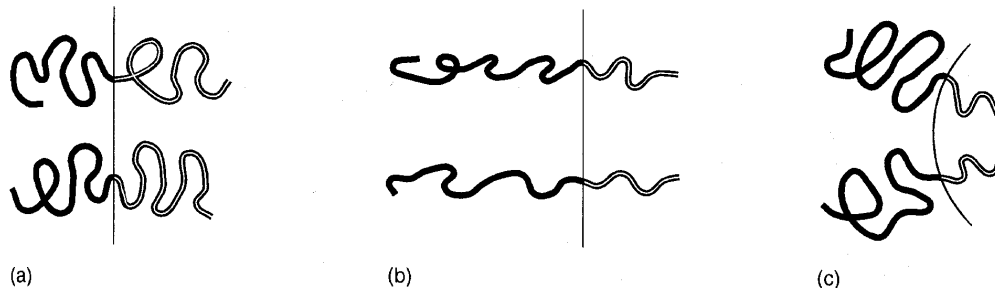


Figure 2.2: Schematics of chain conformation at the microphase-separated state; a) stable flat interface from a compositionally symmetric AB block copolymer i.e. $\Phi_A = \Phi_B$, b) an unstable flat interface in the case $\Phi_A \gg \Phi_B$ and c) a stable curved interface in the case of $\Phi_A \gg \Phi_B$ [11].

One of the most important factors determining the phase morphology in block copolymer is their composition. It is easily understood that the shape of the polymer/polymer interface varies with the relative chain length of the component polymer. A compositionally symmetric AB diblock copolymer (i.e., when volume fractions of both the components are the same) forms a flat interface as shown in figure 2.2 (a). As the volume fraction of a component continues to increase (say of A) relative to that of the other (i.e., as the copolymer becomes compositionally asymmetric) it is more likely that a curved interface is formed because the A chains must stretch sufficiently (fig 2.2b) to allow the formation of a planer interface. In this case the conformational entropy loss of the major component (here A) is too high. Therefore, the A chains tend to expand along the direction parallel to the interface to gain the conformational entropy under the condition that segment densities of both of the block chains have to be kept constant and must be the same as that of the bulk densities of the homopolymers. As a consequence the interface becomes convex towards the minor component (fig 2.2c). This effect of interface curvature becomes more and more pronounced as the composition of the block copolymer becomes further asymmetric. The morphological variations with composition observed in a two-component block copolymer are shown in fig 2.3 [15].

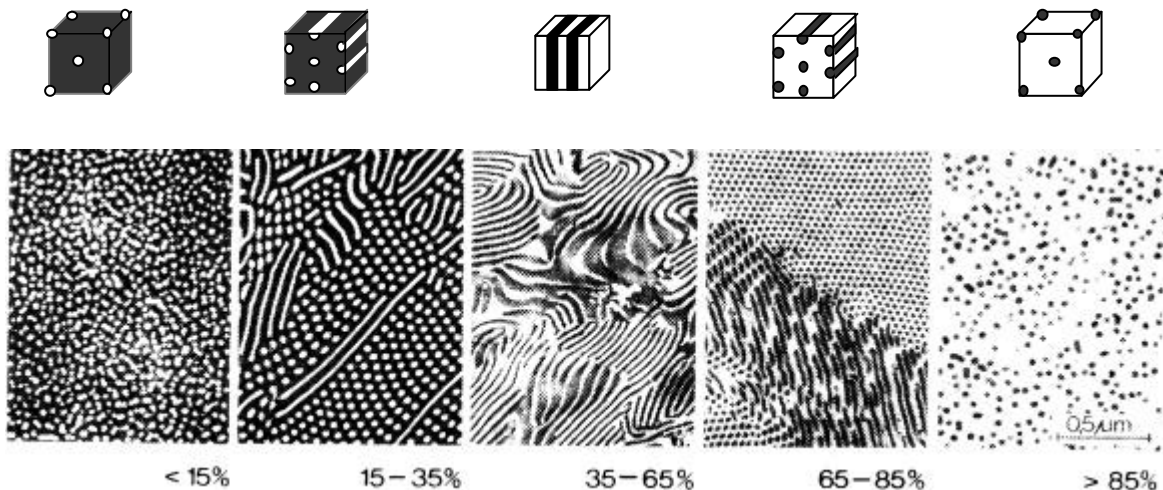


Figure 2.3: TEM images showing classical morphology of the block copolymers exemplified by that observed in an SI-diblock copolymer (A = PS and B = PI, the TEM images are from ref. [15]).

The most asymmetric block copolymer possesses spherical morphology comprising body centred cubic (bcc) spheres of the minor component dispersed in the matrix of the major component. As the volume fraction of the minor component increases cylindrical morphology (hexagonal packed cylinders hpc of minor component in the matrix of major component) evolves.

Symmetric block copolymer exhibit a lamellar morphology consisting of alternating layers of the components. With increasing volume fraction of the component A the morphology appears in reversed order (i.e. hexagonal B cylinders in A matrix and A spheres in A matrix) [11,14]. In the strong segregation limit, the following sequence of phases is observed for PS/PI diblocks: $f_{PS} < 0.17$, bcc; $0.17 < f_{PS} < 0.28$, hex; $0.28 < f_{PS} < 0.34$, gyroid; $0.34 < f_{PS} < 0.62$, lam; $0.62 < f_{PS} < 0.66$, gyroid; $0.66 < f_{PS} < 0.77$, hex; and $0.77 < f_{PS}$, bcc [14].

The morphologies discussed above and illustrated in fig 2.3 are classical ones and are experimentally verified by different workers in several styrene/diene systems [16,17]. Recently, new non-classical bicontinuous morphologies have been found in SI diblock and star block copolymers and called ordered bicontinuous double diamond (OBDD) or 'gyroid' morphologies [18,19]. Hexagonal perforated layer structures (HPL), hexagonal modulated lamellar (HML) structures have been studied in various block copolymer systems both experimentally and theoretically (discussed by Hamley in [2]). Recent experimental results suggest that HML phase may be a transient, and the HPL a long-lived metastable phase. In contrast, gyroid morphology has been identified as one of the stable phases which consists of interpenetrating tetragonal network of the minor phase dispersed in three dimensionally continuous major phase matrix [18,19].

A number of unconventional morphologies were observed by Mogi et al. [20,21,22] and Hashimoto et al. [23] as well as Stadler and co-workers [24-26] and in ABC triblock copolymers which have opened new potential for controlling properties of these nanostructured materials. A few of these morphologies are cited in fig 2.4. Existence of a richer variety of morphology in ABC triblock copolymers is attributable to the presence of more interaction parameters (χ_{AB} , χ_{BC} , χ_{AC}), and the morphological features are often complicated imposing difficulties in physical interpretation [2,20-26]. These studies show that entirely different structures are formed in ABC triblock copolymers depending on the relative composition and interaction between the constituents. More complex morphologies have been recently predicted in three-component multi-block copolymers by Drolet and Fredrickson [27] and Bohbot-Raviv and Wang [28] using self consistent field (SCF) calculations which are yet to be experimentally confirmed. A few of these morphologies are indexed in Appendix 2.2.

2.2 Morphology Control via Architectural Modification

Development of living polymerisation techniques have enabled the chemists to design block copolymer molecules of well defined architectures. The block copolymer chains may range from simple two-component linear molecules to the multi-component radial and branched chains (star, miktoarm star, graft etc.). Most frequently studied important block copolymer architectures are schematically illustrated in figure 2.5. Various block copolymer architectures are dealt with in detail in recent monographs and reviews [2,29]. Architectural modification (modification of interface, chain topology, block symmetry etc.) may lead to a significant deviation in morphology and physical properties of the block copolymers. The strategies mainly adopted are briefly reviewed in the following paragraphs with special reference to two-component systems.

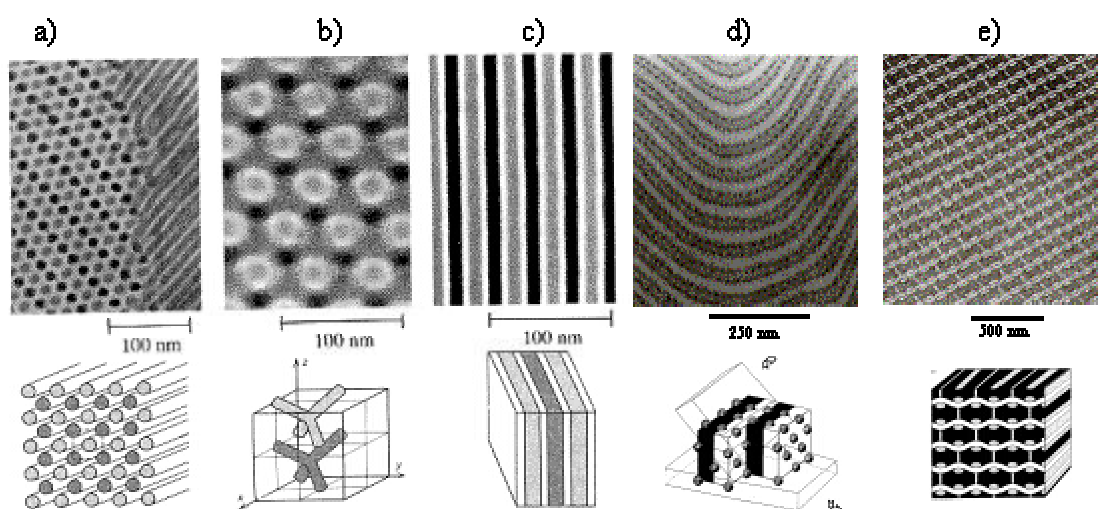


Figure 2.4: Scheme showing few newly discovered morphologies in three-component ABC triblock copolymers; a) tetragonal cylinder b) OTDD structure c) three-phase four-layer structure d) spheres between the lamellae and e) knitting pattern morphology; a-c are from Mogi et al. [20-22] and d-e are from Stadler et al. [25,26].

2.2.1 Variation of Chain Topology

This route consists of combining the block chains into different topologies: linear (diblock, triblock, multiblock), radial (simple star, miktoarm star), graft copolymers etc [2]. Hadjichristidis and co-workers have synthesised a wide range of graft block copolymers, and studied their morphology formation and physical properties. Their works have been documented in recent articles and reviews [29-33]. A pronounced shift in phase behaviour of graft block copolymers with respect to corresponding diblock copolymers was observed. For example, lamellar morphology was observed in a PS/PI/PB miktoarm star block copolymer in a composition range in which a cylindrical morphology would be expected for a diblock copolymer having equivalent composition [30]. The discrepancy in phase behaviour has been explained on the basis of packing frustration. Since both the elastomeric chains emanate from a common junction point in this particular star block copolymer, the chains tend to avoid chain stretching (and achieve maximum possible entropy) by relaxing and forming a curved interface [30-32]. Experimental

observation of ‘Mesh and strut’ structures by Hashimoto et al. [34], lamellae like structures (not exactly lamellae) by Yamaoka and Kimura [35] and of bicontinuous structures (later identified as Gyroid [18,19], in a composition range for cylindrical morphology in a linear block copolymer) by Thomas and co-workers in different star block copolymers are additional evidences illustrating the influence of block copolymer chain topology on their phase behaviour.

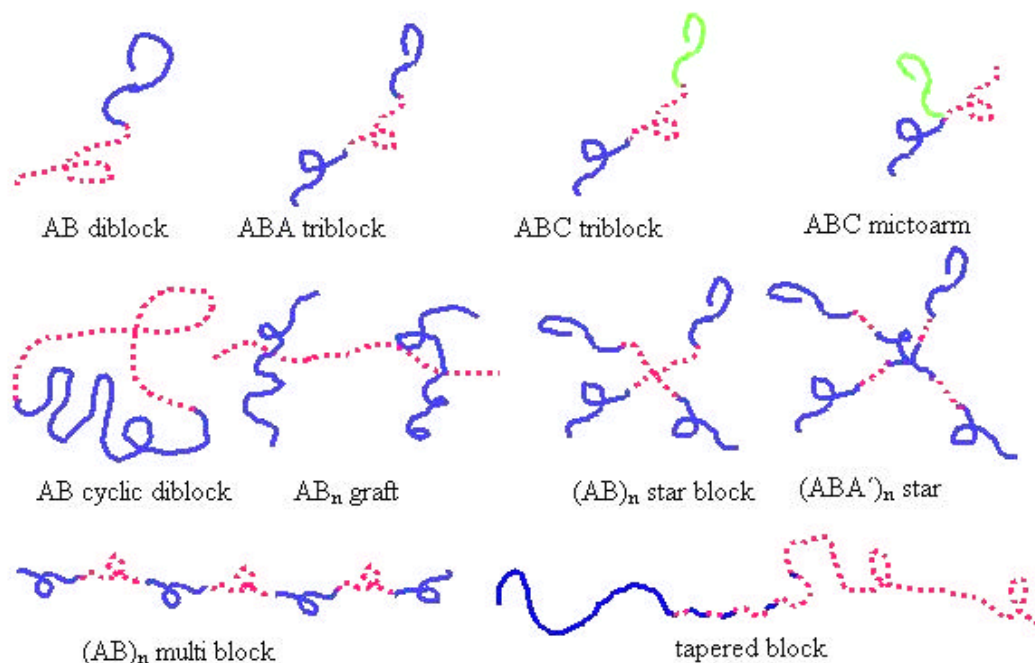


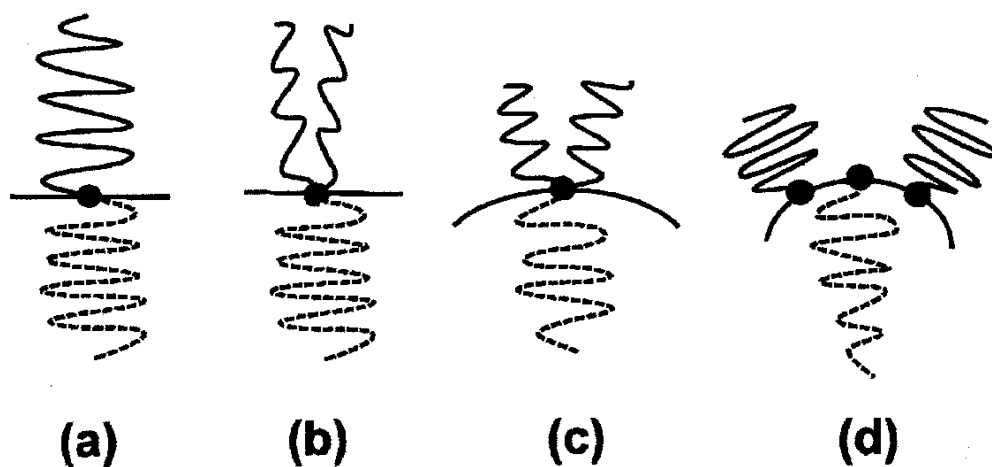
Figure 2.5: Block copolymers of various molecular architectures (A denotes the glassy block).

With the development of new synthetic methods, experimental studies on more complex architectures began to emerge, which, in turn, inspired new theoretical studies of the effect of molecular architecture on morphological behaviour. Milner calculated phase diagrams of asymmetric miktoarm star block copolymers and demonstrated that stability windows for a particular morphology is dramatically shifted as a function of block copolymer architecture [36]. According to Milner’s theory, for example, lamellar morphology would be expected for a styrene/diene miktoarm star (A_2B type) having styrene content as high as 81 vol %, for which composition bcc spheres are expected in a diblock analogue. Particularly, the influence of asymmetry was analysed taking into consideration the *molecular asymmetry parameter* ϵ which constitutes both molecular architecture and conformational asymmetry. The theory has successfully predicted the phase behaviour of miktoarm star block copolymers and graft block copolymers.

The situation of morphology formation in an A_2B type miktoarm star block copolymer is schematically illustrated in fig 2.6 [30,32]. For a compositionally symmetric AB diblock (here named as $(2A)B$ diblock), a flat interface is expected. If a trifunctional branching point (fig 2.6b) exists for A_2B miktoarm star block copolymer, the A chains have to highly stretch perpendicular

to the interface in order to maintain the domain spacing constant. However, it is thermodynamically unfavourable, and the higher stretching of the two **A** arms can be partially alleviated by allowing the interface to curve away from them (fig 2.6c). Thus, multiple arms of block type **A** at a single junction result in an enhanced preference for these arms to remain on the convex side of the interface. This preference causes the shifts of order-order transition (OOT) lines towards higher **B** block volume fractions in morphology diagrams. The effect becomes more pronounced for a graft block copolymer (fig 2.6d).

Previously phase diagrams of asymmetric ABA triblock copolymers and star block copolymers was calculated by Dobrynin and Erukhimovich [37]. These authors have shown the shift of phase boundaries with respect to the number of arms and symmetry of the arms of star block copolymers. Recent studies of Floudas [38] and Matsen and Schick [39] dealt also with phase diagrams of star block copolymers. Most recently, Morozov and Fraaije [40] have analysed the phase diagrams of the block copolymer melts with arbitrary architectures using the highly branched tree-like structures (dendrimers). Topology of the molecules was shown to considerably affect the spinodal temperature and asymmetry of the phase diagrams, but not their type and order.



2.6: Schematic of A-B junction points on an interface for a) $(2A)B$ linear diblock copolymers, b) A_2B block copolymers with a trifunctional branch point at a flat interface, c) A_2B single graft block copolymer with a trifunctional branch point at a curved interface and d) A_2B block copolymers with approximation of equal spacing between the grafted **A** blocks. The curvature of the interface represents the shifts of the OOT lines towards higher **B** volume fractions on the morphology diagrams [30,32].

It should be mentioned that star block copolymers are earning special academic and technical interests due to their preferred rheological and mechanical properties [41-48]. Recently, Kennedy and co-workers have explored the synthesis of star block thermoplastic elastomers using living cationic polymerisation [45-48]. This group has intensively investigated the mechanical and rheological behaviour of linear and star block copolymers and shown that star copolymers possess enhanced properties than their linear counterparts [44].

2.2.2 Asymmetric Block Structure

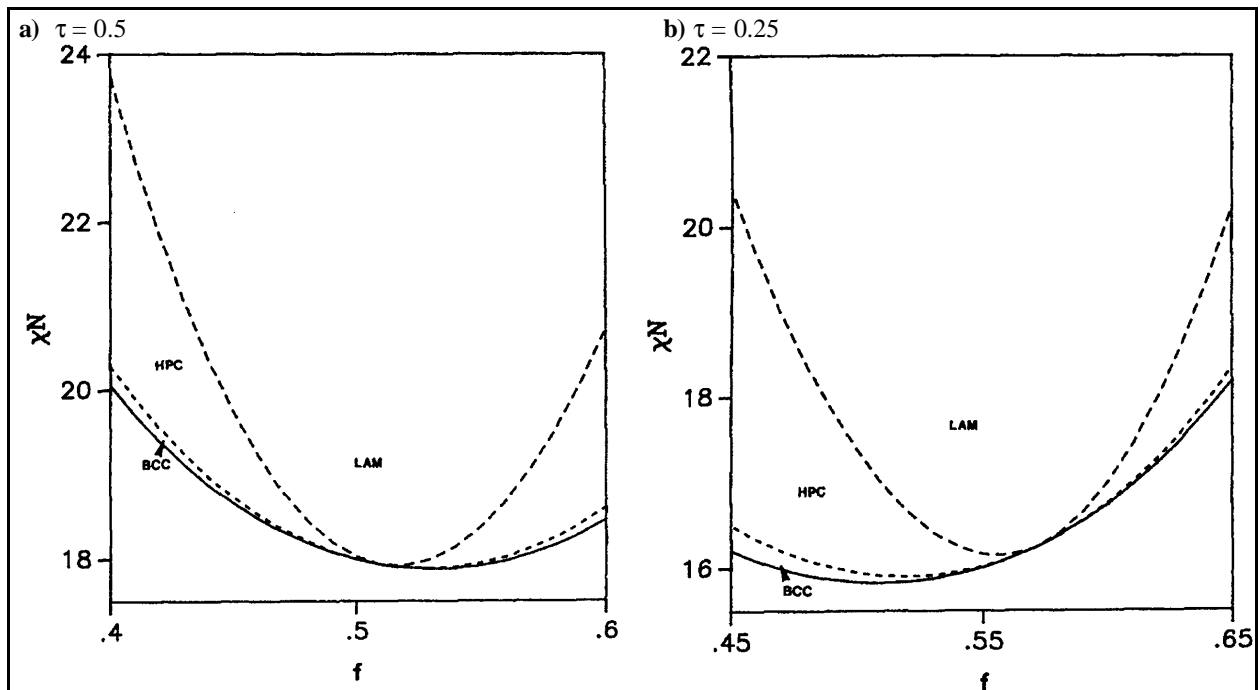


Figure 2. 7: Landau mean field phase diagram for an asymmetric ABA triblock copolymer with a) $\tau = 0.5$ and b) $\tau = 0.25$ [49,51].

A_1BA_2 type copolymers having asymmetric block structure (where A and B are glassy and rubbery blocks respectively; and $M_{A1}/M_{A2} \neq 1$) are of special technical importance. Highly asymmetric A_1BA_2 block copolymers may combine the deformability of the shorter glassy end blocks with strength of longer ones [42,52,53]. Asymmetry in block lengths is demonstrated to cause a significant morphological deviation both experimentally [31-33,41] and theoretically [36,37,39,49-51]. In ref. [37], it has been demonstrated that regions of phase stability in graft copolymers, asymmetric triblocks, linear multiblocks and polygraft copolymers are shifted with respect to diblock copolymer phase diagram. Mayes and Olvera de la Cruz [49,50] have extended Leibler's theory to asymmetric triblocks and $(AB)_n$ star block copolymer melts and generalised the influence of asymmetry as a reason for asymmetric phase diagram. They showed that the phase diagrams of ABA triblock copolymers (compositionally symmetric or asymmetric) are highly asymmetric. The composition (f_c), at which the continuous transition from disordered to lamellar phase occurs, was found to shift as a function of symmetry parameter. The points of continuous transition are also shifted in star block copolymers depending on the number of arms. Unlike in AB diblock copolymer, where a direct transition from disordered to lamellar phase occurs at $f = 0.5$, a transition from the disordered to hex and then to lam phase was predicted for a symmetric ABA triblock copolymer at this composition (asymmetric parameter, $\tau = N_{A1}/N_{A1} + N_{A2} = 0.5$). For a symmetric ABA triblock copolymer at $\chi N = 19$ ($\tau = 0.50$), where the melt is

disordered at $f = 0.40$ while it is predicted to have a hex phase at $f = 0.60$ (fig 2.7a). Meanwhile, for an asymmetric triblock copolymer, broad zones of bcc and hex stability are predicted (e.g., $\tau = 0.25$, fig 2.7b).

The asymmetry of phase diagrams in an ABA triblock copolymer melts can be explained as follows: at $f_A = 0.40$ (and $f_B = 0.60$), it is entropically more difficult to confine two A blocks into domains than a single B block, i.e., as the matrix component, the central B blocks must deform to accommodate the outer A blocks into A domains. Hence, the melt tends to be disordered. This problem is more notable for multiple arm stars with a core of connected B blocks. This causes the f_c points to shift towards higher A volume fraction in $(AB)_n$ stars.

Recently, Matsen has examined the phase behaviour of asymmetric ABA triblock copolymer melt using self consistent field theory (SCFT) and pointed out that shift in phase transition lines results from their different segment distribution compared with that of symmetric triblocks as illustrated in fig 2.8 [54]. As the value of τ deviates from 0.5 (a AB diblock case), the A segment distribution moves away from the interface without stretching the A chains, and this causes an increase in domain spacing (fig 2.8b). Hence, the stretching energy in A domains is decreased. Further, the spontaneous curvature changes, since transferring some of the B domain stretching to the softer A domain by curving the interface away from B domains lowers the overall energy. This change in spontaneous curvatures shifts the OOTs toward larger f_A as τ decreases from 0.5, i.e., when the outer blocks become more asymmetric.

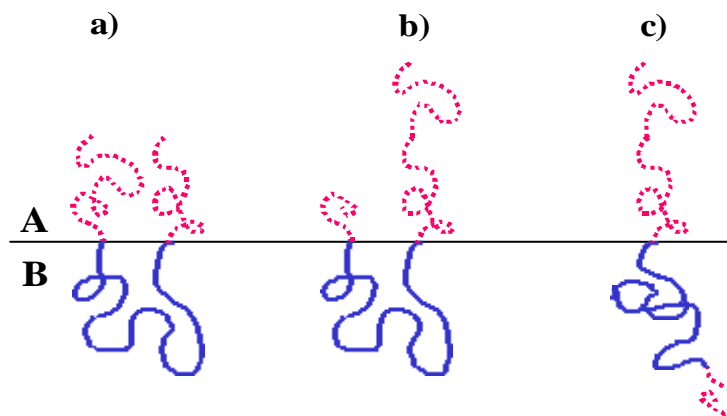


Figure 2.8: Schematic diagram showing three triblock configurations all with equal degrees of chain stretching. A and B chains are represented by dotted and solid lines, respectively. a) symmetric triblock having its segments closest to the interface, b) asymmetric triblock with its segments away from the interface and c) asymmetric triblock having its shorter A block extracted from the A domains [54].

At sufficiently large asymmetry, the A chains begin to pull out of their domains. Although unfavourable interactions occur when A blocks leave A domains, it is more than compensated for by the fact that its B domains can relax. Figs 2.8b and 2.8c demonstrate how the extraction of A blocks allows the B segments shift away from the interface without further stretching of the molecule. The Extraction of short A blocks has a significant influence on the domain spacing of

the ordered morphologies. Generally, the domain periodicity is larger in asymmetric block copolymers than in equivalent symmetric triblocks and diblocks.

Furthermore, role of dispersity (e.g., polydispersity or even bidispersity as explained above) on the morphology formation was studied by Gerberding et al. using SBS triblock copolymers of variable molecular weight distribution of styrene and butadiene blocks [55]. At a wide PS block molecular weight distribution, the bulk morphology was shifted to lower total volume fraction of polystyrene. Likewise, the morphology was shifted to lower PB content when the butadiene centre block possessed a wide molecular weight distribution.

2.2.3 Interfacial Modification

Introduction of a tapered or statistical chain between the incompatible blocks may further modify the block copolymer phase behaviour as demonstrated by several experimental [56-63] and a few analytical studies [64,65]. These studies have, in general, shown that presence of a tapered or statistical chain between the incompatible blocks results in a broadened interface due to enhanced mixing at the interface. In a systematic study, Gronski and co-workers [56,57] measured the thickness of interface in a series of styrene/diene copolymers as a function of length of tapered chain, and observed a broadened interfacial width (extended interface) with increasing length of the tapered chain. They have observed even three different phases in a two-component block copolymer system. Further interfacial modification in styrene/isoprene diblock copolymers was shown to change the interfacial tension (or the effective interaction parameter) and influence strongly the domain dimensions.

Zielinski and Spontak have modelled the equilibrium thermodynamics of A(A/B)B block copolymers (statistical or tapered middle block) by employing the confined chain statistics [64]. Their model treats such systems as three component ABC block copolymers. In tapered block copolymers (fixed composition and molecular weight), the interfacial volume increased and domain periodicity decreased as the volume fraction of tapered block was increased. Both of these functional relationships suggests that a composition gradient imposed across the middle A/B block enhances the interfacial mixing. These predictions are in agreement with the findings of Gronski and co-workers [56,57].

However, microstructural characteristics of a series of compositionally symmetric tapered styrene/isoprene triblock copolymers investigated using TEM and SANS by Sameth et al. showed no dependence of domain periodicity with wt fraction of middle tapered block [58]. Their study indicated, nevertheless, morphological deviations in A(A/B)B block copolymers having middle statistical or tapered block.

Recently, Knoll [52], Asai [61], Moctezuma and co-workers [60] have studied the influence of modified interface on the phase behaviour and mechanical properties of block copolymers. These

and similar studies [66] have indicated that the tapered transition may cause a significant increase in the effective volume fraction of the rubbery component and an improvement of ductility of the copolymers. In such block copolymers, the free energy component of the interface is sufficiently increased, and the system is driven towards order-disorder transition (ODT). Some block copolymer architectures having extended interface are schematically outlined in fig 2.9.

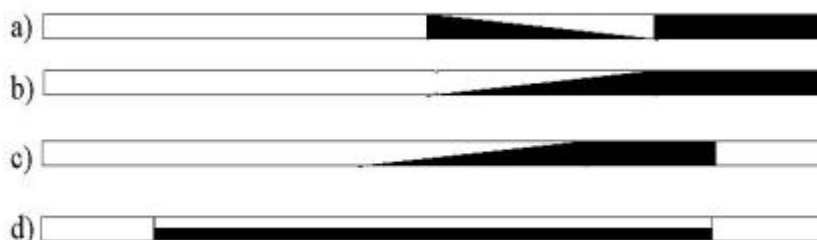


Figure 2.9: Block copolymers having broadened interface, a) inverse and b) normal tapered block copolymers [63] c) normal tapered triblock and d) triblock with a random A/B block [66]; white and black blocks represent glassy and rubbery chains, respectively.

Styrene/diene tapered block copolymers are intensively studied by Hashimoto and co-workers [67]. THF was used as randomiser during the simultaneous copolymerization of styrene and diene using *s*-BuLi and benzene as initiator and solvent, respectively. They observed a rod-like morphology instead of lamellae in nearly symmetric copolymers. They have pointed out two phenomena that may be responsible for a shift in structural and thermomechanical properties of the block copolymers: domain boundary mixing (broadening of interface) and mixing in domain (incorporation of unlike segments into a particular domain).

Worm-like structures are observed by Knoll and Nießner in a highly asymmetric tapered SBS star block copolymer [52]. More recently, Hadjichristidis and co-workers [63] have studied the phase behaviour of *normal* and *inverse* tapered block copolymers, and demonstrated that *inverse* tapered sequences lead to higher compatibility (wider interfacial width) than the *normal* ones. Further, the spinodal lines are shifted towards higher values of χN , which is in consistence with the theoretical predictions of Aksimentiev and Holyst [65]. The latter authors have calculated the phase diagram of a gradient block copolymer melt using Landau-Ginzburg model, and predicted the stability of bcc, hex, gyroid and lam phases, similar to that of a diblock copolymer melt. However, the direct transition from disordered melt to lamellar phase was observed at $\chi N = 11.906$, in contrast to a value of 10.495 in a diblock copolymer. It has been mentioned that the ordering is caused at a larger characteristic length than in the diblock copolymer melt due to diffuse boundary between the blocks A and B.

Block copolymers possessing one or more of the variables discussed above (i.e. complex topology, asymmetric end blocks and broad interface) are expected to exhibit a complex phase behaviour which may have an important consequence on morphology formation, mechanical properties and deformation behaviour.

2.3 Blends Containing Block Copolymers

2.3.1 Block Copolymer/Homopolymer Blends

Block copolymers are often used in combination with other polymers or additives [52,62,68-70]. One of the important ways of morphology control in these materials is given by blending with homopolymers. A two component block copolymer may be blended with homopolymers which are identical with block copolymer's constituent blocks or with homopolymers which are chemically different from that of the constituent homopolymers. Of particular industrial interests are the binary blends of styrene/butadiene block copolymers with polystyrene [52,68].

The length of the homopolymer chain compared to that of block copolymer primarily governs the phase behaviour of a binary blend of a block copolymer and a homopolymer. There is interplay between microphase and macrophase separation; and which effect predominates depends on the composition of the mixture [2,11,71-76]. Hashimoto et al. have explored the phase behaviour of binary blends consisting of styrene/diene copolymers and homopolymers by varying the molecular weight of homopolymer, composition of the blends, block copolymer architecture (AB diblock or ABA triblock) and by using homopolymers having different interaction with the block copolymer [71-76].

For styrenic block copolymer/homopolystyrene mixtures, three regimes have been identified depending on the degree of polymerisation of the homopolystyrene (N_{hPS}) and that of the same component of the block copolymer ($N_{\text{PS-block}}$).

- a. If $N_{\text{hPS}} < N_{\text{PS-block}}$, the hPS molecules tend to be selectively solubilized in the PS domain of the microphase-separated copolymer, and is weakly segregated towards the domain centre leading to an increase in interfacial area per block and causing a swelling of the polystyrene block. This, in turn, can lead to a change in morphology (illustrated later in fig 2.11). This regime has been termed as 'wet brush' regime because the copolymer chains in the weak segregation regime can be considered to be polymeric brushes, and in this case they are 'wetted' by the penetration of homopolymer chains.
- b. If $N_{\text{hPS}} \approx N_{\text{PS-block}}$, the hPS is still selectively solubilized in the PS domains of the microphase separated block copolymer. The hPS molecules tend to be localised in the middle of the PS domains. Hence, the interfacial area is not significantly affected, and the

conformations of another component chains are not significantly perturbed. In this ‘dry brush’ regime, PS block chains are not significantly swelled.

- c. If $N_{hPS} > N_{PS-block}$, macrophase separation takes place leading to the formation of hPS particles in the microphase-separated copolymer matrix or vice versa. Which component forms the matrix depends on the mixture composition.

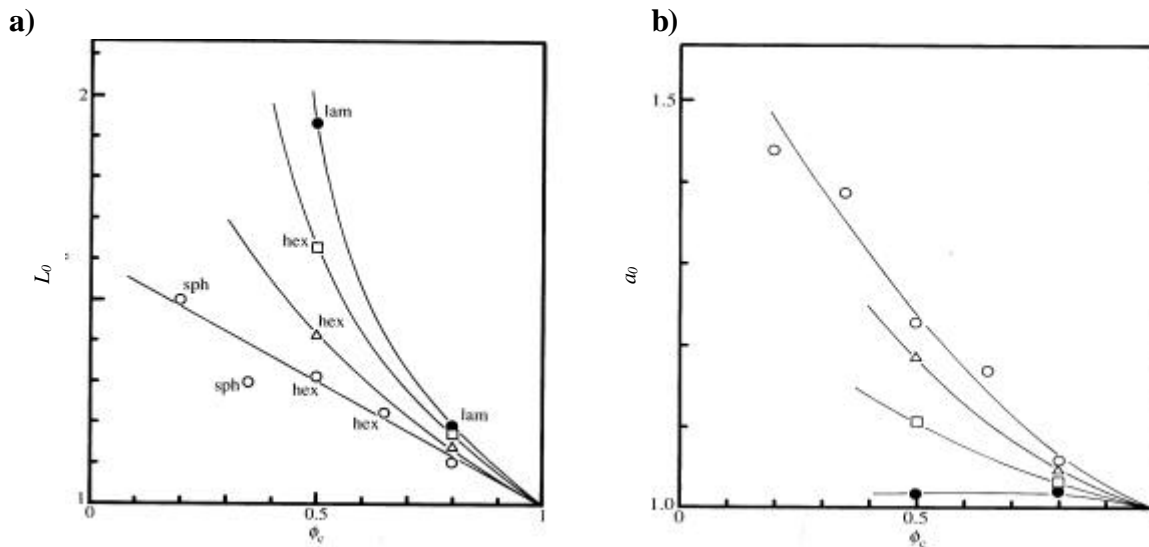


Figure 2.10: a) Average interdomain distance L/L_0 and b) average distance between the chemical junction a/a_0 points along the interface relative to that of pure PI diblock copolymer measured by SAXS with $d_0 = 26.7$ nm and $a_0 = 2$ nm in the regime $M_{A-block} > M_{hA}$ [72].

Comprehensive studies on the phase behaviour of binary block copolymer/homopolymer blends was made by Hashimoto et al. [71-76] and Winey et al. [77,78]. Domain spacing and interfacial area per block were investigated in binary PS-PI block copolymer/PS blends using SAXS by Hashimoto and co-workers [72]. For $\alpha \leq 1$ (where α is the ratio $N_{hPS}/N_{PS-block}$), the domain spacing (L) and average distance between the junction points (a) were found to increase with increasing homopolymer concentration in the blends (fig 2.10). This suggests that the homopolymer chains have swelled the PS block domains. Furthermore, the magnitude of L increased with increasing α at given blend composition indicating the tendency of segregation of homopolymer chains towards the domain centre with increasing α .

Transitions from the lamellar phase of a neat PS-PI diblock copolymer to cylindrical and then to spherical structures were observed by Hashimoto [71,76] on addition of hPS. These morphological changes have been explained on the basis of changes in interfacial curvature and packing density as illustrated in fig 2.11. Addition of hPS chains causes the swelling of block PS chains of the copolymer leaving the PI blocks unswollen. This leads to a difference in segmental density in PS and PI phase. In order to retain normal liquid-like densities, the PS block must stretch and/or PI block must contract (fig 2.11b). However, an alternative is to curve the interface placing PS on its convex side (fig 2.11c). The latter situation predominates when the

conformational entropy loss due to chain stretching is outweighed by the interfacial curvature penalty.

Based on a series of experimental results on blends of styrene/diene diblock copolymers and hPS, Winey et al. have constructed a phase diagram at constant copolymer composition (about 50 vol %) by varying blend composition and α which show the region of existence of different phases which nearly correspond to that observed in pure block copolymers at corresponding overall composition. At larger value of α , homopolymer chains are completely expelled out of corresponding block domains which form a separate macrophase as shown by different studies [77,78].

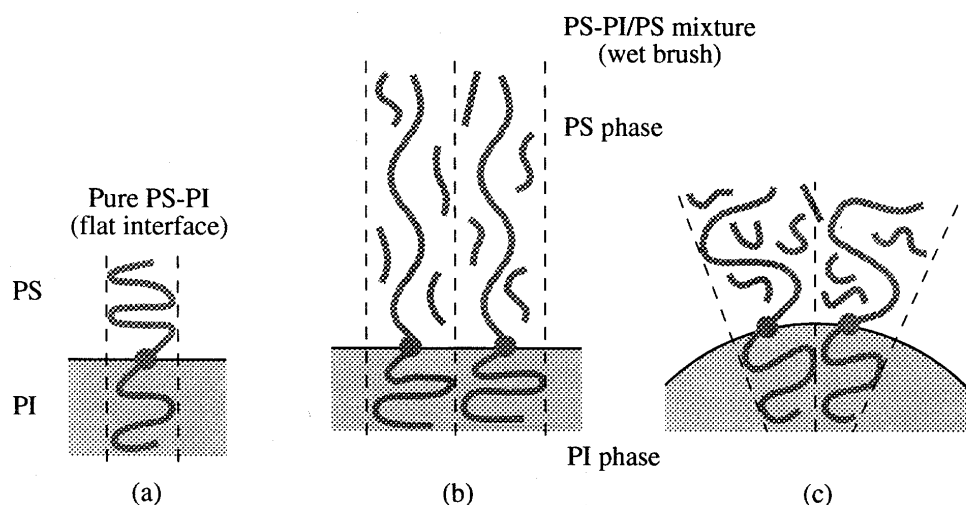


Figure 2.11: Schematic illustration of chain packing: a) pure SI diblock copolymer chain with symmetrical volume fraction forming a flat interface, b) swelling of PS lamellae by uniform solubilization of hPS molecules causes stretching of PS-block chains and/or compression of PI-block chains resulting in a decrease in conformational entropy, c) alternatively a curved interface is formed to gain entropy [76].

Effect of copolymer architecture (star and triblock) on miscibility and mechanical properties of styrene/butadiene block copolymer/hPS was recently studied by Feng et al. [79-81]. These authors have suggested that there is a molecular weight range of hPS for which the mechanical properties are enhanced. Depending on the M_{hPS} , added hPS was found to exist both in PS and PB phases. The influence of block copolymer architecture on the miscibility of the blends was, however, not found.

In addition to classical phases, complex phases have been identified in block copolymer/homopolymer blends too [34,42,82]. Winey et al. [82] observed OBDD phase (later reassigned as 'gyroid' phase) in PS-PI diblock/hPS blends at a overall composition range $\Phi_{PS} = 0.64-0.67$ which is approximately same as the composition range in which this phase was observed in a pure PS-PI diblock copolymer ($\Phi_{PS} = 0.62-0.66$) [17]. Hashimoto and co-workers [34] observed 'mesh and strut' structures in a styrene/butadiene star block copolymer/hPS blend.

These structures and ‘catenoid lamellar structures’ reported by Disko et al. [83] resembled the HPL structures observed in diblock copolymer melts [17].

Low molecular weight hPS, though most soluble in the corresponding block domains of the block copolymers, is generally not desirable for technical applications. This, of course, may reduce the cost but also deteriorates the mechanical properties. Due to lack of stable entanglements, the products don’t possess optimum strength level. Therefore, hPS with quite higher molecular weights (~ 100 kg/mole) is used. The molecular weight of hPS and PS block of the copolymer should be optimized since hPS tends to macrophase segregate when N_{hPS} approaches $N_{\text{PS-block}}$, also undesirable because it may lead to loss in transparency.

Recently, Yamaoka has studied the morphology and toughness behavior of the blends of K-Resin 05 and a PS-co-PMMA (MS) using compression molded samples. His results show a macrophase separation of MS in K-Resin matrix [84,85]. Knoll and Nießner have studied the morphology and tensile properties of blends consisting of highly asymmetric star block copolymer and hPS using compression moulded samples [42]. In spite of a large difference in the molecular weight of homopolystyrene and PS block of the block copolymer, no macrophase separation was observed. The star block copolymer was found to be especially compatible to the added homopolymer.

2.3.2 Binary Block Copolymer Blends

Compared to an intensive investigation of thermodynamics and phase behaviour of block copolymers, only limited information is available on their blends. Hoffman et al. investigated binary blends of SB diblocks and reported a microscopic demixing of blends, with two maxima in the domain size distribution [86]. Jiang et al. [87], Hadziioannou et al. [88] and Hashimoto et al. [76,89,90] investigated binary blends consisting of diblocks and triblocks. In these studies, the blends were microphase separated; and depending on the blend composition and molecular weight of the copolymers, morphology transitions were also observed.

Studies of Hadziioannou et al. and Hashimoto et al. on a series of blends of lamellar diblocks and triblocks consisting of polystyrene and polyisoprene demonstrated that the phase behaviour of the binary block copolymer mixtures is mainly governed by copolymer composition, blend composition and molecular weight ratio (i.e M_1/M_2) of the copolymers [88-90]. If $M_1/M_2 < 5$, complete miscibility of the block copolymers was observed in which the domain periodicity followed the power law: $L \sim M_n^{2/3}$, where M_n is the sum of mole fraction of each block copolymer multiplied by corresponding number average molecular weight. When $M_1/M_2 > 10$, only a partial miscibility of two lamellar block copolymers resulted in macrophase separation of lamellae having different lamellar periodicity [91]. The morphology fundamentally different

from that of parent block copolymers was reported in blends of styrene/butadiene star block copolymers with nearly same chemical composition ($\Phi_{PS} = 0.7$) by Jiang et al. [87]. Particularly, coexistence of cylindrical and worm-like structures was observed. The molecular weight one of the star block copolymers was about 7 times higher than that of the other. The blends showed macrophase separated composite structures containing microphase separated composites. More recently, more complex structures are reported by Knoll and Nießner in blends of star block and triblock copolymers consisting of styrene and butadiene [42].

Recent investigations of Spontak et al. on the blends of symmetric ($\Phi_{PS} = 0.5$) and asymmetric block copolymers ($\Phi_{PS} = 0.85$) showed that the blends show same microstructure as the pure diblock having equivalent overall composition [92].

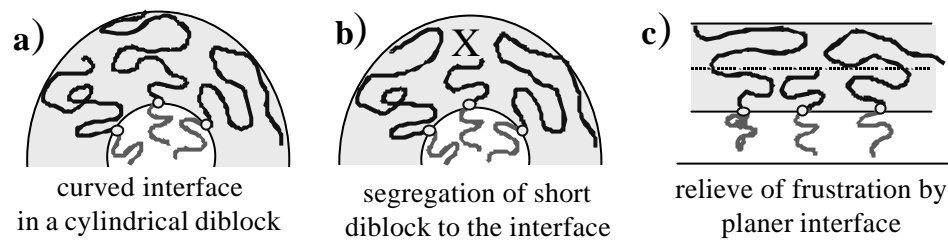


Figure 2.12: Schematic illustrating packing frustration induced by addition of short diblock to a microphase of a long diblock [76].

It was shown that blending of a lamellar-forming diblock with $\Phi_{PS} = 0.32$ and one with $\Phi_{PS} = 0.60$ can induce the formation of bicontinuous cubic structure in certain ranges of composition. In contrast, blending of a diblock forming a lamellar phase with $\Phi_{PS} = 0.44$ with a diblock forming a bicontinuous cubic structure with $\Phi_{PS} = 0.66$ resulted in the formation of lamellar phase even when the overall composition was $\Phi_{PS} = 0.62$ (composition in which bicontinuous structure is expected in a diblock) [76]. It means that a single phase approximation cannot be used while considering the phase behaviour of blends of block copolymers having different molecular weights i.e., the blend morphology doesn't necessarily reflect the morphology of a pure copolymer with an equivalent composition.

The morphology change may be induced by the interfacial curvature and packing density as schematically illustrated in fig 2.12 [76]. Fig 2.12a shows a cylindrical block copolymer with B cylinders in the matrix of A. Exchanging one of the chains by a symmetric AB diblock (lamellae forming) leads to a situation shown in fig 2.12b. The segregation of a short diblock copolymer molecule to the interface leads to the low packing density (denoted by letter X in fig 2.12b where the copolymer is depleted leading to packing frustration). This frustration is relieved when the interface adopts a planer geometry which, in turn, leads to a transition from cylindrical to lamellar morphology (fig 2.12c).

More recently, Hashimoto et al. have studied the blends of AB diblocks with AC diblocks and reported the morphology as would be expected for ABC triblock copolymers [93]. Abetz and Goldacker have reviewed morphology of ABC triblock copolymers and their blends, and shown the existence of hierarchies of microphase separated structures in binary ABC triblock copolymer blends [24]. Through a systematic small angle neutron scattering (SANS) study of binary lamellar forming diblock copolymers, Papadakis et al. have constructed a phase diagram for such systems and demonstrated that a competition between microphase and macrophase separation takes place depending on the chain length ratio and composition [94,95].

These discussions reveal that research interests are growing in the study of phase behaviour of binary blends of block copolymers. These materials have, however, found no considerable industrial interest because of higher manufacturing costs of both the blend components. As a consequence, less (or almost no) attention has been paid in the deformation behaviour and mechanical properties of these blends.

2.4 Mechanical Properties and Deformation Behaviour

In the preceding section, morphology formation in block copolymers and the blends containing block copolymers is briefly reviewed. Now, a short review of micromechanical deformation processes observed in amorphous block copolymers as a function of microphase morphologies is presented. First the thermomechanical and mechanical properties of the polymeric materials are introduced.

2.4.1 Thermomechanical Properties

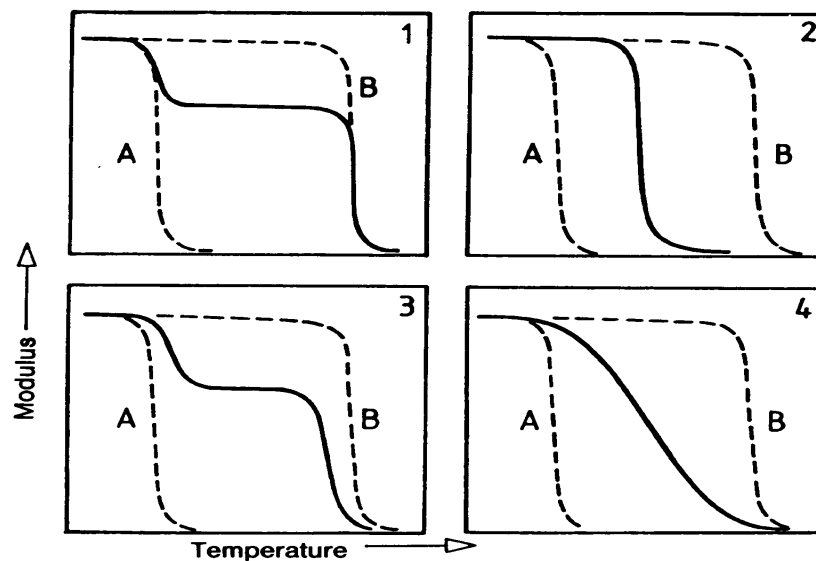


Figure 2.13: Dependence of complex modulus of elasticity as a function of temperature in different polymer pairs (schematic), case 1) immiscible polymers, 2) completely miscible polymers, 3) partially miscible polymers and 4) multitude of phases [8].

Mechanical properties of heterogeneous polymer systems are primarily determined by interaction between the phases and morphology resulting therefrom. Hence, analysis of miscibility of the components may provide an important insight into micromechanical and mechanical behaviour of heterogeneous systems including block copolymers.

Different spectroscopic and microscopic techniques, scattering methods and calorimetry can be employed to examine the miscibility and phase interaction in polymer pairs. However, the measurement of complex modulus as a function of temperature is the most important method for determining the miscibility of polymer mixtures. Four possible cases are schematically represented in fig 2.13 [8]. Solid and broken lines stand for the mixture and pure components, respectively. *Case 1* shows a solid curve indicating two distinct temperatures of glass transitions corresponding to those of the individual components A and B (broken lines). Here, two polymers are completely immiscible and are present as two separate phases. Amorphous two-component block copolymers generally belong to this class [43,69]. *Case 2* shows a sharp glass transition roughly in between those of the two components. In this case, the polymers are completely miscible and exist as a single homogeneous phase. For example, a mixture of PMMA and PEO or PS and PPO represents this system [8]. The curve in *Case 3* indicates two separate glass transitions, but these are shifted with respect to the component homopolymers, i.e., both the phases are of mixed compositions. Weakly segregated block copolymers are known to form a partially miscible phase and hence exhibit a shift in glass transition temperature of constituents [96]. Sometimes, three distinct phases may be observed in a two-component systems: two pure phases and a mixed phase as demonstrated by some block copolymers possessing broad interface [56,57]. *Case 4* shows a broad, ill-defined glass transition reflecting the presence of a multitude of phases with a slightly different composition.

If the miscibility is desired, it can be realised by introducing a third 'component' to the binary polymer mixtures. Phase compatibiliser used in polymer blends, for example, enhance the miscibility (and hence phase adhesion) between the components. Of particular interest in the present work is to qualitatively analyse how the molecular architecture of the block copolymers influences their miscibility and phase behaviour.

2.4.2 Mechanical Behaviour of Polymers

Tensile experiments (stress-strain curves) offer a simple and straightforward way of characterising and comparing mechanical behaviour of polymeric materials. The total deformation of the test specimen comprises different material responses toward external stress: linear elastic, linear viscoelastic, non-linear viscoelastic and plastic deformation [1,8,98]. Linear elastic behaviour, which involves only the reversible alteration of inter-atomic distances without

breakage of chemical bond, is explained by the Hooke's law. This region corresponds to less than 0.1% strain in thermoplastics. At higher strain (up to 0.5% strain), the deformation is no more linear elastic, and this region is termed as linear viscoelastic region, in which the strain-reversibility is time and temperature dependent. At strain $>0.5\%$, the deformation is additionally a function of extent of loading besides time and temperature and called non-linear viscoelastic region. This region, where the molecular flow processes begin, follows the region of plastic deformation (stationary plastic flow) which finally leads to the specimen fracture. Depending on the phase morphology and micromechanical processes of deformation, mechanical behaviour observed in polymers can be classified as schematically summarised in figure 2.14 [1].

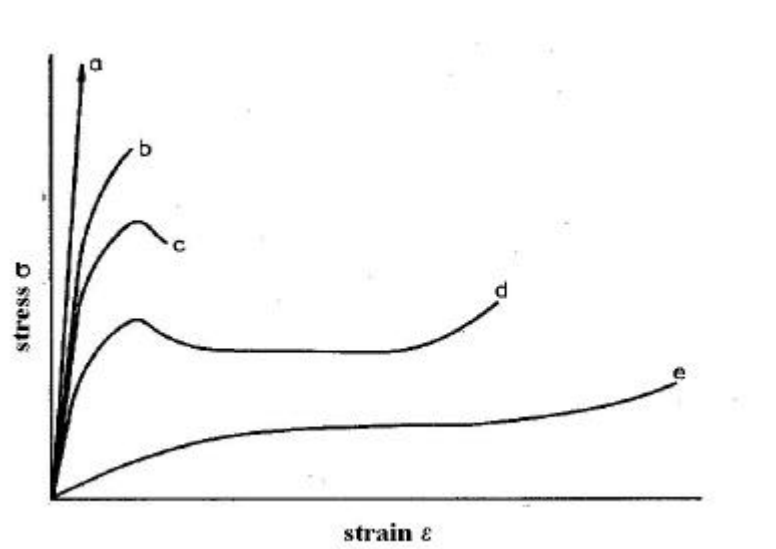


Figure 2.14: Characteristic stress-strain curves (schematic) of different polymers [1].

- a) High modulus fibres (e.g., highly oriented fibres, reinforced thermoplastics): These materials are exclusively linear elastic. The stress increases linearly with strain leading to a high tensile strength a low elongation at break.
- b) Brittle behaviour (e.g., unmodified PS, PMMA): The stress rises almost linearly with strain up to fracture. Stress increases slowly as the plastic deformation process like crazing onsets. The maximum strain is small ($<10\%$).
- c) Ductile behaviour (e.g., rubber modified thermoplastics, PVC): The stress increases with strain but drops after reaching the yield point. Macroscopic neck formation and stress whitening is observed.
- d) Cold drawing (e.g., semicrystalline thermoplastics like PE, PP): The stress level remains practically constant after the strain softening (as observed in curve c in figure 2.14) when the neck expands over the whole specimen. The necking zone is stabilised by orientation hardening. This kind of behaviour is also found in some toughened thermoplastics like block copolymers.

- e) Homogeneous deformation (e.g., TPEs, filled and unfilled rubbers): A slow and continuous increase in stress with strain is observed. The deformation is predominantly entropy elastic; yield points (if there are any) are diffuse.

Strain rate and test temperature have a strong influence on the mechanical properties of polymers (time temperature superposition principle [1,97,98]). Increasing strain rate and decreasing test temperature results in increasing tendency towards imbrittlement of samples which causes the mechanical behaviour of the polymers shift from right to left in fig 2.14. In ABA type block copolymers (where A and B are glassy and rubbery blocks, respectively), almost all the behaviours shown in fig 2.14 may be achieved by simply adjusting the copolymer composition at a temperature between T_g of both the components [43,68,69].

The mechanical behaviour of polymers outlined in fig 2.14 is closely associated with the underlying deformation mechanisms under given loading conditions. A sample which is brittle at a given test conditions may behave ductile under another set of conditions. Hence, the deformation mechanism changes from one test condition to the another. This behaviour is a consequence of pronounced viscoelastic property of the polymeric materials. The deformation mechanisms and resulting mechanical properties are further controlled by molecular and supramolecular parameters including nature of interface in the heterogeneous systems, dimension and organisation of the microscopic building blocks etc. [99-105]. Recently, unusual mechanical behaviours have been observed in the composites consisting of heterogeneous layers with dimensions in the range of few tens of nanometers [99,100]. The micromechanical behaviour of amorphous PS was found to differ considerably depending on molecular structure. In contrast to a linear PS which is characterised by the formation of fibrillated crazes under tension at room temperature, branched PS showed more ductile behaviour and homogeneous crazing under same set of conditions [101].

2.4.3 Micromechanical Construction of Polymers

Due to presence of a large variety of molecular and supramolecular structures, polymeric materials possess a wide variety of morphology. This makes it possible to modify their properties by altering one or more of these variables. How these variables finally lead to particular mechanical properties of polymeric materials is determined by the processes occurring in different length scales, from molecular to macroscopic level, as a response of the materials against external mechanical loading. These processes include displacement and scission of the chains, different yielding phenomena up to crack initiation, propagation and fracture [1,102,103]. These processes depend strongly on diverse molecular structures, morphology as well as loading conditions e.g., temperature, loading speed or stress state as already mentioned. Hence,

comprehensive knowledge of these *micromechanical processes* provides a direct way of designing polymeric materials with improved mechanical properties [103-105].

The fundamental deformation mechanisms observed in heterogeneous polymeric materials are discussed in [103,106]. Knowledge of these mechanisms is required to avoid the materials from undergoing premature failure, one of the main goals of polymer science and engineering. Inducing an intense plastic deformation over a large part of the sample and arresting the crack growth are generally useful to enhance toughness and strength of polymeric materials as schematically outlined in fig 2.15. A common idea of the toughening mechanisms outlined in fig 2.15A is to initiate a large number of local yielding zones (enhancing energy absorbing phenomena) which can be realised in the following ways [103]:

- a. Initiation of a number of microcracks by inorganic fillers, short fibers e.g.; CaCO_3 , glass fibers, carbon fibers etc.
- b. Incorporation of ductile fillers in brittle matrix which are stretched in the area of crack tip (bridging mechanism).
- c. Inducing the formation of small local plastic zones (crazes or shear bands) which is induced by stress concentration at weak particles; a typical mechanism in rubber-toughened plastics.
- d. Cavitation at or inside the filler particles, with subsequent stretching of the matrix ligament between the microvoids

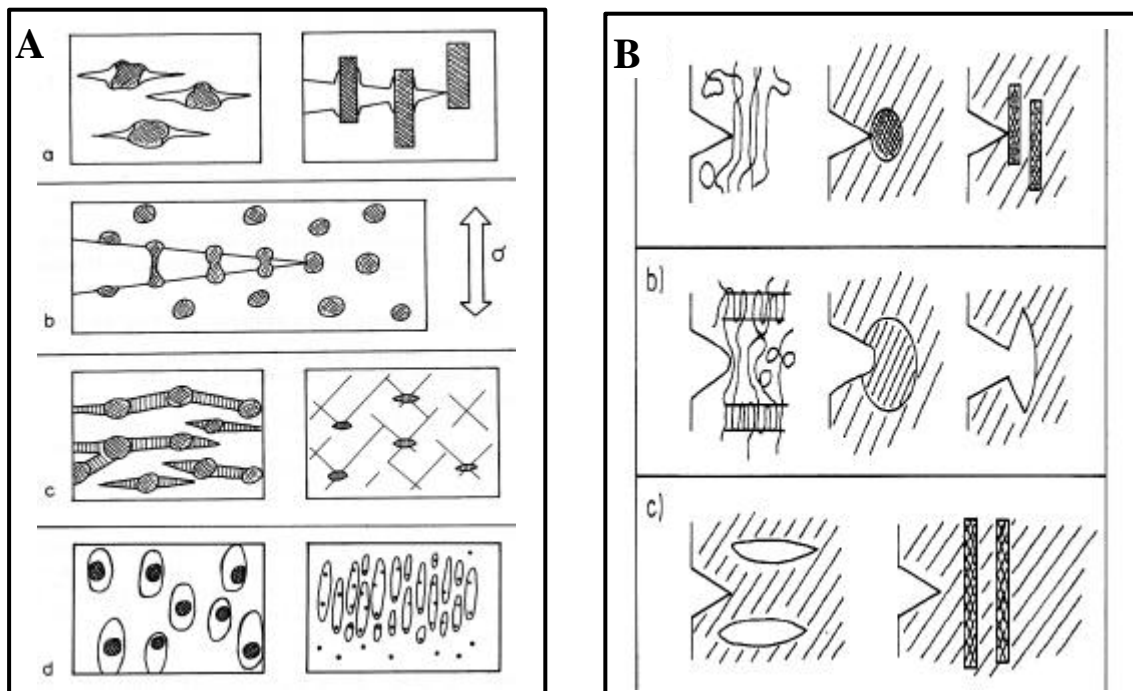


Figure 2.15: Schematic representation of some general micromechanical mechanisms in heterogeneous polymers: A) mechanisms of enhancing the toughness and B) crack-stop mechanisms (cross-hatched areas are inorganic particles, fibres or weak particles dispersed in the bulk polymer matrix; σ stands for tensile stress) [103].

Crack arresting mechanisms, useful in avoiding premature failure of polymers, are induced by different modifications as demonstrated in fig 2.15B.

- a. A rapidly propagating crack may be delayed or stopped by a local volume of higher strength (oriented chains, particles or fibres with a higher strength).
- b. Crack tip blunting by rapid relaxation processes or by propagation of the crack into a weak second phase or other microcracks
- c. Crack-diversion by strong fibres or crack propagation into the regions of unloaded regions between other cracks

Polymer combinations are generally characterised by a heterogeneous structure or morphology. A few of these structural details (not all of them) play decisive role in determining the mechanical and micromechanical behaviour of polymers. Since the optimisation of these structures leads to the optimal micromechanisms (and hence optimal mechanical properties), these structures are known as *properties-determining structures*.

The basic micromechanical mechanisms encountered in block copolymers are slightly different than those discussed above due to existence of *properties-determining structures* in much smaller length scales than in polymers blends and compounds. Here, the response of these structures (generally referred to as microphase separated structure, MSS) are highly coupled with their detailed molecular structure.

2.4.4 Deformation Behaviour of Styrenic Block Copolymers

Among amorphous block copolymers, thermoplastic elastomers (TPEs) have been of greatest technical significance. SBS and SIS TPEs have been investigated extensively which combine straightforward processing of thermoplastics with the elastomeric properties of the final products [2,12,68,69].

Domain theory was proposed to describe the mechanical properties of SBS TPEs in early sixties [68,69] which postulates that the TPEs consist of glassy domains dispersed in rubbery matrix holding the elastomeric network together by means of physical cross links. Electron microscopic images of various block copolymers have proved the validity of this theory, and this is accepted as a basic structural model in explaining the mechanical properties of block copolymers.

Styrene/butadiene block copolymers provide model systems for the study of structure-property correlations of phase separated block copolymers. In figure 2.16a, stress-strain behaviour of SBS block copolymers with different morphologies are illustrated [107]. The figures assigned to different morphologies stand for the styrene content of the SBS triblock copolymer.

At the composition range $\Phi_{PS} = 0.10-0.15$, where spherical PS domains are formed in PB matrix, the block copolymer behaves as a weakly cross-linked rubber due to relatively large inter-

domain spacing. Increasing PS content to about $\Phi_{PS} = 0.30$ results in formation of spheres in a bcc lattice with relatively smaller inter-domain distance, and the copolymer behaves as a cross linked elastomer showing a steep increase in tensile strength. Further increase in styrene content to about $\Phi_{PS} = 0.40$ causes an increase in strength when the PS cylinders in PB matrix are formed. Most commercial TPEs have the composition in the range of $\Phi_{PS} = 0.20$ -0.40.

Recently, in a narrow composition range ($\Phi_{PS} = 0.34$ -0.38), stable gyroid phase has been observed in SIS triblock copolymers [19,20] which shows predominantly elastomeric properties and deforms by the formation of a neck in tensile test [108,109].

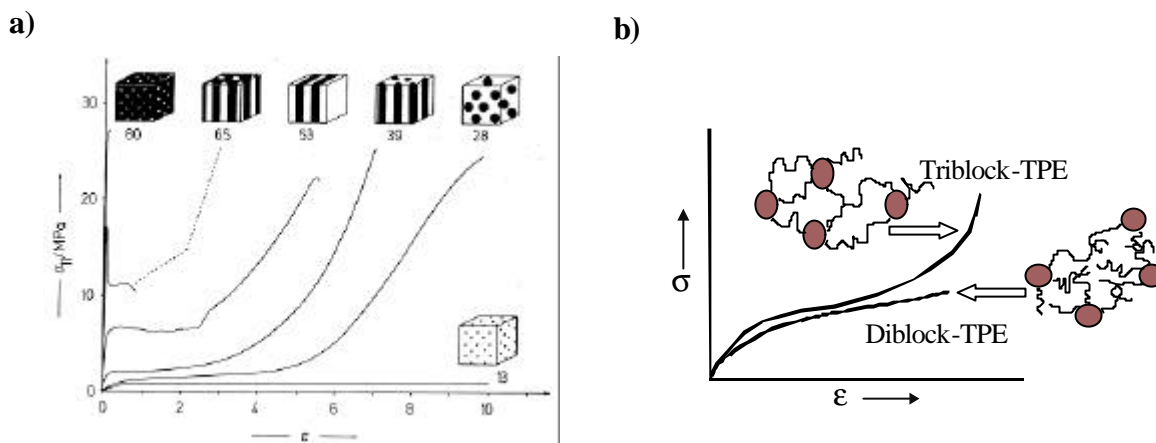


Figure 2.16: a) Stress-strain behaviour of SBS triblock copolymers as a function of styrene content; styrene domains are black [107]; b) Comparison of AB diblock and ABA triblock copolymer TPEs showing the influence of molecular architecture on mechanical properties.

As the block copolymer approaches a compositional symmetry, alternating layers of PS and PB phases are formed, and the macroscopic neck formation prevails during tensile deformation. With increasing styrene content, as the morphology reverses, yield stress increases and elongation at break decreases due to localisation of deformation. Block copolymers with dispersed cylindrical PB domains break in a quite brittle manner.

Architecture of copolymer molecule plays a decisive role in determining mechanical behaviour as illustrated schematically in fig 2.16b. ABA triblock copolymer (where A and B blocks are glassy and rubbery sequences, respectively) have properties essentially different from that of BAB triblock and AB diblock copolymers. From the materials scientific point of view, ABA type copolymers are more important than the latter types because in the former, practically stronger physical networks are formed at both the ends of covalently linked middle elastomeric block.

Interesting mechanical properties were observed in polystyrene/polyalkyl methacrylate block copolymers. Unlike strongly segregated SB or SI diblock copolymer, weakly or intermediately segregated systems may show improvements in desired mechanical properties even with diblock

architecture. Irrespective of molecular architecture (diblock, triblock or star block copolymer) [96,110], tensile strength and Young's modulus of these block copolymers were found to exceed that of both the constituent homopolymers at a certain composition range (fig 2.17). The enhanced tensile properties of these block copolymers have been discussed in terms of broad interface resulting from phase mixing at the interface. Triblock copolymers (even with PBMA outer block) were found to possess tensile properties superior than that of diblock counterparts. It has been concluded that a increasing compatibility and interfacial width between the components were associated with an enhancement of mechanical properties in these systems [111].

Previous studies on deformation behaviour of amorphous block copolymers provide important insight into the correlation between their morphology and mechanical properties. In the following, a brief review of deformation studies on amorphous block copolymer is presented with special reference to styrene/diene block copolymers.

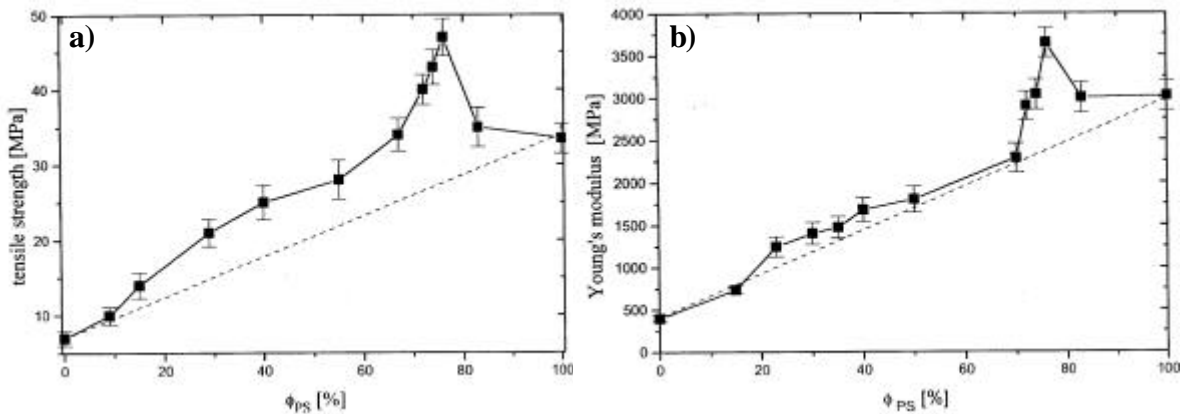


Figure 2.17: a) Tensile strength and b) Young's modulus of PS/PBMA diblock copolymers as a function of polystyrene volume fraction [96,111].

a) Copolymers having rubbery domains in glassy matrix

Pioneering works on the micromechanical mechanisms in S/B block copolymers date back to mid eighties when Argon and co-workers proposed cavitation mechanism in styrene/butadiene diblock copolymers [112-114]. Based mainly on TEM investigations they proposed a two step craze growth mechanism in S/B diblock copolymers having PB domains in PS matrix (fig 2.18a).

1. In the first stage PB domains are strongly deformed till the cavitation stress of PB is reached. The PB domains, as a consequence, tear up or cavitate resulting in the formation of voids organised in the meander-like fashion.
2. The first step is followed by necking and drawing of PS matrix strand caused by tensile stress.

Craze-like deformation zones observed by Argon and co-workers in SB diblock copolymers were thicker than those observed in PS homopolymer and not always formed perpendicular to

the principal stress direction indicating the influence of grain structure on the propagation of deformation bands. They found that the craze propagation takes place preferentially in the regions where the PB cylinders are perpendicular to the external stress direction.

Baer and co-workers [115] investigated SBS copolymer samples having 20%, 30% and 50% PS. Using methyl ethyl ketone (MEK) as solvent they produced PB spheres in PS matrix in every case. In some cases, the craze fibrils were found to start from the PB domains. The dragging of rubber particles into the crazes was also reported by other authors [116,117]. With this process the fibrils are stabilised which enhances the local deformation.

Recently, deformation behaviour of triblock and graft copolymers with glassy outer blocks have been studied by electron microscopic and FTIR spectroscopic methods [118-120]. It has been demonstrated that the craze goes through the glassy matrix leaving the rubbery phase uncavitated. A large orientation of PS chains in an SBS triblock copolymer in the initial stage of deformation is a strong evidence in favour of cavitation in glassy PS matrix [118,120]. These results (i.e., the cavitation induced in the glassy phase) are in contrast to the rubber phase cavitation observed in styrene/butadiene diblock copolymers [113]. A possible explanation is: the PB chain ends in PB domains of diblock copolymer lead to a drastic reduction in the cavitation stress, and at the same time act as the starting points for cavitation. Since the SBS triblock copolymers have only PS chain ends, which occupy a position in the PS phase nearly at the middle of two neighbouring PB domains, there is a possibility of initiation of cavitation mechanism.

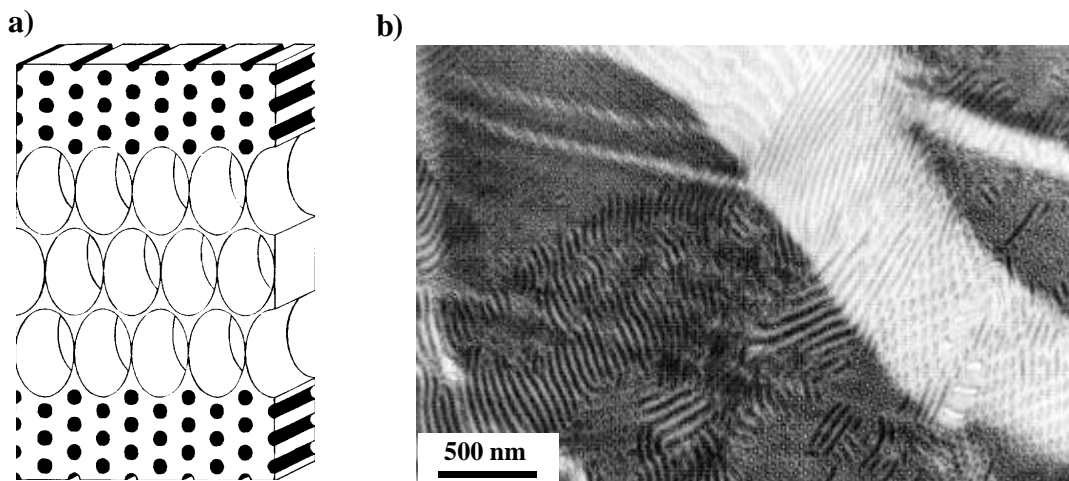


Figure 2.18: a) Cavitation model proposed by Argon et al. [113] and b) cellular structure formed by cavitation mechanism in a weakly segregated PS/PBMA diblock copolymer, $\Phi_{PS} = 0.76$ [111].

Cavitation mechanism proposed for styrene/butadiene diblock copolymers was found to operate unanimously in weakly segregated PS/PBMA diblock copolymers [96,111,119]. In a diblock copolymer having PBMA cylinders in PS matrix, for example, cavitation mechanism resulting in

the formation of cellular structures as previously pointed out by Argon et al. was observed (fig 2.18b).

b) Copolymers having alternating glassy and rubbery layers (lamellae)

Several authors have studied the deformation and fracture processes in lamellar block copolymers [121-124]. Fujimura and co-workers studied [122] the deformation of unoriented lamellar SBS triblock copolymer using SAXS and TEM. Stretching the spin cast films having multigrain structure beyond yield point resulted in chevron-like morphology. Chevron-like morphology was characterised by four point small angle scattering pattern [123,124]. The tilt-angle was found to increase unanimously with increasing strain. At moderate strains, the deformation process was discussed in terms of shearing, kinking, and break down of PS lamellae. At very high strains, PS lamellae were fragmented to form a morphology with dispersed PS fragments in PB matrix (plastic-to-rubber transition).

Later, Seguela and Prud'homme investigated hydrogenated version of lamellar SBS block copolymers with TEM and SAXS and also reported the observation of four point SAXS pattern characteristic of chevron-morphology [125]. They proposed that the anisotropic grains of lamellae rotate in response to the applied strain. As the stacking axis (i.e. the long axis) of these grains rotate towards the stretching direction, the lamellae are sheared relative to each other within the grains without appreciable change in their orientation. Yamaoka and Kimura [35] studied injection and compression mouldings of a lamellar SBS star block copolymer and observed the break down of PS lamellae into small fragments. They also observed the microvoid formation in PB phase of the block copolymer.

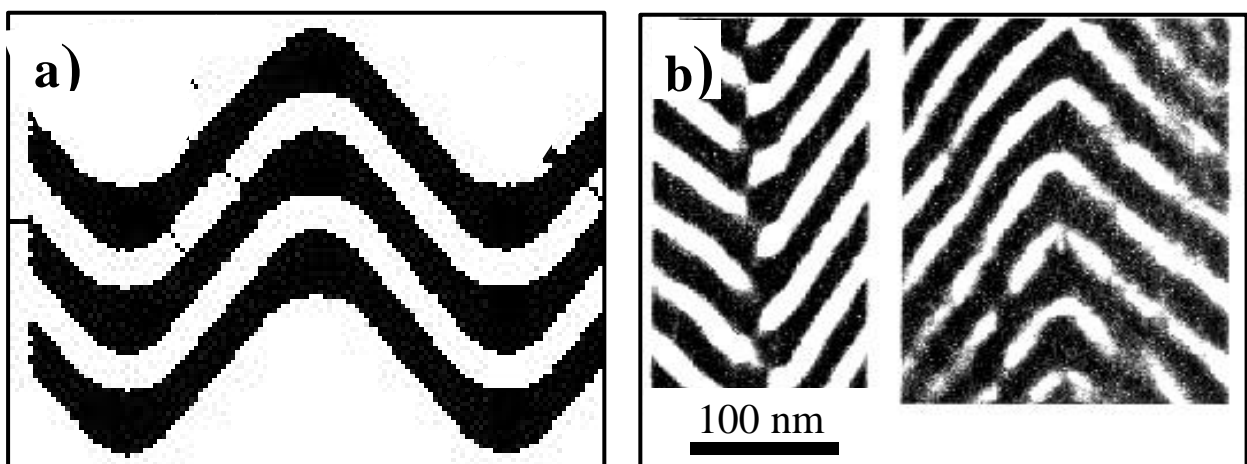


Figure 2.19: Perpendicular deformation of oriented SBS block copolymer: a) scheme showing layer undulation leading to the chevron formation and b) TEM images showing fracture of glassy layers at hinges (left) and Ω -like grain boundary (right) [126].

Recently, Cohen and co-workers have explored systematically the deformation mechanisms in lamellar SBS triblock copolymer using roll cast films. These authors have monitored strain

induced structural changes in nearly single crystal lamellar samples by means of TEM, SFM and SAXS [126-128]. They collected the SAXS patterns for different levels of deformation by loading the sample parallel, perpendicular and diagonal to the lamellar orientation direction. During perpendicular orientation, layer undulation mechanism leading to the formation of chevrons was observed. The undulation of layered structures in response to an extensional force perpendicular to the layers is known in many systems including smectic liquid crystals, sedimentary rocks, predicted in lamellar block copolymers as explained in detail in ref. [128]. Recent analytical studies have shown that there exists a critical undulation instability in a perfectly aligned lamellar block copolymer structure subjected to perpendicular deformation under constrained boundary conditions. This allows a significant part of deformation to be accommodated by shearing of the rubbery layers between the glassy layers. In order to keep the layers parallel to each other, the undulations with large wave lengths are not allowed. Cohen and co-workers further suggest the nucleation of chevron morphology at the regions of local defects (e.g., edge dislocation). The layers in the vicinity of these defects are slightly misaligned, and hence may be the first to respond to the applied stress by rotating their normals away from the strain direction. Opposite rotations of the layers in the vicinity of defects may result in nucleation of kink bands. With increasing strain, the kink bands propagate parallel to the deformation axis into neighbouring layers.

The evolution of four point SAXS patterns is associated with folding of layers into chevron morphology [122-125]. While forming the chevron morphology the layer counter is predominantly in the form of straight 'limbs' and bending of the layers is localised to the 'hinge' regions. The lamellar spacing is found to increase in the 'hinge' regions where the rubbery layers are more dilated than the glassy layers.

At much higher strains (>300%), kink grain boundaries are formed parallel to the deformation direction separating grains which are long in the strain direction but narrow in the lateral direction. Two kinds of kink boundaries were found: one having the continuous PS and PB layers where PB layers are more dilated giving them a "Ω" grain boundary-like appearance and the other one having the layers fractured at the kink boundary (see fig 2.19b, left).

On parallel deformation, the long period of the lamellae was found to decrease right after the yield point indicating the shearing of the layers past one another. Then the lamellar structure was continuously destroyed. The lamellae are broken down into smaller fragments allowing the rubbery phase, now unconstrained by the glassy phase, to undergo a high level of stretching resulting in a large elongation at break. On unloading the sample, lamellae structure was reformed. The lamellar spacing was found to be much smaller than the original values arising from the plastic deformation of PS lamellae.

Sakurai et al. have studied the lamellar orientation in cross-linked SBS polygranular triblock copolymer that was uniaxially drawn at 130°C (above the glass transition temperature of polystyrene) [121]. They observed that in contrast of the formation of herringbone structure in samples drawn at room temperature, the lamellar normal preferentially oriented perpendicular to the stretching direction resulting in parallel array of lamellae aligned in along the stretching direction.

Morphology development in lamellar PS/P2VP diblock copolymers during shear deformation were studied by Winey and co-workers [129,130]. They have interpreted the evolution of 'kink bands' as a result of lamellar rotation at the slip planes. Evidence of lamellar rotation leading to 'kink band' formation was assessed by on-line small angle X-ray scattering (SAXS).

Deformation of lamellar morphology further depends on the glass transition temperatures of the components. Crazing was observed in lamellar diblock and triblock copolymers consisting of PS and P2VP where both the components undergo glass transitions well above room temperature [132]. Extension ratio of craze fibrils λ was found to be always greater if lamellae were oriented perpendicular to the external strain direction: $I_{fibrils\ (perpend)} > I_{fibrils\ (parallel)}$. This observation provided the first direct experimental evidence of stretched chain conformation normal to the phase interface in block copolymers [132].

Morphology and deformation behaviour of PS/PBMA block copolymers with different architectures were widely investigated [131]. The investigations have shown that the phase behaviour of block copolymers has a pronounced influence on deformation mechanisms as well as deformation structures. The disordered block copolymers showed the same deformation mechanism as the corresponding homopolymers while a shift in deformation mechanism was observed at the ODT. It was possible to dictate the deformation behaviour by the strength of segregation, χN . Within the WSL, a cavitation mechanism was observed, while the ISR was associated with deformation mechanisms such as diversion and termination of crazes, craze-tip blunting etc. besides rotation and drawing of lamellae. In this way, a generalised scheme showing a correlation between phase behaviour and deformation mechanisms was presented.

The deformation structures in diblock copolymers are, however, different than those observed in SBS triblock copolymers. In diblock copolymers, the deformation was primarily localised in the form of craze-like bands. Chevron-like morphology and large plastic deformation of glassy lamellae generally observed in SBS lamellar samples were not reported.

c) Deformation of block copolymers having glassy domains in the rubbery matrix

SBS triblock copolymers having PS domains are the most widely investigated systems. Seguela and Prud'homme have studied the deformation behaviour of SBS triblock copolymers having spherical and cylindrical PS domains in the PB matrix using SAXS [133], and they have established the deformation of spherical PS domains to ellipsoids along stress axis. The cylinders were found to align along the external stress direction.

Previously, Pedemonte et al. [134] had investigated the correlation between morphology and tensile properties of cylindrical SBS block copolymer using compression moulded, extruded and solution cast samples. These authors, had already suggested a breaking off of the weaker polystyrene ties as a mechanism responsible for stress softening behaviour. Few years later, Tarasov et al. [135] carried out large strain deformation behaviour of press moulded samples using SAXS. They reported the breakdown of glassy cylinders into long rodlets which remain aligned along the deformation axis when the sample was deformed parallel to the cylinder axis. They also proposed the break down of glassy cylinders into chevron pattern on deforming the sample perpendicular to the cylinder orientation direction. Pakula et al. [136] studied compression moulded cylindrical block copolymer using SAXS and reported the evolution of same final morphology for every kind of orientation of the cylinders with respect to the stretching direction (fig 2.20A). This universal high deformation was also found for the sample having polygranular structure. Investigation of Pakula and co-workers indicated that the high strain deformation of cylindrical block copolymers is controlled by the molecular orientation of the rubbery blocks, while at low strains it is controlled by the initial morphology of the samples. The first detailed evidence of the break down of the glassy cylinders into smaller fragments (formation of rodlets about 70-110 nm long) was provided by the TEM micrographs of an oriented SBS block copolymers published by Odell and Keller [137,138]. They modelled yielding as a progressive breaking of the cylinders into shorter fragments that can bear a higher load. Another model used was the random break model, which provided values for the lengths of the broken rods that are in good agreement with rod lengths measured in TEM images. They calculated the elastic constants of the oriented SBS copolymers and found that the ratio of moduli perpendicular and parallel to the cylinder axis was about 1:100. At moderate strains, the deformation of cylinders parallel to the orientation direction was affine only up to about 3% (yield point) while the deformation in the direction perpendicular to the cylinders was affine up to 20% strain.

The deformation studies on the SBS block copolymers comprising glassy domains in the rubbery matrix have demonstrated that there is a competition between the domain orientation and molecular orientation along the stretching direction. The strain is accommodated primarily in the

soft rubbery matrix with the rubbery chains orienting along the stretching direction. The glassy domains tend to rotate their long axis towards the stretch axis. Since the aspect ratio of the glassy cylinders is exceptionally high (in the range of 1000:1 for a polygranular sample and essentially infinite for single crystals samples), the reorientation process must be highly co-operative, involving whole grains or reorganisation of the cylinders into chevrons.

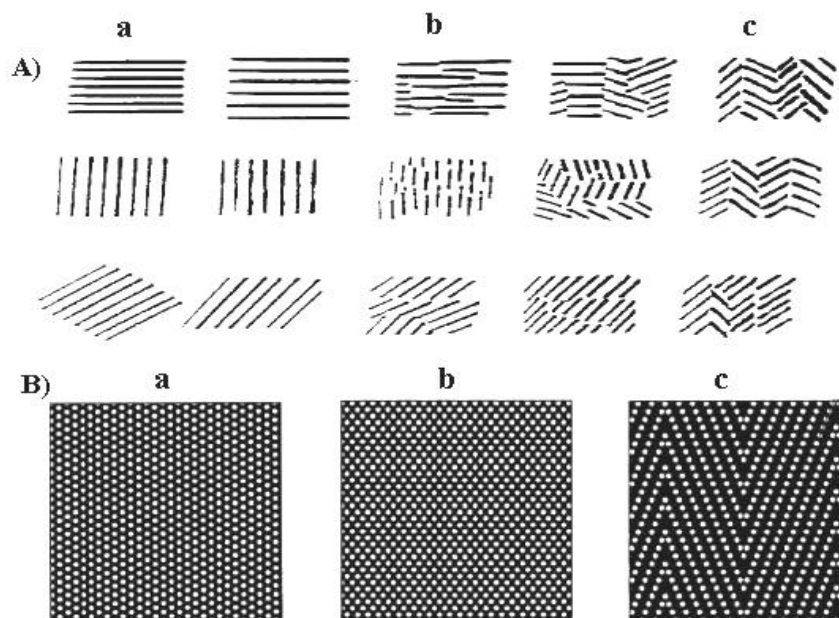


Figure 2.20: Schemes showing deformation mechanisms in cylindrical block copolymers having glassy cylinders in rubbery matrix suggested by Pakula (top, A) [136] and Honeker (bottom, B) [143]. Deformation direction vertical; a, b, and c stand for before deformation, intermediate deformation and high deformation, respectively.

Sakurai and Sakamoto [139,140] investigated the deformation behaviour of symmetrical SBS triblock copolymer by producing solvent induced lamellar, cylindrical and bicontinuous structures. The lamellar morphology led to the highest tensile strength while the cylindrical (PB cylinders) to the least [140].

Recently, perpendicular deformation of nearly single crystal cylindrical SIS block copolymer has been reported by Honeker and co-workers [141-143]. These authors have strained the macroscopically oriented block copolymer films perpendicular to the cylinder orientation direction and monitored the strain induced structural changes in PS cylinders and rubbery matrix by means of TEM [143] and in-situ and SAXS [142]. Since the rubbery block is covalently bonded to the glassy blocks on either side, the deformation of the cylinders have been considered as the markers for the deformation of rubbery phase as well. At small strains (until about 100%) the deformation has been found to be affine i.e., the microscopic change deformation is nearly equivalent to the macroscopic strain of the sample. At higher strains, a transition from affine deformation of rubbery matrix to the kinking of oriented cylinders into a chevron morphology occurs (see fig 2.20B). The kinking instability in which the cylinders are turned to chevron morphology was ascribed to the regions of local misorientation. Post kink deformation involves

a two step shearing plus-dilation mechanism: shearing of the cylinders along the stretching direction (decrease in cylinder spacing) and dilation of the matrix (recovery of the cylinder spacing) [143].

d) Copolymers having complex morphologies

Mechanical properties and deformation behaviour of complex phases are least understood. Even the phase behaviour is not fully explored. The complex phases (viz., gyroid, OBDD, catenoid or mesh and strut structures, HPL etc., reviewed in ref. [2]) are newly discovered. Some of them such as HPL has not been recognised as a stable equilibrium phase. Therefore, there are very few studies concerning the mechanical properties and deformation behaviour of these phases. The first deformation study on HPL and bicontinuous structure was performed in weakly segregated diblock copolymers [96]. These structures were observed in PS/PBMA diblocks at a composition of $\Phi_{PS} = 0.40$ and $\Phi_{PS} = 0.39$, respectively. These samples showed similar stress-strain behaviour as the lamellar samples.

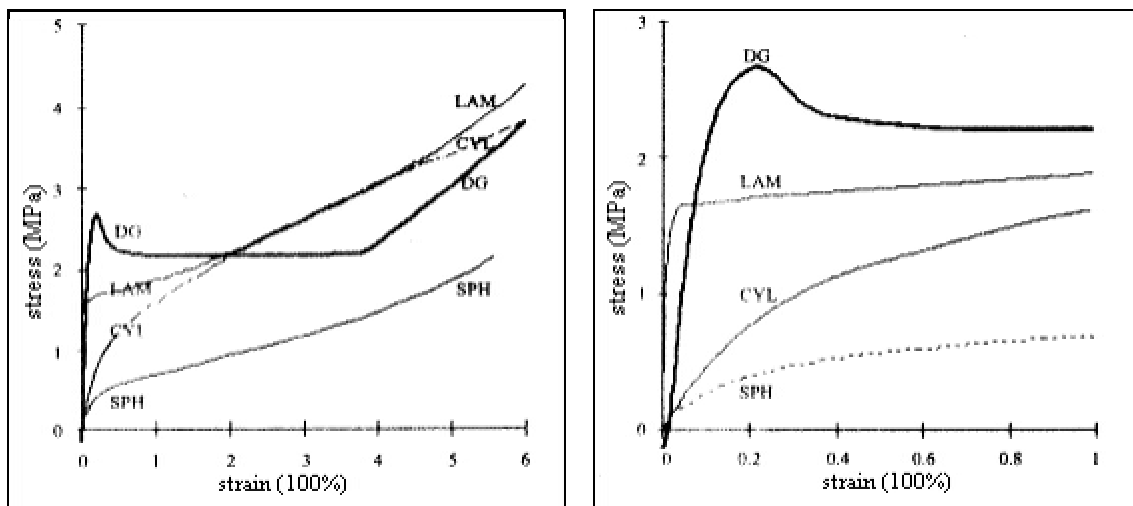


Figure 2.21: Stress-strain behaviour of SIS triblock copolymers having different morphologies: DG double gyroid, LAM lamellae, CYL cylinders (PS) and SPH spherical (PS spheres) [108]

Recently, Dair et al. [108,109] have studied morphology, tensile properties and deformation behaviour of double gyroid (DG) phase in SIS triblock copolymer using both unoriented and oriented roll cast films. They have compared the stress-strain behaviour of solution cast SIS gyroid phase with the SIS samples having other classical morphologies, and have shown that gyroid specimens show a pronounced yielding during tensile testing and attain stress level higher than corresponding lamellar and spherical (PS spheres) SIS block copolymers (fig 2.21). The enhanced mechanical properties of the gyroid morphologies over classical ones are discussed in terms of presence of 3D interpenetrating network of glassy domains in the three dimensionally continuous rubbery matrix. Oriented DG sample showed pronounced anisotropy as in oriented lamellar [126] and cylindrical [143] block copolymers. However, the stress-strain curves of

isotropic polygranular solution cast unoriented film was intermediate between the parallel and perpendicular stretches of the oriented samples, indicating that properties of the DG are not as strongly dependent on the stretching direction as the lamellar [126,127] and cylindrical [141-143] samples. Young's modulus in the [111] direction was found to be approximately five times higher than in the transverse direction. The yielding and plastic flow of PS struts have been suggested as the principal deformation mechanism of the DG phase, where the molecular weight of outer styrene blocks of the SIS triblock copolymer they used was 13.6 kg/mole. However, no microscopic evidence of 'nanonecking' and drawing was provided during the deformation of double gyroid morphology. It should be emphasised that deformation studies of the complex phases is indeed in the stage infancy and should be further explored.

In this section, the deformation mechanisms have been reviewed with special reference to tensile deformation of styrene/diene block copolymers at room temperature.

It has been, however, pointed out that the deformation mechanisms may vary with extent of segregation χ_N , kinds of monomers etc. In fact, temperature and strain rates may play a decisive role in determining the deformation. For example, a block copolymer consisting of only glassy components may show crazing at room temperature irrespective of the microphase separated morphology they possess.

e) Deformation of block copolymer/homopolymer blends

Though a great deal of works have been devoted to the deformation behaviour of ternary blends containing two homopolymers and a block copolymer compatibiliser (*which is outside the scope of this work*), only limited investigations are made on binary block copolymer/homopolymer blends and binary block copolymer blends. Micromechanical behaviour of styrene/butadiene block copolymer/polystyrene blends was discussed by Argon and co-workers [112] and Aggarwal [62]. In both the cases role of block copolymer as impact modifier was analysed. Block copolymer particles dispersed in the PS matrix were able to both initiate and terminate the crazes. Aggarwal has even argued the superior mechanical properties of block copolymer modified PS than the conventional rubber modified one.

Yamaoka studied intensively the morphology and mechanical properties of blends consisting of styrene/butadiene star block copolymer and a statistical copolymer of methyl methacrylate and styrene (MS) [144-146]. At a MS content of about 20 wt %, a maximum in Izod impact toughness was observed when the particles had a diameter of 300-500 nm. Hashimoto and co-workers investigated morphology and strain induced structural changes in blends consisting of SBS triblock copolymers and polystyrene [123,147]. Particularly, the healing of deformed domain structures on annealing was investigated. Determining the strain induced structural changes in SBS triblock copolymer/homopolymer blends, they demonstrated the hindrance of

healing process by added homopolymers. Till the date, almost no references are available on micromechanical behaviour of binary block copolymer blends.

2.4.5 Molecular Architecture vs. Micromechanics

As discussed above, there exists an inherent relationship between the molecular parameters (chain architecture, nature of interface, chain topology etc.), phase behaviour, and mechanical as well as micromechanical behaviour of block copolymers (illustrated in fig 2.22), where the dimension of structural variables vary from molecular to microscopic and macroscopic level from top to bottom.

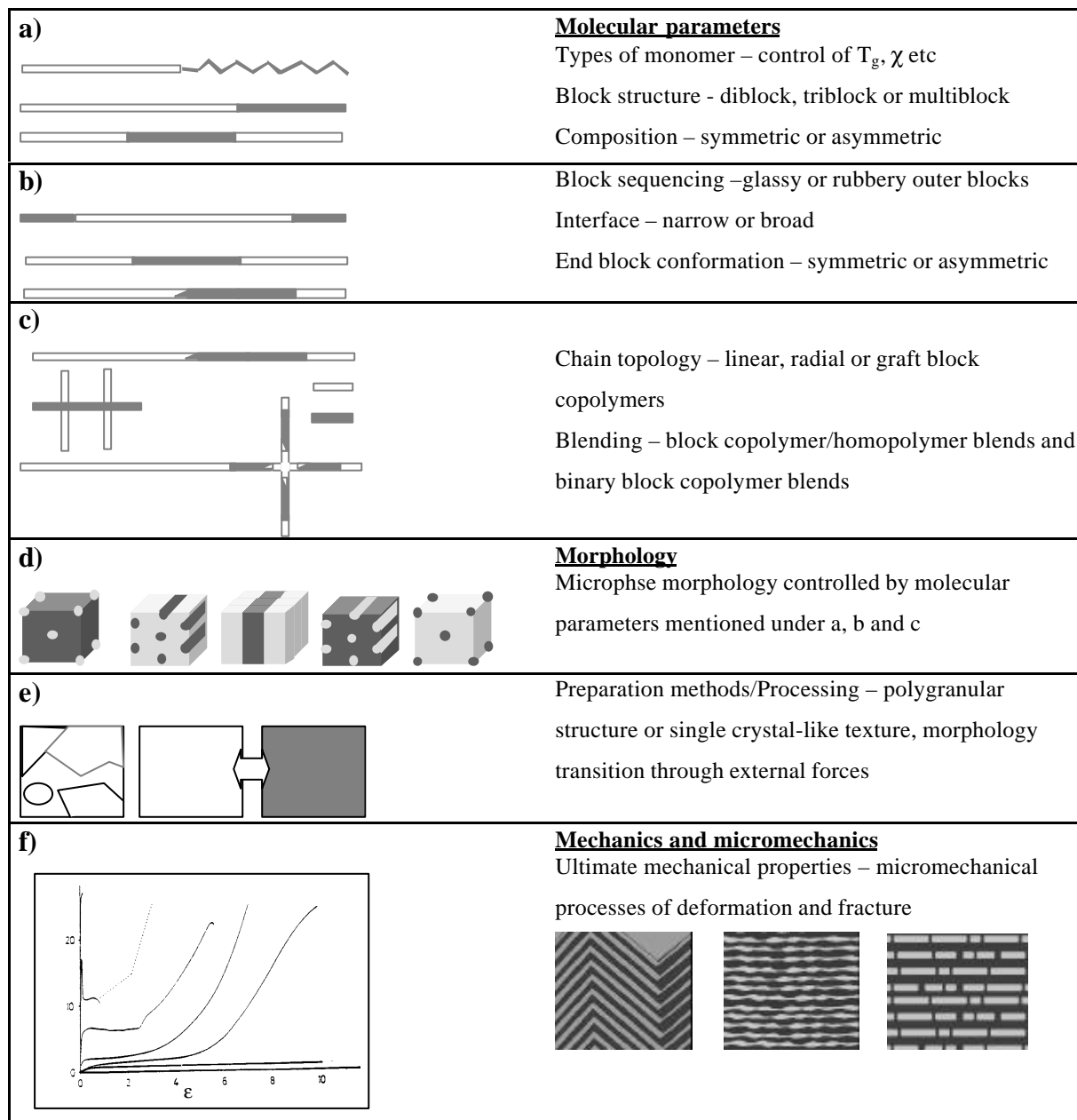


Figure 2.22: Scheme showing the correlation between molecular parameters, morphology and mechanical properties of block copolymer.

Mechanical behaviour of these materials may be mainly dictated in terms of microphase separated structures, their size and orientation, grain size etc. The morphology control, which

forms an important aspect of applied block copolymer engineering, is supplemented by blending with other block copolymers and homopolymers. Finally, these structures are optimised by adjusting the processing conditions. The response of these structures towards external force is coupled with the architecture of the molecules under consideration. This is evidenced by different deformation behaviour exhibited by SB diblock and SBS triblock copolymers. Symmetry of end blocks and placement of glassy block(s) in the molecular backbone further plays a decisive role in the mechanical behaviour of the copolymer. For example, SBS triblock copolymers become tougher when styrene outer blocks are made more and more asymmetric [52]. What kinds of monomers are chosen as the block chains determines the extent of chemical incompatibility and hence the degree of segregation. The latter has an important influence on phase behaviour of the block copolymer to be produced. Further, it determines the T_g of the phases that decides the upper and lower service temperature of the final products. Poly(methyl styrene-*b*-butadiene-*b*-methyl styrene) TPEs, for example, have higher upper service temperature than styrene/diene block copolymers [68,69].

To achieve a satisfactory level of mechanical properties in styrene/diene block copolymers, the terminal PS blocks must exceed a critical molecular weight so that strong physical cross-links may be formed which held the glassy chains firmly in PS domains. The minimum length of PS sequence required for a good phase separation depends on the nature of diene middle block. The molecular weight should be optimised due to rheological reasons as well [52]. Overall molecular weight of the copolymer and molecular weight distribution (monomodal, multimodal etc.) should be optimised to achieve desired deformability and processability.

Mechanical behaviour of the block copolymers may be strongly influenced by the speciality of molecular architecture. Star block copolymers have been found, for example, to possess preferred rheological and mechanical properties compared to their linear analogues and less sensitive to diblock contamination. Graft copolymers offer new possibilities of fine-tuning mechanical properties, but the probability of deterioration of mechanical properties due to presence of undesirable rubbery end blocks should be taken into account [68].

In spite of a lot of works on the phase behaviour of simple linear block copolymers, the attention paid to their structure-property correlation seems to be still insufficient. With development of more complex molecular architectures, complexities have been introduced in their phase behaviour and structure-property correlation, as well. A systematic study of correlation between morphology, mechanical properties and deformation mechanisms with respect to these complex architectures (schematically proposed in fig 2.22) is yet to be explored and will be an important aim of this thesis.

3. EXPERIMENTAL PART

3.1 Materials

3.1.1 Pure Block Copolymers

Characteristics of the block copolymers covered in this work are listed in table 3.1. Samples were prepared by solution casting, compression moulding, injection moulding and extrusion. (results and discussion in chapter 4).

Table 3.1 Characteristic of investigated block copolymer samples

sample designation	** M_n (g/mole)	M_w/M_n	* Φ_{ST}	remarks
ST1-S74	91,800	1.99	0.74	sharp transition, PB core, asymmetric SB arm
ST2-S74	109,200	1.69	0.74	tapered transition, PS core, asymmetric SBS arm
LN1-S74	82,000	1.07	0.74	sharp transition, symmetric PS end blocks
LN2-S74	93,000	1.13	0.74	tapered transition, asymmetric PS end blocks
LN4-S65	116,000	1.20	0.65	random S/B middle block, symmetric PS end blocks

ST – star block; LN – linear block copolymer; * total volume fraction of styrene determined by double bonds titration using the Wijs method; ** determined by GPC using PS calibration.

3.1.2 Block Copolymer/Homopolystyrene (hPS) Blends

Blends of ST2-S74 (and LN2-S74) with hPS were prepared with weight ratios 80/20, 60/40, 40/60 and 20/80 by solution casting and injection moulding. Characteristic data of polystyrene samples used in blending are listed in table 3.2 (results and discussion in chapter 5).

Table 3.2: Characteristic of polystyrene samples used to prepare blends with ST2 and LN2

samples	M_n (g/mole)	M_w (g/mole)	M_w/M_n	preparation
PS015	11,800	15,200	1.29	radical polymerisation
PS033	18,300	33,100	1.81	"
PS190	82,600	190,000	2.30	"

3.1.3 Binary Block Copolymer Blends

Binary blends of star block copolymer ST2-S74 and LN4-S65 are prepared by solution casting as well as injection moulding with weight ratios 80/20, 60/40, 40/60 and 20/80. (results and discussion in chapter 6).

3.1.4 Synthesis of Block Copolymers

The block copolymer samples used in this study were provided by the BASF. Details about synthesis of styrene/butadiene block copolymers can be found elsewhere [42-44,52,63,155,156]. A brief account of synthesis of such block copolymers via living anionic polymerization shall be

presented taking example of alkyllithium (e.g., *sec*-BuLi) initiated sequential polymerisation of styrene and butadiene using an inert hydrocarbon solvent such as cyclohexane or toluene.

It is necessary to rigorously exclude oxygen, water or any other impurities that may react with the highly active propagating species so that the molecular weight of the polymer blocks can be precisely controlled. The anionic polymerization comprises the following three steps:

- Chain initiation by an initiator (e.g., organolithium compounds such as *sec*-butyllithium, BuLi) leading to the formation of a “living” anion,
- Propagation of the living chain by sequential addition of monomers and
- Termination of living chain

a. Initiation reaction

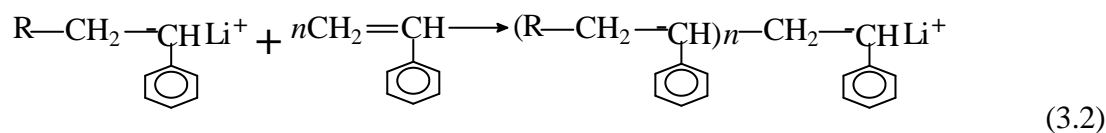
The initiator R^-Li^+ first reacts with a molecule of styrene monomer to form a reactive species. The rate of initiation reaction is high compared to the subsequent chain propagation which insures the narrow molecular weight distribution of the blocks.



b. Chain propagation reaction

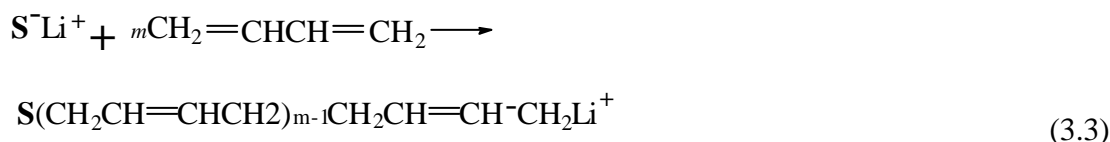
i. First styrene outer block

The next step is to join more styrene monomers to the reactive species (propagation of the chain) leading to the formation of poly(styryl) lithium (S^-Li^+) which is also an anion.



ii. Butadiene block

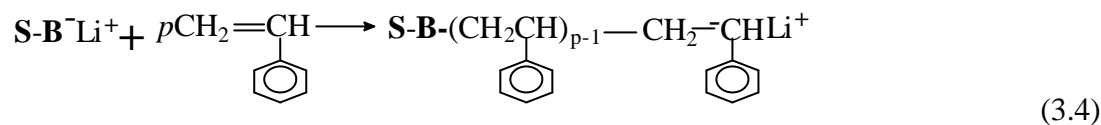
The end product propagation step S^-Li^+ can initiate further polymerisation. Hence butadiene block may be added to the living styrene block. The polymerisation of butadiene chain via 1,4-addition may be represented as:



iii. Second styrene block

The end product of above step designated as $S-B^-Li^+$ can again act as initiator for another styrene outer block. The rate of initiation of styrene polymerisation by $S-B^-Li^+$ is slow compared to subsequent propagation reaction. This may lead to the wide molecular weight distribution of the

final styrene block of resulting SBS triblock copolymer. The problem can be avoided by addition of solvating agents like ethers just before the styrene monomer is added.



c. Termination reaction

When the last reaction is complete, the reaction can be terminated by the addition of a protonating agent such as an alcohol.

ABA triblock copolymers and the molecular architectures derived therefrom are the most important styrenic block copolymers, where A and B stand for polystyrene and polydienes (polybutadiene or polyisoprene) respectively. Generally, these block copolymers are synthesised by adopting following three routes.

i. *Three-step Method Using Monofunctional Initiator*

The *sec*-BuLi initiated sequential polymerisation of styrene and butadiene blocks as discussed above allows the preparation of ABA triblock copolymers with well defined block length. Both symmetric and asymmetric PS end blocks can be prepared by adjusting the number of monomers being added to corresponding block.

This method also allows the preparation of tapered triblock copolymers when a mixture of styrene and diene is added to the reaction mixture after the completion of first styrene block. In this case, due to higher reaction rate of diene monomers over the styrene monomers polybutadiene chain is preferentially constructed allowing a gradual addition of styrene monomers. This leads to a gradual variation of composition along the chain backbone at the interfacial region (tapered transition).

ii. *Two-step Method Using Bifunctional Initiator*

This method requires a bifunctional initiator which allows the formation of middle diene block by dianionic polymerization. The diene chain has, therefore, two living ends which can cross over slowly with the styrene end blocks. This method is especially useful in the case of unidirectional block copolymerization, i.e., when the living B block initiates A block and not vice versa.

iii. *Two-step Method Using Monofunctional Initiator*

Formation of an ABA triblock copolymer by coupling two living AB diblocks at B requires in addition to the monofunctional initiator a suitable linking agent like dihalide or ester to join the lithium chain ends of the diblocks. This method has the advantage of monomer addition only for

two times as in the bifunctional initiation, thereby reducing the problem of introduction of impurities. The biggest difficulty lies in the fact that one should exactly adjust the ratio of linking agent to the chain end concentration. Any deviation from exact stoichiometry leading to the formation of free diblocks has a dramatic effect on the strength of material.

Star Block Copolymers

Several methods are employed to prepare symmetric star block copolymers. The “core first” method uses a multifunctional initiator to start the anionic polymerization, and the desired monomers are sequentially added. The “core last” method comprises the coupling of living diblocks or multiblocks using an oligofunctional linking agent. Initiating the outer blocks (generally the PS block) at various intervals after the begin of the polymerization in the same system star block copolymers of asymmetric block conformation may be synthesized.

3.2 Sample Preparation

3.2.1 *Solution Casting*

About 0.5 mm thick films of the samples were prepared by solution casting. The samples were dissolved in toluene to prepare an about 3% (w/v) solution and the solvent was evaporated over a period of two weeks to allow the formation of well ordered equilibrium structures. The films were dried at room temperature for several days and vacuum-annealed for 48 hours. Thin films for SFM studies were cast onto a freshly cleaved mica surface.

3.2.2 *Injection and Compression Moulding*

For injection moulding, the melt at 225°C was injected into a mould maintained at a temperature of 45°C to rapidly cool it. Compression moulding was performed using the following program: ca.1 min melted at 190°C, 5 min pressed at a pressure of 50-200 bar. Finally the plates were cooled for 3 minutes at a pressure of 200 bar. Tensile bars were prepared by cutting the plates using a suitable form.

3.2.3 *Extrusion*

0.5 mm thick and 100 mm wide sheets of block copolymer samples were extruded using a laboratory extruder at a temperature range 170-190°C.

3.3 Mechanical Properties

Mechanical behaviour of the samples was characterised by uniaxial tensile testing and fracture mechanics method.

3.3.1 Tensile Testing

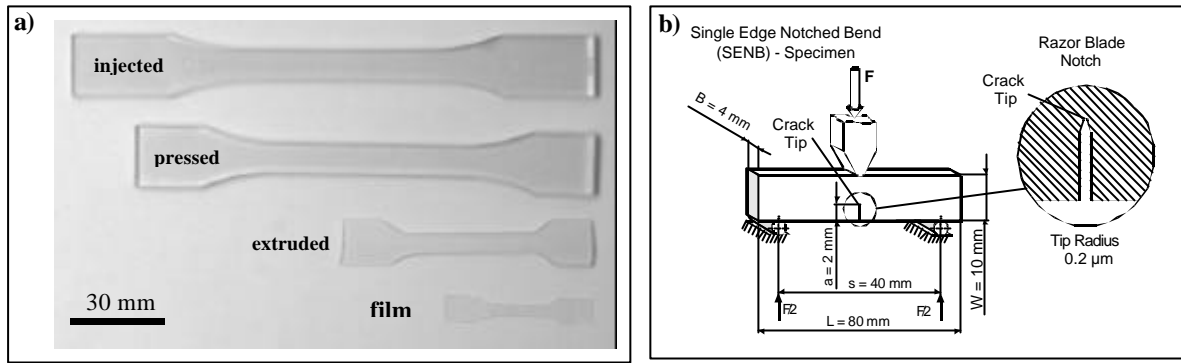


Figure 3.1 a) Light microscopic pictures of the tensile bars showing their relative size and b) Schematic showing three-point bend test specimens used for fracture mechanics measurements

Tensile tests were performed using a universal testing machine (Zwick 1425 and Instron 4507) at variable cross head speeds and temperature according to ISO 3167 and ISO 527. At least 10 samples were measured in order to prevent preparation artefacts and to get a good statistics of data. Relative size of the tensile specimens is shown in figure 3.1a. The main objective of this test is to have a comparative insight into the mechanical behaviour of the investigated samples. Stress-strain curves were recorded using following equations for the calculation of stress (σ) and strain (ϵ). The modulus of elasticity (Young's modulus) was determined by the slope of initial portion of stress-strain curves.

$$\text{stress, } \mathbf{s} = \frac{F}{A} \quad (3.5)$$

where F and A stand for the load experienced by the specimen in Newtons and initial cross section of the specimen in mm^2 , respectively.

$$\text{Strain, } \mathbf{e} = \frac{L - L_0}{L_0} \cdot 100\% = \frac{\Delta L}{L_0} \cdot 100\% \quad (3.6)$$

where ΔL is the change in the length of the specimen relative to the initial test length L_0 .

3.3.2 Fracture Mechanics

a. Determination of fracture mechanics parameters

In order to quantify the toughness behavior of the samples, an instrumented Charpy impact tester of 4J total work capacity was used. The single edge notched bend (SENB) specimens according to the norms of ISO 179 have the following dimension: length $L = 80$ mm, width $W = 10$ mm and thickness $B = 4$ mm (fig 3.1b). The specimens are notched with a razor blade (notch tip radius = ca. $0.13 \mu\text{m}$). For the measurement of fracture mechanics parameters as resistance against unstable and stable crack growth, the initial crack length of 2 mm and 4.5 mm, respectively were cut at the middle of the specimens through their thickness [149]. To minimize the specimen vibration, the span length was set to 40 mm, and the pendulum hammer speed at

strike was 1m/s. The determination of Young's modulus and yield strength under impact loading conditions as well as the fracture mechanics parameters as resistance against unstable crack initiation was carried out using the procedures described in ref. [149]. The J-values enable, on the basis of energetical definition of J-integral, the quantification of energy dissipation during the process of crack growth while the critical crack-tip opening displacement (CTOD, δ_{dk})-values takes into account the deformation of polymeric materials close to the crack tip. The δ -values are determined on the basis of plastic hinge model where the maximum deflection f_{max} is substituted by notch contribution of the deflection.

b. Determination of crack resistance (R-) curves

Toughness of binary block copolymer blends as resistance against stable crack initiation and growth was characterized by means of crack resistance (R-) concept of elastic-plastic fracture mechanics.

Crack resistance curves (R-Curves) represent the functional dependence of loading parameters (J-integral or δ) with the stable crack growth Δa . These curves makes it possible to derive the fracture mechanics parameters as resistance against stable crack initiation and propagation.

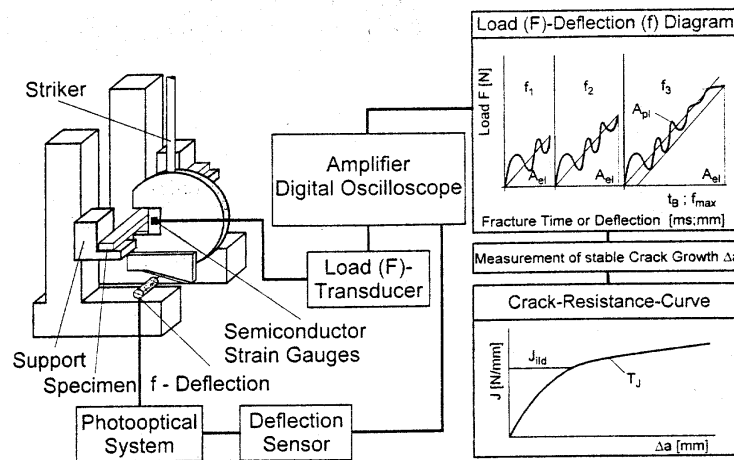


Figure 3.2: Instrumentation of stop-block method for the determination of R-curves via multi-specimens technique.

R-curves can be obtained by loading the specimens in such a way that the stable cracks having different lengths are formed. A special experimental technique is needed to record the dynamic crack resistance curves, which make it possible to supply different energy values to the specimens. Among various experimental methods of R-curves determination, the multi-specimen method in the stop-block-technique (see fig 3.2) has been found especially suitable for polymeric materials [149,150]

The J-values determined by using equation (3.7) [149-151], which is suggested for the determination of R-curves in polymers, are found to be in excellent agreement with that calculated by an iterative approach [150,151]:

$$J = \mathbf{h}_{el} \frac{A_{el}}{B(W-a)} + \mathbf{h}_{pl} \frac{A_{pl}}{B(W-a)} \left(1 - \frac{(0.75\mathbf{h}_{el} - 1)\Delta a}{W-a} \right) \quad (3.7)$$

where A_{el} and A_{pl} are elastic and plastic part of total deformation energy while η_{el} and η_{pl} represent the corresponding correction factors [149]. The letters W, B and a stand for specimen width, thickness and the notch depth respectively. Because J-integral is, exactly speaking, defined only for the stationary crack, it is necessary to introduce a correction factor for a growing crack, to allow the consideration of a finite crack propagation Δa and effect of instationary stress field ahead the crack tip. In this way, as shown in ref. [150], the requirement of limitation of stable-crack-growth-contribution formulated in the Standard draft ESIS TC4 protocol [148], should be considered. The discussions on specimen geometry and test of geometry-independence of the fracture mechanics parameters derived from the R-curves, like parameters as resistance against stable crack initiation, can be found elsewhere [149,150,152,153]. Further details on determination and evaluation of R-curves under impact loading conditions are discussed in [149].

3.4 Microscopic Techniques

Different microscopic techniques (scanning electron microscopy SEM, transmission electron microscopy TEM, high voltage electron microscopy, HVEM and scanning force microscopy, SFM) were used to investigate morphology and deformation behaviour of the samples. Detailed references on different microscopic techniques may be found in [154].

3.4.1 Electron Microscopy

Scanning electron microscope (SEM, Jeol) was used to study the fracture surfaces of the samples broken in tensile as well as impact tests. The fracture surfaces were sputtered with about 10 nm thick gold film prior to the SEM investigations.

Microstructures of the samples were studied by transmission electron microscope (100 kV TEM, Jeol and BS 500). For TEM studies, ultra-thin sections (ca. 70 nm thickness) were cut from a block of the bulk sample immersed for several days in aqueous osmium tetroxide (OsO_4) solution in order to selectively stain butadiene phase of the styrene/butadiene block copolymers. To complement the deformation behaviour of few selected samples, semi-thin sections (ca. 500 nm) were studied using high voltage electron microscope (1000 kV Joel HVEM). The semi-thin

sections were strained in a special tensile device to a certain strain and fixed in the strained state. The sections were stained by OsO₄ prior to the HVEM investigations.

3.4.2 Scanning Force Microscopy

For comparable study of morphology and deformation structures of the samples, scanning force microscope (SFM, Multimode, Digital Instruments) was used. The microscope was operated in tapping mode at room temperature. The samples were microtomed at a temperature of -120°C to prepare a fresh surface, and the cut face was scanned using a silicon cantilever (resonant frequency 300- 400 kHz and spring constant 15 N/m). Thin films were directly imaged without further preparation.

3.5 Additional Characterisation Methods

3.5.1 Thermomechanical Properties and Glass Transitions

Dynamic mechanical analysis (DMA) was employed to characterise thermomechanical properties and primary glass transitions in block copolymers using DMTA Mark 3E (Rheometric Scientific) in torsion and temperature sweep mode. The measurements were performed with a frequency of 1 Hz, at a temperature range from -120°C to 120°C and at heating rate of 1 °C/min. Test specimens cut from compression moulded plaques had the dimensions 30 mm×10 mm×2 mm. Additionally, differential scanning calorimetry (DSC) measurements were carried out to locate the glass transition temperature of component blocks using Mettler DSC 820 in the temperature range from -120 °C to 150 °C with a rate of 10 °C/min using the cycle heating – cooling – heating. The heat flow and the second derivative of the heating scans are used for the analysis of the glass temperature. The weight of each sample was approximately 10 mg.

3.5.2 Determination of Molecular Weight and Composition

Molecular weight of the samples were determined by gas permeation chromatography (GPC) using tetrahydrofuran (THF) as solvent using PS calibration. Volume fraction of styrene and butadiene in block copolymers were determined by double bonds titration using the Wijs method. The results of these investigations were provided by the BASF.

4. STRUCTURE-PROPERTY CORRELATIONS IN DIFFERENT BLOCK COPOLYMER ARCHITECTURES

4.1 Phase Behaviour and Morphology

4.1.1 Correlation Between Molecular Architecture and Phase Behaviour

Molecular architecture of the styrene/butadiene block copolymers studied here is schematically outlined in fig 4.1 (detail molecular parameters in table 3.1). The total styrene volume fraction of the samples is between 0.65 and 0.74. The linear copolymer LN1, a neat SBS triblock, has symmetric styrene end blocks separated from butadiene centre block by a sharp interface. Sample LN2, in contrast, has a tapered transition (shown by an oblique line between PB and PS blocks), and comprises asymmetric PS end blocks, the larger block being about 4-5 times longer than the shorter one. The molecular weight of longer polystyrene block is in the range of 50,000-70,000 g/mole. Sample LN4 consists of short PS end blocks ($M_n \sim 18,000$ g/mole) connected by a rubbery block made up of a random styrene/butadiene copolymer. The styrene volume fraction of the hard block is about 0.32.

sample	molecular structure	morphology
LN1-S74		
LN2-S74		
LN4-S65		
ST1-S74		
ST2-S74		

Figure 4.1: Molecular architectures of the block copolymers studied; Sxx indicates the volume fraction of styrene in the block copolymers. The oblique line between the blocks stand for a tapered transition; white and black colours stand for styrene and butadiene phases, respectively.

The star molecules have about four asymmetric arms, one of them being much longer than the others whose molecular weight ranges from 60,000 to 90,000g/mole. ST1 is a neat block copolymer (sharp interface) while ST2 is a tapered one with a wide interface between centre

butadiene block and styrene core. The diverse molecular architecture (chain topology, block asymmetry, nature of interface etc.) of these block copolymers leads to remarkably different phase behaviour and mechanical properties as discussed below.

Dynamic mechanical analysis (DMA) of the block copolymers (fig 4.2a,b) gives an important insight into their phase behaviour. The shift of glass transition temperature of the components relative to that of the corresponding homopolymers may provide valuable information on the miscibility of the constituent blocks. In spite of equivalent chemical composition the samples (except LN4 which contains 65 vol. % styrene) exhibit an appreciably different behaviour in DMA plots. Especially noteworthy is the shift in glass transition temperature of butadiene phase T_{g-PB} . The glass transition temperatures of respective block copolymers is determined by the location of loss-tangent peak ($\tan \delta = G''/G'$) in DMA spectra. The neat linear triblock copolymer LN1 has a T_{g-PB} and T_{g-PS} at -98°C and 102°C that correspond to the glass transition temperatures of polybutadiene and polystyrene homopolymers, respectively. This behaviour would be expected from the chemical incompatibility between PS and PB, which are separated by a fairly sharp interface (strong segregation). In other samples, the T_{g-PS} remains more or less constant but T_{g-PB} is shifted towards substantially higher temperatures in the following order: ST1 (-76°C), ST2 (-73°C), LN2 (-44°C) and LN4 (-17°C). The shifts in T_{g-PB} of the block copolymers is also supported by DSC measurements (Appendix 4.1). A significant shift in T_{g-PB} towards higher temperatures implies that a considerable amount of styrene units having bulky pendant groups is mixed to the butadiene phase. Styrene units mixed to the butadiene phase hinder the mobility of flexible polybutadiene phase increasing its glass transition temperature.

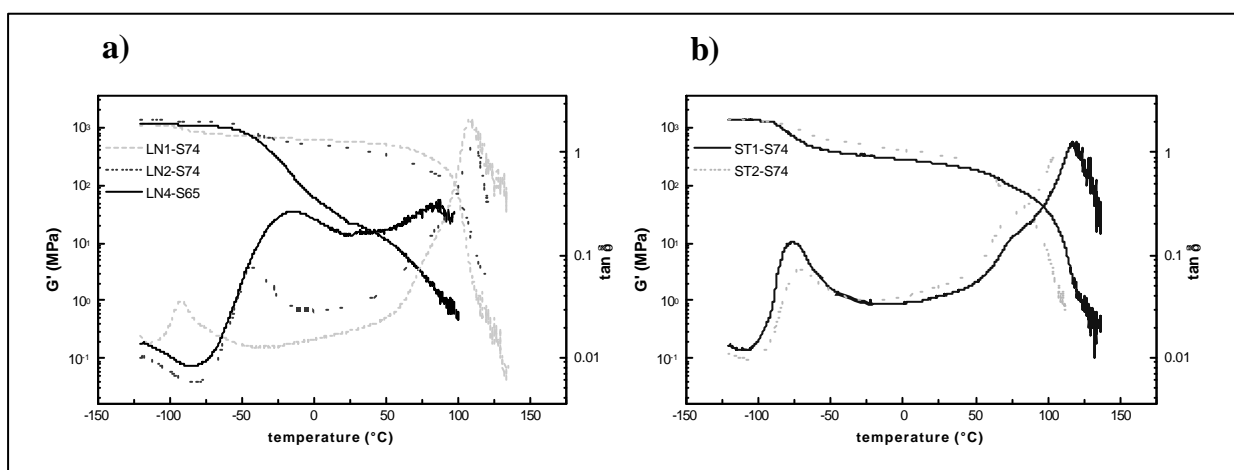


Figure 4.2: Dynamic mechanical spectra of different block copolymer showing storage elastic modulus (G') and loss tangent ($\tan \delta$); a) triblock copolymers b) star block copolymers.

Furthermore, the tapered interface between PB and PS blocks in LN2 and ST2, as shown by an oblique line between the dissimilar blocks in figure 4.1, results in the situation that a part of stiff styrene segments is trapped in butadiene phase. These segments further contribute to cause an

increase in T_{g-PB} . The tapered sequence behaves mostly as a styrene-butadiene-rubber (SBR) and practically belongs to the rubbery phase. It follows, hence, that the effective volume fraction of the soft phase would be increased in the tapered block copolymers. Larger shift in T_{g-PB} in LN2 compared to that of ST2 indicates the presence of relatively longer tapered chain in the former.

The molecules of LN2, ST1 and ST2 are highly asymmetric (i.e., the molecules contain unequal PS end blocks). Molecular weight of the shorter PS chains in LN2 is around 12,000 g/mole, and it is still lower in the star block copolymers. These shorter chains may be partly pulled into the PB domains as suggested recently by Matsen [54] for asymmetric ABA triblock copolymers (to be discussed later in fig 2.8). This explains the massive increase in T_{g-PB} in the LN2, ST1 and ST2. It may further provide reason for an additional glass peak observed at about 75°C in ST1, ST2 and LN2, which may be assigned to the relaxation of short PS chains partly mixed to the butadiene phase leading to an increase in T_{g-PB} .

Fox and Flory have suggested an empirical equation to explain the molecular weight dependence of glass transition temperature (T_g) of polystyrene (from p. 353 of ref. [7]):

$$T_g = 106^\circ\text{C} - \frac{1.8 \times 10^5}{M_n}, \text{ where } M_n \text{ is number average molecular weight of the polymer.}$$

Using this equation, a number average molecular weight (M_n) of 7,200 g/mole may be calculated for polystyrene chains having a glass transition temperature of 75°C (fig 4.3). This polystyrene chain length is close to the molecular weight range of short polystyrene chains present in LN2, ST1 and ST2. It is particularly noteworthy that this additional T_{g-PS} peak is very pronounced in sample ST2 implying the presence of an additional PS phase (i.e., PS domains embedded in PB lamellae) that would explain the existence of “two-component three-phase” morphology of this sample to be discussed later. But a separate PS phase has not been detected in samples ST1 and LN2 by microscopic techniques.

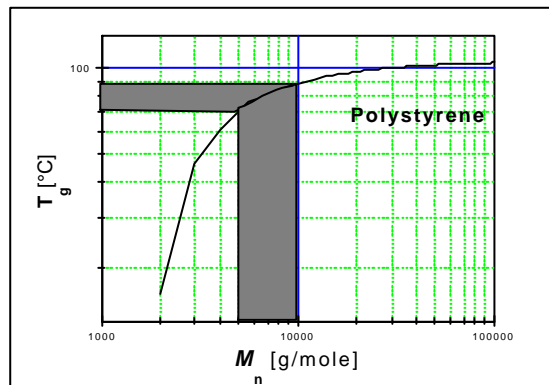


Figure 4.3: Plot of Fox's equation for PS; the shaded area shows the range of molecular weight and corresponding glass transition temperature of short polystyrene chains contained by the block copolymers LN1, ST1 and ST2.

DMA plots in fig 4.2a shows that glass transition temperature of butadiene phase is most significantly shifted in LN4. A glass temperature of -17°C (the soft phase in LN4) is almost

intermediate between the glass transition temperature of pure polystyrene and polybutadiene homopolymers. Thus, glass transition at -17°C results from the random copolymer centre block in LN4.

In the tapered block copolymers, in which the composition at the interface does not suddenly change, the interfacial width may increase due to enhanced phase mixing. The same is true in case of block copolymers having PS domains held fixed by random S/B copolymer (for instance LN4) chains. In such cases, the whole system can be driven towards the order-disorder transition (ODT), and a weak segregation behaviour may be observed [41,59]. This phenomenon may have important consequences in the mechanical properties of the block copolymers.

Analysis of DMA spectra, especially the size of plateau modulus and level of the loss tangent ($\tan\delta$), further allows to draw qualitative inferences about the interfacial width of the block copolymers. Here, this aspect is illustrated taking linear block copolymers as example. The modulus level in the rubbery plateau region, which primarily depends on the hard block (i.e., polystyrene) concentration, is the highest and flattest for LN1 and decreases in the order: LN1, LN2, LN4. This suggests that the extent to which pure phases are formed decreases in the same order. In other words, LN1 forms the 'purest phases' and has smallest mixed phase volume or narrowest interface. Hence, the interface width increases from LN1 to LN2 to LN4. Since the material at the interface will have transitions between those for pure PS and pure PB, the level of $\tan\delta$ in the rubbery plateau region will be increased by interfacial volume [157]. This reiterates that the interfacial volume and the interfacial width increase in the order: LN1, LN2, and LN4.

4.1.2 *Equilibrium Morphologies*

Microphase separated structures of the block copolymers examined by TEM and SFM are compared in figs 4.4 and 4.5. Since the phase detection in tapping mode SFM is sensitive to the material heterogeneity, phase signals can be used to identify different phases in the multiphase polymeric materials [158-161]. It has been demonstrated that the contrast in tapping mode phase images changes with the force used (i.e. the ratio of applied set point relative to that of the free oscillation) [159,160]. Under low or moderate tapping forces, the brighter and darker phase signals in SFM images correspond to the higher and lower modulus phases, respectively [159]. Since the SFM images are collected under moderate force, the brighter phase signals should correspond to the hard phase (PS in this case) and so on.

Interpretation of SFM phase signals in styrene/butadiene block copolymers is discussed in recent publication [66,158]. Since the butadiene phase has been selectively stained with OsO_4 for TEM imaging, white and dark regions in TEM images stand for PS and PB, respectively. As evident from fig 4.4, sample LN1 has a cylindrical morphology with hexagonal PB cylinders in PS

matrix as expected from its net chemical composition [2,11,14]. The cylinders are partly parallel and partly orthogonal to the plane of micrographs. The long period of the PB domains as measured in Fourier transformed images is given in table 4.1.

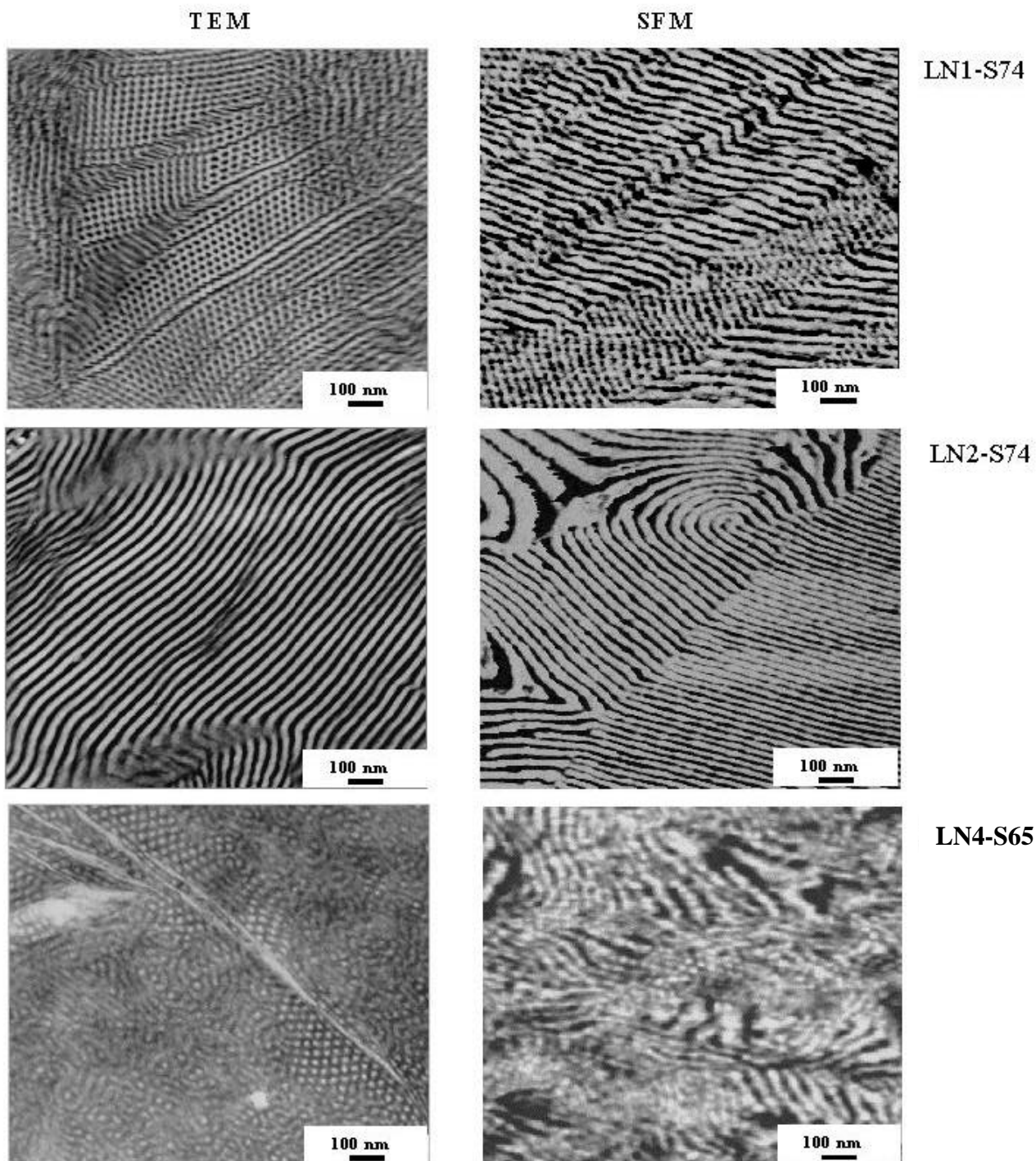


Figure 4.4: Representative TEM (left) and SFM phase (right) images of triblock copolymers; characteristic dimensions of the microdomains are given in table 4.1.

LN2 shows, in contrast, a lamellar arrangement of alternating layers of PS and PB despite its composition identical to that of LN1. The molecular structure of LN2 should be responsible for the appearance of “finger print pattern” characteristic of lamellar morphology rather than a

cylindrical one. Flat-on as well as edge-on views of lamellae are clearly demonstrated by the SFM micrographs. For the evolution of lamellar structure, however, the effective volume fraction of the component must be more or less symmetric [14]. This is only possible if a part of polystyrene (or styrene segments) is mixed in the PB phase and practically belongs to the soft phase.

First, this block copolymer has asymmetric PS end blocks, the shorter ones having a molecular weight in the range of 12,000 g/mole. A part of these short PS chains may be mixed to the PB phase leading to an increase in T_{g-PB} as discussed in previous section. Since PS chains with molecular weight of about 10,000g/mole is sufficient for the formation of its own domains in linear SB block copolymers [43,68], a major part of the shorter PS arms is expected to phase segregate to form lamellae. The stretching energy of a bidisperse polymer brush (e.g., A block in asymmetric ABA triblock) is known to be less than that of a monodisperse one (e.g., symmetric ABA triblock). Hence, polystyrene has lower stretching energy in asymmetric SBS triblock copolymer than that in symmetric one. The stretching energy will be balanced, as suggested recently by Matsen, if a part of short PS chains are dragged into the PB domains which results in a decrease in stretching energy of PB domains [54]. Styrene units present in the tapered chain (indicated by oblique lines in fig 4.1) are the another candidates to be fully mixed with PB phase. Both of these effects would contribute to reduce the effective volume fraction of polystyrene to such an extent that the whole system is driven towards compositional symmetry; and the formation of lamellae will be possible. This argument is in consistence with a strong shift of T_{g-PB} in sample LN2 towards higher temperature (to -44°C in contrast to T_{g-PB} at -98°C in sample LN1) as observed in DMA curves given in fig 4.2.

Recent theoretical calculations [36,37,50,54] and experimental works on graft block copolymers [30-32] have shown that a considerable shift in phase diagram occurs depending on molecular architecture of the block copolymers. Mayes and de la Cruz [49,50] have, for example, analysed how molecular architecture modifies the phase behaviour of block copolymer melts. They have predicted a notable shift in stability windows for different morphologies at a given composition for asymmetric triblock copolymers and star block copolymers. Several authors have studied the phase behaviour of graft copolymers both theoretically [36] and experimentally [29,31] and observed a substantial shift from classical picture of morphology of diblock copolymers. Phase behaviour of LN2 experimentally determined in this work is especially consistent with recent prediction of Matsen [54] on equilibrium behaviour of asymmetric block copolymers. Since the ratio of long to the short PS blocks in LN2 ≥ 4 , a considerable shift in boundary of microphase morphology may be expected.

Finally, sample LN4-S74 consists of physical networks of polystyrene phase in random S/B copolymer matrix. The polystyrene volume content as hard blocks (terminal blocks) in this block sample is about 0.32 which is in the composition range of conventional styrenic thermoplastic elastomers (TPEs). Hence, dispersed PS domains in S/B rubbery matrix are expected (figure 4.4, bottom).

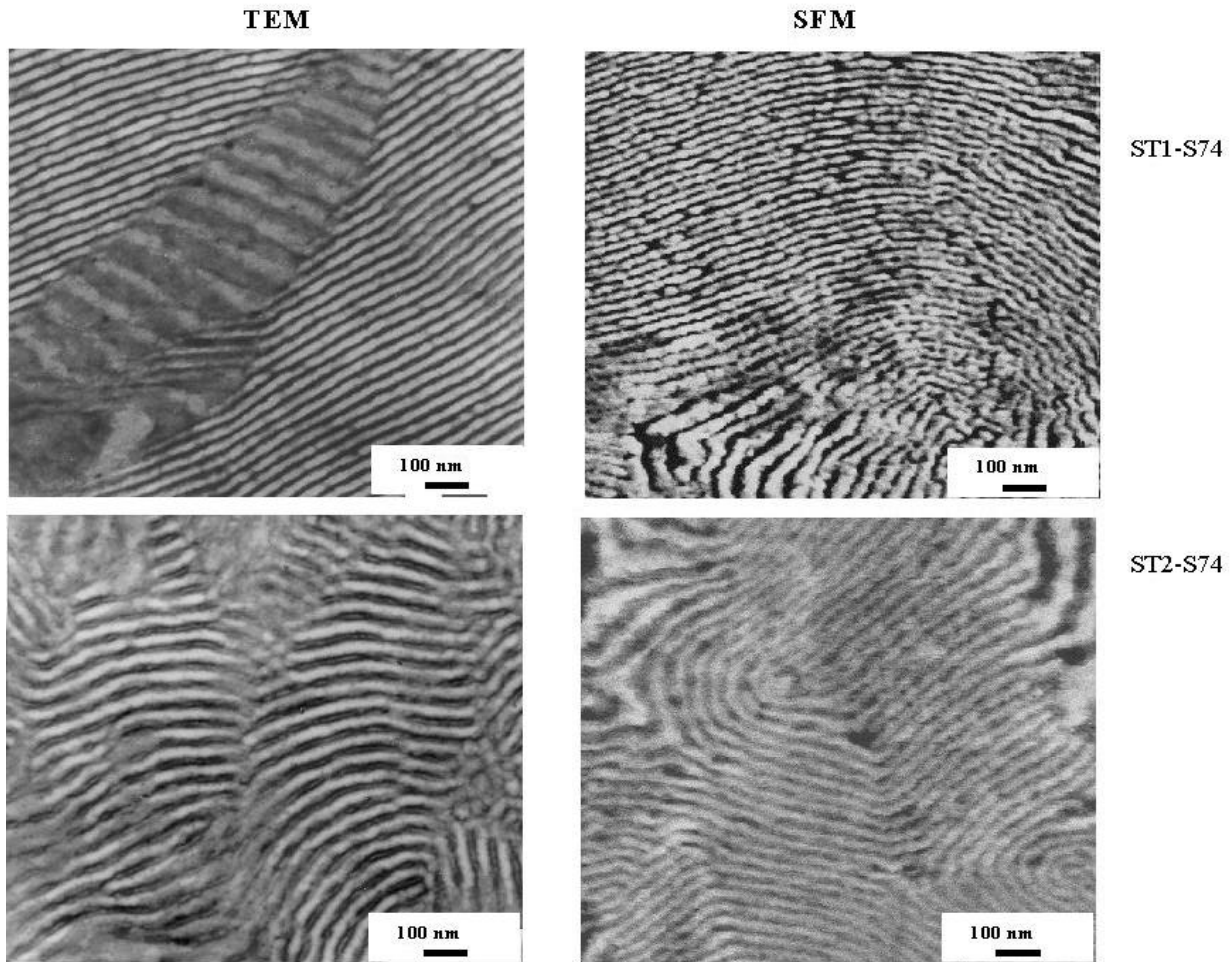


Figure 4.5: Representative TEM (left) and SFM phase (right) images of radial block copolymers; characteristic dimensions of the microstructures are given in table 4.1.

Two-phase morphology with dispersed hard phase in the rubbery matrix has been observed in SIS and SBS TPEs. The dispersed phase consists generally of hexagonal packed PS cylinders in such TPEs [43,68]. In this respect, sample LN4 has structural similarity with classical styrenic thermoplastic elastomers. However, contrasting the classical styrenic TPEs (which contain about 30 vol. % polystyrene), LN4 does not possess highly ordered microstructures. The lack of a hexagonal lattice in this sample implies a broadened interface typical of a system close to the order-disorder transition (ODT) [41,59]. The morphology of this sample, which may be called as *randomly distributed cylinders* in random S/B copolymer matrix is, indeed, very complex.

Lamellae-like morphology is observed in sample ST1-S74 and ST2-S74 (fig 4.5). Characteristic SAXS reflexes for lamellar morphology are, however, not observed in both of these block

copolymers [162]. In a diblock copolymer of equivalent composition, hexagonal arrangement of PB domains in PS matrix would be expected. TEM and SFM micrographs of these samples, however, show both flat-on and edge-on views of the microstructures that may be expected only in case of layered morphology. Flat on view of ‘lamellae’ is especially visible in the SFM phase image of sample ST2.

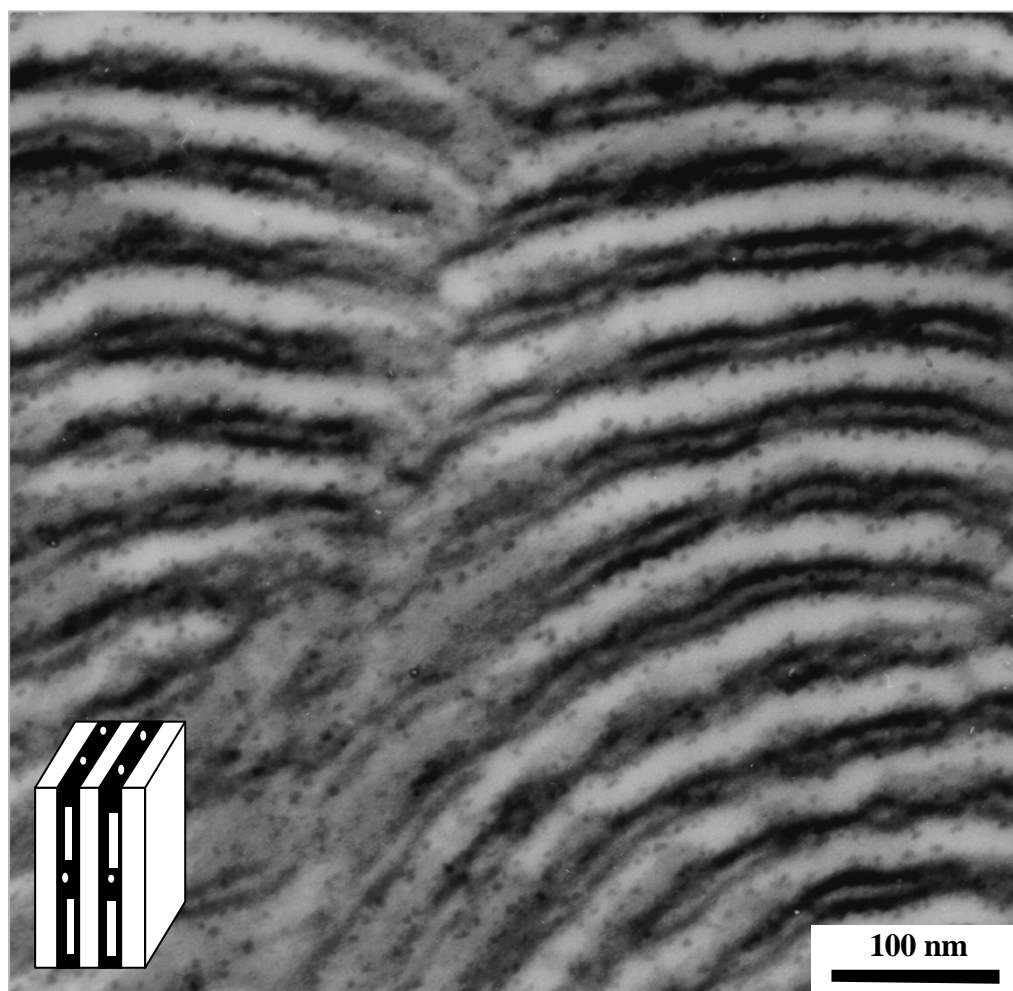


Figure 4.6: High magnification of TEM image showing “Two-component three-phase” morphology observed in ST2-S74.

The deviation in morphology (formation of lamellae-like structures instead of hexagonal PB cylinders) in these radial block copolymers can be assigned to their special molecular structures (block asymmetry, star architecture). It should be stressed that the influence of end block asymmetry as discussed above while elucidating the morphology and phase behaviour of sample LN2 is applicable in star block copolymers as well. Indeed, the ratio of longer to shorter PS outer blocks in star block copolymers is still higher than in LN2, and a stronger shift in their phase behaviour seems reasonable. An increase in T_{g-PB} in ST1 and ST2 (fig 4.2b), for example, implies the presence of PS sequences in the butadiene phase. A higher shift of T_{g-PB} in ST2 than in ST1 may be attributed to the presence of tapered transition (fig 4.1), where the PS chains mixed with the PB phase hinder the mobility of the latter, and leads to an increase in T_{g-PB} .

The star molecules are prepared by coupling living the chains using oligofunctional coupling agent [41,156]. Since the coupling is a statistical process, it results in stars of varying arm numbers and compositions. Hence, star block copolymer samples are, indeed, a mixture of several kinds of stars which introduces further complexity in their solid state morphology.

As mentioned earlier, theoretical works of Matsen [39], Olvera de la Cruz [49,50], Milner [36] and Dobrynin [37] have demonstrated a shift in phase behaviour of star block copolymers compared to their linear analogues. Most recent analysis of Morozov and Fraaije [40] has also demonstrated that the topology of molecules affects the spinodal temperature and asymmetry of phase diagrams. Olvera de la Cruz reported the first theoretical calculations concerning the phase stability of star block copolymers, simple graft copolymers, and miktoarm A_nB_n star copolymers [49]. Irrespective of the position of the branch point, the minimum value at the spinodal was predicted to occur at volume fraction $f = 0.5$. Star copolymers of the A_nB_n type are predicted to have a critical point at $(\chi N)_s = 10.5$, (χ is the Flory-Huggin's interaction parameter and N is overall degree of polymerisation) the same value as for diblocks, when $f = 0.5$. But for $(AB)_n$ star copolymers, the critical value of $(\chi N)_s$ does not occur at $f = 0.5$, and the minimum value of $(\chi N)_s$ decreases by increasing the number of arms. In other words, the tendency towards phase separation increases with increasing number of arms.

On the other hand, increasing the number of junction points along any arm (e.g., ABA structure instead of AB structure of the arm) may further favour phase separation due to decreased entropic contribution to free energy resulting from chain stretching. If each arm consists of asymmetric A blocks (structure analogous to that of LN2, fig 4.1), the phase boundaries tend to shift again. Hence, giving each arm an asymmetric ABA triblock (or AB diblock) structure may introduce complex phase behaviour in block copolymers. Exactly this complex situation exists in ST1 and ST2 which makes the formation of well defined morphology more difficult.

Furthermore, studying the compositionally symmetric styrene/isoprene inverse star-block copolymers, Thomas and co-workers observed experimentally the morphological transition from lamellar to OBDD structure at higher outer to inner block asymmetry. This transformation was attributed to a preferred interfacial curvature induced by the change of the architecture in these asymmetric (in the arm diblock level) but symmetric (in overall composition) star copolymers [163].

Morphology of ST2, consisting of alternating PS and PB layers with PB layers embedding scattered PS domains about 6-9 nm in thickness, deviates most significantly from the classical picture of morphology of styrene/butadiene block copolymers (fig 4.6). Obviously, the PS domains found inside the PB lamellae, which may be regarded as a separate phase, act as reinforcing filler, which simultaneously increases the effective volume fraction of PB. Therefore,

the unique morphology of this star block copolymer can be termed as “two-component three-phase” morphology. Three-phase morphologies have been observed in ABC triblock copolymers by several authors (summarised in chapter 2.2.3 of Ref. [3]). Morphology very similar to that of ST2 was observed in an ABC triblock copolymer by Hashimoto et al. [23] in which one of the minority end block C (24 wt %) formed sphere-like domains in the matrix of majority B (39 wt %) phase lamellae. The existence of complex three phase morphology in asymmetric styrene/butadiene star block copolymer was first reported by Knoll and Nießner [41]. Irrespective of sample preparation methods, this morphology has been found to persist. These results have shown that “two-components three-phase” morphology is characteristic of an asymmetric S/B block copolymer with SBS triblock arm structure.

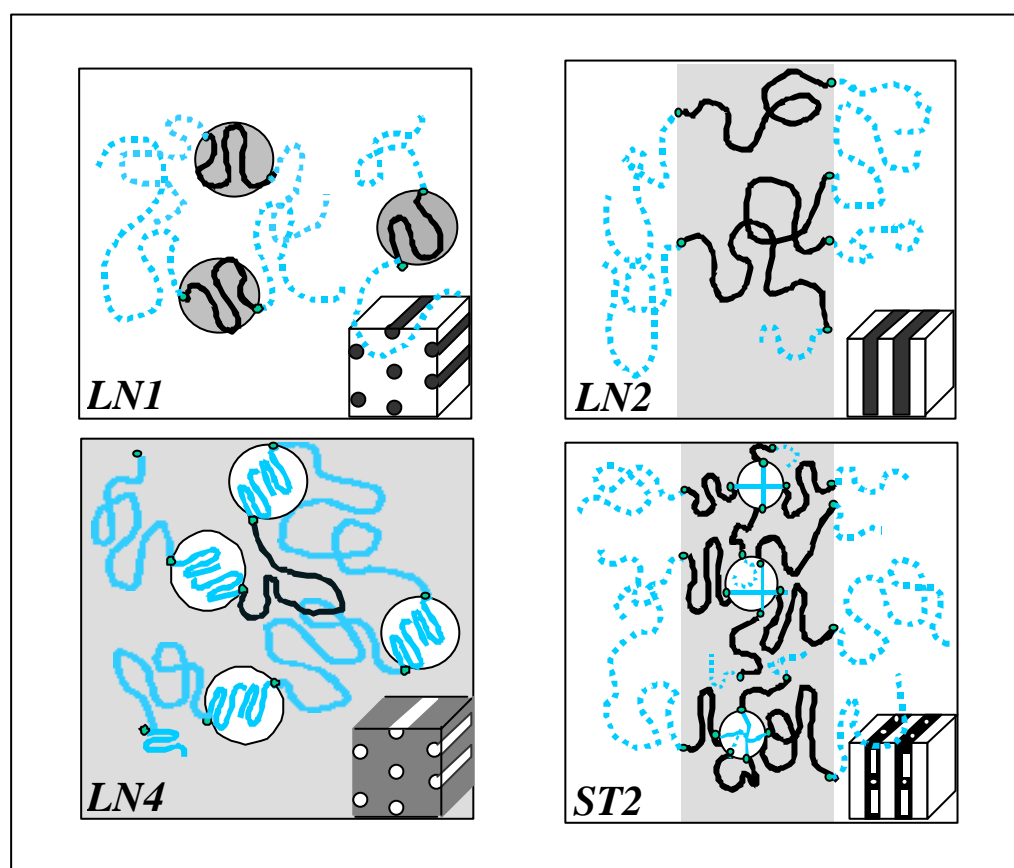


Figure 4.7: Scheme showing conformation of constituent block chains in the investigated block copolymers.

The formation of PS domains inside the PB lamellae leading to the “two-component three-phase” morphology in ST2 stems from its special molecular architecture. Its molecule has a small PS core with molecular weight sufficient for the formation of PS domains (i.e., >10000 mole). Therefore, the scattered PS domains found in PB phase appear to originate from the PS core of the star molecules. That another star block copolymer ST1 does not possess PS domains in the PB phase supports this notion. These domains observed in TEM micrographs of ST2 could

not be resolved satisfactorily in the SFM images, since the resolution of SFM may be limited by tip radius [159,160] which might blunt on prolonged scanning over the sample surface.

It should be admitted that the morphologies of the block copolymers having asymmetric block conformations are very complex, and their evolution is not fully understood. On the basis of results discussed above, a simple schematic picture of morphology formation is presented in fig 4.7.

Table 4.1: Mean long period (\bar{L}) and average thickness of PS (\bar{D}_{PS}) or PB (\bar{D}_{PB}) domains measured in TEM and SFM micrographs of investigated solution cast samples.

samples	\bar{L}_{TEM} (nm)	\bar{L}_{SFM} (nm)	$\bar{D}_{PS,TEM}$ (nm)	$\bar{D}_{PB,TEM}$ (nm)
LN1-S74	28	29	-	13
LN2-S74	36	42	20	-
LN4-S65	33	37	15	-
ST1-S74	37	41	22	-
ST2-S74	47	45	21	-

4.1.3 Effects of Sample Preparation Methods

In preceding section, equilibrium morphologies of the block copolymers have been discussed. Such structures are, however, non-realistic in samples prepared by usual processing methods like press moulding, injection moulding, extrusion etc., where the molecular mobility leading to the formation of ordered structures is highly constrained. In presence of external forces like shearing, pressure etc., the thermodynamic conditions favourable for a particular morphology are not attained, and non-equilibrium morphologies may prevail. Especially important in this respect are the domain orientation and phase transitions brought about by the external forces like shearing [35,164,165].

Fig 4.8 compares TEM micrographs of two linear block copolymers LN1 and LN2 prepared by two different methods: compression moulding and injection moulding. At the first glance, it may be seen that the microphase separated structures have an enhanced orientation along the direction parallel to the machine direction in contrast to ‘polygranular’ structure of solution cast samples. These structures are qualitatively similar to the equilibrium ones (compare with fig 4.4 and 4.5). In each case, the basic morphology has been maintained. In injection mould, the microstructures (lamellae or cylinders) are aligned but often more disrupted. The orientation of microstructures arises from the shear stress operating during the process of injection moulding.

Orientation of block copolymer microdomains is intensively studied in the literature [35,126-130,165]. Winey and co-workers have studied the orientation of lamellar block copolymer samples under large amplitude oscillatory shear (LAOS) [129,130] while Bates et al. [165] have

investigated the shear orientation and phase transitions in block copolymers with lamellar and cylindrical structures. Yamaoka and co-workers have studied the morphology of injection moulded and compression moulded lamellar block copolymers and observed different degree of orientation [35]. Nearly single crystal-like textures in a lamellar and a cylindrical sample have been recently prepared by Thomas et al. using roll cast technique [109,126-128]. These studies have shown that microphase morphology of the block copolymers may be significantly altered by an application of external forces like shearing. The influence of processing conditions on morphology and mechanical properties of star block copolymers is discussed by Michler et al. in a recent publication [166].

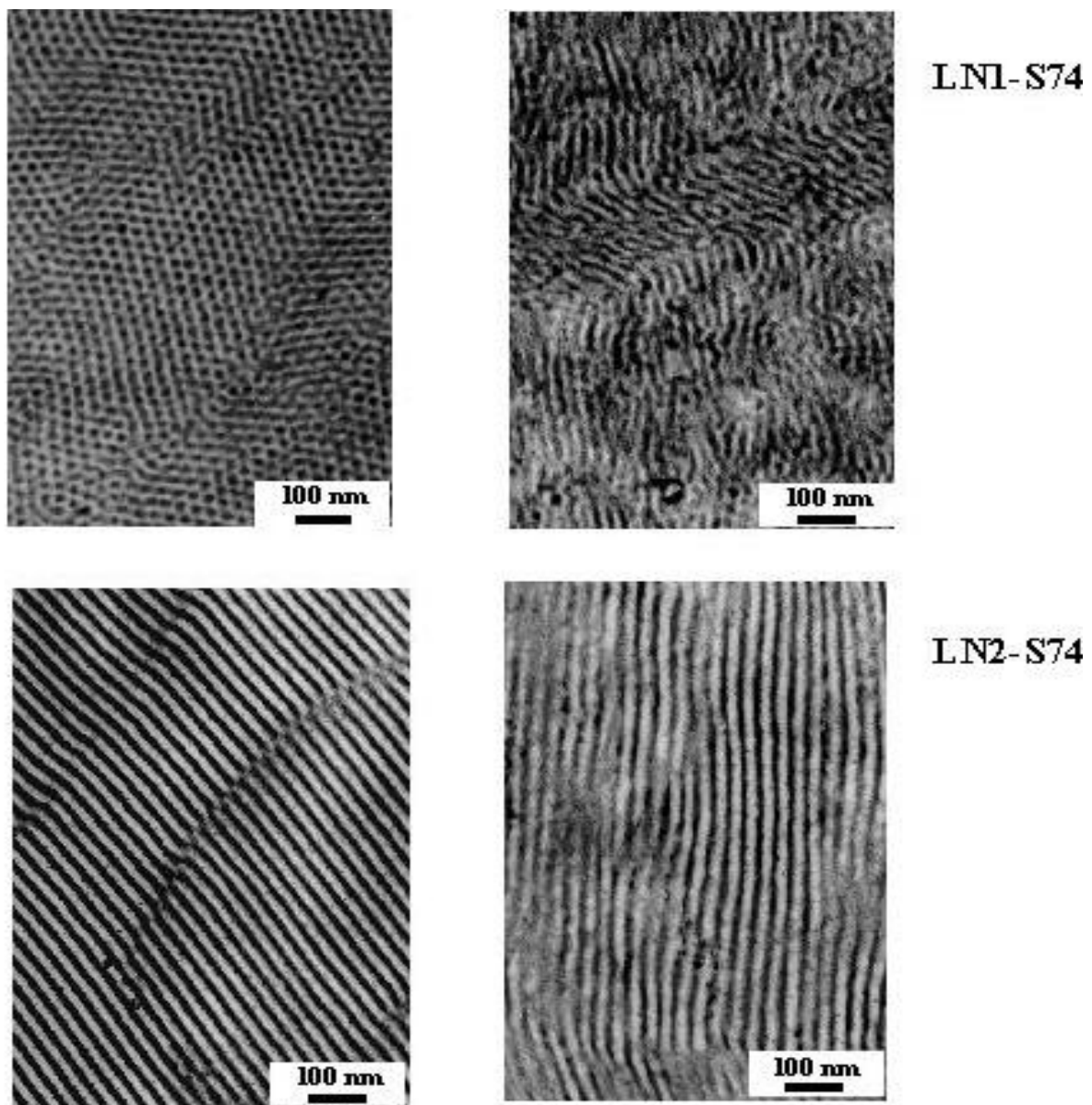


Figure 4.8: TEM images showing morphology of LN1-S74 and LN2-S74 prepared by press moulding (left) and injection moulding (right); injection direction vertical.

No preferential orientation of microstructures is observed in compression moulded samples. These are randomly arranged, and still show a very pronounced long range order. The

microphase separated structures in compression moulds are quite equivalent to the equilibrium ones.

It should be emphasised that the morphology in injection moulded samples can change even from layer to layer and the distance from the injection mouth because of extremely rapid cooling conditions (a large difference in melt and mould temperature). Presence of anisotropic 'skin core' morphologies in injection moulded bars have been observed in various polymers including block copolymers [70,167]. Generally, the sample is strongly stressed towards the 'skin layer' than the 'core layer'; the microstructures are often irregularly arranged, possess more defects and hence deviate from the equilibrium structures.

4.2 Mechanical Properties

Mechanical behaviour of ABA type block copolymers are mainly governed by their microphase separated structures [68,111,118,138]. Hence, their mechanical properties may be discussed with respect to the corresponding morphology. Molecular parameters like asymmetry, topology etc. generally exercise indirect control over mechanical properties mainly by affecting the phase behaviour.

4.2.1 Tensile Behaviour

Stress-strain curves of solution cast and injection moulded samples are given in fig 4.9. The parameters obtained from solution cast films and injection moulds are, however, not directly comparable due to different geometry of tensile specimens (table 4.2). If these were neat linear block copolymers with symmetric outer PS blocks, LN1, LN2, ST1 and ST2 all would have formed PB cylinders in PS matrix; and their stress-strain curves would resemble that of LN1. Similarly, LN4 would have given rise to a lamellar morphology; and a corresponding stress-strain curve would be similar to that of a lamellar SBS triblock copolymer. But the morphology of investigated block copolymers deviate strongly from the classical picture and consequently a significant shift in mechanical and micromechanical behaviour is observed. With respect to phase behaviour and morphologies, the investigated block copolymers show three kinds of behaviour:

- a. Brittle behaviour – high yield stress, low elongation at break, stress whitening, (e.g., LN1-S74, PB cylinders in PS matrix)
- b. High impact behaviour – low yield stress, very high elongation at break, strain hardening, large plastic deformation (e.g., LN2-S74, ST1-S74 and ST2-S74; lamellar structure)
- c. Thermoplastic elastomeric behaviour – no pronounced yield point, high elongation at break, excellent recovery (e.g., LN4-S65, PS domains in rubbery matrix)

Sample LN1 has the highest yield stress suggesting the highest resistance to plastic deformation attributable to the presence of a PS matrix. After reaching the yield point strain softening prevails, and the sample breaks at a strain of about 10-20%. A macroscopic stress whitening, indicative of microvoid formation, is observed during tensile testing.

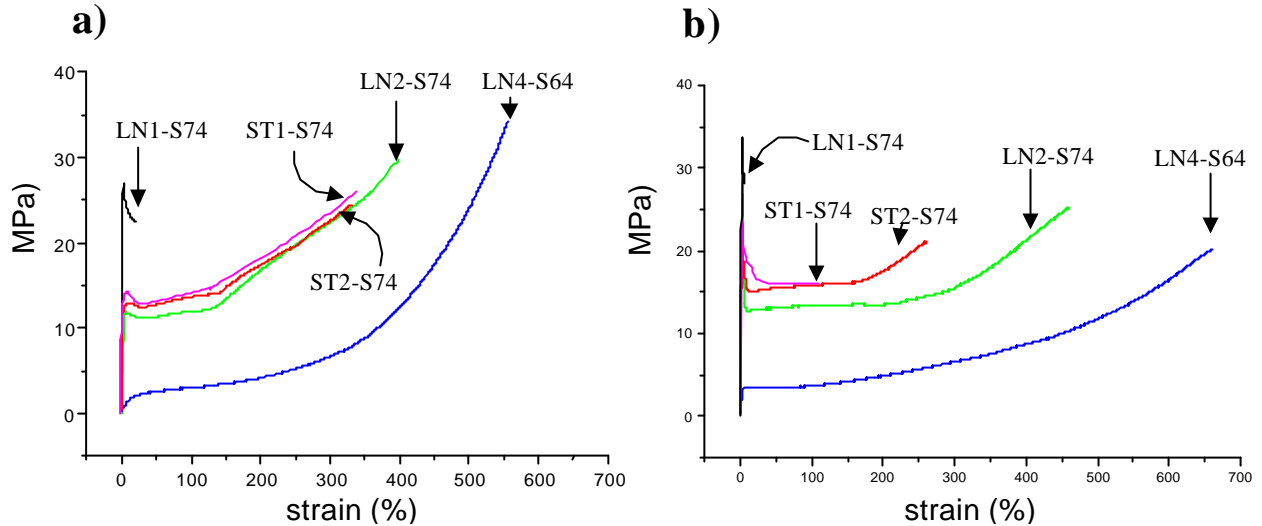


Figure 4.9: Stress-strain curves of the block copolymers; a) solution cast films and b) injection moulds; tensile test at a cross head speed of 50 mm/min.

A diffuse yielding is observed in solution cast lamellar samples LN2, ST1 and ST2 in consistence with earlier results by Sakurai et al. [140] in polygranular samples. The yielding, which has been treated as a beginning of successive fragmentation of glassy lamellae leading to the formation of glassy domains in the rubbery matrix, indicates the onset of plastic deformation. In block copolymer literature, this process has been referred to as plastic-to-rubber transition [123-127,135-138]. During the drawing process, the stress level remains nearly constant, which again rises (strain hardening) until the fracture of tensile specimens. All the lamellar block copolymers exhibit finally similar mechanical behaviour regardless of the molecular architecture they possess. It suggests that the polygranular lamellar samples deform via similar mechanism. Nevertheless, the linear block copolymer LN2 shows still a higher elongation at break than the other lamellar samples. This difference is more pronounced in the injection moulded samples, which might be explained by the higher effective rubber content in LN2 resulting from mixing of styrene units in butadiene phase at the phase boundary (tapered interface). This notion is strongly supported by a larger shift of T_{g-PB} in this sample towards higher temperature than the other lamellar samples ST1 and ST2.

Moreover, triblock chains have longer counter length than the star block chains at constant molecular weight which would eventually contribute to higher macroscopic elongation. Higher stretching further leads to higher chain orientation of the chains (higher orientation hardening)

leading to higher stress at break. Higher rubber toughening via increased T_{g-PB} may, however, have unwanted consequences on the low temperature toughness of the block copolymers. At comparable molecular weights, star block copolymers have preferred rheological properties over triblock copolymers [43-45,52].

Table 4.2: Mechanical properties of investigated block copolymers, injection moulds (inj) and compression moulds (prs) are tested according to the norms ISO 527; solution cast film (sol) has a thickness and total length of about 0.5 mm and 50 mm, respectively. All the samples are tested at a cross head speed of 50 mm/min at room temperature.

sample code	preparation	Young's modulus (MPa)	yield stress σ_Y (MPa)	stress at break σ_B (MPa)	strain at break ϵ_B (%)
LN1-S74	inj	1810±8	29,8±0,2	23,9±0,3	8,8±1,0
	prs	1623±27	28,8±0,3	24,6±0,3	14,2±1,0
	sol	-	26,6±2,2	22,5±2,4	19,4±1,9
LN2-S74	inj	1268±16	28,9±0,5	25,5±1,4	436±14
	prs	568±49	11,4±0,3	26,1±1,5	369±23
	sol	-	11,9±0,7	33,6±4,0	416±23
LN4-S65	inj	79±10	ca. 3,2	20,2±0,7	605±9
	prs	38±11	-	18,0±0,7	597±9
	sol	-	-	32,5±3,7	550±12
ST1-S74	inj	1573±8	26,8±0,2	16,1±0,5	110±37
	sol	-	-	27,6±2,4	368±35
ST2-S74	inj	1205±14	23,7±0,3	19,3±0,8	257±15
	prs	1014±48	16,8±0,7	27,7±1,6	387±26
	sol	-	12,5±0,7	26,4±2,8	363±33

Low yield strength of solution cast lamellar samples arises from their polygranular nature. In contrast, sample LN4 does not have a well-defined yield point due to its homogeneous deformation. Appearance of a shoulder at about 10% strain may imply the beginning of successive fragmentation of PS cylinders at higher strains (to be discussed later in section 4.3.1). It is evident that the ultimate mechanical properties (e.g., maximum achievable stress level, maximum elongation etc.) of solution cast samples are, in general, superior than that of injection moulds. It is attributable to nearly equilibrium structures of solution cast films in which the incompatible domains are well phase separated [43,69].

Since the injection moulded samples are loaded along the injection direction (parallel to the orientation of microstructures), these samples show higher yield stress. This results from the cumulative resistance of all the glassy layers against plastic deformation. These samples achieve, however, lower stress level during tensile deformation, arising from unfavourable conditions for phase separation during the processing. It is especially true for sample LN4 in which polystyrene domains are dispersed in rubbery matrix. In thermoplastic elastomers, the ultimate strength is mainly determined by the strength of physical cross links of dispersed PS domains which depends on the extent of phase separation.

In injection moulds, the styrene domains are more or less spherical in contrast to disordered short cylinders of solution cast sample (compare fig 4.14a and 4.15a). That PS cylinders can withstand higher stress level than PS spheres explains further the higher level of strength of solution cast LN4 than the injection mould.

4.2.2 Mechanical Anisotropy in Oriented Samples

The orientation of microdomains may have a significant impact on deformation behaviour and mechanical properties of the block copolymers as recently shown by Thomas and co-workers in samples having lamellar [126-128], cylindrical [141-143] and gyroid [108,109] morphologies. Different extension ratio of craze fibrils was measured by Kramer and co-workers depending on the orientation of lamellae with respect to the external stress direction [132].

The mechanical properties of oriented styrene/diene block copolymers are highly anisotropic which is associated with the orientation of microstructures with respect to the loading direction. Here, this mechanical anisotropy in oriented samples is discussed taking lamellar copolymer LN2 as an example. In extruded LN2, where the lamellae are oriented along the extrusion direction in macroscopic scale (e.g., fig 4.10a), dissimilar stress-strain curves are obtained on loading the samples parallel and perpendicular to the lamellar orientation direction (fig 4.10b). It is clearly noticed that the sample has yield stress of about 15 MPa and 10 MPa when loaded parallel and perpendicular to the lamellar orientation direction, respectively.

Ultimately, the tensile strength and elongation at break of the specimens under perpendicular loading exceeds that under parallel loading. These observations are partly consistent with recent findings of Thomas et al. [126,127]. These authors have demonstrated the formation of characteristic chevron morphology when the lamellar sample is subjected to tensile loading perpendicular to the orientation direction and observed that both the deformations (both parallel and perpendicular to the lamellar orientation direction) led ultimately to the same value of strain and stress at break. A reason of this discrepancy may be due to the different specimens geometry and strain rate used in their experiment. It may also be associated with different degree of

misorientation in the samples used by in this work and Thomas and his co-workers. Nevertheless, different deformation mechanisms seem to hold at the strains close to the specimen fracture.

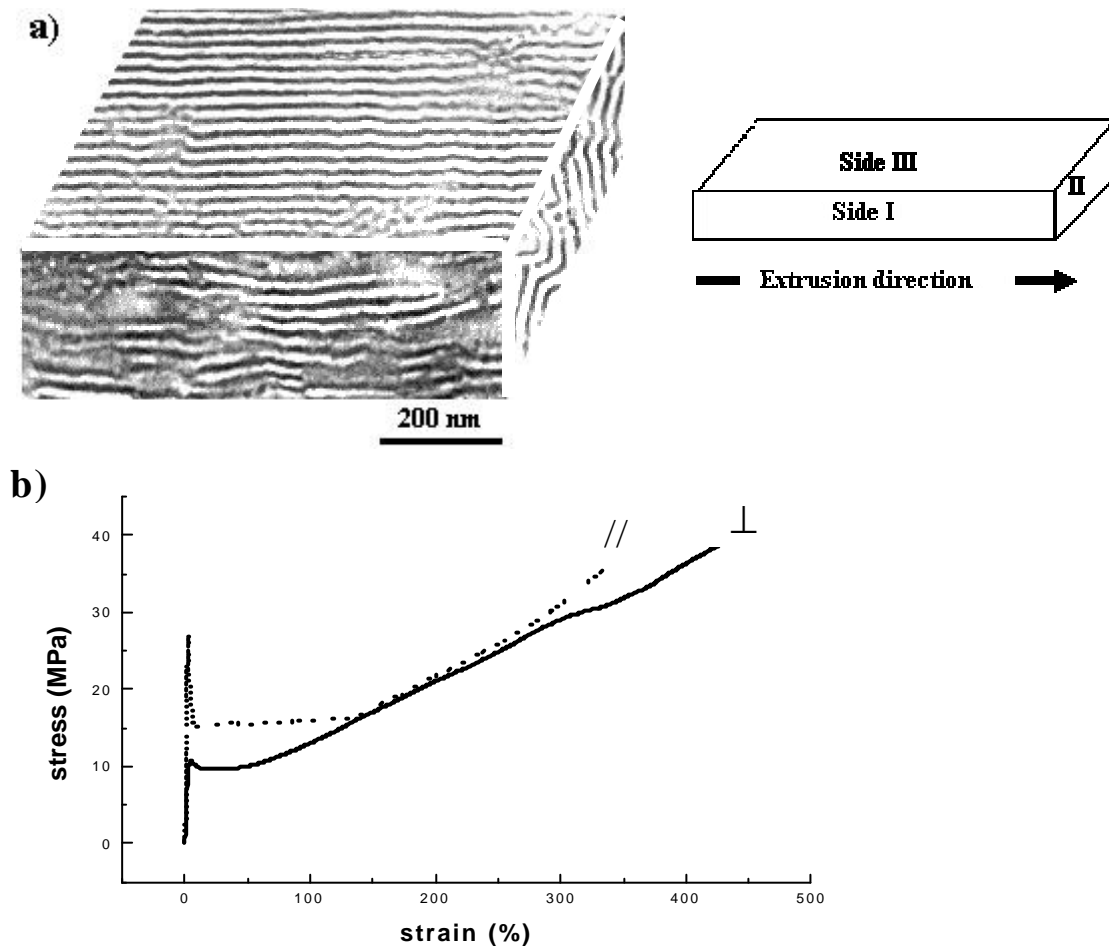


Figure 4.10: a) TEM images showing morphology of extruded lamellar copolymer LN2; the numbers I, II and III stand for different directions in which the specimens are taken from the extruded sheets schematically outlined at the right side and b) stress-strain curves obtained on loading the samples parallel (//) and perpendicular (\perp) to the lamellar orientation direction.

4.3 Micromechanical Behaviour

4.3.1 Influence of Microphase Morphology

In the preceding section, the mechanical properties of solution cast samplers are classified in three headings on the basis of morphology. Accordingly, deformation structures can be discussed with respect to microphase morphology of the samples: PB domains in PS matrix, alternating layers and PS domains in rubbery matrix.

a. Deformation of block copolymer with PB domains (e.g., LN1-S74)

HVEM micrographs of the sample LN1-S74 in fig 4.11 reveal the fine structures in craze-like deformation zones. Such local deformation zones in block copolymers having rubbery domains in glassy matrix are already reported in the literature [111,113-115,168]. A precise inspection of

these zones makes it noticeable that the “microcrack” goes through the PS matrix leaving the PB domains often uncavitated. This observation is fundamentally different from the results obtained in SB diblock copolymers [112-114], weakly segregated block copolymers [111] and star block copolymers with rubbery outer blocks [168].

According to the cavitation model proposed by Argon and Schrier [113] for SB diblock copolymers, cavitation of rubbery PB domains is followed by micronecking in the surrounding glassy PS matrix. The deformation of glassy matrix leads to the formation of cellular structures made up of microvoids and drawn PS fibrils.

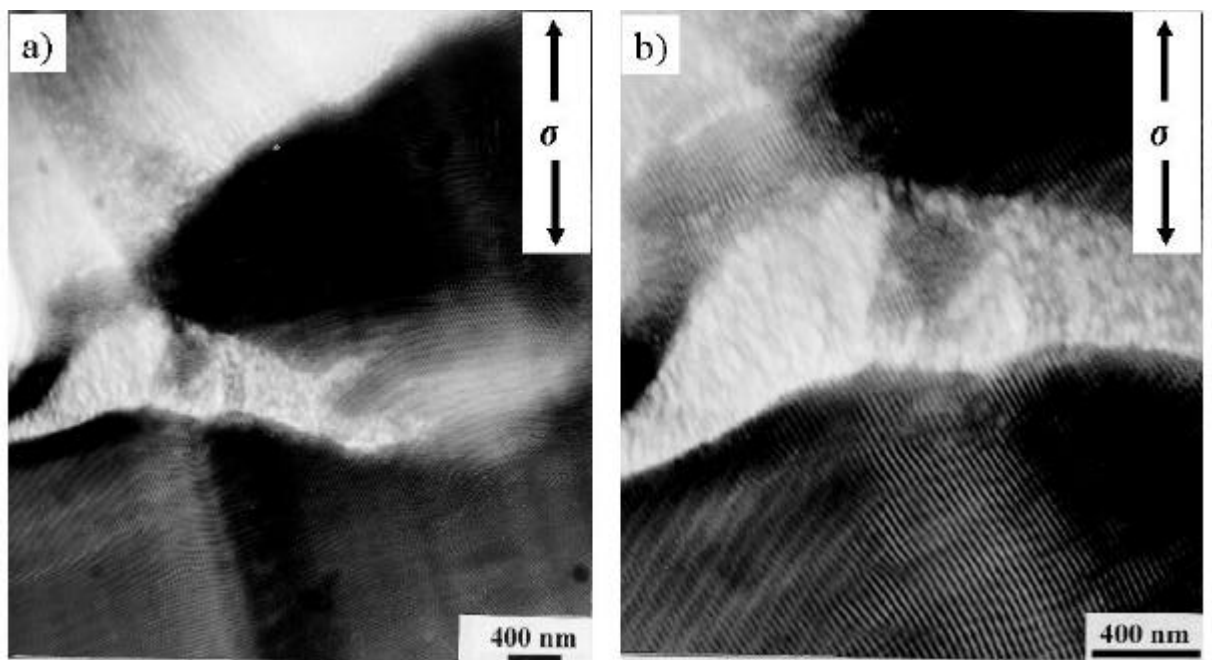


Figure 4.11: a) Lower and b) higher magnification of HVEM micrographs showing crazing in polystyrene matrix in sample LN1-S74; deformation direction indicated by arrow.

In contrast to this cavitation model, cavitation of the glassy phase prevails during tensile deformation in SBS triblock copolymer. Similar deformation behaviour has been observed in ABC triblock copolymers having both glassy terminal blocks and styrene/isoprene multigraft copolymers [119]. For SBS triblock copolymers, rupture of styrene domains (cavitation in the PS phase) has been reported previously by Baer and co-workers [115]. Those results indicate that the cavitation mechanism proposed for SB diblock copolymers is no more valid for SBS triblock copolymers irrespective of the type of microphase separated structures present in them. The cavitation in block copolymers is, therefore, clearly related to the location of glassy blocks in their molecules.

The cavitation of rubbery phase under concentrated stress ahead the craze tip in SB diblocks may be attributed to the presence of one half of the chain ends in the rubbery domains. As another half of the chain ends are terminated in glassy matrix, flexible rubbery chains are prone to pull out of the rubbery domains (disentanglement), and cavitation in the rubbery domains takes place.

Since both the chain ends are terminated in the PS matrix in SBS triblock copolymers, there is more likelihood that the glassy chains slide past one another favouring microvoid formation in the glassy matrix.

Craze fibrils in PS matrix in sample LN1 are highly stretched. However, the macroscopic elongation of the specimens is limited to few percents. Localisation of deformation in craze-like deformation zones is the reason of observed low elongation at break. Presence of PS matrix accounts for the high yield stress and high elastic modulus of this sample.

Table 4.3: Long period (L) and average thickness of PS domains (D_{PS}) measured in TEM micrographs of injection molded samples before and after deformation. The figures inside parenthesis corresponds to the peak of distribution. *PB domains about 13 nm in diameter which either remain almost unchanged or slightly stretched plastically in craze-like regions in deformed samples.

samples	L (nm)		D_{PS} (nm)	
	before def.	after def.	before def.	after def.
LN1-S74	20-25 (23)	-	-*	-
LN2-S74	25-30 (28)	11-17 (14)	05-23 (16)	3-17 (10)
LN4-S65	18-33 (22)	-	12-28 (15)	-
ST1-S74	33-46 (40)	12-30 (21)	14-32 (22)	6-25 (14)
ST2-S74	37-42 (39)	12-26 (18)	10-36 (20)	8-22 (14)

b. Deformation of lamellar block copolymers (e.g., LN2-S74)

Due to presence of alternating PS and PB layers, sample LN2 deforms through a different mechanism than LN1. The morphology of sample LN2 deformed in tensile test is shown in fig 4.12. In the deformed specimen, the lamellar long period has been partly decreased locally up to 1/3 of the original value (fig 4.12a, upper right). Assuming equivalent deformation in the direction normal to the image surface, a local elongation of PS lamellae of about 200% can be estimated which is in the same order as the macroscopically observed strain at break of the specimen (fig 4.9a). The deformed lamellae have been aligned strongly in the deformation direction indicating the rotation of the lamellae towards the strain direction. Recent studies on the deformation behaviour of lamellar block copolymers using TEM and in-situ scattering techniques by Thomas et al. [126,127] have shown that oriented lamellar “single crystals” deform via formation of chevron fold-like morphology nucleated from pre-existing local defects (like edge dislocation) when the sample is subjected to tensile deformation perpendicular to the lamellar orientation direction. They have demonstrated that macroscopic strain of a few hundred percent can be achieved simply through the lamellar folding (formation of chevron folds) without noticeable stretching of the lamellae itself in the strain direction. A similar chevron fold-

like morphology has been observed in solution cast polygranular sample LN2, which might have been formed by rotation or folding of the lamellae situated perpendicular to the stress direction (fig 4.12b). The narrow kink boundaries are mostly asymmetric, and the PS lamellae are partly broken at the hinges. The lamellar long period at the hinges is larger than that in the limbs indicating the dilation of rubbery layers. Most importantly, the deformation is not localised in the form of craze-like zones in contrast to sample LN1. Since the lamellae are randomly oriented, observed high ductility of this sample can be assigned to be the result of combined effect of both lamellar *folding* and lamellar *stretching* along the deformation direction.

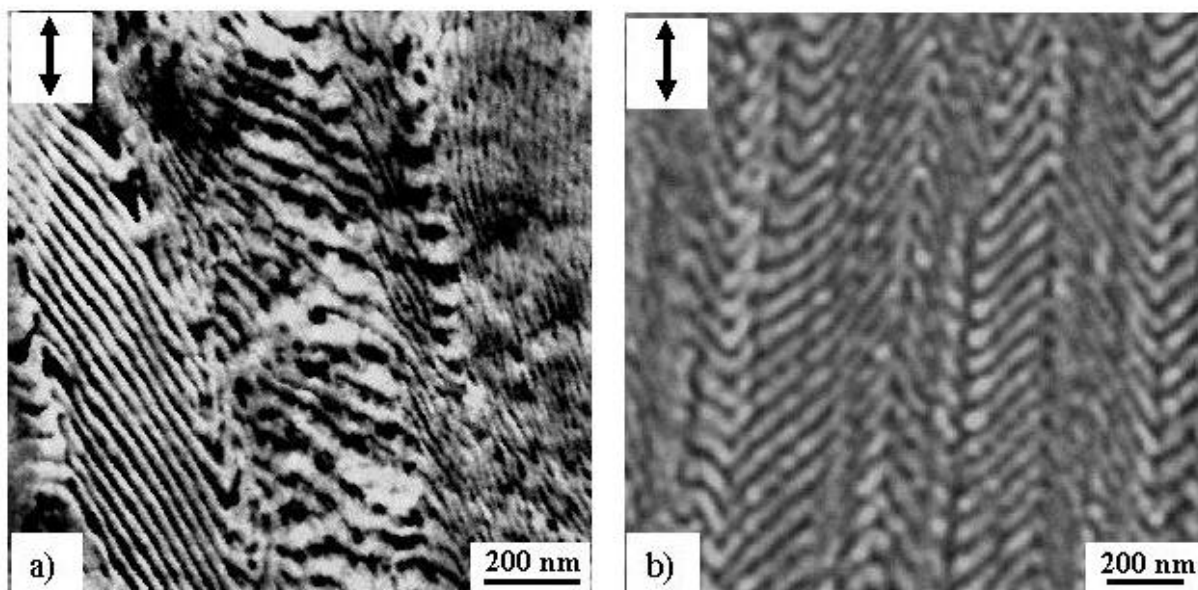


Figure 4.12: SFM phase images showing chevron fold-like morphology in lamellar block copolymer LN2-S74 formed by tensile deformation, deformation direction vertical.

Similar deformation mechanism hold in lamellar star block copolymers. TEM images of ST2 strained in the tensile test is shown in fig 4.13a, and the thickness distribution of PS lamellae before and after deformation is given in fig 4.13b. It can be noticed in fig 4.13a that there are two different deformation zones: one with plastically deformed lamellae (shown by letter H) and the other with lamellae forming fish-bone pattern (shown by letter F). In the former, PS lamellae thickness has reduced by over 50% while in the latter PS lamellae are simply bent towards the strain direction or turned into kink boundaries. As in sample LN2, the lamellar long period in this region is significantly higher than in undeformed sample resulting from the dilation of rubbery layers.

Moreover, high ductility of lamellar samples LN2 and ST2 may be related to their molecular structure. Unlike sample LN1, which comprises the symmetric PS end blocks and has a sharp interface between the blocks, the chains of sample LN2 and ST2 contain asymmetric PS terminal blocks and a tapered transition resulting in a broadened interface. Enhanced mechanical

properties due to broadened interface have been discussed in weakly segregated block copolymers [111,131]. The asymmetric nature of the hard blocks leads to a twofold advantages: the longer end block contributes to the strength of the block copolymer, whereas the shorter blocks enhance the deformability and processability [53]. To summarise, deformation via similar micromechanism (e.g., plastic stretching and folding of lamellae into chevron-like texture) leads to similar tensile properties of solution cast lamellar samples.

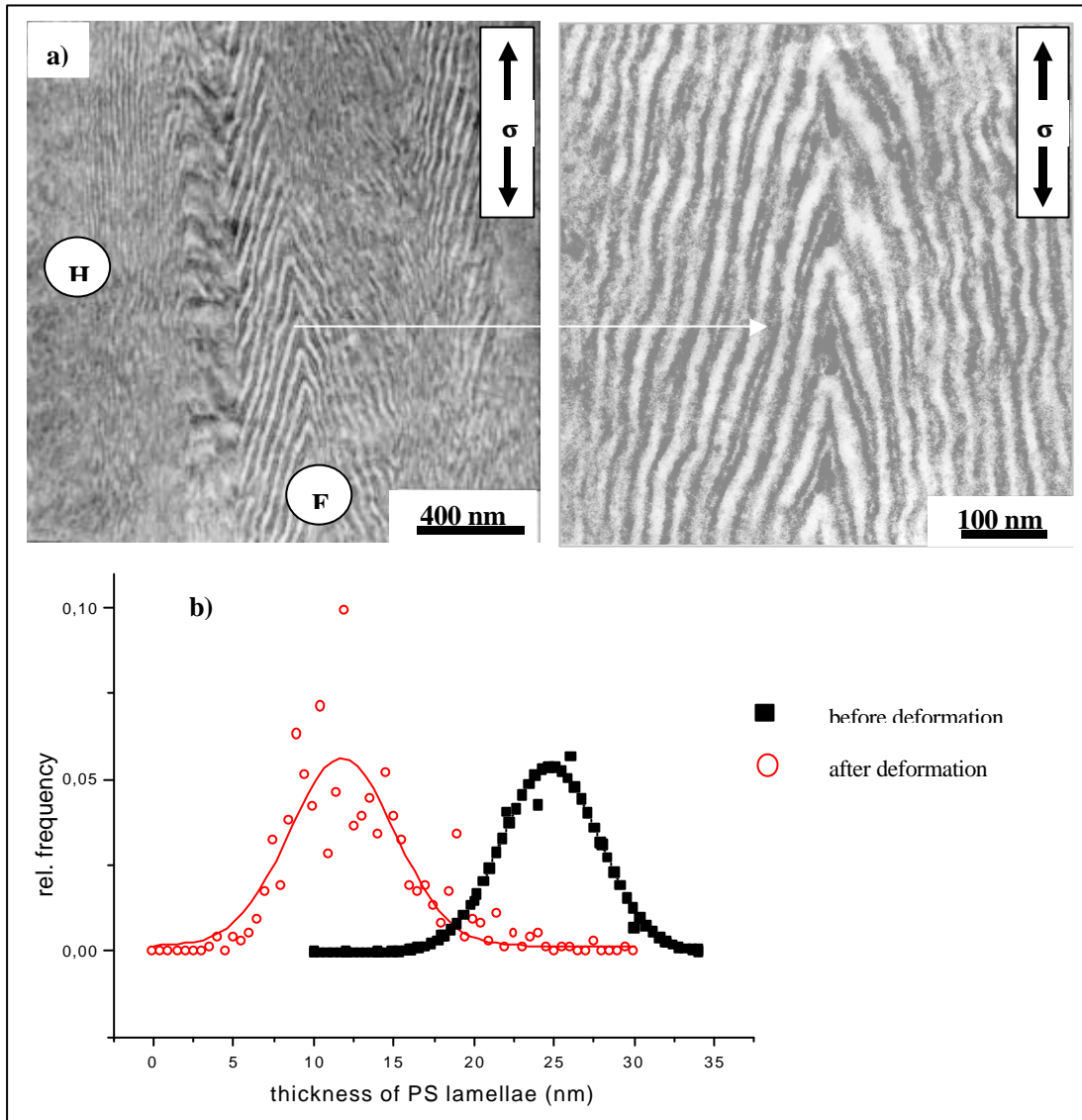


Figure 4.13: TEM micrographs showing deformation structures in solution cast ST2 (top) and distribution of thickness of PS lamellae fitted to a Gaussian function.

c. Deformation of block copolymer with PS domains (e.g., LN4-S65)

Due to presence of rubbery random S/B matrix with glassy PS domains dispersed in it, sample LN4-S65 shows a large degree of non-linear elastic behaviour. This accounts for the observed large elongation at break, low yield strength and excellent recovery. In spite of observation of a few quite regular hexagonal array of dispersed PS phase in rubbery matrix, majority of the cylinders (fig 4.4 bottom) are too short and disordered. So, it is difficult to map the deformation

structures in this copolymer with the help of thin sections from the specimens strained in tensile test. Nevertheless, the glassy domains take nearly ellipsoidal shape and are aligned in the strain direction (fig 4.14b). This observation is in agreement with the previous observation of Seguela and Prud'homme [133]. However, fragmented glassy domains cannot be distinguished.

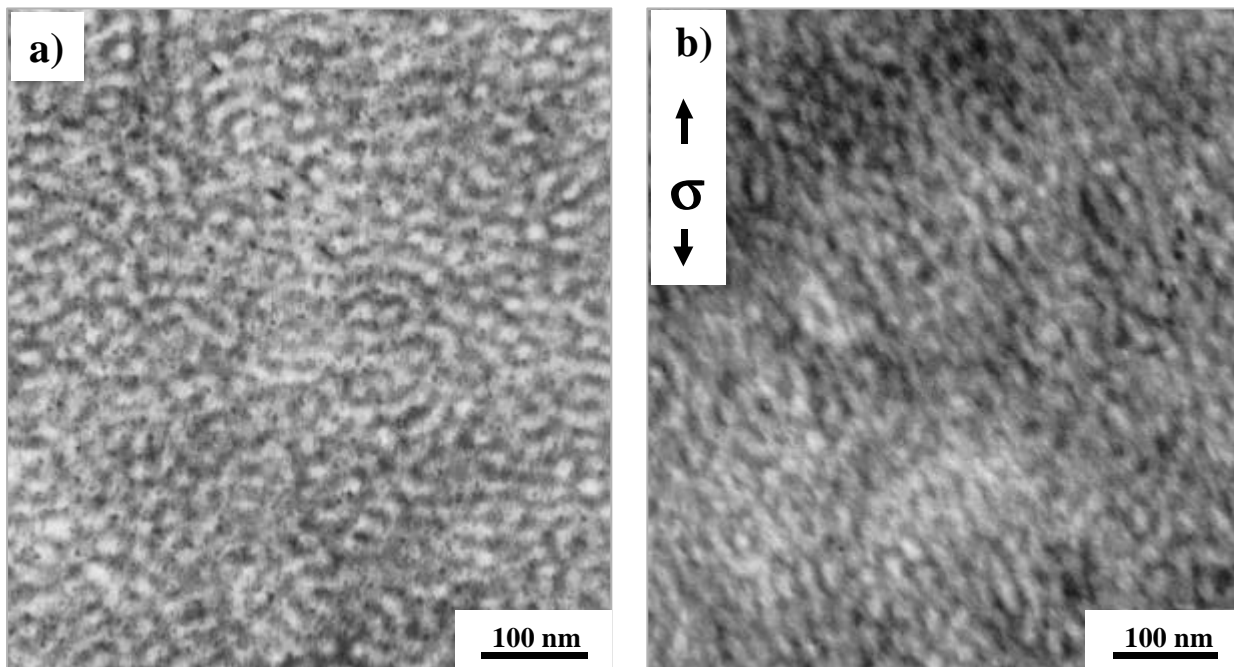


Figure 4.14: TEM images showing a) morphology and b) deformation structures in LN4-S65; deformation structures are imaged after the relaxation of the sample strained in the tensile test; injection moulding and strain direction vertical.

Thin films of LN4 cast from its toluene solution was slowly strained using a special external tensile device to different strains, and deformation structures were imaged by the SFM. The results are presented in fig 4.15. The morphology of this sample in thin film shows the randomly arranged short styrene cylinders in S/B rubber matrix (Fig 4.15a). The periodicity of domains is about 37 nm. At about 100% strain, the original domain structure of LN4 is distorted. The cylinder-like domains are partly broken forming bead-like structures (shown by a white circle in fig 4.15b) and rearranged in chevron-like manner. Like LN2 and ST2, the average long period of domains in chevron region is higher than in the undeformed sample. The bead-like structures are interconnected by thin fibrils. Nevertheless, the deformation behavior of this sample resembles that of conventional styrenic thermoplastic elastomer as discussed below.

In order to study the deformation of glassy cylinders in a triblock copolymer, strain induced structural changes in a commercial SEBS thermoplastic elastomer (Kraton) was investigated straining thin films to different levels of strain [169]. The results are summarised in fig 4.16. The morphology consists of light PS cylinders in dark rubbery matrix. On slow evaporation of solvent, glassy cylinders were predominantly aligned parallel to the substrate. Until about 20% strain, no significant change is noticed. At higher strains (~100% strain), the cylinders are partly

broken; and chevron fold-like morphology appears which may be nucleated at local defects like edge dislocations [127,128,142].

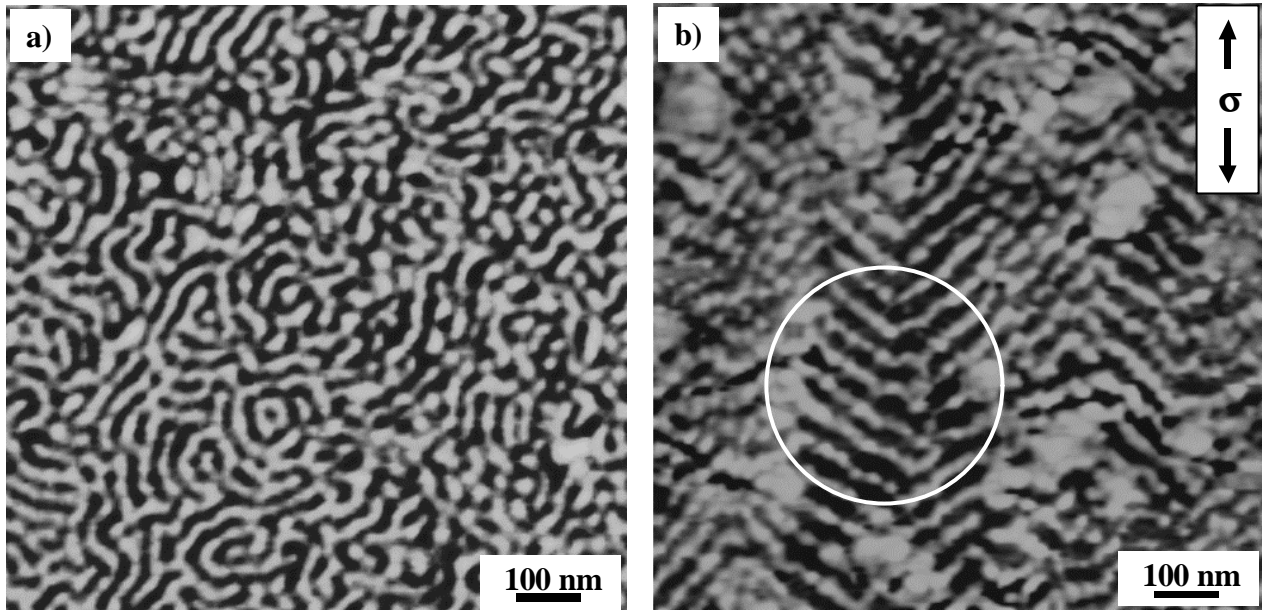


Figure 4.15: SFM phase images showing a) morphology and b) deformation structures in sample LN4, surface of solution cast films imaged in the strained state.

The cylinders lying along the strain direction are further broken down into smaller fragments at higher strains, while the rubbery matrix at the chevron folds are further dilated resulting in larger long period of the cylinders at these regions: long period of glassy cylinders at the chevrons is about 34 nm compared to about 28 nm in undeformed sample. Dilation of rubbery layers in chevrons is an additional reason for observed higher molecular orientation in the rubbery phase recorded by Fourier transformed infrared (FTIR) spectroscopy [169].

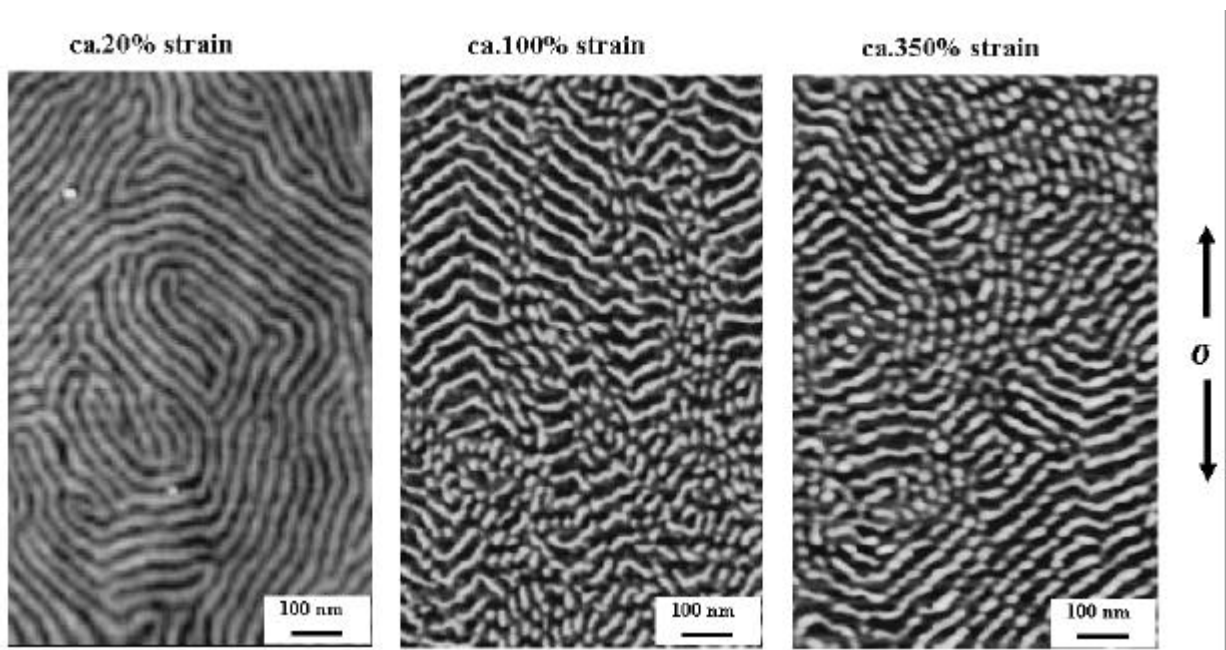


Figure 4.16: SFM phase images showing different stages of deformation of glassy cylinders in SEBS triblock copolymers [169].

The SFM micrographs presented in fig 4.16 provide the direct evidence of fragmentation of glassy cylinders into smaller rodlets under strain. This is in accordance with the previous results of Keller and Odell [137] and recent results of Honeker and Thomas [141]. With increasing strain, population of chevron morphology is found to decrease which qualitatively suggest the successive break down of cylinders even at the regions of chevrons.

4.3.2 Influence of Molecular Structure

The influence of molecular architecture of star block copolymers on morphology has been already discussed. It was mentioned that the presence of a tapered transition and PS core in the asymmetric star block copolymer may yield an important effect on the deformation behaviour and mechanical properties. Now, the mechanical properties of oriented star block copolymers ST1 and ST2 are examined on the basis of micromechanical processes of deformation.

Figure 4.17 compares morphology (top) and deformation structures (bottom) observed in injection moulded star block copolymers. Stress-strain curves of these samples compared with linear triblock copolymer LN1 are separately presented in fig 4.18. Stress-strain behaviour is characterised by a well-defined yield point. The degree of plastic deformation is, however, quite different. Both ST1 and ST2 show a much larger plastic deformation than LN1. The area under the corresponding σ - ϵ curves, which is a measure of the absorbed energy, is much larger for the star block copolymers. The deformation of both star blocks occurs by neck formation and subsequent elongation, while the SBS triblock undergoes a brittle fracture. ST1 and ST2 show a unexpectedly large elongation at break of about 110% and 260%, respectively.

In spite of their similar molecular topology (i.e., asymmetric star, fig 4.1) and similar morphology (fig 4.17, top) the tapered star block copolymer ST2 shows a more ductile behaviour than the neat copolymer ST1. This discrepancy should be found in different architectural and interfacial structures of these copolymers. Detailed study of influence of molecular structure on mechanical properties has been discussed in [166].

As already stated, the asymmetric architecture is associated with two advantages: the longer PS arms improve the strength of the materials, while the shorter PS arms simultaneously enhance their deformability. This reason for the observed ductility is present in both the copolymers ST1 and ST2. When subjected to tensile strain, shorter PS chains present in a PS lamellae may easily loosen and act as precursors for the drawing of PS chains, which form the entanglement network. This could be the reason for the formation of alternating thicker and thinner regions along a PS lamella in deformed samples (fig 4.17, bottom). Thus, homogeneous plastic deformation of both PS and PB lamellae is the principle deformation mechanism of the star block copolymers. The PS lamellae have been drawn locally up to a few hundred percent.

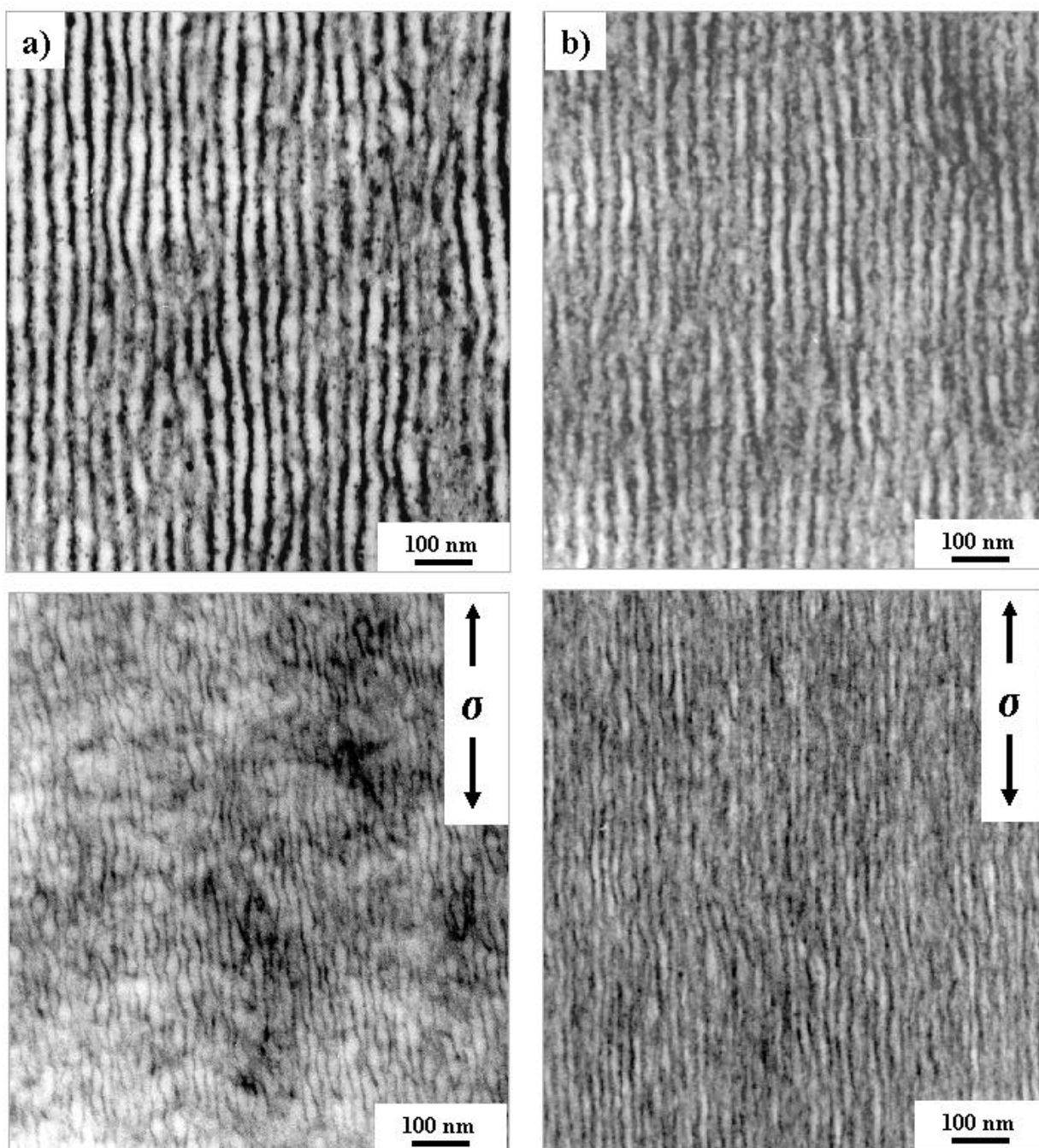


Figure 4.17: TEM images showing morphology (top) and deformation structures (bottom) in a) neat star block copolymer ST1 and b) tapered star block copolymer ST2; injection moulds, injection direction vertical; the samples are loaded parallel to the lamellar orientation.

The PS domains scattered in the PB lamellae in ST2, chemically coupled to the butadiene phase, may act as additional “energy sinks” [43], which may delay failure by elastically absorbing a part of energy. These domains further act as ‘filler’ in rubbery phase and enhance the effective strength of PB lamellae.

It was demonstrated that mechanical properties such as toughness and tensile strength of tapered block copolymers exceed that of common neat block copolymers [60,61]. Recently, Asai [61] has observed a strong improvement of tensile properties in a tapered SB diblock copolymer and

explained it by enhanced energy dissipation. Incorporation of tapered chains in a block copolymer results in a decreased interfacial energy due to enhanced mixing of the phases [59]. This enhanced miscibility is connected with an increasing interfacial width, and then the phase behaviour is close to a weakly segregated system. Weidisch, Michler and co-workers have shown [111,131] that an increasing interfacial width is responsible for a significant improvement of tensile properties of block copolymers.

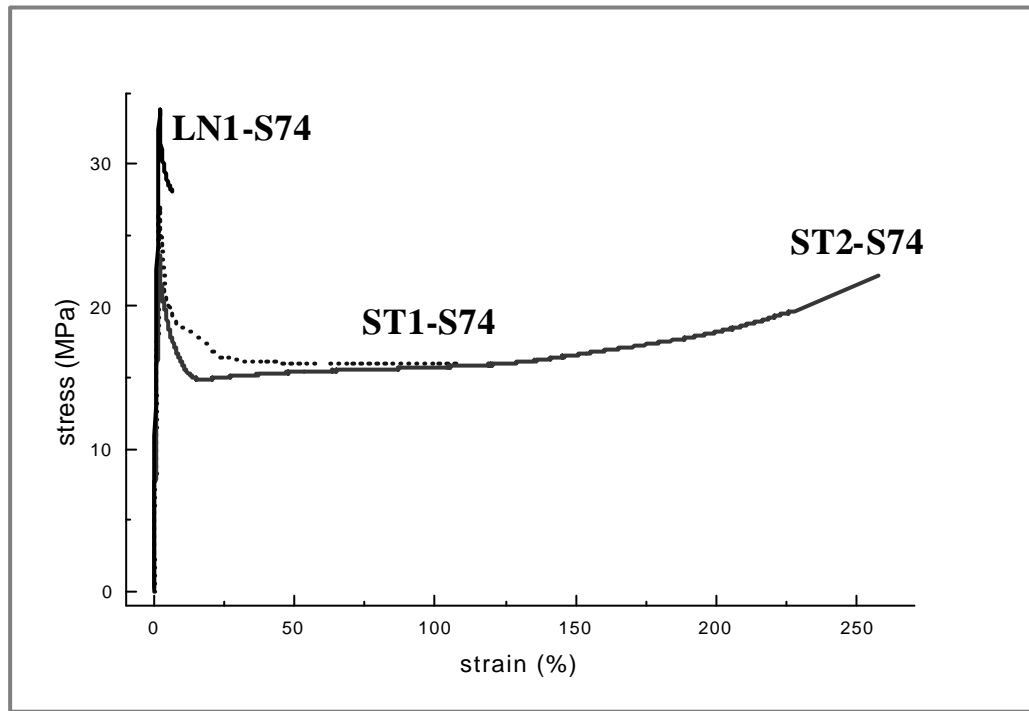


Figure 4.18: Stress-strain behaviour of injection moulded star block copolymers ST1 and ST2 compared to the neat linear block copolymer LN1.

In the deformed samples, alternating thinner and thicker regions in ST1 are more pronounced than in ST2 (fig 4.17, bottom). This indicates that the PS lamellae show locally an inhomogeneous deformation (lamellar necking). This necking process leads to a premature failure of PS lamellae. The PS lamellae in ST2-S74 are more homogeneously deformed i.e., the neck has been stabilised during the drawing process. More homogeneous deformation of PS lamellae in ST2 is the reason for its higher ductility.

The observed high ductility of the star block copolymers can be correlated with a large plastic deformation of PS lamellae. Quantitative analysis shows that the average PS lamellar thickness is reduced to about the half during deformation in ST1 and ST2 (table 4.3, fig 4.13,4.20). However, locally the PS lamellae show a larger plastic deformation ($\lambda_{PS} > 4$). This indicates that an inhomogeneous plastic flow of PS lamellae occurs via micronecking and drawing and a

subsequent rupture of necked PS lamellae into small fragments. The necking process of the PS lamellae is accompanied by chain orientation and strain hardening.

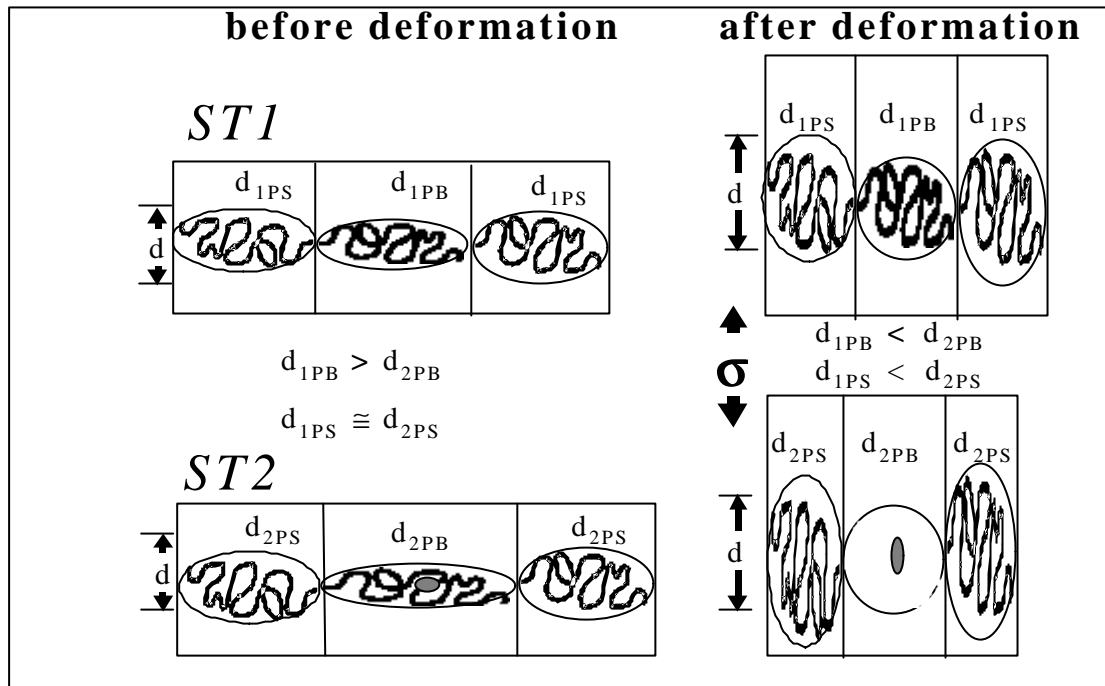


Figure 4.19: A schematic drawing showing the chain conformation in ST1 and ST2; the letter **d** stands for the diameter of the of the perturbed coil parallel to the interface, and the subscript 1 and 2 denote star block copolymers ST1 and ST2, respectively.

More homogeneous drawing of PS lamellae, that is believed to be the reason of enhanced ductility of ST2 over ST1, may be explained by examining the molecular structure of the copolymers. The possible chain conformation in ST1 and ST2 is schematically presented in fig 4.19. According to the theoretical consideration of chain dimensions in block copolymers, the corresponding homopolymer chains in a copolymer assume an ellipsoidal conformation with the major axis of the ellipse normal to the interface [11]. At the same time, the block copolymer chains are shrunk in the direction parallel to the interface so as to compensate the elongation in the perpendicular direction.

By determining the extension ratio of craze fibrils in lamellar triblock copolymers as a function of fibril direction with respect to lamellar orientation direction, also Kramer and co-workers have demonstrated the stretching of copolymer chains in a direction normal to the microdomain interface [132]. Each arm in ST1 and ST2 has a diblock and triblock structure, respectively (fig 4.1). Hence, every butadiene chain in ST2 is connected twice with the styrene chains, whereas it is connected only to outer PS block in ST1. This means that the butadiene chains in ST2 have higher entropy loss due to chain stretching normal to the interface, leading to more perturbed chain conformation than in ST1. Based on this model, it can be easily estimated that butadiene

phase in ST2 allows higher extension ratio parallel to the lamellar direction to reach the same thickness of the PB lamellae after deformation. Higher extension ratio of the PB phase allows simultaneously larger plastic deformation of the PS lamellae. Eventually, the thickness of both PS and PB lamellae may reduce to a larger extent in ST2 than in ST1 after deformation (i.e., $d_{1PS} < d_{2PS}$ and $d_{1PB} < d_{2PB}$). This results in more homogeneous deformation of PS lamellae in ST2 than in ST1 as mentioned above.

A more general and more simple explanation to this issue would be higher effective rubber content (and hence higher rubber toughening) in the star block copolymer ST2 than in ST1 in spite of identical net styrene content. Increase in effective rubber content in a tapered block copolymer has been already discussed in section 4.1.1. Since the styrene domains inside the butadiene phase may be regarded as ‘fillers’, these domains practically belong to the rubber phase, causing ultimately an increase in rubbery component and simultaneously a decrease in styrene volume fraction. The higher rubber toughening in ST2 than in ST1 is supported by lower yield stress of the former than the latter (24 MPa in ST2 compared to 27 MPa in ST1).

4.3.3 Thin Layer Yielding Mechanism in Lamellar Star Block Copolymers

It has been observed that the lamellar block copolymers included in this study show a large homogeneous plastic deformation of PS lamellae. Based on a detailed study on lamellar block copolymers, a “thin layer yielding” mechanism has been proposed which may be used as an alternative toughening mechanism in glassy polymers [166]. Here, this mechanism is discussed with special reference to ST2-S74.

As already mentioned, homogeneous plastic deformation of PS lamellae is the most striking effect observed in lamellar star block copolymers. As a result, the thickness of PS lamellae decreases from about 10-36 nm to 8-22 nm (i.e., a local thickness reduction of about 50%, compare fig 4.17b top and bottom; see also fig 4.20). Same order of decrease might be expected for the width of the lamellae (i.e., in the direction normal to the micrographs). Similar extent of reduction in the lamellar long period may be evident in fig 4.21. From this, an elongation of about $\lambda \approx 4$ can be estimated, which is of about the same order as the strain at break of bulk specimen. Moreover, this elongation is in the same order as the maximum elongation of craze fibrils in PS [1,170]. Elongation of craze fibrils is limited by entanglements. The maximum extension λ_{max} of craze fibrils is correlated to the maximum deformation ratio of the entanglement network given by $\lambda_{max} = l_e/d \approx 4$, where l_e is the contour length between the adjacent entanglement points and d is the root mean square end-to-end distance of a chain corresponding to entanglement molecular weight [1].

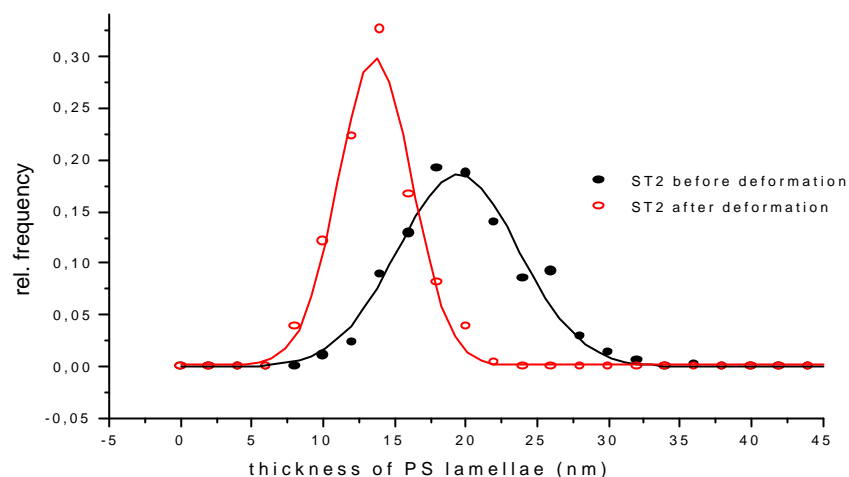


Figure 4.20: Distribution of PS lamellae thickness in ST2-S74 before and after deformation; data points fitted in a Gaussian function.

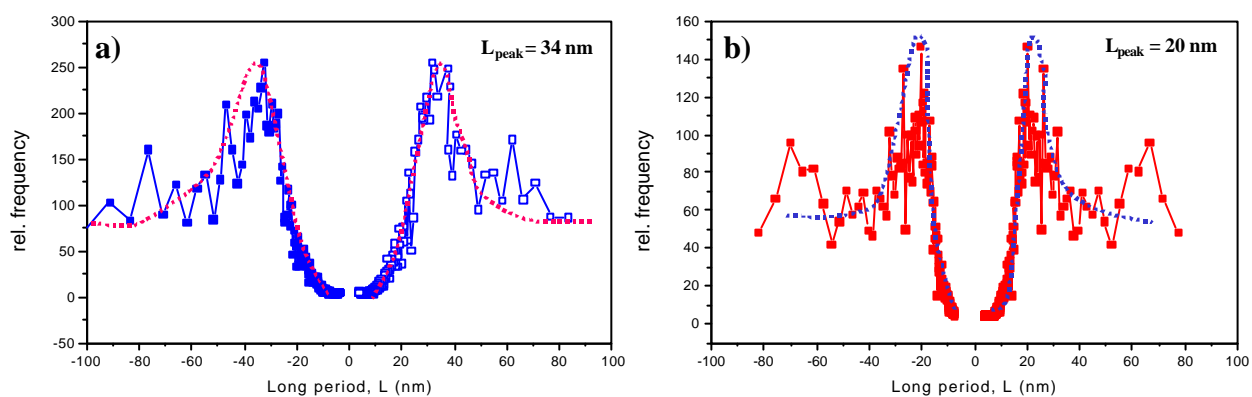


Figure 4.21: Distribution of lamellar long period in injection moulded ST2-S74 determined by Fourier transformation; a) before and b) after deformation; L_{peak} denotes the peak value of lamellar periodicity distribution.

Homogeneous deformation of craze fibrils in PS appears if the thickness of the fibrils lies in the range of about 5-20 nm [1]. In the lamellar block copolymers studied here, the homogeneous deformation of PS lamellae is similar to homogeneous craze fibril deformation in polystyrene. The difference between both mechanisms can be realised in the fact that craze fibrils in PS are stretched between microvoids, whereas the PS lamellae are deformed together with the adjacent PB lamellae. Therefore the PB lamellae may have a function analogous to that of adjacent microvoids and do not hinder the deformation of PS lamellae. Hence, this deformation mechanism can be called as “thin layer yielding”. In contrast to the cavitation mechanism which is usually observed in block copolymers, a homogeneous deformation of PS as well as of adjacent PB lamellae occurs, and local deformation zones or crazes are not observed. The principle of “thin layer yielding mechanism” is schematically represented in fig 4.22a.

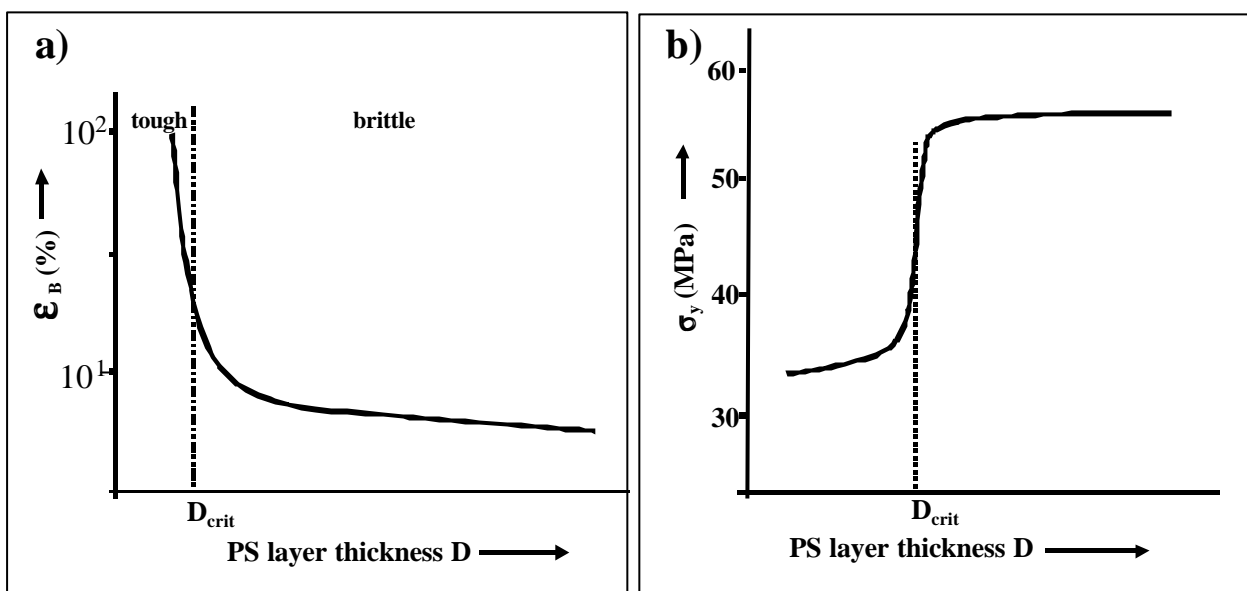


Figure 4.22: a) Scheme showing principle of thin layer yielding and b) σ_y drawn as a function of PS lamellar thickness.

A brittle material with a layer thickness D behaves brittle (characterised by a low strain at break, ϵ_B) as far as the value D is above a critical thickness (about 20 nm in the present case). Below this thickness, a strong transition to a very ductile fracture mode, as shown in fig 4.22a, (large elongation to break, ϵ_B) occurs. Results observed in lamellae forming star block copolymers indicate that this effect can be used as an alternative toughening mechanism in block copolymers.

Similar effects have been observed in heterogeneous polymeric systems having micro- and nanolayered structures [99,100]. In a polystyrene/polyethylene system van der Sanden and Meijer have observed a brittle/ductile transition when the layers had a thickness of about 40 nm [99]. A temperature dependence of layer thickness in these systems was also demonstrated. Hence, it becomes obvious that critical thickness may be highly coupled with the nature of interface between the components.

It can be assumed that the PB lamellae possess only a negligible load bearing capacity. The load is carried mainly by the PS lamellae with an effect of stress concentration. At a PB content of about 30% stress concentration in the PS lamellae can be expected to be about 1.4 times higher than the externally applied stress. Using this value and the yield stress determined by tensile testing of about 24 MPa (for example, star block copolymer ST2-S74), the internal yield stress of the PS lamellae can be estimated to be $\sigma_y^{lam} \approx 34$ MPa. This is significantly lower than the yield stress of 55 MPa for bulk PS (the crazing stress in PS is in the order of 55 MPa [42,97]). Therefore, the schematic illustration of figure 4.22a can be redrawn as shown in fig 4.22b.

Below the critical thickness of PS lamellae, the yield stress of PS lamellae σ_y^{lam} is sufficiently low to induce a large plastic flow of PS lamellae leading to the ductile behaviour of the star block copolymer. If the thickness of PS lamellae exceeds the critical value of about 20 nm, a

strong increase in yield stress of PS lamellae occurs. Hence, the yield stress of thick PS lamellae reaches the crazing stress of polystyrene. Then, the deformation leads to the formation of craze-like deformation zones, and the polymer behaves brittle.

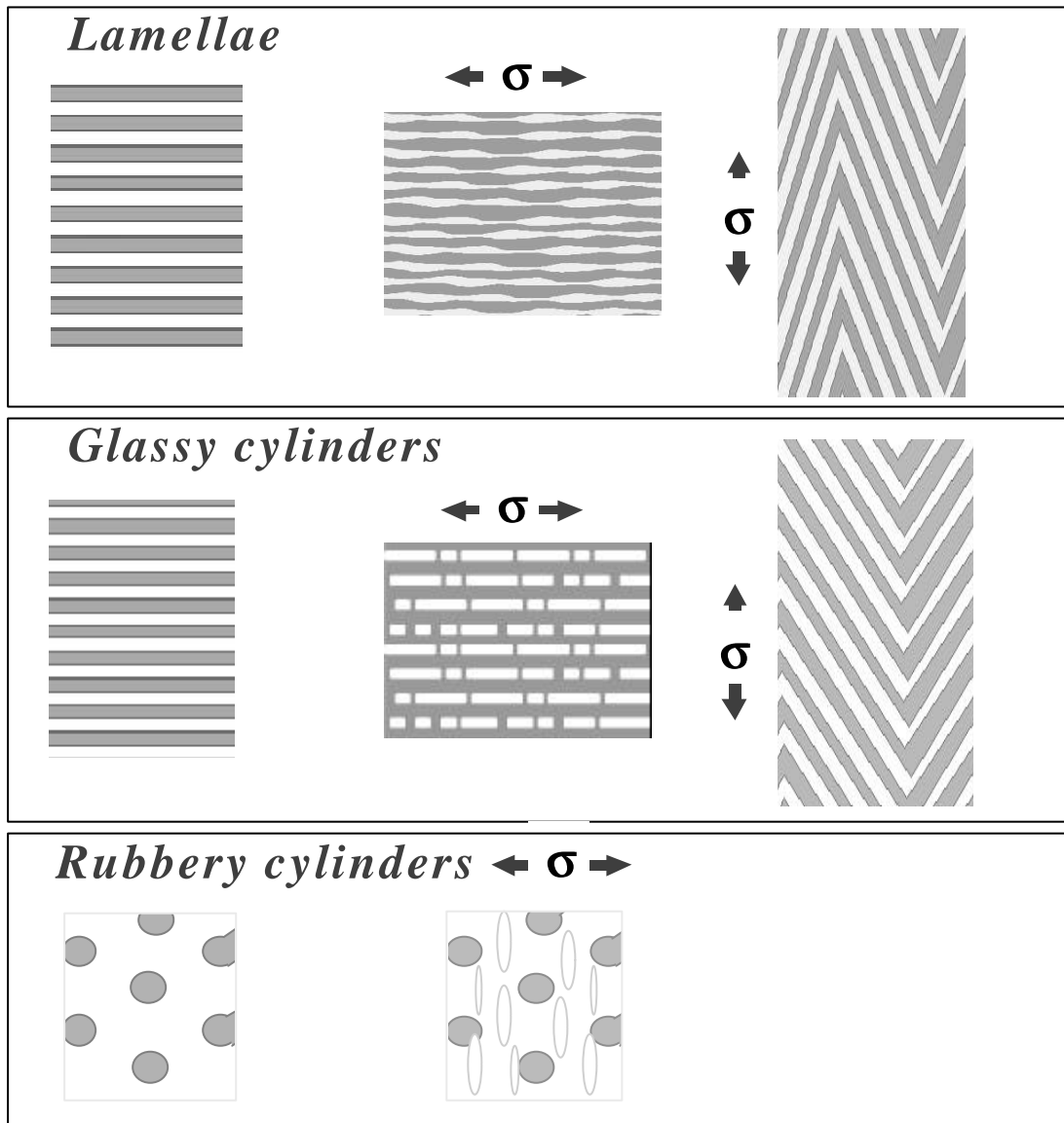


Figure 4.23: Scheme showing deformation mechanisms in ABA triblock copolymers at large strains as a function of morphology.

The reported deformation mechanism of lamellar block copolymers, especially the star block copolymers, is the result of the modified molecular architecture compared to the common diblock copolymers. Firstly, the larger number of arms in star block copolymers enable a better molecular coupling even at low molecular weights. At low molecular weights the properties of diblock copolymers show a molecular weight dependence. This means that in diblock copolymers with the same lamellae thickness a thin layer yielding mechanism cannot be observed because of the low molecular weight of the corresponding blocks which are unable to form entanglements. Thus, SB diblock copolymers with total molecular weights of about 100,000 g/mole appear to be quite brittle. However, for diblock copolymers with higher

molecular weights, the long period increases and thus the thickness of lamellae do not fulfil the conditions proposed in Fig 4.22.

On the basis of the results discussed above, deformation mechanisms in ABA type amorphous block copolymers (where A and B are glassy and rubbery blocks, respectively) with respect to microphase separated morphology may be summarised as illustrated schematically in fig 4.23.

4.3.4 Additional Evidences of Thin Layer Yielding Mechanism

The validity of thin layer yielding mechanism can be alternatively tested by selectively cross-linking the butadiene phase, and examining whether the PS lamellae further show large plastic deformation. For this purpose, tensile bars of two lamellar samples LN2 and ST2 were cross-linked by exposing them at the atmosphere of γ -radiation at different doses. Tensile testing on the samples irradiated at a dose of 40 Mrad demonstrates that the samples show still a high degree of plastic deformation (fig 4.24).

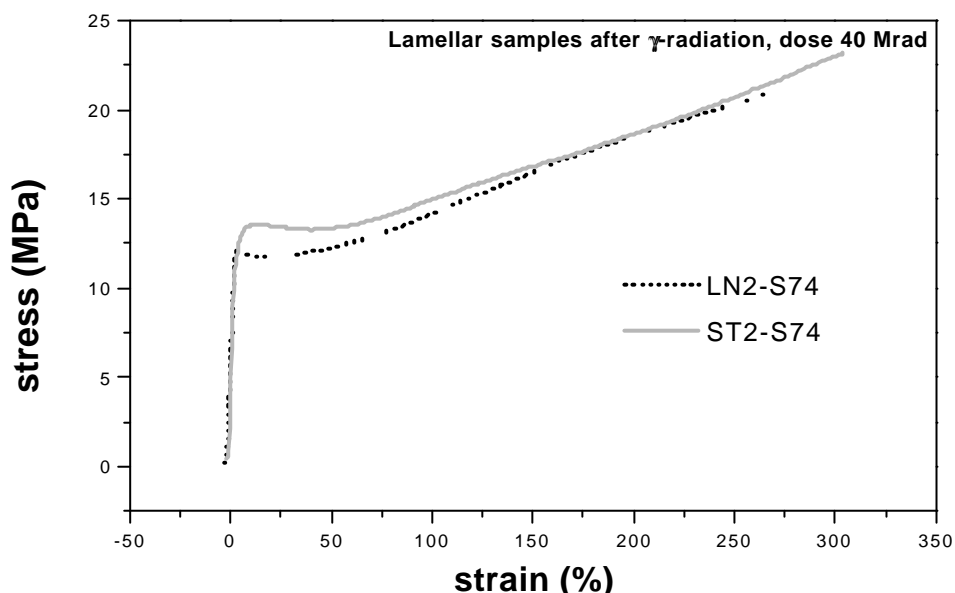


Figure 4.24: Stress-strain curves of two lamellar samples LN2 and ST2 after γ -irradiation (40 Mrad); Note that the samples show still a large degree of plastic deformation.

At higher irradiation doses, the elongation at break was found to decrease, however. Nevertheless, the samples showed a large plastic deformation even after selective cross-linking of butadiene phase as elucidated by TEM micrographs given in fig 4.25 (irradiation dose 60 Mrad). As in the micrographs of the samples without cross-linking (compare 4.25b with fig 4.13a), the micrographs show characteristic chevron-like morphology formed by the lamellae whose normal originally lies parallel to the strain axis. Moreover, the lamellae show locally very large plastic deformation. These results suggest that plastic deformation of PS lamellae, about 20 nm in thickness, is their inherent characteristic. The fact that higher cross-linking (60 Mrad and onwards) led to the imbrittlement of the sample may imply that a thin flexible layer between the glassy layers is essential for the 'thin layer yielding' mechanism.

A further evidence of plastic deformation of PS lamellae may be obtained by testing the sample at variable temperature and strain rate. It may be expected that lowering the temperature (or increasing the strain rate) would shift the critical thickness towards smaller values and vice versa. Tensile tests on lamellar samples were carried out at different temperatures (from room temperature down to glass transition temperature of the rubbery block) and strain rates [171]. At -30°C , for example, star block copolymers ST1 and ST2 show necking and drawing of PS lamellae (fig 4.26).

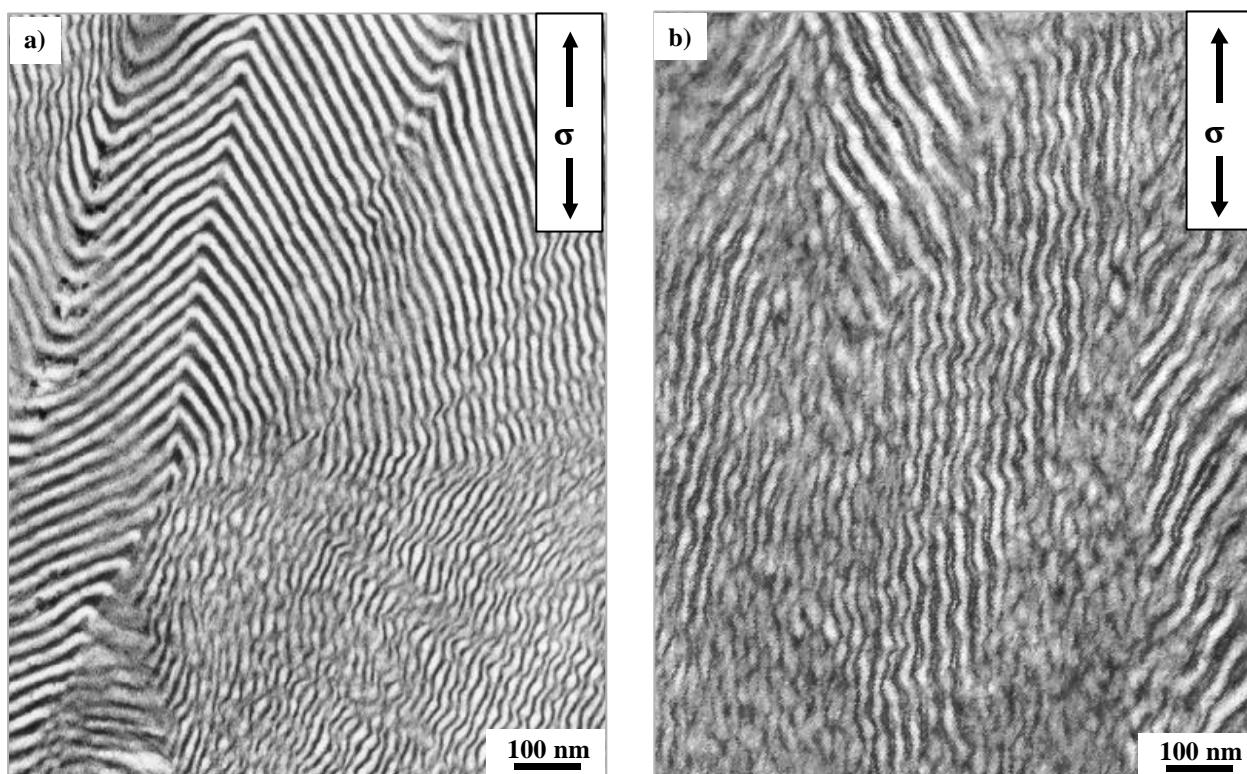


Figure 4.25: TEM images of strained a) LN2 and b) ST2 showing chevron-like morphology and plastically deformed PS and PB lamellae (strained after γ -irradiation).

The local thickness of PS lamellae in the samples deformed at -30°C is close to that of samples deformed at room temperature. But the TEM micrographs make it clear that alternating ‘thicker and thinner regions’ along PS lamellae in ST1 are more pronounced than in ST2. The more homogeneous deformation of ST2 at lower temperature might be a result of its special molecular architecture as discussed earlier, and further indicates the role of adjacent butadiene layers in effective drawing of PS lamellae. Because the adjacent PB layers in ST2 are practically thicker (due to more ellipsoidal conformation and presence of ‘filler’ domains) than that in ST1, the plastic deformation at lower temperature seems to be less hindered in ST2. Nevertheless, more pronounced appearance of alternating thicker and thinner regions along a PS lamella at -30°C (which is more clearly visible in ST1 fig 4.26 a) suggests that yielding of PS lamella is hindered at lower temperature, i.e., the lower the temperature the more difficult would be the ease of plastic deformation of polystyrene lamellae. In other words, the critical thickness would shift

towards smaller value with decreasing temperature and vice versa. Similar effect will exercise the increased strain rate. However, PS lamellae deform still in ductile manner up to a temperature of -30°C .

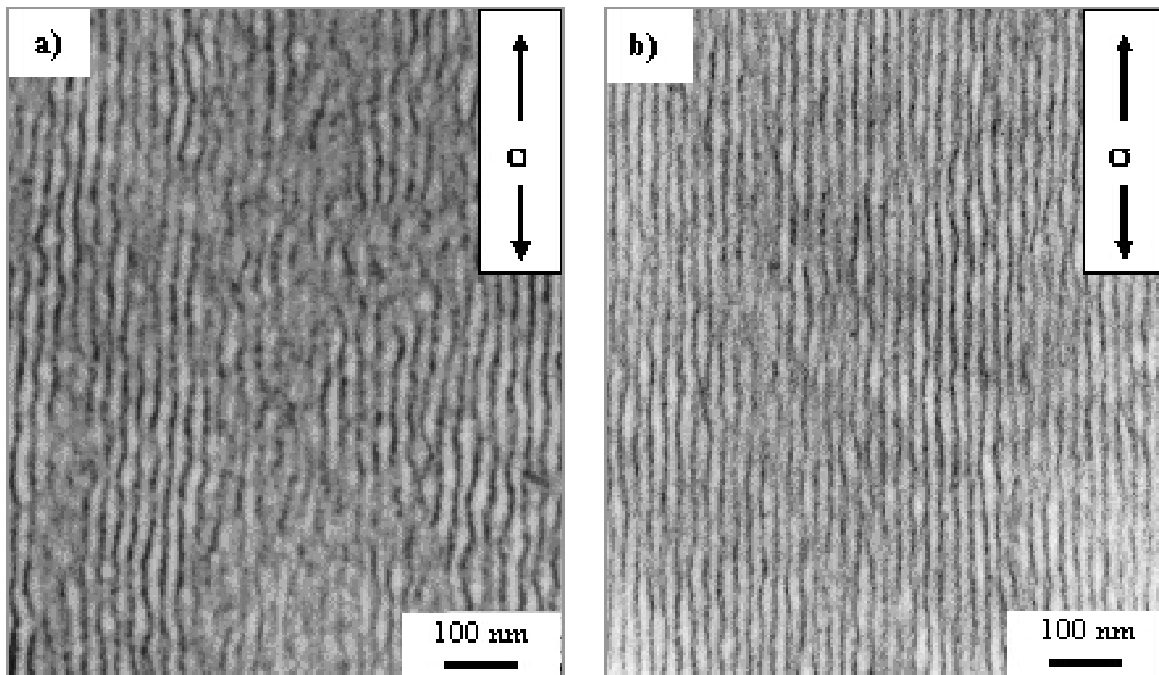


Figure 4.26: TEM micrographs of a) ST1 and b) ST2 showing deformation structures at -30° , injection moulded samples strained at a cross head speed of 50 mm/min.

4.4 Fracture Toughness of the Block Copolymers

For many practical applications of block copolymers, mechanical properties under impact loading conditions are important. Hence, fracture toughness of block copolymers (J -integral, crack-tip opening displacement, δ) are determined using different concepts of elastic-plastic fracture mechanics (J -integral and crack tip opening displacement CTOD-concept).

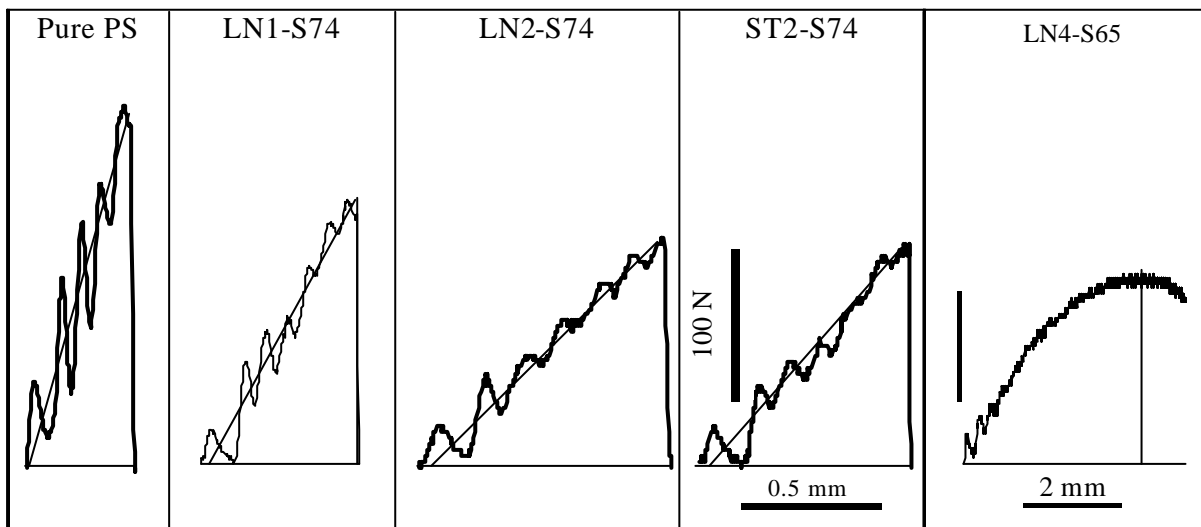


Figure 4.27: F-f diagrams of different block copolymers compared to pure polystyrene, injection moulded SENB specimens loaded at a rate of 1.5m/s perpendicular to the injection direction;. The scale bars for the first three samples are same as that for ST2-S74.

Representative load-deflection (F-f) curves of few block copolymers compared with that of pure PS are given in fig 4.27 and the corresponding fracture toughness values (defined by J -integral J , and CTOD value δ_{dk}) determined by evaluating the F-f curves are indexed in table 4.4.

From F-f-diagrams of the block copolymers presented in fig 4.27, at a first glance, it may be seen that the block copolymers having $\Phi_{\text{Styrene}} = 0.74$ show principally same behaviour as pure polystyrene under impact loading conditions: nearly linear-elastic behaviour and predominantly unstable crack propagation. The existence of exclusively small plastic deformation (small scale yielding) can be shown by fracture surface morphology of specimens that broke in a brittle manner (demonstrated on example of ST1 in fig 4.28). The fracture surface reveals a small region of stable crack growth and a small CTOD-value. Only the linear triblock copolymer LN4 shows elastic-plastic behaviour combined with predominantly stable crack propagation.

Table 4.4: J-integral and CTOD-values of investigated block copolymers.

materials	J -integral values (N/mm)	CTOD-values (10^{-3} mm)	s_{dY} (MPa)	E_d (MPa)	behaviour
LN1-S74	2.8±0.4	17±2	66.9±1.5	1409±36	linear elastic
LN2-S74	4.2±0.5	45±7	31.4±5.8	798±19	linear elastic
LN4-S65	-	-	4.9±0.5	168±12	elastic-plastic
ST1-S74	4.3±0.4	45±7	23.1±0.5	710±19	linear elastic
ST2-S74	3.3±0.1	35±5	38.3±4.3	965±49	linear elastic

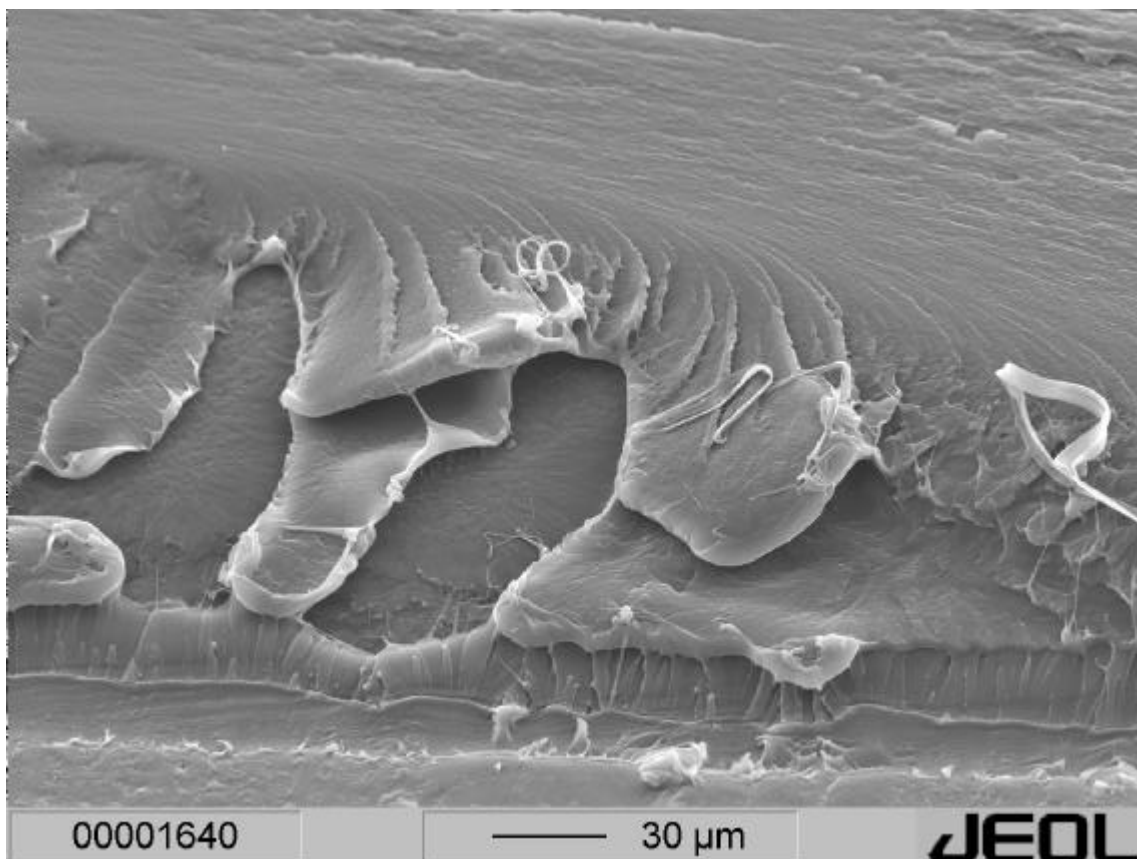


Figure 4.28: SEM micrograph showing fracture surface morphology of lamellar star block copolymer ST1.

In other words, the lamellar block copolymers that were found to be ‘tough’ in quasi-static tensile testing behave ‘brittle’ under impact loading conditions. It is, however, very easy to notice that the lamellar block copolymer have higher value of J-integral and crack tip opening displacement (δ_{dk}) values than cylindrical block copolymer LN1 indicating a larger amount of energy dissipation (table 4.4). On the fracture surface morphology of sample ST2 (fig 4.28), the sharp razor blade notch is followed by a stretch zone formed by notch tip blunting. Behind the stretch zone, there is a narrow zone showing a small scale yielding.

The brittle behaviour of lamellar block copolymers under impact loading may provide reason for loading rate dependence of thin layer yielding mechanism discussed in section 4.3.3. It may be assumed that the critical thickness of PS layers shifts towards smaller value at elevated strain rate.

4.5 Conclusions

In this chapter, correlation between molecular architecture, morphology formation and deformation behaviour of asymmetric styrene/butadiene block copolymers ($\Phi_{\text{Styrene}} \sim 0.70$) has been discussed. In the investigated narrow composition range, all the principal classical morphologies (viz., PS domains, alternating PS and PB lamellae, PB domains) have been observed.

While PB cylinders in PS matrix are observed in a symmetric linear SBS triblock copolymer (LN1-S74), lamellar morphology is found in an asymmetric linear triblock copolymer (LN2-S74) having identical composition. The star block copolymers ST1-S74 and ST2-S74 possessing identical chemical composition as LN1 reveal lamellae-like morphology, as well. Particularly, a “two-component three-phase” morphology has been observed in the tapered star block copolymer ST2-S74 which consists of alternating PS and PB lamellae with PB lamellae embedding cylinder-like polystyrene domains.

A symmetric triblock copolymer containing a styrene-co-butadiene middle block (LN4-S65) show randomly distributed cylinders in rubbery matrix due presence of styrene-co-butadiene middle block and 32 vol % of polystyrene outer blocks. This morphology resembles that of a system close to the order-disorder transition (ODT) in spite of sufficiently high molecular weight of outer polystyrene blocks (~ 18000 g/mole).

The observed lamellar structure of the asymmetric block copolymers (LN2, ST1 and ST2; all with $\Phi_{\text{Styrene}} \sim 0.74$) corresponds to the morphology that would be expected in a symmetric diblock having lower polystyrene content (i.e., $\Phi_{\text{Styrene}} \sim 0.50$). That means, the order-order transitions (OOT) are shifted towards higher polystyrene content. These results provide qualitative experimental evidences on the shift of block copolymer phase diagram (with respect

to $(\chi N)_{\text{crit}}$ and Φ_{eff} as schematically illustrated in fig 4.29) by a change in molecular architecture. Hence, by altering the phase behaviour of the block copolymers via architectural modification and choosing suitable preparation conditions, one can exercise considerable control over their deformation mechanisms and mechanical properties.

In contrast to diblock copolymers with PB domains in PS matrix, where the rubber phase cavitation is followed by necking and drawing of glassy phase, PS phase cavitation is found to predominate in SBS triblock copolymer having analogous morphology. The deformation of lamellae is strongly dependent on their orientation. For the lamellae situated parallel to strain direction, ‘thin layer yielding’ mechanism prevails while the formation of chevron morphology predominates for the lamellae aligned originally perpendicular to the strain direction. Interplay between glassy domains fragmentation and chevron formation occurs in block copolymers having PS domains in rubbery matrix.

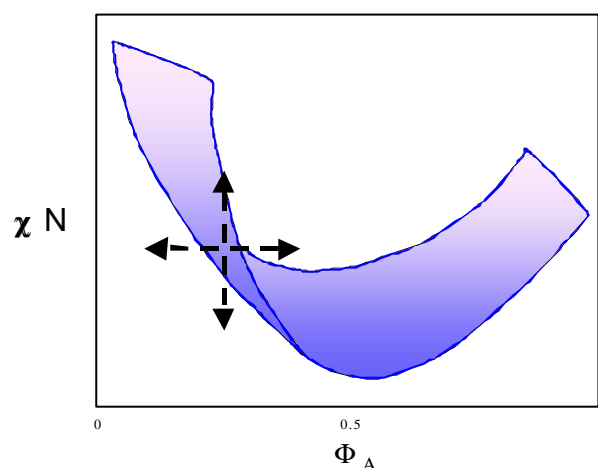


Figure 4.29: Schematic representation of shift in block copolymer phase diagram via architectural modification; the arrows stand for the direction of shift of phase boundaries.

Asymmetric styrene/butadiene block copolymers forming lamellar structure show a homogeneous plastic flow of glassy and rubbery layers (the ‘thin layer yielding’ mechanism) provided that the glassy layers meet the criterion of critical layer thickness D_{crit} . This mechanism may be used as alternative toughening mechanisms in glassy polymers. In styrene/butadiene block copolymers, the $D_{\text{crit-PS}}$ is found to be ~ 20 nm. However, a more precise quantification of this criterion requires the systematic variation of layer thickness and corresponding micromechanical investigation as a function of loading condition (e.g., temperature, strain rate).

The investigated block copolymers with modified architecture in a narrow composition range ($\Phi_{\text{Styrene}} \sim 0.70$) exhibit mechanical behaviours which would be expected in classical block copolymers in a broad composition range ($\Phi_{\text{PS}} \sim 0.25-0.75$). Thus, to generalise, architectural modification in ABA type block copolymers (A and B are glassy and rubbery blocks, respectively) opens a novel way of micromechanical construction of these nanostructured polymeric materials.

5. STRUCTURE-PROPERTY-CORRELATIONS IN BLOCK COPOLYMER/PS BLENDS

5.1 Phase Behaviour and Morphology

In this section, star block copolymer ST2-S74 is blended with polystyrene homopolymer (hPS) with variation of hPS molecular weight (M_{hPS}) and blend composition (Φ_{hPS}). The characteristics of used hPS are listed in table 3.2 in chapter 3. Homopolystyrene samples having weight average molecular weight of 15.2, 33.1 and 190.0 kg/mole are designated as PS015, PS033 and PS190, respectively. First, influence of M_{hPS} on the miscibility and mechanical properties of the blends is examined changing the M_{hPS} and keeping the blend composition constant ($\Phi_{\text{hPS}} = 20 \text{ wt } \%$) using solution cast samples. Then, ST2 is melt blended with general purpose polystyrene (GPPS, designated as PS190 in table 3.2) in a wide composition range and processed via injection moulding.

5.1.1 Dynamic Mechanical Properties

Results from dynamic mechanical analysis (DMA) presented in fig 5.1 are helpful to understand the compatibility between ST2 and added polystyrene in relation to the molecular weight of hPS (i.e., M_{hPS}). Two hPS samples are chosen: PS015 whose molecular weight is much smaller than the longest PS block of the block copolymer ($M_{\text{hPS}} \ll M_{\text{PS-block}}$) and PS190 whose molecular weight is higher than that of corresponding block of the copolymer ($M_{\text{hPS}} > M_{\text{PS-block}}$).

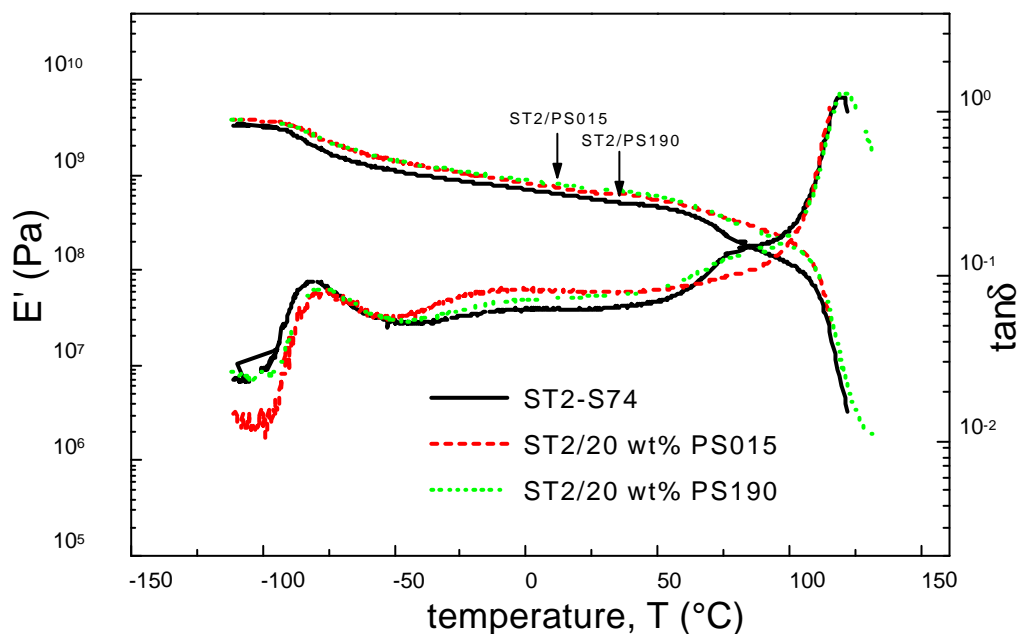


Figure 5.1: DMA spectra of star block copolymer/hPS blends as a function of hPS molecular weight, ($\Phi_{\text{hPS}} = 20 \text{ wt } \%$); solution cast sample about 0.5 mm thick measured at 1Hz (the storage modulus curves of the blends are very close to each other).

The glass transition temperatures of the butadiene phase ($T_{\text{g-PB}}$) in the pure star block copolymer ST2-S74 and both ST2/PS015 and ST2/PS190 blends (determined by peaks $\tan\delta$ vs. T curves) are located nearly at the same position. A closure look, however, reveals that $T_{\text{g-PB}}$ in the blends

are shifted slightly towards higher temperature (Although it is a small shift, this observation is supported by a number of experiments). In contrast, the glass transition temperature of the polystyrene phase T_{g-PS} doesn't change. During the DMA experiment, the blend containing polystyrene homopolymer with higher molecular weight (PS190) is found to be more stable at higher temperatures close to T_{g-PS} which may be attributed to the formation of stronger entanglement networks by the added polystyrene. In general, the T_{g-PS} peak observed at about 75°C in star block copolymer (discussed in section 4.1.1 in detail) appears in the Star block copolymer/hPS blends as well.

These observations are in line with recent results of Feng et al. [79,80] who investigated the compatibility of added hPS with block copolymer by blending polystyrene with variable molecular weights with star and triblock copolymers. These authors have suggested that there exists a range of M_{hPS} for the added homopolystyrene to be compatible with the block copolymer. They found the dissolution of a part of low molecular weight polystyrene in the butadiene phase which was manifested by an increase in glass transition temperature of the butadiene phase (T_{g-PB}).

Regardless of M_{hPS} , a part of added hPS is mixed to the butadiene phase which is attributed to the presence of broad molecular weight distribution of the hPS, low molecular weight fraction of which may be easily assimilated by butadiene phase as already discussed in the literature [79]. Low molecular weight fraction of a hPS may be mixed to the butadiene phase due to greater entropic contribution to mixing which results in an increase in T_{g-PB} . The area under the T_{g-PB} peak in ST2/PS015 is greater than the corresponding area in ST2/PS190 blend which indicates higher interaction between PB and styrene segments in the former blend.

5.1.2 Influence of hPS Molecular Weight on Morphology

The influence of homopolystyrene molecular weight on phase behaviour of block copolymer/hPS blends is demonstrated by TEM micrographs presented in fig 5.2 (data about the internal details of blend morphology in Table 5.1). The molecular weight of hPS lies in the following range: $M_{hPS} \ll M_{PS-block}$, $M_{hPS} < M_{PS-block}$ and $M_{hPS} > M_{PS-block}$. The composition of the blends is fixed at 20 wt % hPS in each case. The observed morphology can be explained on the basis of molecular weight of the homopolymer relative to that of the corresponding block of block copolymer ($M_{hPS}/M_{PS-block}$).

An interplay between microphase and macrophase separation is observed in these blends. The molecular weight of added PS015 ($M_n = 11,800$ g/mole) is much smaller than that of the longest PS block of the star block copolymer ($M_n \sim 70,000$ g/mole) but is slightly higher than that of the smaller blocks ($M_n \sim 7,000$ g/mole). Hence, according to the situation discussed in section 2.3

[74-78], most of the hPS is solubilized into the PS domains of the block copolymer leading to the microphase separated structures given in fig 5.2a.

Due to solubilization of homopolymer in corresponding copolymer block, respective domain size may expand both laterally and normal to the interface. The expansion of PS lamellae normal to the interface is indicated by an increase in the thickness of the PS lamellae (table 5.1 and fig 5.3). The mixing entropy of hPS increases with the ratio $M_{PS\text{-block}}/M_{hPS}$. Since this ratio is quite high in ST2/PS015 blend, the hPS molecules are able to penetrate deeply into the PS domains close to the chemical junction points [76]. As a result, the junction points are shifted apart. To compensate this shift and to make up entropy loss, butadiene phase has to contract which causes a decrease in lamellar long period. The decrease in the PB lamellae thickness should be more than compensated for by an addition of a small amount of low molecular fraction of PS015 in the butadiene phase as indicated by an increase in $T_{g\text{-PB}}$.

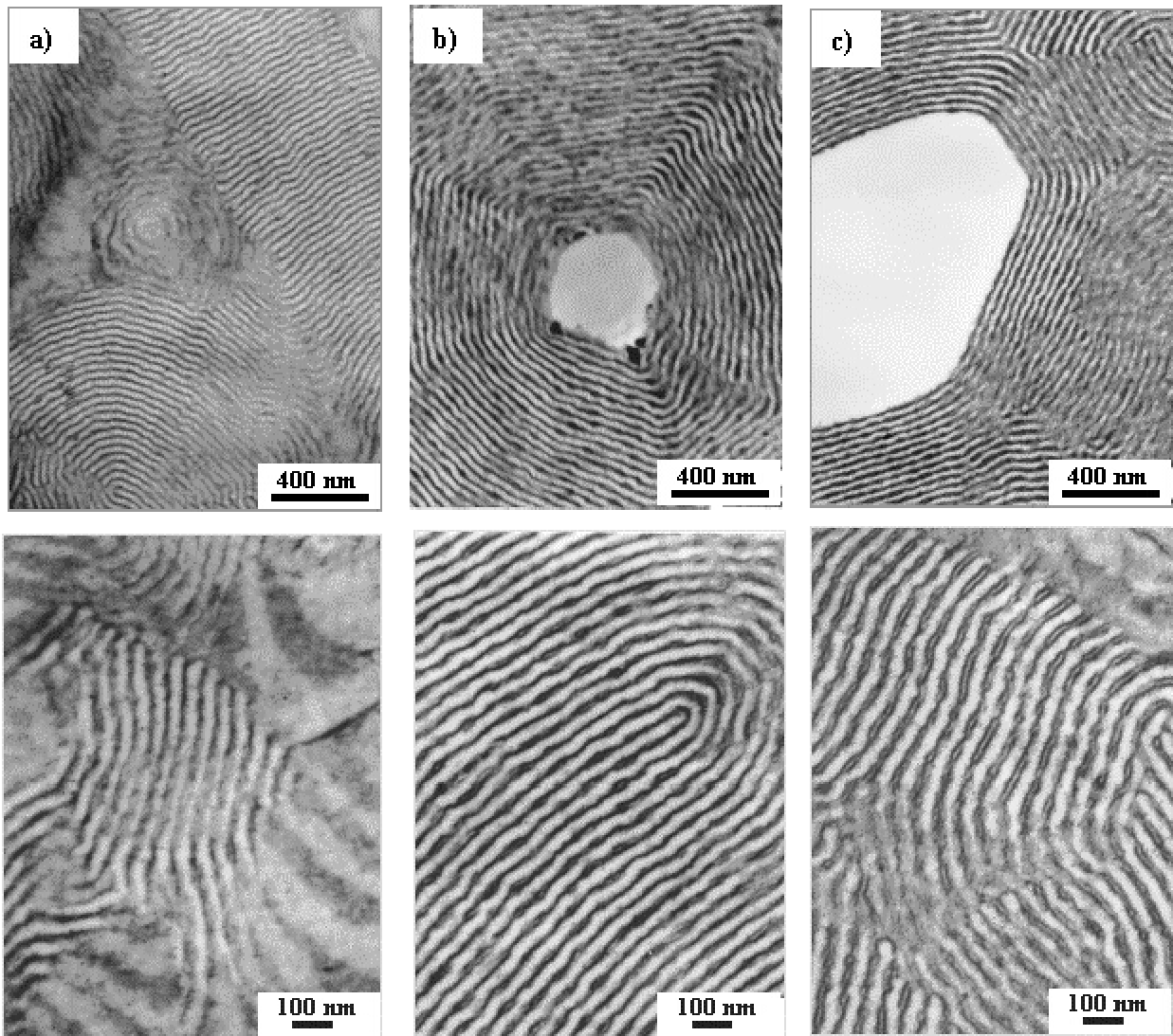


Figure 5.2 Lower (top) and higher (bottom) magnification of TEM images showing morphology of solution cast ST2/hPS blends as a function of hPS molecular weight (M_{hPS}); a) ST2/PS015, b) ST2/PS033 and c) ST2/PS190; blend composition in each case is $\Phi_{hPS} = 20$ wt %.

As M_{hPS} approaches $M_{\text{PS-block}}$, mixing entropy of the homopolymer chains is decreased, and these chains become less successful to wet the copolymer brush effectively. The hPS and PS block become, hence, less miscible. As a result the copolymer shrinks, and the hPS chains tend to be segregated in the middle of the PS domains or even completely expelled from the microdomains to form the macrophase separated PS particles (chapter 2 in ref. [2]). Nearly this situation is present in ST2/PS033 blend. Since a large part of PS033 molecules tend to segregate to the centre of the PS lamellae, the thickness of PS lamellae increases (table 5.1) while the junction points are not displaced. Hence, the PB lamellae thickness is again maintained. This causes a small increase in lamellar long period in sample ST2/PS033. However, a part of hPS is expelled out of the PS lamellae which forms hPS particles few hundred nanometers in diameter (fig 5.2b).

Table 5.1: Average lamellar long period (\bar{L}) and PS lamellae thickness (\bar{D}_{PS}) measured in TEM images of solution cast ST2/20 wt % hPS blends (Variation of hPS molecular weight). The values correspond the peak of corresponding Gaussian fitting of the data.

blends	\bar{L} (nm)	\bar{D}_{PS} (nm)	remarks
pure ST2	39-54	20.2	-
ST2/PS015	37-43	22.2	hPS completely solubilized in PS block of ST2-S74
ST2/PS033	42-58	22.1	hPS only partly solubilized, hPS particles about 0.3-1.0 μm in diameter
ST2/PS190	49-54	21.2	hPS almost completely macrophase separated, hPS particles about 1-4 μm in diameter

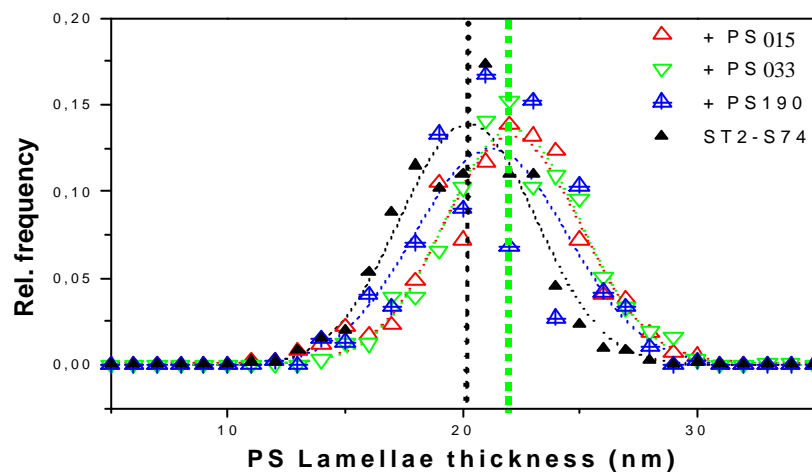


Figure 5.3: PS lamella thickness distribution in ST2/hPS blends as a function of M_{hPS} compared to pure ST2.

Molecular weight of PS190 is much larger than that of any PS blocks of ST2 (i.e., $M_{\text{hPS}} > M_{\text{PS-block}}$). Hence, the hPS molecules tend to phase-separate forming large hPS particles in block copolymer matrix (fig 5.2c). The three-phase morphology of the matrix is again maintained, and large PS190 particles few microns in diameter are formed. Nevertheless, owing to a broad molecular weight distribution of polystyrene, a part of lower molecular weight fraction of PS190 may be expected to solubilize in the PS domains.

It may be, in general, assumed that criteria for solubilization of homopolymers in the corresponding block of copolymers discussed is valid for investigated asymmetric star block copolymer/hPS blends. So, an increase in concentration of PS190 would lead to further macrophase separation, and finally, block copolymer particles in PS190 matrix are expected at higher PS190 concentration. Detailed analysis of morphology formation in ST2/hPS blends is, however, outside the scope of this work.

5.1.3 Morphology of Injection Moulds

Variation of sample preparation methods, especially the choice of solvents may have a dramatic effect on morphology of block copolymer/hPS blends. Common processing methods like injection moulding, compression moulding, extrusion etc. can cause a remarkable deviation from the equilibrium structures, which can ultimately influence their deformation behaviour.

Morphology of injection moulded star block copolymer ST2-S74 as discussed in chapter 4 consists of alternating PS and PB lamellae with PB layers embedding scattered PS domains about 6-9 nm in diameter. The PS and PB lamellae are about 22 nm and 12 nm thick, respectively. The PS lamellae are often disconnected. The lamellae are aligned parallel to the injection moulding direction (section 4.3.2).

Injection moulded ST2-S74/PS190 blend with $\Phi_{\text{hPS}} = 20$ wt % maintains the lamellar morphology of the host star block copolymer (fig 5.4). The PS lamellae in this blend are more continuous in contrast to the partly disconnected 'worm-like' PS lamellae of pure injection moulded ST2. Quantification of PS lamellae thickness reveals that it is increased by about 20% (fig 5.5). The PB phase still embeds scattered PS domains.

Precise inspection of low magnification electron micrographs in fig 5.4 (a,b) reveals two distinct regions: one of them contain more polystyrene and appear lighter (shown by letter **L**). The other regions contain lesser polystyrene and appears darker (shown by letter **D**). Both the regions have lamellar structure. PS lamellae in the former are, obviously, thicker than the latter. This appearance suggests that added polystyrene is unevenly distributed in the corresponding block of the block copolymer. However, appearance of few thick polystyrene layers (thickness up to few hundred nanometers) further implies that added PS190 would macrophase-separate under equilibrium conditions.

Presence of lamellar stripes, containing higher and lesser amount of styrene (lighter **L** and darker **D** regions in fig 5.4, respectively), in the blends can be possibly explained on the basis of molecular structure of the star block copolymer.

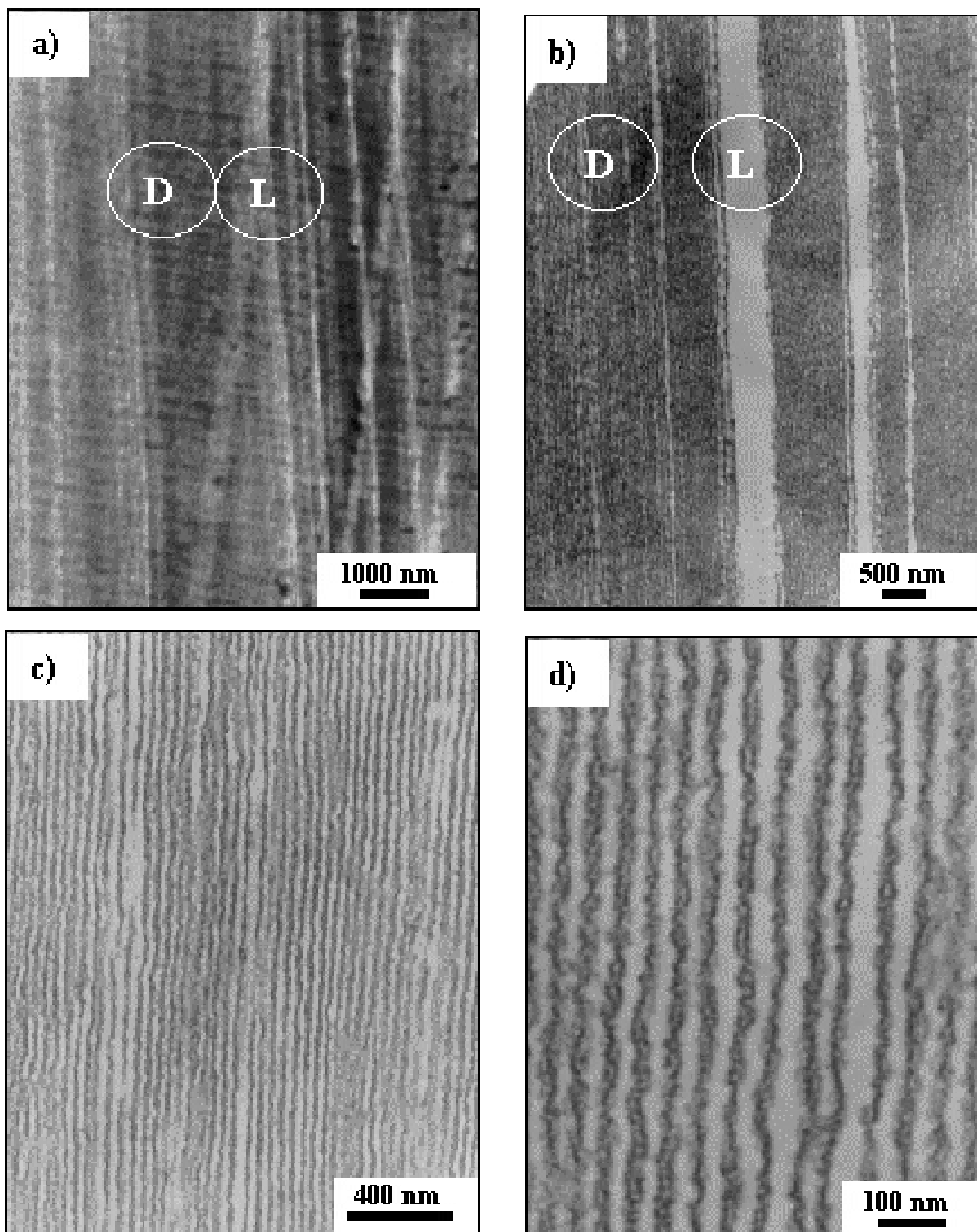


Figure 5.4: Representative electron micrographs showing morphology of injection moulded ST2-S74/20 wt % PS190 blend ($\Phi_{\text{hPS}} = 20$ wt %): a-b) Lower magnification of HVEM (left) and TEM (right) images at the middle of the tensile bar; c-d) Lower (left) and higher (right) magnification of TEM images close to surface; injection moulding direction vertical.

ST2 molecules are prepared by coupling tapered SBS triblocks of different lengths (both styrene-rich and butadiene-rich triblocks) using an oligofunctional coupling agent. Since the coupling is a statistical process it may result in stars having different number of arms. The stars can differ in net chemical composition as well [41,42]. Detailed analysis has shown that the stars possess

about four arms (personal communication with the an author of Ref. [41]), and among them one long arm in average (see fig 4.1). But there is a probability of formation of stars with two or more long arms. These stars are styrene-rich since each long arm already contains excess styrene. The polystyrene blocks of these styrene-rich stars, as one would expect, can solubilize more amount of added PS190. Hence, preferential solubilization of added PS190 in these styrene-rich stars leads to the formation of lamellar stripes having more amount of PS due to swelling of PS lamellae of the host copolymer (lighter regions indicated by **L** in fig 5.4).

Representative micrographs of samples with $\Phi_{\text{hPS}} = 40, 60, \text{ and } 80$ wt % of PS190 given in fig 5.6 reveal the following observations:

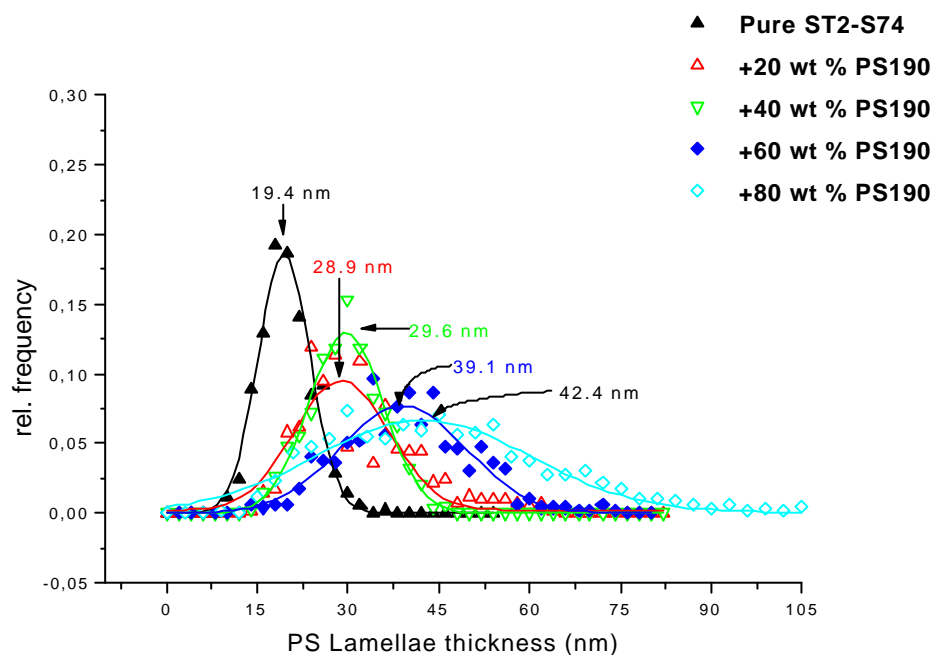


Figure 5.5: Distribution of PS lamellae thickness measured in TEM micrographs of injection moulded ST2/PS190 blends using a special image processing program; the distribution is fitted to a Gaussian function.

a) PS lamellae become thicker and thicker with increasing PS190 content while the PB lamellae also show a slight increase in thickness. At higher PS190 content (≥ 60 wt %), the PS lamellae fuse to form PS matrix which embed elongated “PB islands”. PS domains scattered in the PB phase are present irrespective of the blend composition.

b) Despite presence of few unusually thicker PS layers (thickness up to few hundred nm, fig 5.4), no particle-matrix morphology, typical of most polymer blends, is observed. This is the reason of why the blends are nearly as transparent as the block copolymer itself. The structures are too small to scatter light.

c) The microstructures are always oriented in flow direction as a result of the shear forces operating in the injection moulding process.

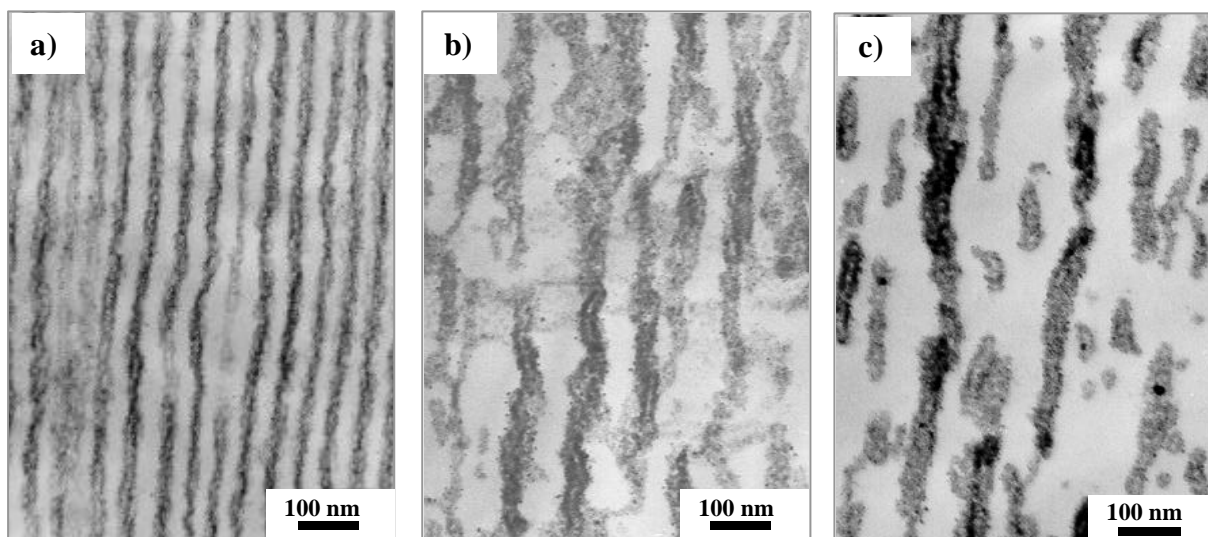


Figure 5.6: Representative TEM micrographs of samples containing a) 40%, b) 60% and c) 80 % by weight of PS190 in injection moulds; injection moulding direction vertical.

As the PS lamellae fuse to form PS matrix at higher PS190 content, it becomes more difficult to measure thickness of PS lamellae accurately. However, it is still possible to measure the thickness of PS domains which still assume “lamellar form”. With increasing hPS content, the thickness of PS lamellae (D_{PS}) and their distribution shift towards higher value. A continuous increase in D_{PS} as well as long period L (table 5.2) in these blends attests that a major part of PS190 has been added to the corresponding blocks of ST2. Further, the PB lamellae become wider at higher PS190 content (compare micrographs in fig 5.5d and 5.6) suggesting that a part of added PS190 is trapped by the butadiene phase as well.

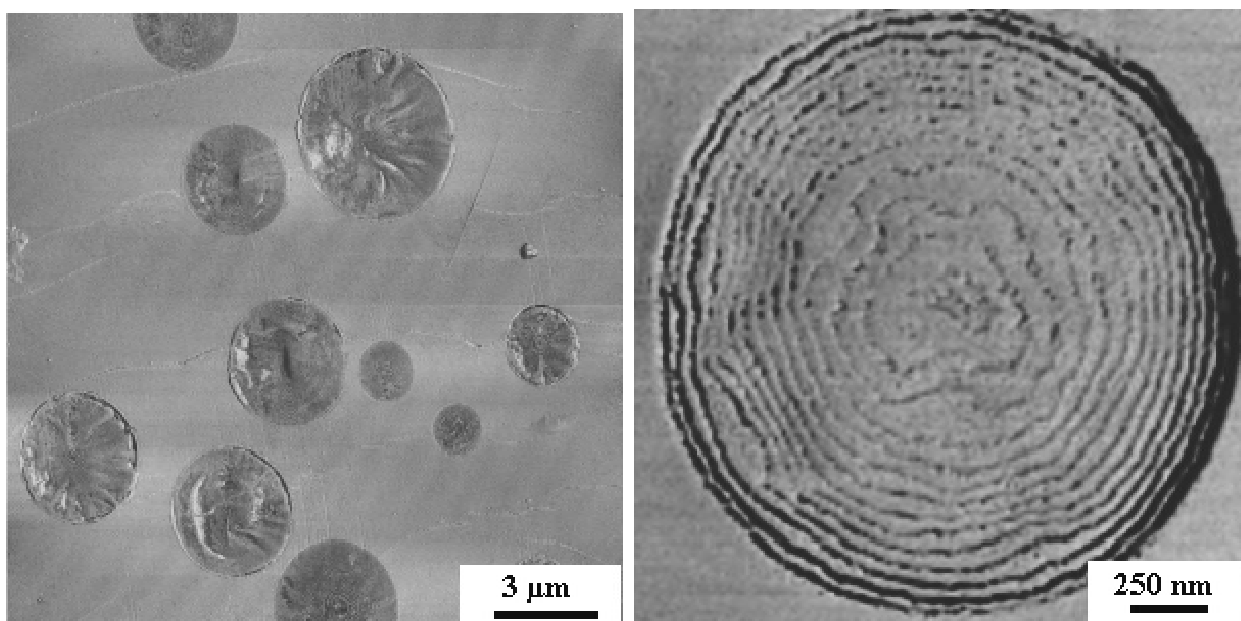


Figure 5.7: SFM phase images showing microphase separated ST2 particles in PS190 matrix; solution cast sample ($\Phi_{hPS} = 80$ wt %); the morphology of particles resembles that of concentric spherical shell (CSS) structures discussed in [114].

Under equilibrium condition, PB lamellae would not significantly widen. Neither would the blend maintain the layer structure. The blend would macrophase separate under equilibrium conditions. An example of macrophase separation of ST2/PS blend at higher PS content ($\Phi_{\text{hPS}} = 80$ wt %) is demonstrated by SFM phase images presented in fig 5.7.

In spite of presence of a few much thicker PS layers in injection moulded blends (see fig 5.4), pronounced macrophase separation is not observed. Hence, processing conditions seem to play very important role during structure formation in ST2-S74/PS190 blends. High shear stress of injection moulding process causes a forced miscibility in the melt state preventing the formation of large particles. If the melt is rapidly cooled, the microphase separated structures are frozen in. Moreover, a part of low-molecular-weight component of PS190 may be easily mixed to the PS (and even PB block as suggested by DMA results) blocks of the copolymer. These observations are in agreement with recent results of Knoll and Nießner [41,42]. These authors also found no macrophase-separated particles in compression moulded star block copolymer/hPS blends. Therefore, complex molecular structure of ST2-S74 seems to exercise a significant influence on miscibility with hPS.

Table 5.2: Average lamellar long period (\bar{L}) and PS lamellae thickness (\bar{D}_{PS}) measured in TEM images of injection moulded ST2/PS190 blends (variation of composition).

PS190 content	\bar{L} (nm)	\bar{D}_{PS} (nm)	remarks
0 (pure ST2)	42	20	-
20 wt %	46	29	50-230 nm thick PS layers are locally present
40 wt %	50	30	presence of thicker PS layers > 50 nm thick
60 wt %	72	39	-
80 wt %	85	42	-

5.2 Mechanical Properties

5.2.1 Tensile Behaviour

a. M_{hPS} dependence of tensile properties

Mechanical behaviour of block copolymers and their blends with homopolymers is determined mainly by their phase morphology. Stress-strain curves of solution cast ST2/hPS blends as a function of hPS molecular weight are given in fig 5.8 (corresponding morphologies in fig 5.2). The composition is fixed at 20 wt % hPS. Independent of hPS molecular weight, addition of hPS to the star block copolymer generally increases the load that the samples can withstand, but causes a decrease in elongation at break (ϵ_B) from about 350% to below 250%. The blends have ϵ_B of about 40 % smaller and yield strength (σ_Y) about 40% higher than that of pure block

copolymer. The stress level achieved by the blend ST2/PS190 is substantially higher than that of ST2/PS015 and ST2/PS033 blends.

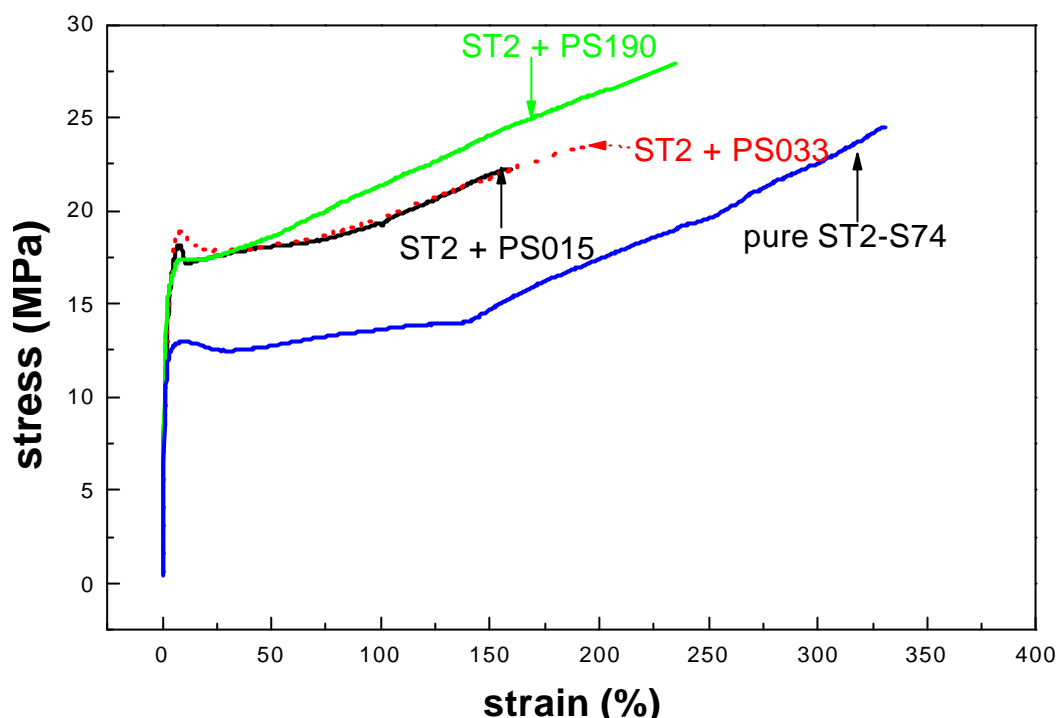


Figure 5.8: Stress-strain behaviour of star block copolymer/hPS blends as a function of hPS molecular weight; hPS content 20 wt % in each case, solution cast samples strained at a cross head speed of 50 mm/min.

The increase in strength arises from increasing overall PS content while a strong decrease in elongation at break ϵ_B is associated with the difference in deformability. Value of ϵ_B for the ST2/PS015 is still lower in spite of the absence of hPS particles. It may be attributed to the weakening of entanglements or plasticizing effect by the low molecular hPS ($M_n = 11,800$ g/mole and $M_w/M_n = 1.29$). During tensile testing, no pronounced macroscopic stress whitening was observed in this blend while it was pronounced in the others.

Mechanical properties of polymers are dependent on their molecular weights. To achieve a desirable level of strength, the polymers must exceed two times of a critical molecular weight (called entanglement molecular weight M_e ; for PS it is about 19,100 g/mole) which is essential for the formation of stable ‘molecular knots’ or entanglements [1]. The strength of ST2/hPS blends clearly shows molecular weight dependence of the added polystyrene (M_{hPS}): the lower the molecular weight the higher is the chance that the mechanical properties worsen. The lower level of strength of blends containing PS015 and PS033 (and even much lower elongation at break for ST2/PS015) results from the fact that their molecular weight is below (or nearly equal to) the entanglement molecular weight M_e of PS. The low molecular weight PS act as defect points and may lead to premature fracture. Conversely, enhanced strength of the blend ST2/PS190 may be explained by its molecular weight which is several times higher than M_e .

b. Tensile properties of injection moulded samples

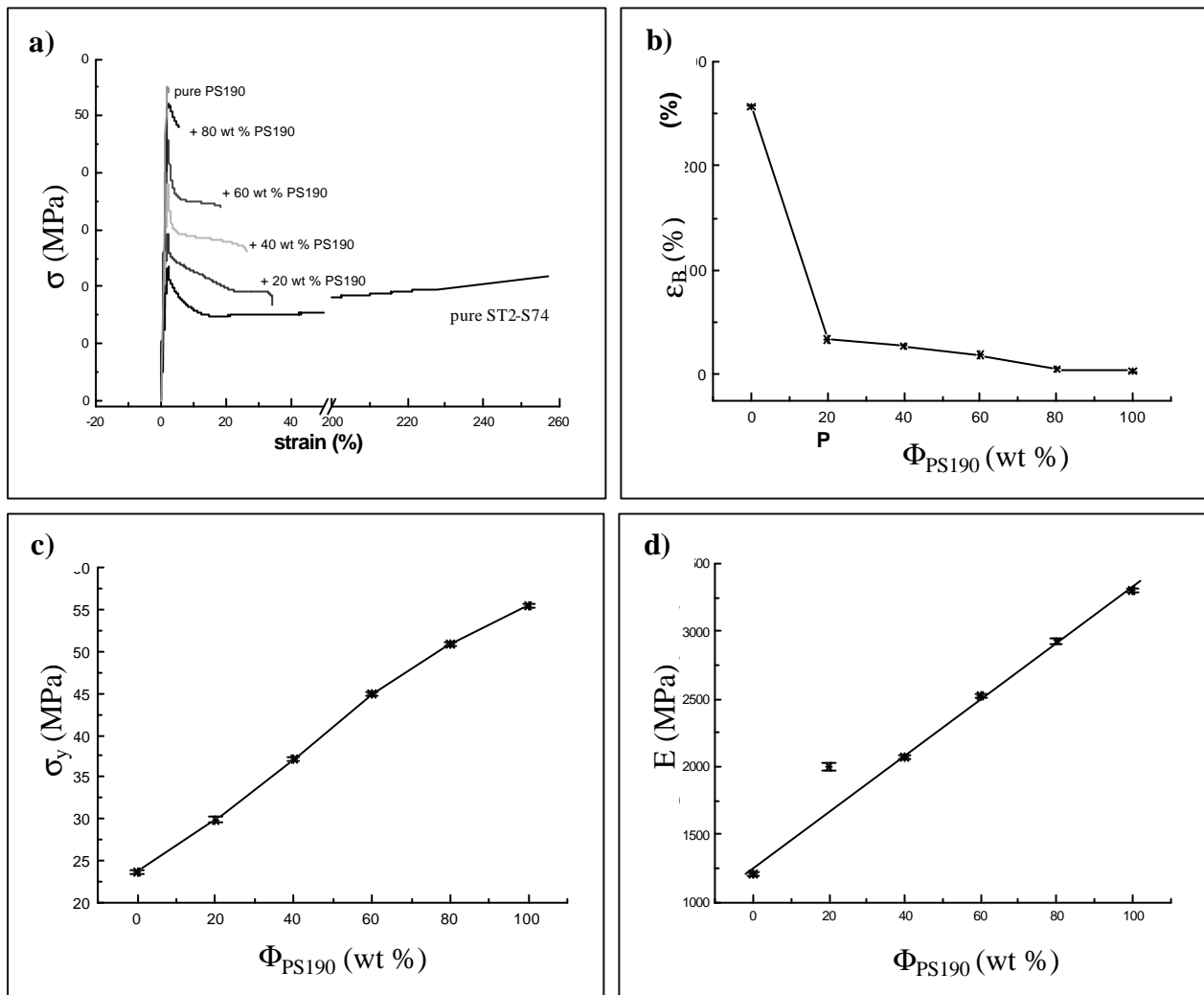


Figure 5.9: Stress-strain behaviour of injection moulded star block copolymer/GPPS blends as a function of PS190 concentration, tensile testing 50 mm/min at room temperature; a) σ - ϵ curves, b) elongation at break, c) yield stress and d) Young's modulus

Mechanical properties of solution cast samples are non-realistic in practical applications. Hence, tensile properties of injection moulded ST2/hPS blends over a wide composition range are studied. For this purpose, PS190 has been chosen for blending with ST2 since ST2/PS190 showed desirable mechanical properties even in solution cast films (fig 5.8). The stress-strain curves of these blends, given in fig 5.9a, differ from that of solution cast ones due to presence of dissimilar morphologies. Most significant differences are observed in the values of σ_y and ϵ_B . Injection moulded blends (e.g., one with 20 wt % PS190 in fig 5.9a) show higher yield strength (σ_y) and lower elongation at break (ϵ_B) than the solution cast films (fig 5.8). Higher yield strength of injection moulded samples results from higher thickness of PS lamellae (fig 5.4) and the orientation of microdomains. Elongation at break ϵ_B , yield stress σ_y and Young's modulus E of the blends are plotted as a function of blend composition in fig 5.9 (b-d). Yield strength and Young's modulus increase with increasing polystyrene content. The magnitude of ϵ_B falls

drastically at $\Phi_{\text{PS190}} = 20$ wt % suggesting a transition in deformation mechanism which shall be discussed in section 5.3.

A well-defined yield point appears during tensile deformation of pure ST2. After this point, the stress falls rapidly (strain softening), reaches a minimum and again rises slowly (strain hardening). This sample undergoes fracture at a strain and stress of 257% and 20 MPa, respectively. Macroscopically, the deformation occurs via necking and drawing of tensile specimen.

Yield point appear in injection moulded ST2-S74/PS190 blends as well. However, they show only strain softening. With increasing PS190 content, the extent to which the neck can elongate (drawing of the tensile bar) decreases and the tendency of brittle failure increases. Additionally, the blends exhibit a macroscopic stress whitening that indicate the formation of local deformation zones. The stress whitening becomes pronounced until a PS190 content of 40 wt %, and it becomes less pronounced at higher PS content.

Table 5.3: Mechanical properties of injection moulded ST2/PS190 blends, tensile testing 50 mm/min at room temperature; the errors are less than 5% in each case.

PS190 content	Young's mod. (Mpa)	yield stress (MPa)	stress at break (MPa)	strain at break (%)
0 (pure ST2)	1205	24	20	257
20 wt %	1296	30	19	34
40 wt %	2072	37	26	27
60 wt %	2522	45	33	18
80 wt %	2926	51	47	5
Pure PS190	3300	55	54	3

5.2.2 Fracture Mechanics

Fracture toughness of pure block copolymers was discussed in section 4.4. Lower toughness of lamellar block copolymers (which showed ductile behaviour in tensile test) was interpreted in terms of notch sensitivity of these materials and strain rate dependence of thin layer yielding mechanism. It is, therefore, plausible to assume that the notch sensitivity will strengthen with increasing PS190 content in the blends. Under impact loading conditions, injection moulded ST2/PS190 blends show similar behaviour as pure ST2: nearly linear elastic behaviour and predominantly unstable crack propagation combined with small scale yielding.

Fracture mechanics parameters determined as resistance against unstable crack propagation (J and δ_{dk}) are plotted as a function of blend composition Φ_{PS190} (wt %) in fig 5.10 which show a decreasing tendency of toughness with increasing PS190 content. Young's modulus (E_d) and

yield stress (σ_{yd}) increase with PS190 content. A sharp transition in fracture mechanics parameters as well as E_d and σ_{yd} occurs at a PS190 content of about 50 wt %. (Alternatively, an increase in toughness takes place at an ST2 content of about 50 wt %). It is quite interesting to note that this change takes place when the morphology changes from alternating lamellae to the presence of PS matrix. Decreasing tendency of toughness with increasing PS190 content in these blends may be attributed to increasing notch sensitivity.

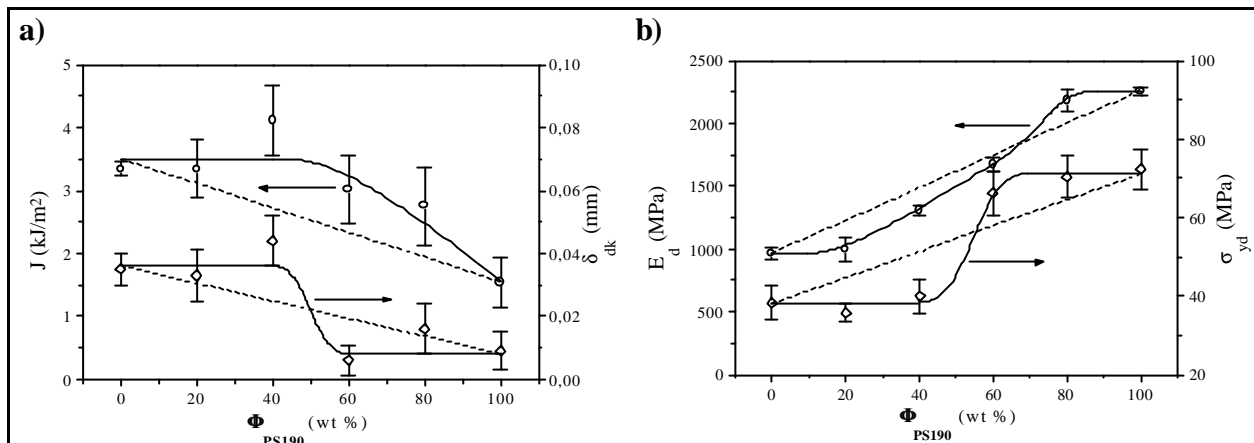


Figure 5.10: a) J-integral values (J) and CTOD values (δ_{dk}) plotted as a function of composition in injection moulded ST2/PS190 blends loaded perpendicular to the moulding direction; b) Young's modulus (E_d) and yield stress (σ_{yd}) in dependence of blend composition.

In contrast to the results of Yamaoka [144-146] who reported an increase in toughness of lamellar block copolymer by an addition of 20 wt % styrene-co-methacrylate copolymer (MS), the toughness level in injection moulded ST2/PS190 blends doesn't increase. This inconsistency arises from different morphology of the blends. In the blends containing stiff particles, the toughness may be enhanced by void formation at the poles of the particles and large plastic deformation of the surrounding matrix. This process is absent in injection moulded ST2/PS190 blends due to predominantly microphase separated morphology (fig 5.4 and 5.6).

One reason of the enhanced notch sensitivity and resulting lower toughness could be the orientation of molecules in injection moulded samples normal to the lamellar orientation direction, i.e., the chains assume elliptical coil conformation perpendicular to the lamellar orientation direction. [11,132] On loading the samples normal to the lamellar orientation direction (or injection direction), hence, the molecules are stressed parallel to the chain direction. So, the loading mode is most favourable for lowest toughness. Fracture toughness might be increased by isotropisation of morphology where the domains and the copolymer chains are randomly oriented.

5.3 Micromechanical Deformation Behaviour

5.3.1 Solution Cast Blends

In solution cast ST2/hPS blends, three different types of morphologies were observed depending on hPS molecular weight and blend composition: microphase separated blends (e.g., ST2/20 wt % PS015); macrophase separated blends having ST2 matrix (e.g., ST2/20 wt % PS190) and macrophase separated blends having PS190 matrix (e.g., ST2/80 wt % PS190). Accordingly, the micromechanical mechanisms may be discussed under three headings.

a. Microphase separated blends (e.g., ST2/20 wt % PS015)

In microphase separated blend where thickness of PS lamellae lies in the same range as the pure block copolymer ST2, similar deformation mechanism may be expected, i.e., the homogeneous plastic flow of PS and PB lamellae via thin layer yielding mechanism. Indeed, the deformation structures observed in this blend (fig 5.11) are very similar to that of pure block copolymer (compare to fig 4.13). The lamellae have been partly turned to strain direction and partly stretched strongly along the deformation direction. Chevron folds-like morphology, typically formed by folding of lamellae situated initially perpendicular to the strain direction, are observed too. An alternating array of thicker and thinner regions forming ‘bead-like’ structures along a deformed PS lamellae may further suggest the fluctuation of PS chain density in PS lamellae.

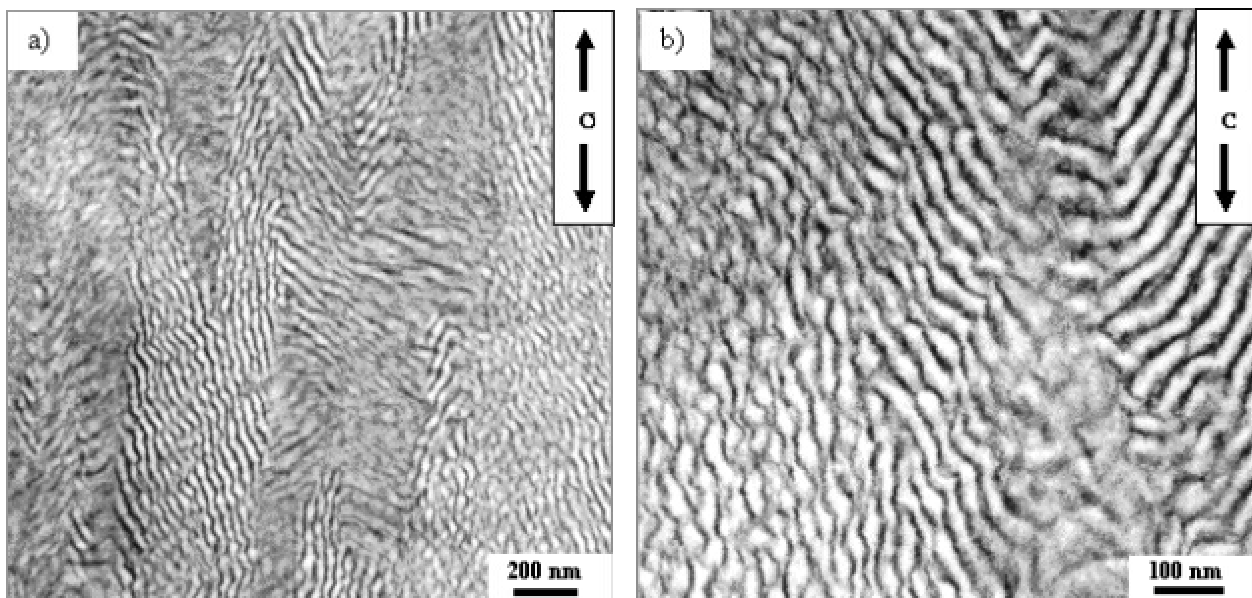


Figure 5.11: a) Lower and b) higher magnification of TEM micrographs revealing strain induced structural changes in microphase separated ST2/20 wt % PS015 blend; strain direction vertical (morphology of undeformed sample in fig 5.2a).

In spite of analogous morphology and similar deformation structures, the elongation at break for this blend is much smaller than the pure ST2 (ref. fig 5.8) which may be explained by the plasticisation of PS lamellae by PS015 whose molecular weight lies below the entanglement

molecular M_e weight of polystyrene ($M_{PS015} \sim 12,000$ g/mole; and M_e for PS 19,100 [1]). But these may partly be mixed to the butadiene phase and act as precursor of microvoid formation leading to premature fracture.

Furthermore, the PB lamellae in this blend are slightly thinner (about 12 nm) than in pure star block copolymer (about 14 nm). In section 4.3.2, it has been shown that maximum elongation of PS lamellae may also depend on the thickness of adjacent PS lamellae. Therefore, the maximum elongation that may be achieved in this sample is restricted by smaller thickness of PB lamellae leading to decreased macroscopic elongation at break. As a result, more pronounced 'bead-like' structure is observed in microphase separated ST2/hPS blend than in pure ST2.

b) Macrophase separated blends having ST2 matrix (e.g., ST2/20 wt % PS190)

Fig 5.12 shows details of deformation structures observed in macrophase separated ST2/20 wt % PS190 blend which possesses PS particles in ST2 matrix. Especially, morphological changes around the PS particles during deformation are very helpful to understand the micromechanical processes.

Growth of microvoids at the poles (i.e., in the direction of stress) of the particles is well known from particle filled polymers [1, 146]. In the present case, the PS190 inclusions act as stiff particles embedded in the soft ST2 matrix. At the pole regions of the PS particles microvoids appear due to stress concentration.

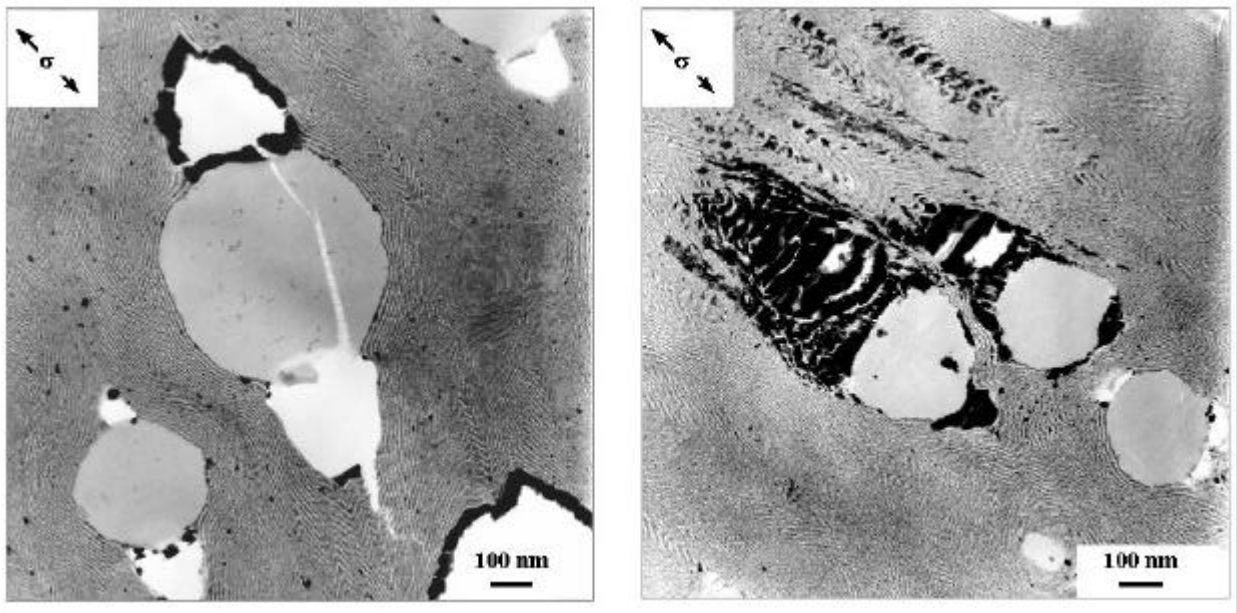


Figure 5.12: TEM images showing deformation of macrophase separated blend ST2/20 wt % PS190, strain direction shown by an arrow; (morphology of undeformed sample in fig 5.2c).

If the elastic modulus of the inclusions is much larger than that of continuous matrix, the stress is reduced at the equator, and a compressive stress component acts at the equators of these spherical PS190 particles yielding a good contact with the matrix. The maximum stress

concentration exists at the poles of the particles which is the reason for void formation as shown in fig 5.12. The PB lamellae can cavitate due to their lower cavitation stress compared to PS lamellae followed by the formation of voids [113]. However, the cavitation of PB lamellae should occur at a higher stress compared to SB diblock copolymers due to the presence of additional PS domains inside the PB lamellae.

Formation of microvoids is followed by a large homogeneous plastic deformation of PS as well as the PB lamellae. The contour length of lamellae around a microvoid is about twice of original length at PS particle surface, indicating a local deformation with an extension ratio of about $\lambda = 2$ (i.e., strain, $\epsilon = 100\%$). Lamellae along and between the PS particles are also plastically deformed which results in a transverse stress component in the sample. This transverse stress is responsible for the initiation of fibrillated crazes within these particles (fig 5.12 left).

Microvoids are heavily stained by OsO_4 in different regions as shown in fig. 5.12 (right). In addition to the staining effect, OsO_4 has an affinity to be deposited at regions with a larger free volume (microvoids). Dark spots formed by heavy deposition of staining agent can be observed in PB lamellae which lie perpendicular to the stress direction. This indicates that the PB lamellae are preferentially deformed followed by void formation which was also reported by Yamaoka [35].

Although this sample shows principally a homogeneous deformation revealed by the large deformation of lamellae, the degree of this deformation is mainly determined by the orientation of lamellae relative to the tensile direction. Since the lamellae are oriented randomly, an anisotropic deformation behaviour on the microscopic scale is observed (This is also true for microphase separated blend mentioned in 5.3.1a and pure block copolymer cast from solution). This type of anisotropy in deformation behaviour resulting from different orientation of lamellae is well known in semicrystalline polymers.

Deformation mechanism revealed by TEM investigations can be correlated with results of tensile tests. After the yield point, where plastic deformation of PS lamellae onsets (fig 5.8), cavitation at the poles of PS particles takes place as a consequence of disentanglement of polystyrene chains between the PS190 phase and the lamellar matrix. This is manifested as stress whitening during tensile testing. Cavitation at the poles of these PS particles acts as precursor for further plastic deformation of lamellar matrix. Large plastic deformation of lamellae surrounding the PS190 particles and existing microvoids leads to further growth of these voids. The ultimate fracture of the specimen occurs via growth of microvoids into cracks and crack propagation.

c) Macrophase separated blends having PS190 matrix (e.g., ST2/80 wt % PS190.)

The morphology of ST2/80 wt % PS190 blend is be similar to that of rubber toughened thermoplastics (fig 5.7). By analogy, the deformation mechanisms observed in ST2/80 wt % PS190 blend (fig 5.13) can be compared to the deformation of rubber modified thermoplastics where the soft inclusions are dispersed in the thermoplast matrix. The effectiveness of rubber toughening depends on the size, distribution and microstructures of the rubber particles [1,103,105,106]. Toughening glassy thermoplastics by block copolymers have been studied by Aggarwal and shown that block copolymer particles can act as good toughening agents if these are able to undergo plastic deformation [62]. The toughening mechanism involves the initiation and/or termination of fibrillated crazes in the thermoplast matrix by the soft block copolymer particles.

Craze-like deformation zones are observed perpendicular to the principal stress direction. The craze fibrils in the deformation zones are highly stretched, and have a thickness of 10-30 nm. Since the block copolymer particles are softer than the polystyrene matrix, the stress concentration occurs at equator of the particles [1,106]. The Young's modulus of PS matrix and star block copolymer is 3300 MPa and 1205 MPa, respectively (table 5.3). This mismatch in Young's modulus is large enough for the nucleation of crazes. The stress concentration may lead to disentanglement of polystyrene chains between the PS matrix and the PS lamellae of the copolymer particle resulting in the formation of voids at their equator. The formation of voids takes place at the yield point, which is manifested as the stress whitening during tensile testing [171].

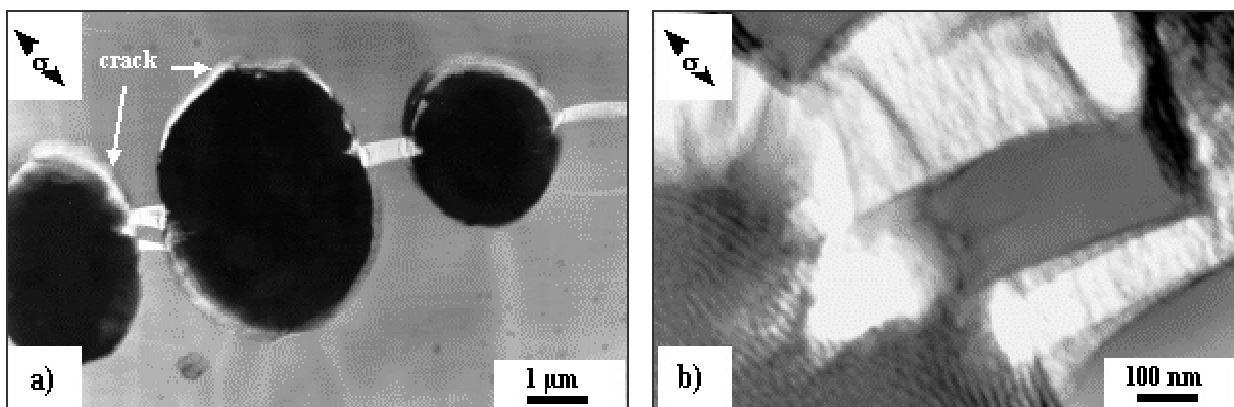


Figure 5.13: HVEM images showing deformation of macrophase separated blend ST2/80 wt % PS190; strained semi-thin sections (~ 500 nm thick), OsO₄ stained, deformation direction indicated by an arrow; (morphology of undeformed sample in fig 5.7).

The effectiveness of block copolymer particles as toughening agent depends on the internal morphology and size of the particles. The molecular parameters (like molecular weight and architecture, i.e., AB or ABA type copolymer, with A as matrix component) may play an

important role in the toughening mechanism. It is desirable that the molecular weight of the end blocks is greater than M_e , so that a strong matrix/particle coupling is possible.

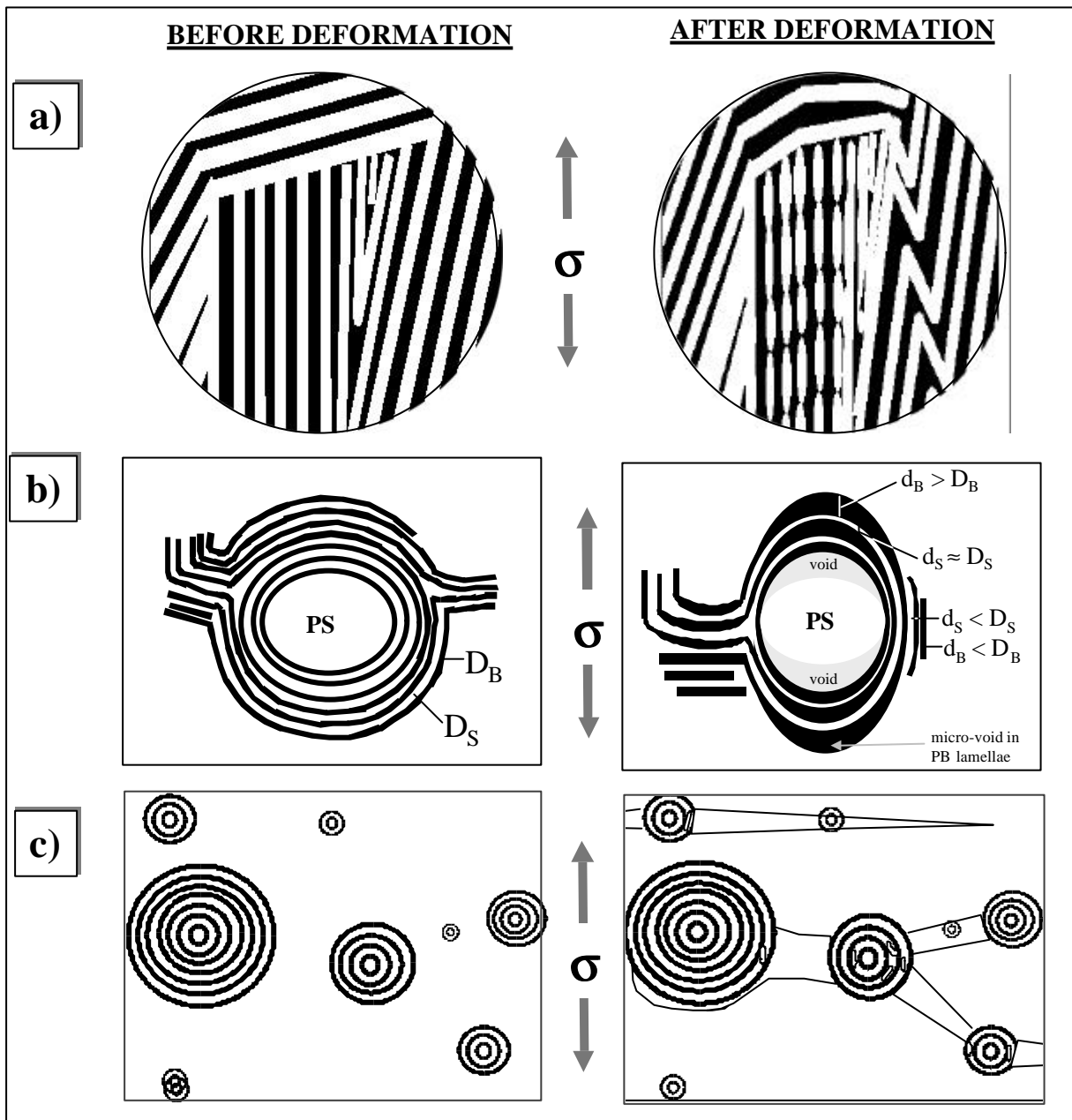


Figure 5.14 Scheme showing deformation mechanisms observed in block copolymer/hPS blends.

The longest PS block of the copolymer has the molecular weight greater than M_e which should make it a good toughening agent. However, a debonding between the particles and the matrix is observed which would be expected only for the polymers having a poor interfacial adhesion.

Due to stress concentration microvoids formation begins at the equatorial regions. In HIPS, the whole particle morphology takes part in the deformation processes allowing a large plastic deformation of particles as well as thermoplastic matrix. However, in ST2/80 wt % PS190 blend, the particles consist of concentric arrangement of alternating glassy and rubbery layers.

On application of external stress, the stress field is built up in all the directions such that yield stress of soft particles is increased (e.g, up to crazing stress of PS or even more) which opposes the plastic deformation. This favours, on the other hand, the fracture of glassy layers leading to micro-crack formation and crack propagation. As a result, the stress level at the vicinity of the equator of copolymer particles is drastically reduced and the lamellae undergo plastic drawing (fig 5.13b).

Taking solubility parameter of used solvent toluene and the components of the block copolymer (polystyrene and polybutadiene) into account*, one can easily predict that PS phase is slightly more soluble in toluene than PB phase. Hence, allowing the solvent to evaporate from the solution of the blend, PB phase would first shrink. Because the PS phase is still in the solution phase when PB phase is already dried, the PS chains are more perturbed after complete solvent evaporation. Especially, the boundary between the matrix and copolymer particles experiences the largest stress because of presence of pure polystyrene matrix in the solution even after the lamellae in the particles are partly solidified. This excess internal stress inside the copolymer particles and between the matrix and particles would favour the propagation of microcrack along the boundary of copolymer particles (fig 5.13a) or along a PS lamella.

5.3.2 Injection Moulded Blends

In contrast to homogeneous deformation of pure ST2, highly localised deformation zones are noticed in injection moulded ST2/PS190 blends. Characteristic deformation structures observed in these blends are shown in fig 5.15. At lower PS190 content ($\Phi_{PS190} \leq 40$ wt %), craze-like zones prevail while 'kink bands'-like morphology is observed at higher PS190 content ($\Phi_{PS190} \geq 60$ wt %).

The deformation zones at lower PS content (e.g., 20 wt % PS190, fig 5.15a) are formed normal to the strain direction which contain highly stretched lamellae and microvoids, and these resemble the crazes frequently observed in thermoplastics and their rubber modified grades [1,105,106]. Quantitative analysis shows that the lamellae in these deformation zones are stretched up to few hundred percents ($\lambda > 3$). Macroscopic strain of about 34% is contributed alone by this deformation.

These crazes are, however, fundamentally different from those observed in homopolymers and rubber modified thermoplastics. The most striking difference is that the fibrils are often separated by highly stretched rubbery domains in addition to the microvoids.

* Since, $\delta_{PS} = 9.10$ (cal/cm³), $\delta_{PB} = 8.40$ (cal/cm³) and $\delta_{Toluene} = 8.90$ (cal/cm³), it follows that $(\delta_{PS} - \delta_{Tol.})^2 < (\delta_{PB} - \delta_{Tol.})^2$ indicating that solubility of PS in toluene is slightly higher than that of PB (data from p. 68 of ref. [7]).

The transition in deformation mechanism from homogeneous stretching of PS and PB lamellae to the formation of local deformation zones is the reason of a drastic reduction in elongation at break in ST2/20 wt % PS190. The localisation of deformation in the form of craze-like zones is a sign of inability of glassy PS layers (which have a thickness of about 30 nm or more, fig 5.4-5.6) to undergo plastic flow, and it provides a strong evidence for ‘thin layer yielding’ mechanism proposed for lamellar block copolymers in section 4.3.3. This hindrance in plastic deformation of PS layers appears to be associated with the thickness of PS lamellae because the transition from ductile to brittle behaviour occurs exactly when the average thickness of PS lamellae D_{PS} shifts from about 20 nm to about 30 nm.

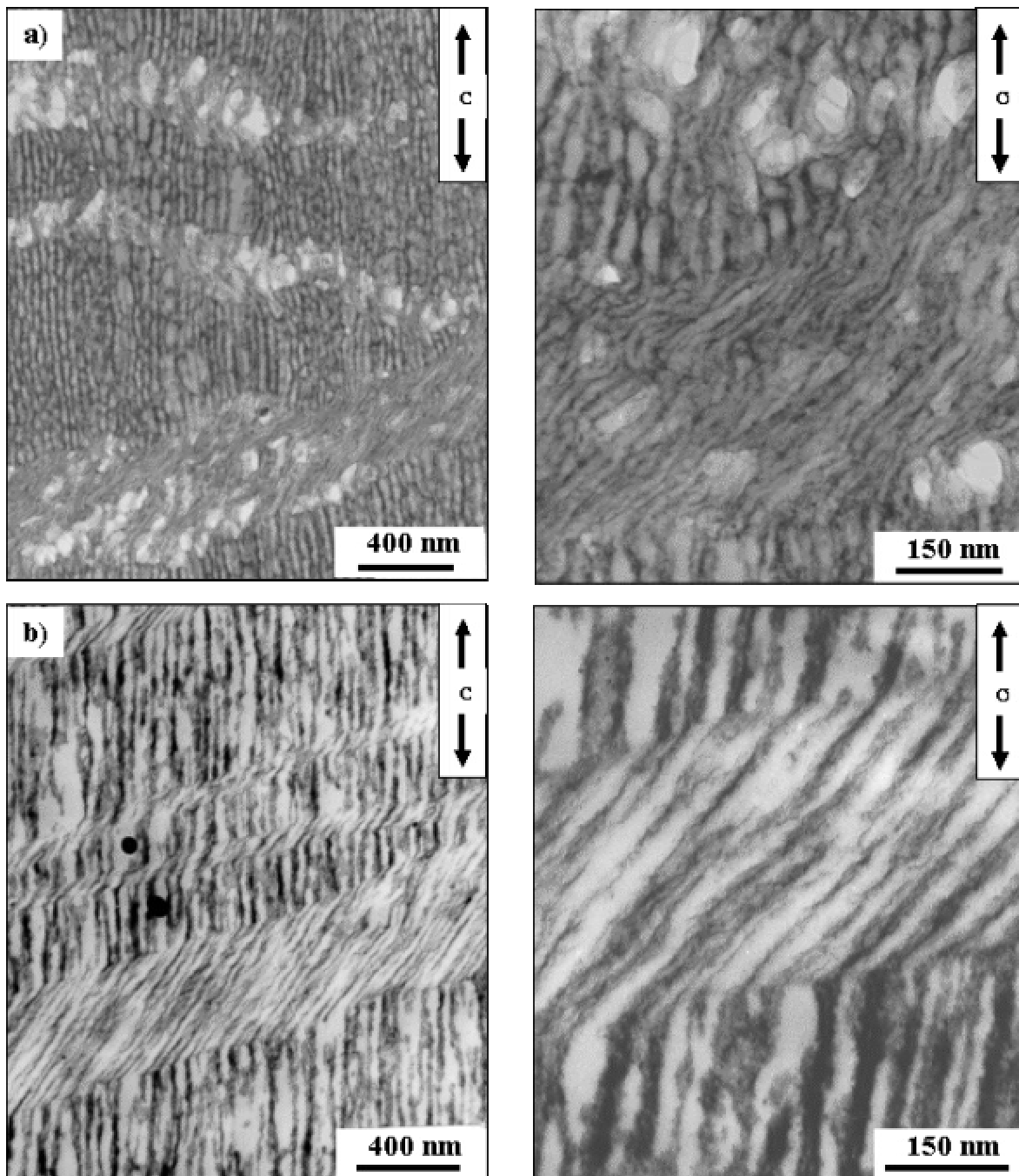


Figure 5.15: Lower (left) and higher (right) magnification of TEM images showing deformation structures observed in injection moulded ST2/GPPS blends: a) 20 wt % PS190 and b) 60 wt % PS190; strain direction is vertical.

As discussed in section 4.3.3 the yield stress of PS lamellae reaches crazing stress of bulk polystyrene when their thickness exceeds the critical thickness (D_{crit}). Then the PS lamellae act as stress concentrators and undergo crazing. Few much thicker PS layers observed at lower PS190 content (fig 5.4) may further favour stress concentration and premature failure of the sample.

The transition in deformation mechanism and mechanical properties at $\Phi_{PS190} = 20$ wt % can be clearly noticed in the scanning electron (SEM) micrographs presented in fig 5.16. While the pure star block copolymer shows a ductile fracture characterised by highly stretched fibrils, the blend containing 20 wt % GPPS undergoes a brittle fracture. Large flat areas on SEM micrographs (fig 5.16b) suggests an unstable crack propagation along the thickness of the tensile bar from one end to the other leading to a brittle fracture.

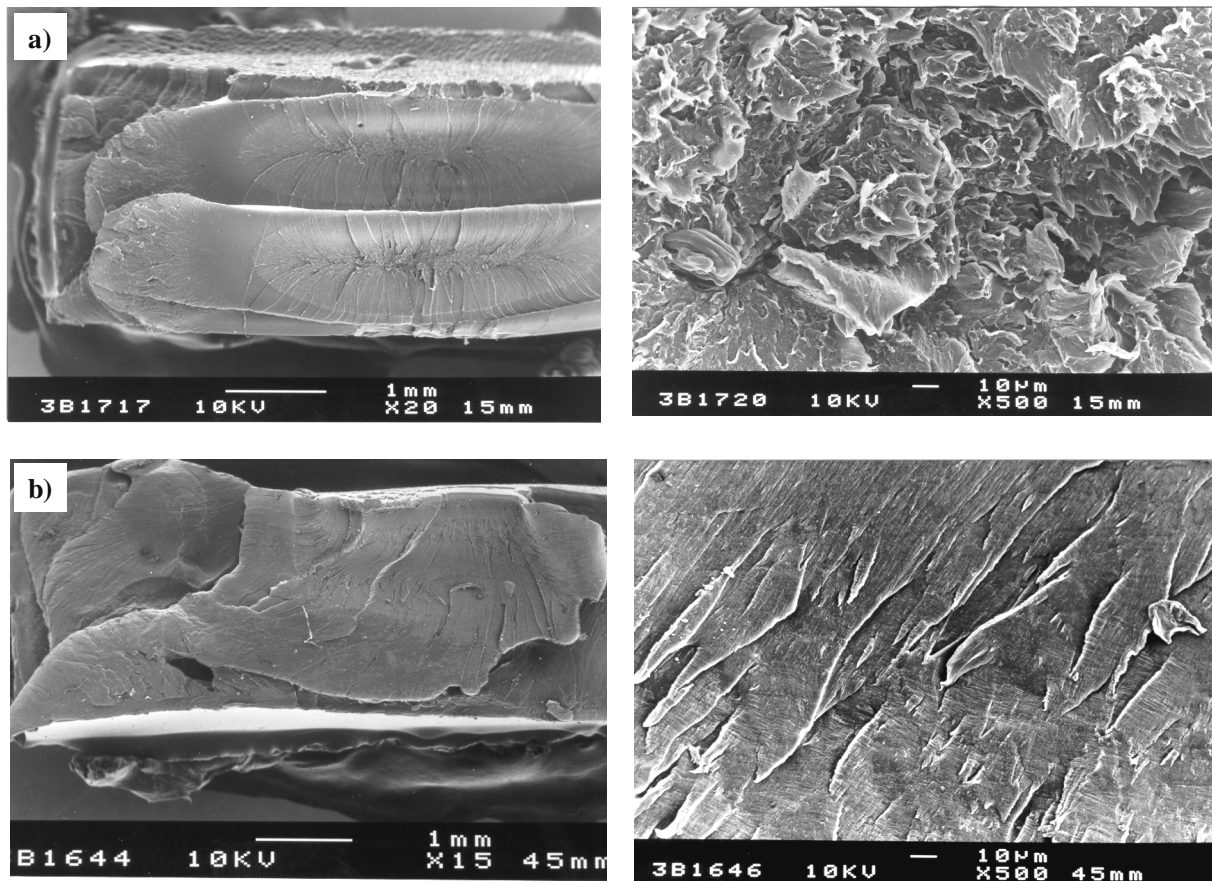


Figure 5.16: SEM micrographs of fracture surfaces of the injection moulded samples broken in tensile test: a) pure star block copolymer ST2 and b) ST2/20 wt % PS190 blend.

The HVEM micrographs of ST2/PS190 blends (fig 5.17) provide additional evidence of ‘thin layer yielding’ mechanism. Regardless of preparation methods (solution casting, extrusion, press moulding etc.), the bulk star block copolymer samples showed no pronounced localisation of deformation [174]. In contrast, their blends with PS190 in injection moulds deform by the formation of local deformation zones. In the blends with $\Phi_{PS190} = 20$ and 40 wt %, the crazes are localised mainly at the lamellar stripes containing more polystyrene (whiter stripes) get stopped

at the regions of lower polystyrene content (darker regions). This kind of craze stop mechanism at the stripe of lamellae containing lesser amount of polystyrene (i.e., those dissolving very less or no added PS190) results from the fact that the darker areas relieve stress by allowing plastic deformation and shearing of lamellae at the craze tip: i.e.,

$$\mathbf{s}_y^{thick_layers} \approx \mathbf{s}_{craze}^{PS} \text{ while } \mathbf{s}_y^{thin_layers} < \mathbf{s}_{craze}^{PS}$$

The mechanisms of craze-tip blunting, craze coalescence and craze diversion in PS-b-PBMA diblock copolymers were investigated by Weidisch and Michler [111]. These mechanisms have been discussed in terms of enhanced mechanical properties of these block copolymers, e.g., synergism in tensile strength. Generally, the craze-tip blunting occurs when the craze has to pass through a stripe of lamellae. In the present case too, the craze-stop mechanism can be discussed in the sense of enhanced mechanical properties because craze-termination in this context means a pronounced energy dissipation due to plastic deformation of thinner PS layers (which would mean an increase in ductility). Absence of crazes rather than craze-stop is, however, desirable for increased ductility in lamellar block copolymers.

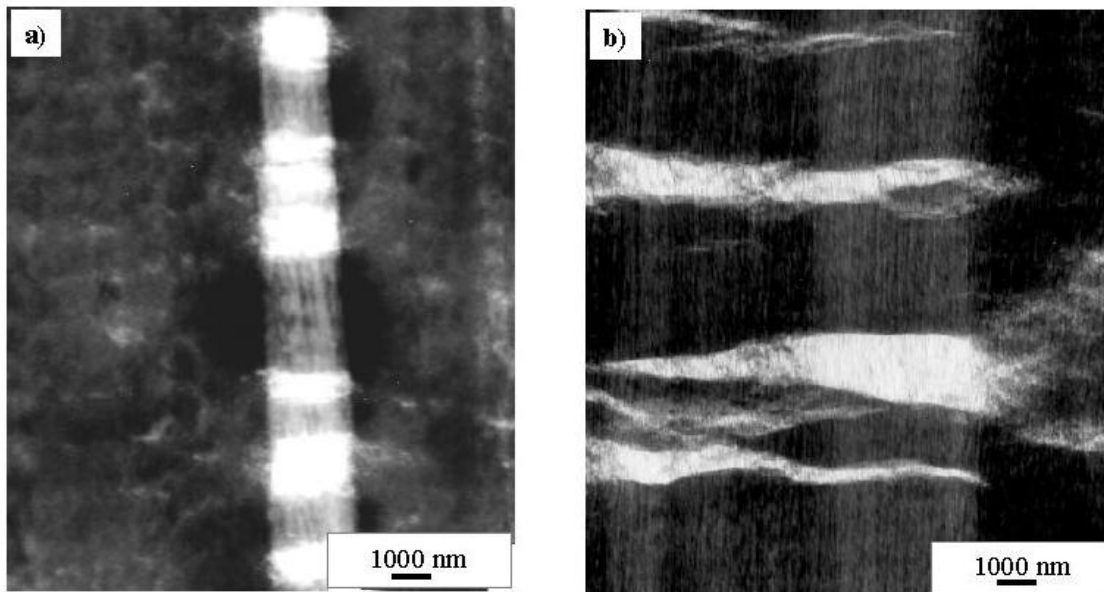


Figure 5.17: HVEM micrographs showing deformation structures in a) ST2/20 wt % PS190 blend and b) ST2/40 wt % PS190 blend: semi-thin sections about 500 nm thick were cut from the middle of the sample. Deformation direction is vertical. Crazes are localised at the regions with thicker PS layers and are stopped at the regions with thinner PS lamellae.

At higher PS190 content ($\Phi_{PS190} \geq 60$ wt %), as PS practically forms the matrix, no craze-stop mechanism was observed [174]. Although not directly comparable, it is worth mentioning that results from fracture mechanics and micromechanics seem to be correlated to each other. It has been shown that the level of toughness characterised by J-integral or CTOD values remain more or less constant up to a PS190 content of about 50 wt % after which a drastic reduction in

fracture mechanics parameters occur (fig 5.10a). This transition takes place, when the micromechanism shifts from craze-stop to the craze-propagation.

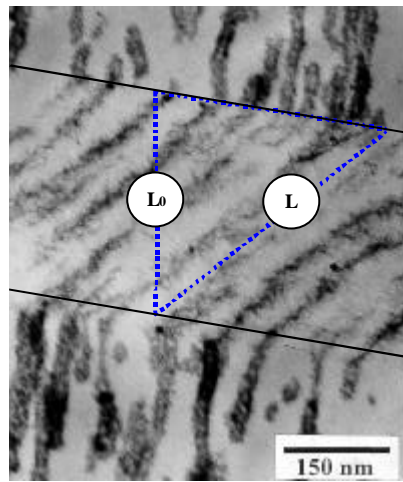
Moreover, peculiar types of narrow, long and sharp-edged deformation bands (fig 5.15b) are revealed by TEM at higher PS content ($\Phi_{\text{PS190}} \geq 60 \text{ wt } \%$).

The deformation bands show the characteristics of both crazes (with respect to their orientation to the external stress direction) and shear bands (with respect to tilt angle of microstructures inside these deformation bands). These bands often propagate perpendicularly to the external stress direction. Inside the deformation bands, the PS and PB lamellae are only slightly deformed and tilted away from strain direction by about 50° . Whole of the macroscopic strain is localised at these deformation bands. Sometimes, the deformation bands are also inclined to an angle with the strain direction. These bands are, however, very different from classical crazes or shear bands observed in homopolymers like PS and rubber toughened thermoplastics [1,105,106]. Unlike crazes, there is no evidence of voiding and unlike shear bands these zones are usually not tilted at 45° towards the direction of external stress.

These bands resemble the 'kink bands' reported recently by Winey et al. in a lamellar diblock copolymer under shear deformation [129,130]. However, the kink bands observed by them are formed simply by rotation of lamellae; and their thickness remains practically unchanged [129]. Clearly, the kinking of lamellae observed in this work is governed by different mechanism than that observed by Winey and co-workers. How these new kinds of deformation structures are evolved; in the present case, is not fully understood and should be further investigated. It can be speculated that these bands are formed by 'turn-back' of weakly stretched lamellar stripe due to release of elastically absorbed energy after external stress has been relieved (i.e., after the specimen fracture). Similar structures are also observed in binary block copolymer blends subjected to tensile deformation (section 6.3.1). The deformed lamellae should have tilted in order to compensate the volume change during deformation. Additionally, the shear component of the tensile stress could have also contributed in the formation of these bands. It should be admitted that the deformation structures observed in injection moulded samples are, in general, not representative of the whole tensile specimen due to presence of non-equilibrium morphology which may change from one end of the bar to the next and even along the cross section of the mould.

By measuring the length of deformed lamellae (L) relative to the width of deformation zones (L_0), an elongation of about 12 % can be estimated (illustrated in fig 5.18). Since the deformation bands are nearly parallel and the lamellae inside these bands are almost equally inclined to the lamellar axis, this local deformation of 12% may be assumed to be valid for the

macroscopic sample. This is in the same range as the macroscopically measured elongation at break of the tensile bar (table 5.3; sample with 60 wt % PS190 has $\epsilon_B=18\%$).



$$\epsilon_{\text{lam}} = (L-L_0/L_0) \times 100$$

$$\sim 12 \%$$

Figure 5.18: Estimation of elongation at break by quantifying the deformation zones in ST2/60 wt % PS190 blend; strain direction is vertical.

That the elongation at break drastically falls when 20 wt % PS190 is blended with ST2 appears a little bit disappointing. But it should not be regarded as a disadvantage of blending block copolymer with homopolymers. In fact, the lamellar block copolymer shows surprisingly high ductility than any other blends of analogous composition under tensile loading. Actually, the elongation at break (a measure of ductility) increases exponentially when the thickness of the PS layers lies in the range of about 20 nm.

A significant advantage of star block copolymer/hPS blends may be judged in the following way. Let us compare the parameters listed in table 5.4 for pure PS and a blend with 40 wt % ST2 (which is the composition range for block copolymer modified standard polystyrene in practical applications). It can be easily noticed that compared to a huge gain in strain at break in the blends, the loss in Young's modulus and yield strength is almost negligible.

Table 5.4: Comparison of tensile properties of pure PS190 and a blend with 40 wt % ST2.

properties	pure PS190	PS/40 wt % ST2	remarks
Young's modulus (MPa)	3300	2520	Modulus loss ca. 24%
Yield strength (MPa)	55	45	Loss in yield strength ca. 17%
elongation at break (%)	3	18	Gain in elongation at break ca. 500%

Compared to the properties of linear block copolymer/polystyrene blends (e.g., LN2/PS190 blends), ST2/PS190 blends studied in the frame of this work possess more desirable mechanical

properties. Elongation at break for LN2/PS190 and ST2/PS190 as compared in fig 5.19 clearly demonstrate that ST2 has clearly higher toughening activity than LN2.

Comparative study of styrene/diene block copolymer/hPS with respect to the block copolymer architecture have been the concern of few recent studies. Feng et al. have [79] studied the dynamic mechanical properties of blends consisting of polystyrene and styrene/butadiene block copolymers with triblock and star architecture. These studies have proved no influence of block copolymer architecture on phase behaviour and mechanical properties of blends with homopolymer. However, recent study of Thompson and Matsen has demonstrated that far more substantial improvements in compatibilisation of homopolymer blends can be achieved by simply introducing polydispersity into the diblock copolymers [175]. Therefore, comparative results on ST2/hPS and LN2/hPS blends are in line with the prediction of Thomson and Matsen because ST2 molecules having a larger dispersity (about 1.6) may be expected to be more compatible with polydisperse homopolystyrene than linear copolymer LN2 having smaller dispersity index (about 1.2).

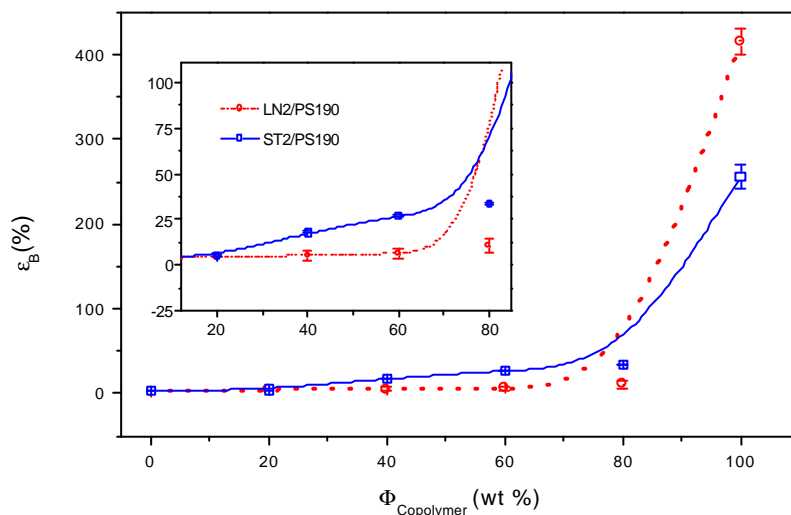


Figure 5.19: Comparison of elongation at break for LN2/PS190 and ST2/PS190 blends; tensile testing ISO 527 at room temperature and cross head speed of 50 mm/min.

An important advantage of star block copolymer lies in the fact that its higher molecular weight and larger number of PS blocks allow better molecular coupling with hPS molecules than the linear copolymer without making any compromise in rheological properties.

5.4 Conclusions

In this chapter, structure-property correlations in star block copolymer/homopolystyrene blends has been studied. The influence of morphology on micromechanical and mechanical behaviour has been analysed. Under equilibrium condition, macrophase as well as microphase separation of added homopolystyrene (hPS) occurs depending on mixture composition and molecular weight of the hPS. Under shear stress of injection moulding, however, macrophase separation is strongly

suppressed that induces miscibility between PS block of the block copolymer and hPS in spite of higher molecular weight of polystyrene. A broad molecular weight distribution of the homopolymer and that of block copolymer may favour the compatibility between the PS block and hPS.

While the ‘thin layer yielding’ mechanism is found to operate in solution cast microphase separated blend in which the thickness of the PS lamellae is still in the range of ~ 20 nm, a more or less pronounced localisation of deformation is observed in macrophase separated blends. In each case, homogeneous plastic deformation is the predominant deformation mechanism of the block copolymer phase.

The injection moulded blends, in which the thickness of PS lamellae is about 30 nm or more, the deformation mechanism switches from homogeneous plastic deformation to the formation of local craze-like deformation zones. The localisation of craze-like zones in the lamellar stripes containing thicker PS lamellae is a direct evidence of ‘thin layer yielding’ mechanism. The hindrance of plastic deformation of PS lamellae imposed by their thickness is the reason of the drastic reduction in elongation at break.

Asymmetric star block copolymer may provide excellent potential for producing highly transparent materials suitable for food packing films, beakers for cold and hot drinks etc. on the basis of the commodity thermoplastic PS. These blends allow fine-tuning of optimum level of strength and stiffness. The ductility of the blends (especially under impact loading conditions) should be, however, improved. Possible routes to improve the ductility of block copolymer/hPS blends are modification of block copolymer architecture and optimising processing conditions (e.g., isotropisation of the morphology).

Future works should further concentrate to clarify the new kinds of deformation structures observed in star block copolymer/hPS blends and enhance the deformability of the layers inside the deformation bands.

6. STRUCTURE-PROPERTY-CORRELATIONS IN BINARY BLOCK COPOLYMER BLENDS

6.1 Motivation – Why Binary Block Copolymer Blends?

An ideal polymer blend is one which combines the useful properties of constituent blend partners. It is desirable to have mixtures or compounds or copolymers whose properties are even superior than that of either components. Interesting examples in this respect are PS/PnBMA diblock copolymers, in which the tensile strength is found to exceed that of both the components in a certain composition window [111].

For practical applications, polymer mixtures are required which allow a balance of important mechanical properties like stiffness, strength and ductility [1]. In practice, however, polymer pairs seldom show linear dependence of mechanical properties with composition. At a given composition, the properties of one of the components often dominate. For example, a sudden change in elongation at break was observed at a hPS content of 20 wt % in star block copolymer/hPS mixtures (chapter 5). Decreased ductility (compared to pure block copolymer) is, indeed, disadvantage of these blends.

Binary block copolymer blends, both blend partners being microphase separated, may offer the possibility of tailoring mechanical properties by reorganising the macromolecular segments. For this reason, morphology-toughness correlation in binary star block copolymer/triblock copolymer blends has been investigated.

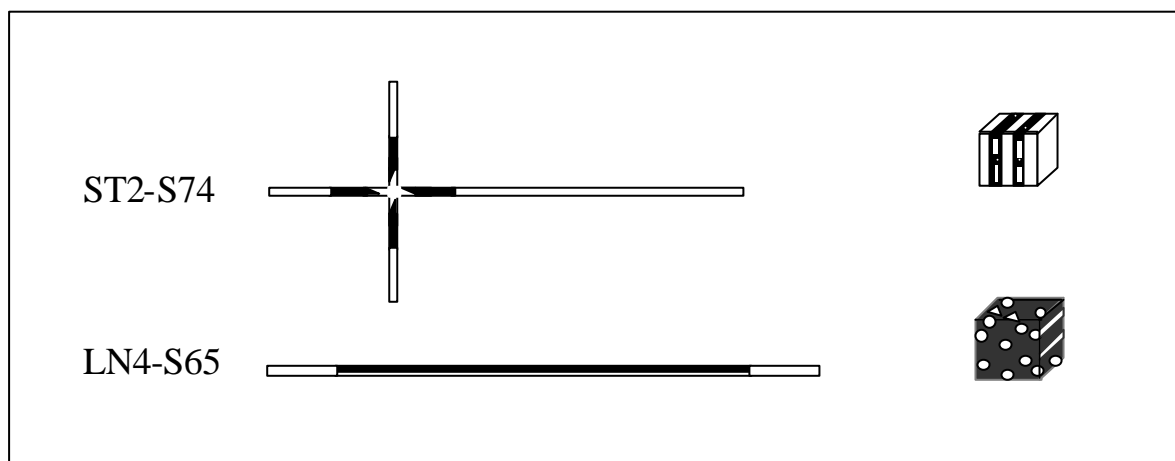


Figure 6.1: Architecture and morphology (schematic) of the copolymers used to prepare binary blends.

To recall the mechanical behaviour of pure block copolymers having different morphologies, lamellar samples showed ductile behaviour under quasi-static loading condition (section 4.2.1). Under impact conditions, most copolymers showed brittle behaviour irrespective of molecular architecture and the type of microphase morphology. From the practical view point, materials which show tough behaviour both under slow as well as impact loading conditions are preferred. The following study demonstrates that investigated binary block copolymer mixtures offer the

possibility to achieve these goals. It is the first systematic study of fracture toughness characterisation of binary blends consisting of asymmetric star block and triblock copolymers using crack resistance concept.

6.2 Phase Behaviour and Morphology

6.2.1 Phase Behaviour and Equilibrium Morphologies

The styrene/butadiene block copolymers used in this section are ST2-S74 and LN4-S65 (fig 6.1): one having thermoplastic properties and another one having thermoplastic elastomeric properties (section 4.2.1). The blends consist of 5, 10, 20, 40, 60 and 80 % by weight of LN4-S65.

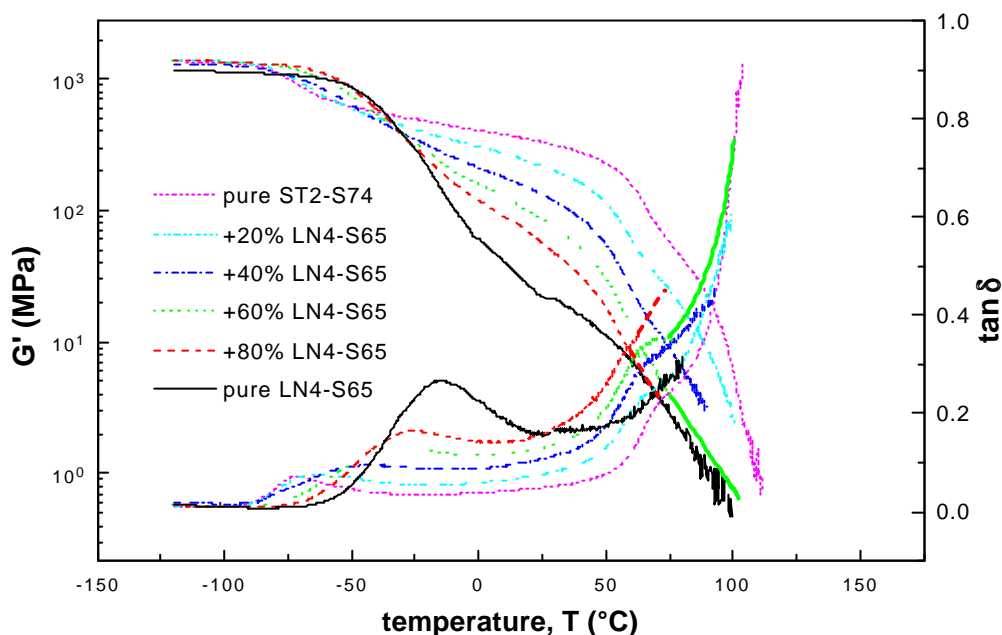


Figure 6.2: DMA spectra of ST2-S74/LN4-S65 blends: note that the T_{g-PB} shows a gradual increase with increasing LN4 content (see also table 6.1), measured at a frequency of 1 Hz.

DMA spectra of the blends given in fig 6.2 make it obvious that glass transition temperature of butadiene phase (T_{g-PB}) increases almost linearly (table 6.1) with increasing LN4 content which is an indication of incorporation of bulky styrene segments in the flexible butadiene phase.

The intensity of loss peaks ($\tan\delta$) and the area thereunder as well as the inclination of plateau region in the G' vs. T curves have been discussed in the literature as indicator for phase miscibility [15,157]. With increasing LN4 content, the intensity of the loss peak for soft phase and the area thereunder increases suggesting that the volume of materials taking part in the interaction at this region has increased with LN4 content, i.e., intensification of mixed phase. A continuous inclination of plateau region in G' vs. T curves further implies the gradual increase in mixed phase which is softer and leads to a decrease in storage modulus. Since LN4 contains already a large part of mixed styrene/butadiene random phase, the increase in mixed phase with increasing LN4 content is quite understandable.

Table 6.1: Glass transition temperature of soft (T_{g-PB}) and hard phases (T_{g-PS}) in ST2/LN2 blends determined by DMA

LN4 wt %	T_{g-PB} (°C)	T_{g-PS} (°C)	remarks
0	-74	~100	-
20	-68	~100	-
40	-53	~100	-
60	-31	~100	-
80	-25	-	Detection of T_{g-PS} difficult due to softening of the sample, DSC indicated a T_{g-PS} of about 87°C for LN4
100	-15	-	

Meanwhile, the glass transition temperature of styrene phase (T_{g-PS}) remains more or less unchanged suggesting the presence of pure polystyrene phase. In every sample except pure LN4-S65, the shoulder located in damping curve at about 75°C persists which would indicate the relaxation of short PS chains of the star block copolymers as already discussed in section 4.1. At higher LN4 content, it was difficult to detect a T_{g-PS} . This suggests the absence of pure polystyrene phase in the samples although it is microscopically evident as will be discussed later. Equilibrium morphology of binary ST2/LN4 blends is given in fig 6.3 and 6.4. An addition of 20 wt % LN4 leads to a transition from an ordered lamellar structure to a worm-like morphology with highly reduced long range order (fig 6.3). With the destruction of lamellae structure, the small PS domains originally embedded in PB lamellae of ST2 becomes less pronounced. With increasing LN4 content, the disordered domain structure persists, but the bright stripes of lamellae, with periodicity smaller than the pure ST2, are always phase separated. The size of PS domains in the blends have nearly same thickness distribution as the pure star block copolymer (~20 nm) which at higher LN4 content (80 wt %) drops to a level of pure LN4 (~15 nm).

In binary blends of block copolymers with well defined morphologies, the phase behaviour may be predicted by ‘single phase approximation’ [92], i.e., the morphology of the blends nearly corresponds to the total phase volume ratio of the components. Since the phase volume ratio and morphologies of both the block copolymers ST2 and LN4 are not well defined, it is impossible to assign the binary block copolymer blends a particular classical morphology. The blend morphologies are fully unconventional and difficult to interpret based on the results obtained so far. However, two points are quite obvious:

- a. The blends show a considerable compatibility which is supported by DMA results as well.
- b. Lamellae forming molecules are segregated from the rest of the others.

The quantification of microphase separated structures show that the polystyrene domains in the blends approach the size of polystyrene lamellae of the star block copolymer (Appendix 6.1).

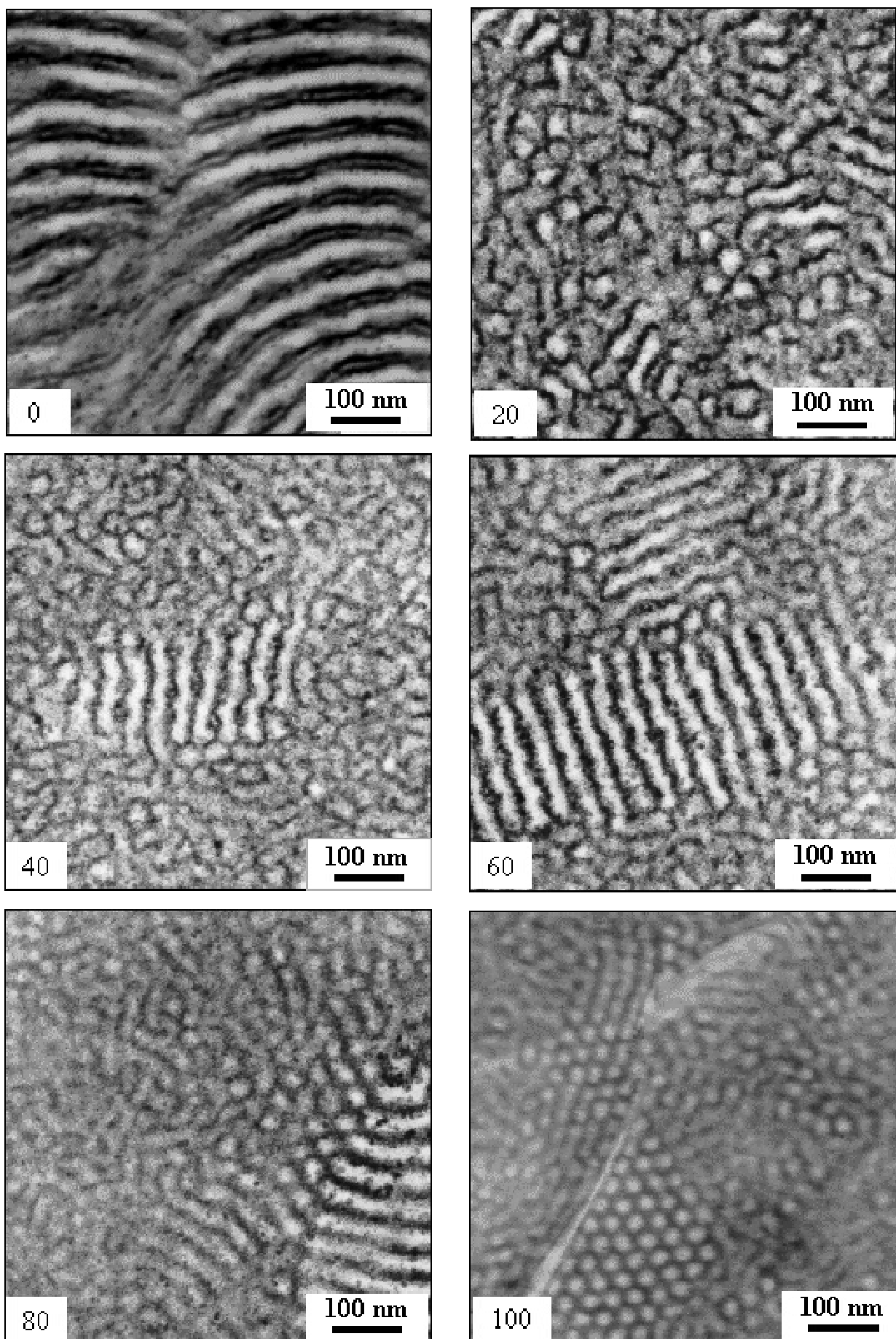


Figure 6.3: TEM images showing Morphology of solution cast ST2/LN4 blends; the figures at the bottom left of each micrograph stands for LN4 wt %.

In TEM images of the blends (fig 6.3), two kinds of domains are apparent: ‘white’ domains almost sharply separated from the ‘dark’ rubbery phase and ‘grey’ domains having diffuse boundary with the rubbery phase. The former domains resemble qualitatively the PS lamellae of pure ST2 while the latter PS domains of pure LN4. Majority of the hard domains in pure LN4 are ‘poorly segregated’ and disordered. The domains with diffuse boundary are especially pronounced at higher LN4 content (>60 wt %) and dominate the corresponding morphology.

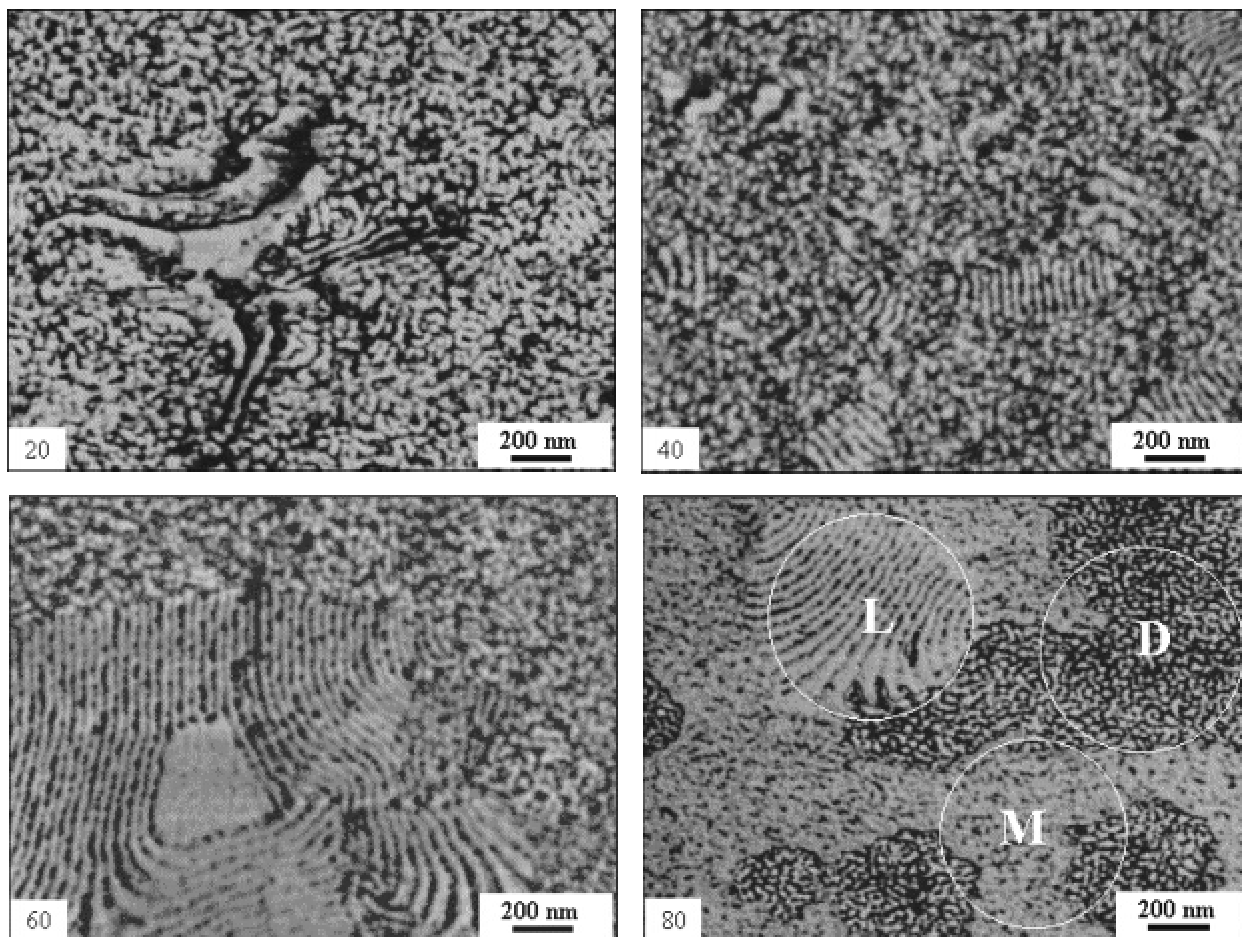


Figure 6.4: SFM phase images showing morphology of solution cast ST2/LN4 blends; note the existence of three distinguishable ‘phases’ at higher LN4 content (LN4 phase, ST2 phase and a mixed phase); at lower LN4 content these phases become indistinguishable; the figures at the bottom left of each micrograph stands for LN4 wt %.

Dark regions in the TEM image are results of preferential staining of double bond containing butadiene phase which also contains a considerable amount of styrene segments especially in the blends. Presence of styrene segments in the butadiene phase is also suggested by an increasing glass transition temperature of the soft phase. These styrene segments which cannot be stained by OsO₄ may reduce the local density of stained material whereby ‘grey’ domains results. The phase behaviour of ST2/LN4 blends is, indeed, very complex compared to conventional polymer blends and even binary block copolymer blends mentioned in the literature [88-91] due to their complex architecture and morphology.

Since the phase signals in SFM are sensitive to materials heterogeneity [158-161], the contrast in the phase images may be used to extract more qualitative information on the phase behaviour of the binary blends. The separation of lamellae forming molecules into separate domains is further supported by SFM phase images presented in fig 6.4 where the regions of alternating layers are more pronounced. Additionally, three phases become apparent especially at higher LN4 content: bright PS *domains* in dark rubbery matrix characteristic of LN4 (indicated by D), alternating *layer* structures (indicated by letter L) and worm-like domains packed close to each other forming an interpenetrating network-like structures (indicated by letter M). The latter might have originated by union of butadiene rich stars and LN4 molecules and may represent the *mixed* phase. Star molecules having higher amount of styrene may phase separate and form lamellar structures (as indicated by L in fig 6.4). The evolution of these domains are schematically illustrated in fig 6.5.

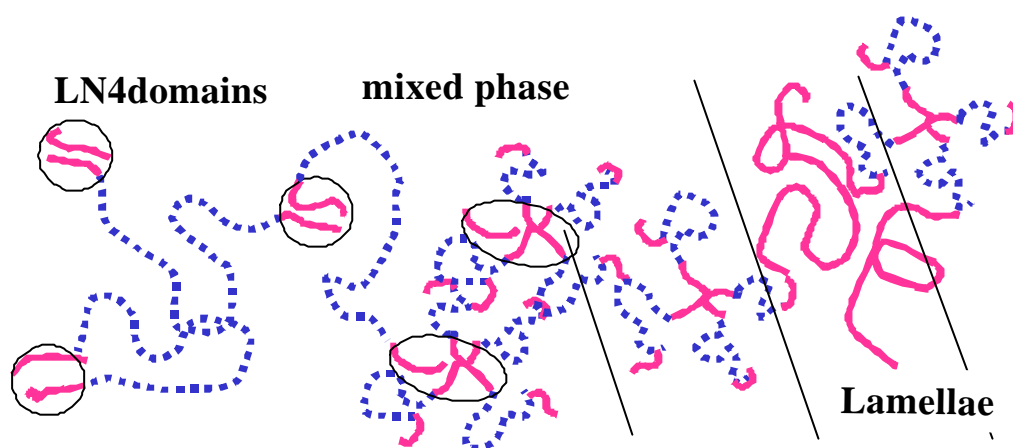


Figure 6.5: Schematic showing chain reorganisation in ST2/LN4 blends forming LN4 domains (**D**), ST2 lamellae (**L**) and mixed phase (**M**).

Since a fraction of stars is butadiene rich and contains nearly as much polystyrene hard block as LN4 molecules (in the range of 18000 g/mole), these stars are compatible with the LN4 molecules and may form common domain structure. This compatibilisation is further favoured by the presence of random copolymer middle block of rather high molecular weight in LN4. Nonetheless, molecules of the block copolymers ST2 and LN4 are clearly phase separated forming domains of different size and geometry.

Macrophase separation of block copolymer molecules resulting in the coexistence of different microphase separated structures was reported by several authors in different systems [86,87,91]. While Hashimoto et al. [91] found the coexistence of lamellae with different periodicity in a blend of copolymers having a large molecular weight difference, Jiang [87] reported the strange structures evolving from the incompatibility between the copolymer molecules of different molecular weights.

The observed incompatibility of the copolymer molecules in spite of identical chemical constitution can be discussed by the consideration of total entropy of the system. If the constituents (styrene blocks and butadiene blocks in the present case) of two different kinds of molecules (having very different molecular weights) have to reside in the like domains, the middle block of the 'smaller' molecules have to stretch which results in decrease in entropy. Since the chemical junctions must be located at the interface the outer block of the these small molecules cannot reach the domain centre which produces a density heterogeneity [87]. Hence, this process is not favourable, and the system tends to gain entropy by phase separation.

6.2.2 Morphology of Injection Moulded Samples

The investigation of block copolymers at thermodynamic equilibrium is the foundation of physical characterisation of these materials, e.g., through phase diagram. In the technical applications of block copolymers, this thermodynamic equilibrium is, however, never attained due especially to the technological constraints like limited processing time and associated economical considerations. Therefore, analysis of correlation between the non-equilibrium structures (i.e. the influence of processing conditions) and mechanical properties should find a more intensive consideration. Hence, morphology of the binary blends is analysed using injection moulded blends (fig 6.6). Injection moulded blends are further used in order to correlate the mechanical behaviour (tensile testing and fracture mechanics) with their micromechanical deformation behaviour.

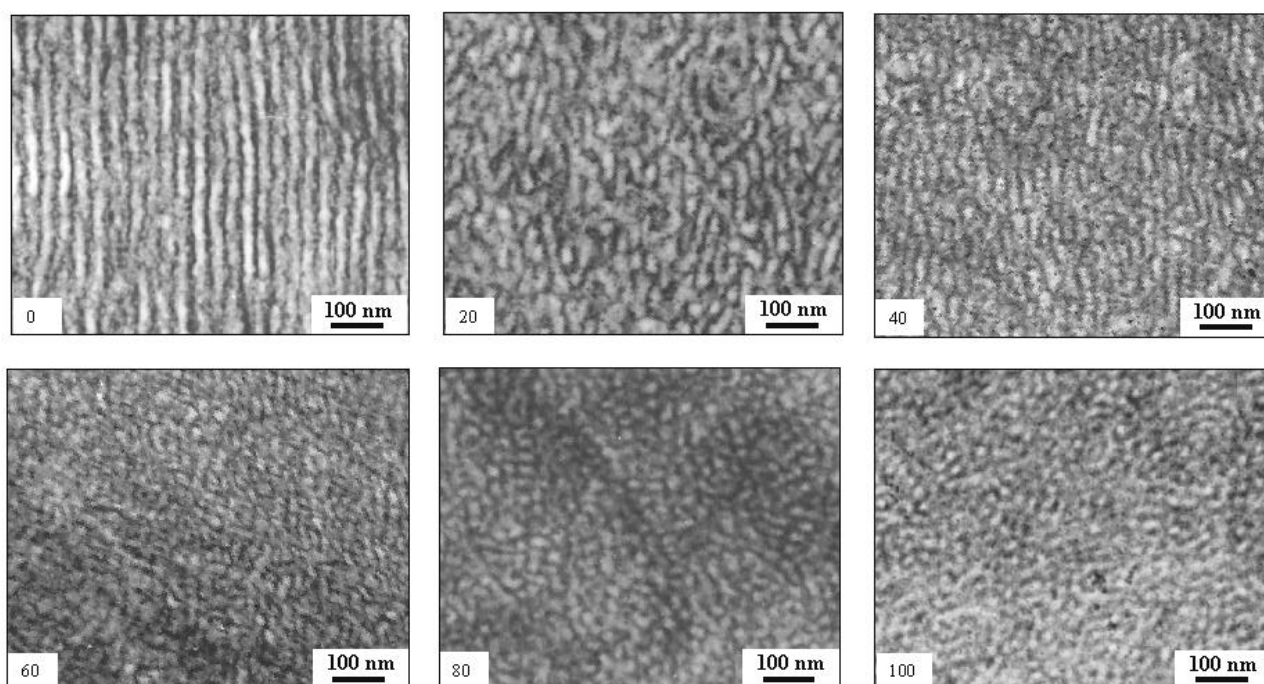


Figure 6.6: TEM images showing morphology of injection moulded ST2/LN4 blends, injection direction vertical; the figures at the bottom left of each micrograph stands for LN4 wt %.

It has been mentioned that the blends show partial miscibility in molecular level. In injection moulded samples, macrophase separation of the component block copolymers is further suppressed by the shear stress. The phase separated lamellar domains observed clearly in the solution cast samples are not distinct. Furthermore, the morphology is qualitatively similar to those observed in solution cast films (predominantly worm-like morphology in both the cases). Hence, it seems reasonable to use bulk injection moulded samples to study the morphology-toughness correlation in these binary block copolymer blends.

Basically, two types of morphologies are apparent: at lower LN4 content (0-20 wt %), lamellar morphology prevails which qualitatively resembles the structure of pure ST2. At higher LN4 content (40-80 wt %), the structures are qualitatively comparable to that of pure LN4. The structural reorganisation (“*disorder*”) appearing with increasing LN4 content has, as will be shown in section 6.3.2, a strong influence on the achieved toughness level and underlying crack propagation mechanisms.

Opposed to the conventional polymer blends, where an amorphous soft phase (e.g., rubber) is dispersed in the matrix of hard phase, no percolation of soft phase (i.e., no phase inversion) may be observed in the blends of ST2 and LN4. This results from the absence of macrophase separation of corresponding block copolymer microdomains. This is partly due to high shear stress of injection moulding and partly to the partial miscibility of the similar block domains of the constituent block copolymers.

6.3 Mechanical Properties and Micromechanical Behaviour

6.3.1 Tensile Properties

Stress-strain curves of binary block copolymer blends given in fig 6.7 provide an excellent example of synergistic blends in which the mechanical properties show almost a linear dependence with composition. These diagrams elucidate how the balance of elastic to plastic deformation shifts with composition. The mechanical behaviour shifts gradually from a thermoplastic to an elastomer with increasing LN4 content.

Gradual disappearance of alternating layer structure (characteristic of the sample ST2) associated with appearance of sphere-like domains dispersed in rubbery matrix (characteristic of LN4) with increasing LN4 content is the reason for the observed continuous shift in mechanical behaviour.

In solution cast samples, where the domains are randomly oriented, the yield stress is lower than that of injection moulded blends. The yield point which is already diffuse in ST2, becomes less pronounced with increasing LN4 concentration. The yield point in the injection moulded samples is visible until an LN4 content of 60 wt %. Appearance of the more pronounced yield point in

injection moulded sample is connected with domain orientation and thicker size of the tensile bars.

A linear dependence of Young's modulus and elongation at break with composition as demonstrated in fig 6.8 manifests the possibility of fine tuning stiffness and ductility of the investigated binary block copolymer blends.

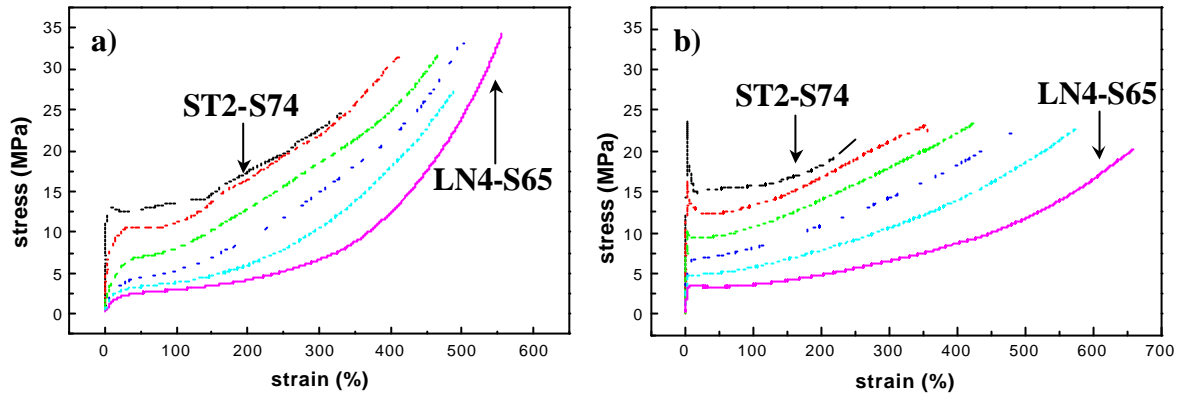


Figure 6.7: Stress-strain behaviour of the binary ST2/LN4 blends at room temperature; a) solution cast samples and b) injection moulded samples, cross head speed 50mm/min.

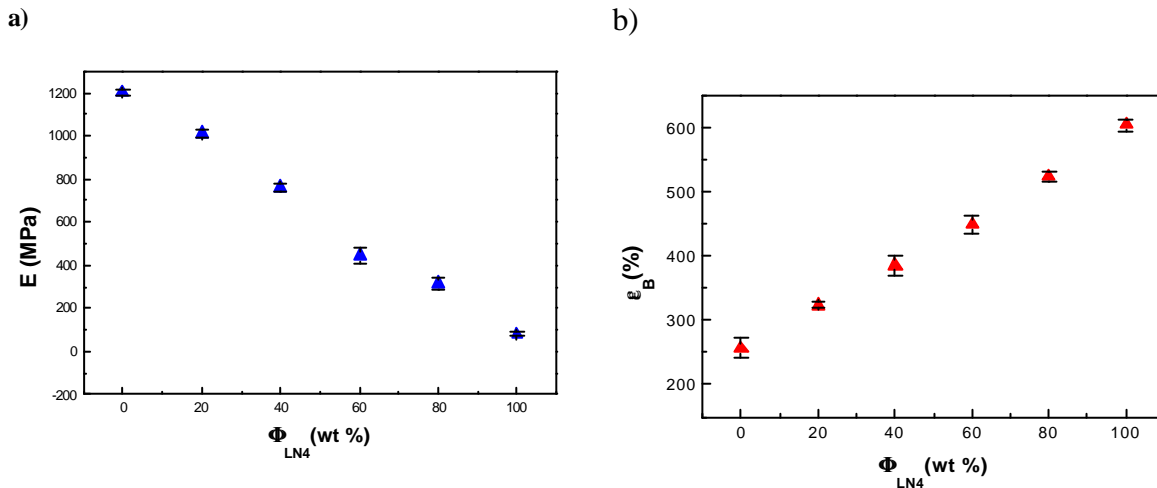


Figure 6.8: a) Young's modulus and b) Elongation at break plotted as a function of blend composition in ST2/LN4 blends (injection moulded samples, 50 mm/min at room temperature).

The elongation at break increases with LN4 concentration while the stress at break remains more or less constant. Higher maximum stress level is achieved in solution cast samples than in injection moulds which is attributable to better phase separation in the former.

With increasing LN4 content, the amount of elastic deformation in the blends progressively increases making it more difficult to analyse the strain induced structural changes. However, important inferences on micromechanical processes of deformation may be obtained by analysing the fracture surfaces of the tensile specimens broken in tensile tests. Representative fracture surface morphology of some binary blends is presented in fig 6.9.

Fracture surface of pure star block copolymer shows ductile fracture of the specimen accompanied with large plastic stretching and fibrillation. The fracture process begins somewhere at the middle and expands towards periphery of the tensile bar (fig 5.16). A transition in deformation behaviour is observed at an LN4 content of 20 wt %, when the fracture surface shows the structures typical of shear deformation. The typical shear lips (fracture paraboles), which represent cracks propagating along different planes, are clearly visible (fig 46.9a).

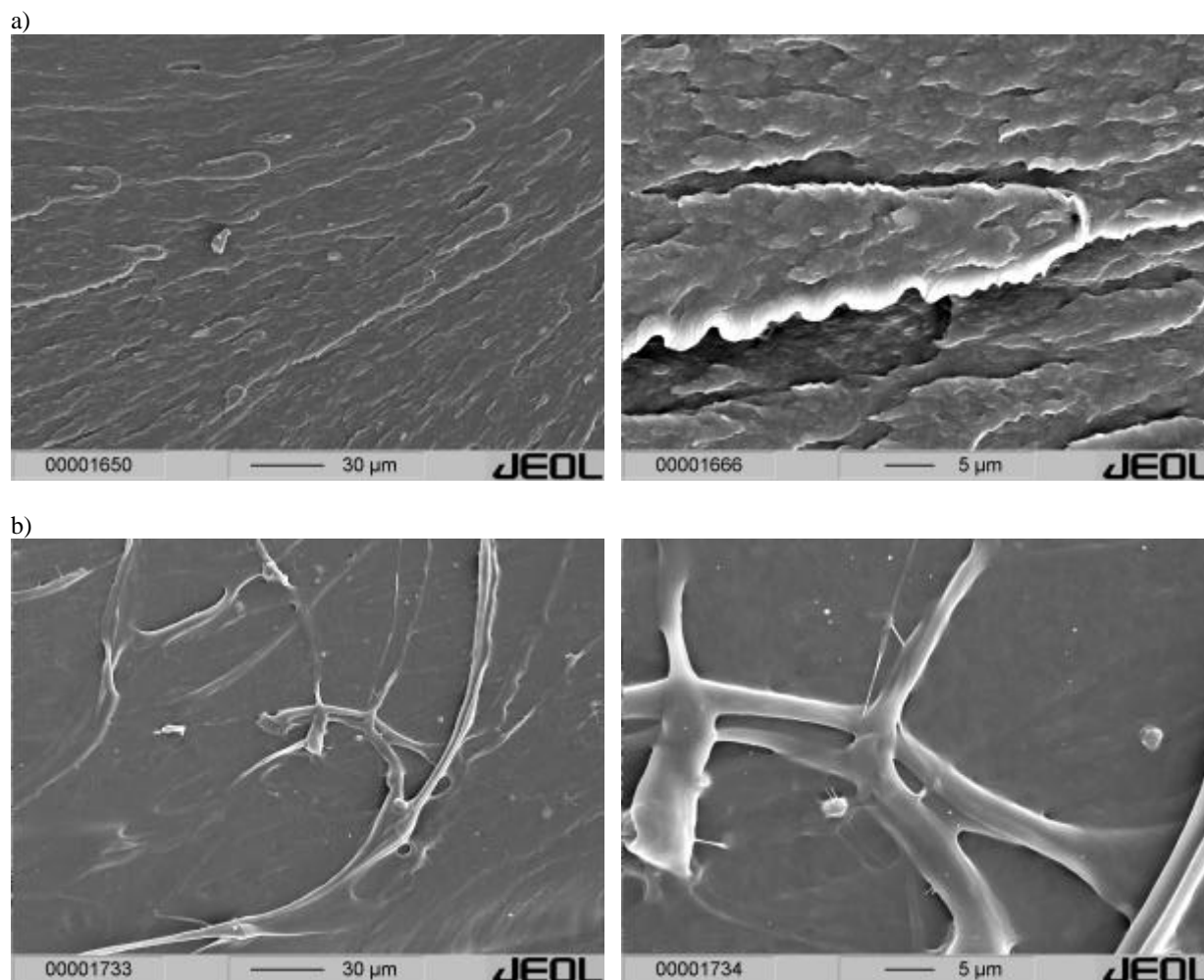


Figure 6.9: Lower (left) and higher (right) magnification of SEM micrographs showing fracture surface morphology of binary ST2/LN4 blends, fracture surfaces from injection moulded bars broken in tensile test a) 20 wt % LN4 and b) 60 wt % LN4

With increasing LN4 content, the fracture surface becomes increasingly smoother suggesting increasing tendency of elastic deformation. The extent of plastic deformation decreases, and the fracture surface shows isolated regions of plastically drawn materials (fig 6.9b).

Micromechanical behaviour of the pure block copolymers ST2 and LN4 has been discussed in section 4.3.1. It has been mentioned that ST1 shows a large homogeneous plastic deformation of PS lamellae while LN4 exhibits principally an elastic behaviour. The deformation mechanisms is coupled with the orientation of microstructures as well.

The morphology of the blends become more complex with increasing LN4 content as the elastic deformation becomes more and more dominating. These factors introduce difficulty in the determination (especially in the quantification) of strain induced structural changes in the samples. Therefore, deformation structures in solution cast blend containing 60 wt % LN4 have been investigated by TEM. The representative TEM micrographs are given in fig 6.10.

In the first glance, it may be noticed that lamellar grains are turned into chevron-like patterns as observed in cylindrical and lamellar block copolymers under tensile deformation [126,143]. Almost all the kink boundaries in these ‘inverse chevrons*’, are, however, perpendicular to the strain direction in contrast to the deformation structures in lamellar block copolymer (e.g, compare with fig 4.12b). Low magnification of TEM image reveals that the ellipsoidal worm-like PS domains in the ‘matrix’ are aligned in the strain direction. This is an indication of plastic deformation of the matrix-domains. Furthermore, the thickness of PS lamellae has been reduced from about 22 nm to about 15 nm due to deformation (Appendix 6.2).

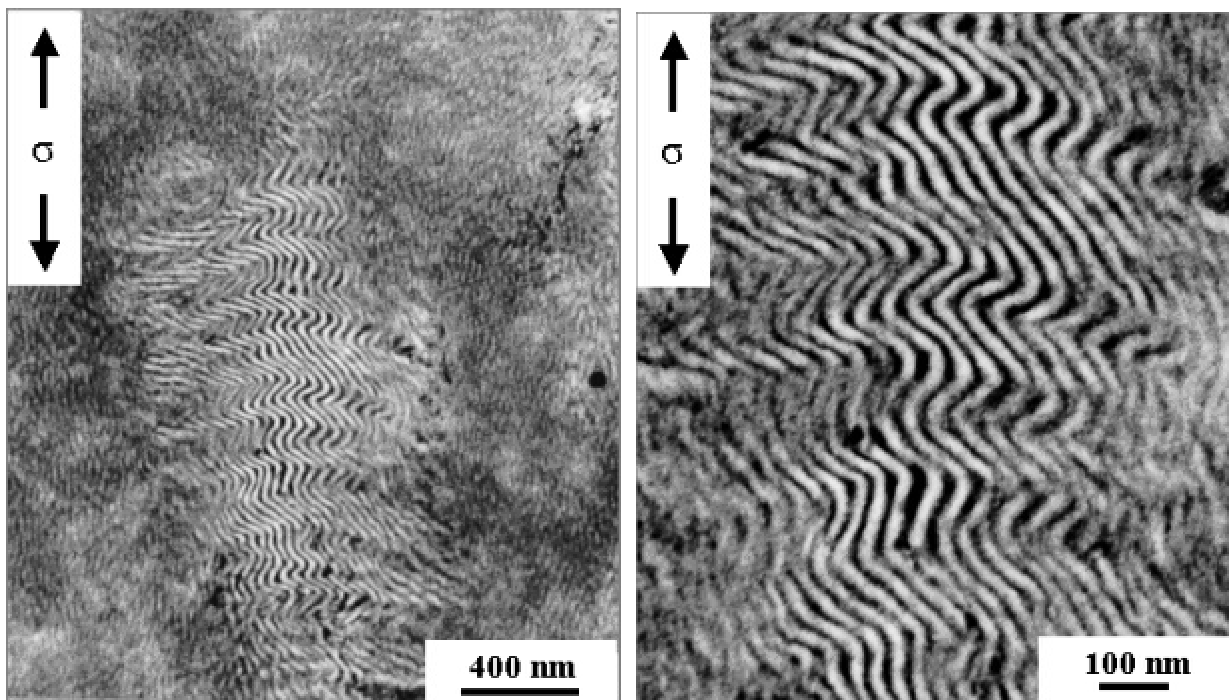


Figure 6.10: TEM micrographs showing strain induced structural changes in solution cast ST2/60 wt % LN4 blend with a deformed lamellar region; sample taken from the specimen broken in the tensile test after relaxation, deformation direction is shown by arrows.

Since the kink boundaries produced by deformation are almost always perpendicular to the strain axis, the dispersed lamellar grains must have rotated. Obviously, the chevrons are formed by the relaxation of the plastically deformed lamellae when the elastic energy absorbed by the matrix

* Because the kink boundaries are almost perpendicular to the strain axis in contrast to chevron formation in lamellar block copolymers, the chevron in the present case may be referred to as ‘inverse chevron morphology’.

phase has been released. This is the same mechanism as proposed for injection moulded ST2/PS190 blends at higher PS content (compare with fig 5.15 and 5.18).

Hence the deformation of this sample is mainly controlled by the predominantly elastic stretching of matrix consisting of dispersed PS domains which allows a large plastic deformation of lamellar grains and at the same time also contributes to delay fracture by elastically absorbing a large part of supplied energy.

6.3.2 Toughness Characterisation by Fracture Mechanics Approach

In this section, results from fracture mechanics experiments using an instrumented Charpy impact tester are discussed. Among others, a main objective of fracture mechanics methodology is to determine fracture mechanics parameter which quantify the materials resistance against unstable and stable crack growth. Three-point bending specimens (single edge notched bend, SENB) having a sharp notch made by razor blade allow the determination of the load-deflection (F-f) curves from which the parameters like stress intensity factor (K), J-integral values (J) and critical crack-tip opening displacement CTOD (δ) can be calculated [149].

a. Load deflection (F-f) curves

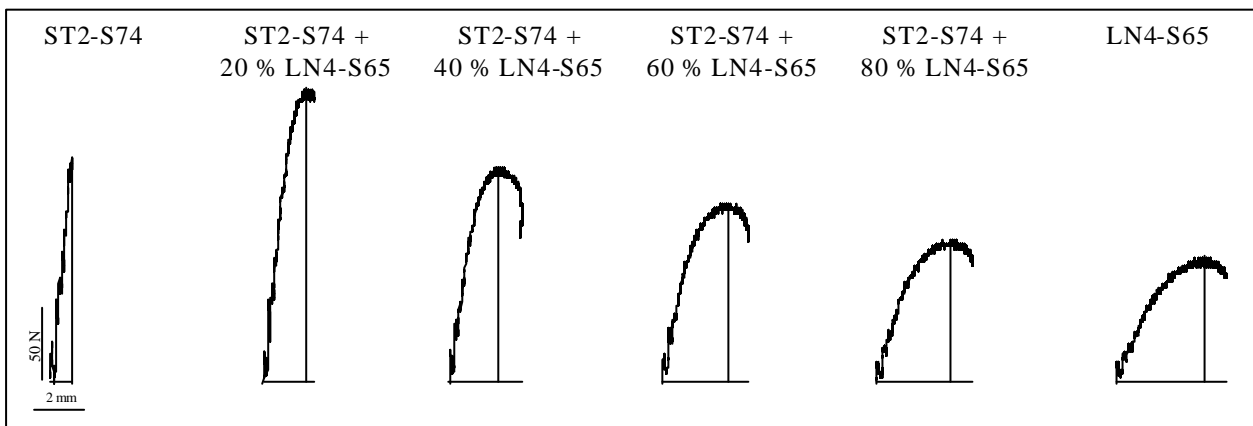


Figure 6.11: Load-deflection (F-f) curves for some binary star block copolymer/triblock copolymer blends; all the samples except ST2-S74 were not broken.

Representative load-deflection (F-f) curves of some of the notched samples are given in fig 6.11. These diagrams give an insight into materials behaviour under impact loading conditions. While pure star block copolymer shows nearly linear elastic behaviour, the blend with ≥ 20 wt % LN4 shows elastic-plastic behaviour combined with crack propagation energy after the load maximum. F-f diagrams recorded with unnotched samples allow the determination of Young's modulus E_d and yield stress σ_{yd} under impact loading conditions (fig 6.12). A continuous

decrease of these parameters with ascending LN4 concentration qualitatively suggests the increasing trend of toughness modification.

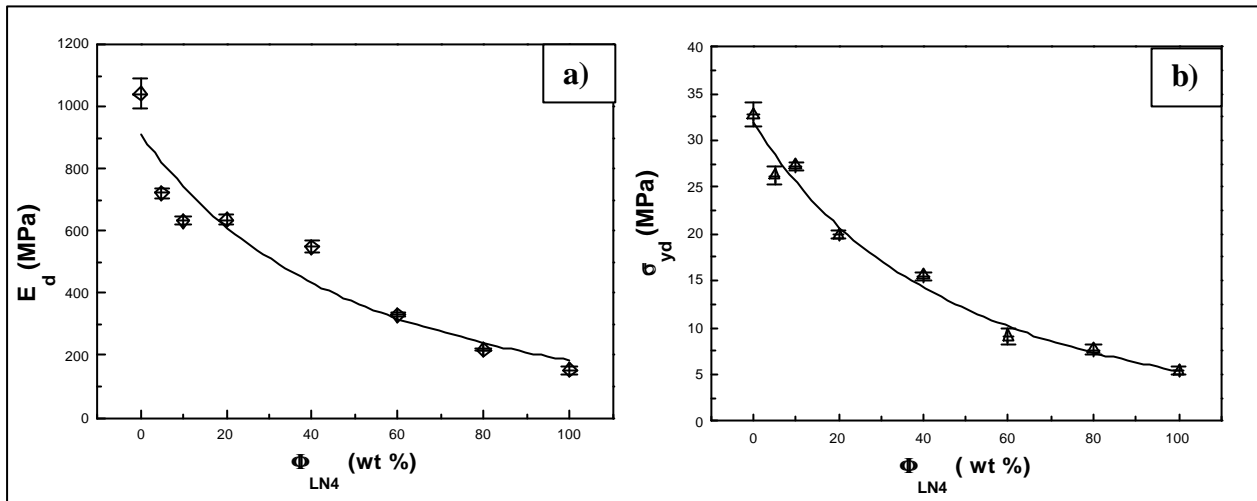


Fig 6.12: Dependence of a) Young's modulus E_d and b) yield stress σ_{yd} as a function of blend composition in ST2/LN4 blends determined by evaluating F-f diagrams of unnotched specimens.

b. Characterisation of Crack Resistance Behaviour

As already mentioned, the pure star block copolymer shows nearly linear elastic behaviour while the blend containing 20 wt % LN4 shows an elastic-plastic behaviour. Meanwhile, this change in F-f behaviour is connected with a transition from predominantly unstable crack growth to stable crack growth leading to a rapid increase in fracture toughness.

For blends containing <20 wt % LN4, very small amount of plastic flow may be ascertained. Since the maximum achievable stable crack growth in this composition range was very small ($\Delta a \leq 70 \mu\text{m}$, small scale yielding), crack arresting was impossible. Hence, the experimental determination of crack resistance curves (R-curves) was possible only at LN4 concentration ≥ 20 wt %. The quantitative description of stable crack propagation behaviour resulting therefrom is based on the quantification of fracture mechanics parameters as resistance against stable crack initiation and propagation.

Crack resistance (R-) curves for ST2/LN4 blends are given in fig 6.13, which show the dependence of fracture mechanics parameters (J-integral J as well as crack-tip opening displacement, CTOD) as a function of stable crack growth Δa . Both J- Δa and δ - Δa curves (i.e., R-curves with J or δ as loading parameter) exhibit the identical behaviour indicating the similar applicability of both the concepts in determining the R-curves of these blends. At 80 wt % LN4, the behaviour is nearly equivalent to that of pure LN4, and hence, these curves may be evaluated simultaneously.

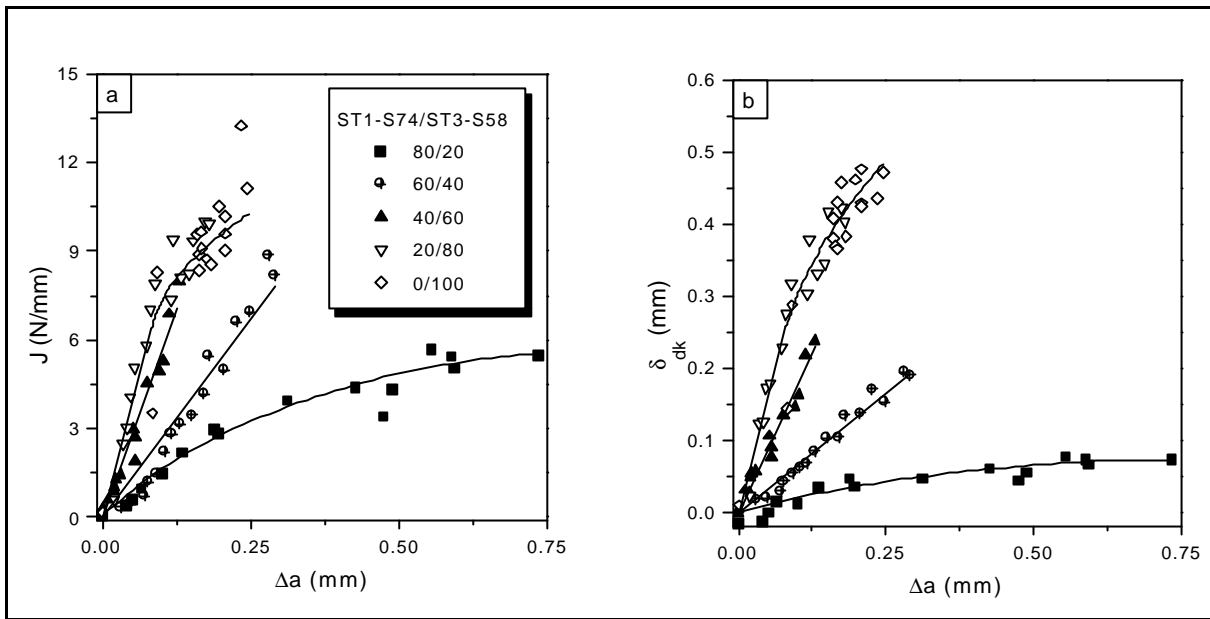


Figure 6.13: a) J- Δa and b) δ - Δa curves of binary ST2/LN4 blends; R-curves determined by using J-integral and δ concepts yield similar results.

The technical crack initiation values ($J_{0.1}$ and $\delta_{0.1}$) are generally employed in order to characterise the stable crack initiation. At these values the predetermined magnitude of small crack growth (e.g., $\Delta a = 0.1$ mm) will be reached. On the other hand, based on the considerations of the kinetics of crack propagation processes, i.e., analysis of different phases of crack growth (like crack-tip blunting, stable crack initiation and propagation, and perhaps the unstable crack propagation) as a function of time, physical crack initiation values (i.e., J_i and δ_i) can be determined. The parameters determined at physical crack initiation points are more theoretically motivated than those at technical ones (e.g., at $J_{0.1}$ and $\delta_{0.1}$ which are determined for stable crack growth $\Delta a = 0.1$ mm). Additionally, inferences about the magnitude of physical crack initiation values can be deduced through the quantitative analysis of stretch zone on the fracture surfaces. Like corresponding R-curves, the crack initiation values based on J-integral and δ concepts show similar tendency. Fracture mechanics parameters as resistance against unstable crack propagation (J_{Id}) and stable crack initiation ($J_{0.1}$, J_i) are plotted in fig 6.14a as a function of blend composition.

As a resistance against stable crack propagation, the slope of the R-curves at $\Delta a = 0.1$ mm (i.e. $dJ/d(\Delta a)|_{0.1}$ and $d\delta/d(\Delta a)|_{0.1}$) and resulting tearing modulus ($T_J = dJ/d(\Delta a)|_{0.1} \times E_d/\sigma_{yd}^2$ and $T_\delta = d\delta/d(\Delta a)|_{0.1} \times E_d/\sigma_{yd}$) can be utilised. As shown in fig 6.14b, the slopes of the R-curves at $\Delta a = 0.1$ mm and the tearing modulus increase up to 80 wt % LN4 after which these values remain constant. This indicates that the increasing ductility of the unnotched samples in the present case with increasing LN4 content associated with decreasing elasticity modulus E_d and yield strength σ_{yd} (fig 6.12) also manifests the resistance against stable crack propagation. It should be,

however, mentioned that this correlation does not have a general validity as shown by recent results (discussed in part II of ref. [118]). The physical crack initiation values (J_i and δ_i , fig. 6.14a) are insensitive to morphology which is in accordance with the previous results obtained for heterophase polymeric systems [176]. Furthermore, it is found that crack initiation values (e.g., $J_{0.1}$ and $\delta_{0.1}$) are generally not (or less pronounced) sensitive to the structure of the materials in contrast to the crack propagation values (like tearing modulus T_J and T_δ , fig. 6.14b).

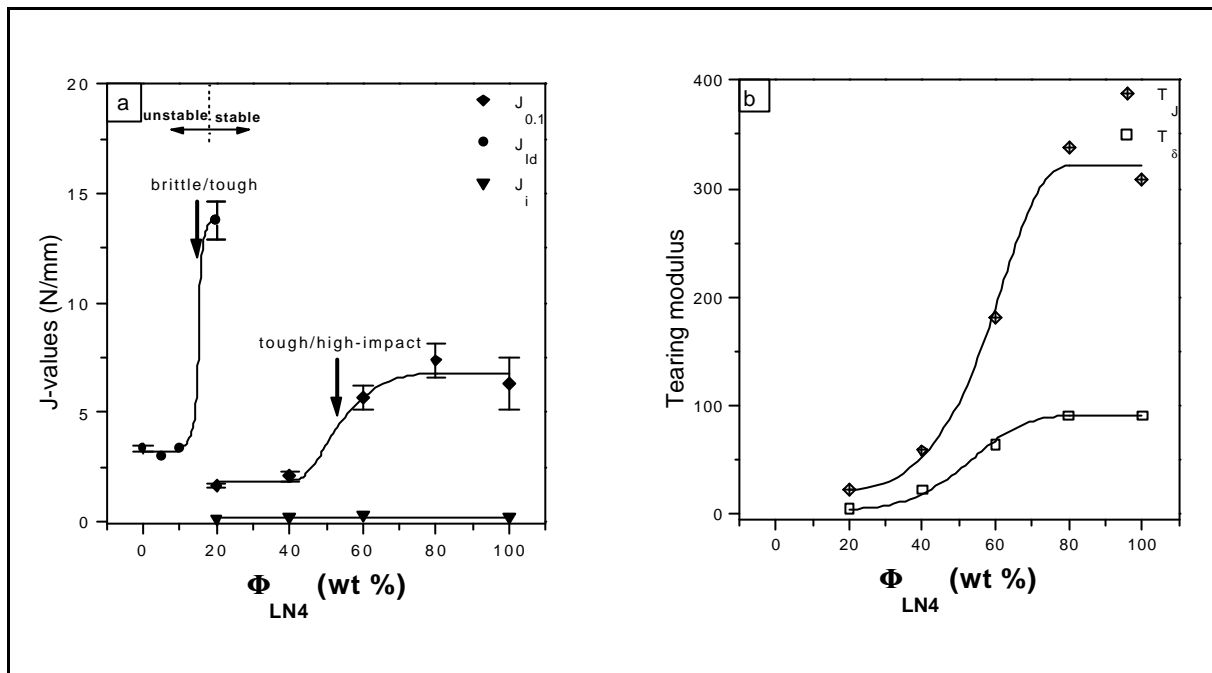


Figure 6.14: Fracture mechanics parameters as a function of blend composition: a) crack initiation and b) crack propagation values.

The kinetics of crack growth, especially the demarcation of each stage of crack growth, can be described by the crack propagation velocity. Additionally, it may be described by values like temporal change of fracture mechanics parameters e.g., CTOD-rate $d\delta/dt$ as a function of stable crack growth. In fig 6.15, the stages of crack propagation are represented by the slopes of $d\delta/dt$ values. Stage (1) is correlated with the region of crack tip blunting, where the original razor-sharp crack blunts resulting in a strong increase in $d\delta/dt$ values. In stage (2), the blunted crack propagates stable but non-stationary, i.e., the $d\delta/dt$ values increase with Δa . In stage (3), the non-stationary stable crack propagation finally reaches a stationary stable crack growth (equilibrium state), and the value of $d\delta/dt$ remains constant. The meaning of the constancy of $d\delta/dt$ values is equivalent to that of crack tip opening angles (CTOA). The maximum value of $d\delta/dt$ attained increase with LN4 content in the blends: 0.05 m/s and 0.09 m/s for 20 and 40 wt % of LN4 respectively and 0.10 m/s for 60 wt % and onwards.

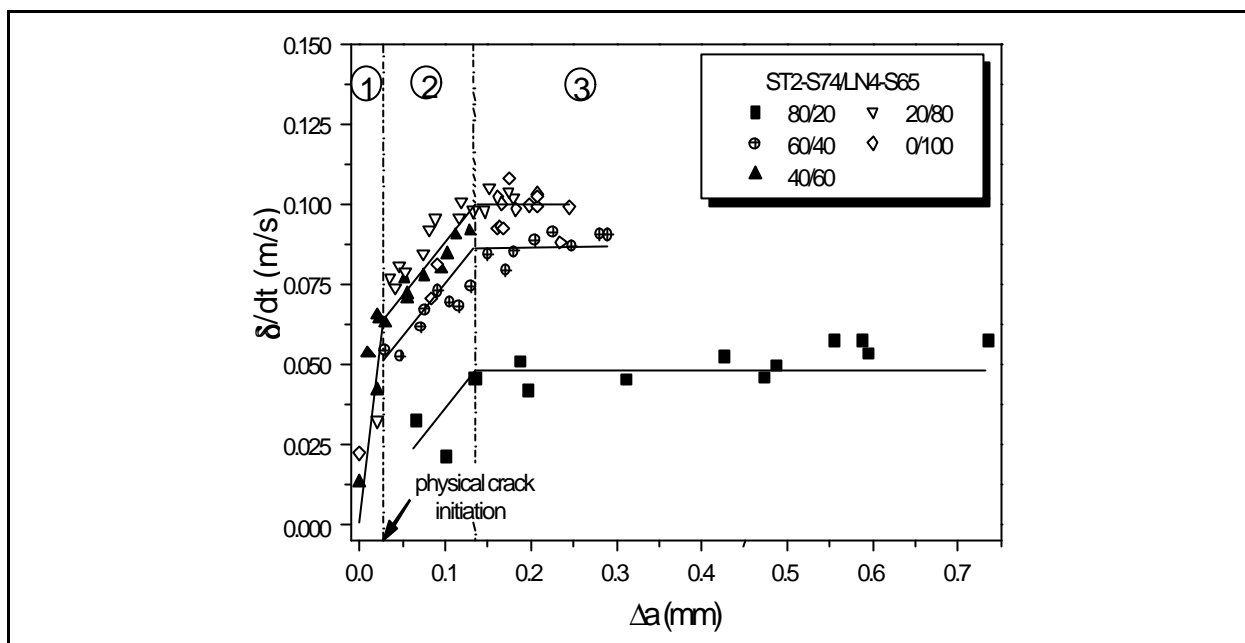


Figure 6.15: Crack-tip opening displacement rate $d\delta/dt$ as a function of stable crack growth and blend composition.

Two different brittle/ductile transitions (BDT) were observed in other heterophase polymers [176,177]: the conventional BDT1 (“brittle/tough” transition) as a measure for the safety against unstable crack propagation and THT (“tough/high-impact” transition) as a measure for the protection against stable crack initiation. In the investigated binary block copolymer blends, a pronounced BDT can be observed at 10-20 wt % LN4 while a quite broad BDT2 is observed between 50 and 60 wt % LN4 (fig 6.14a).

As demonstrated in recent studies [176,177], a shift from THT to BDT occurs if the crack growth mechanism shifts from stable towards unstable one. As discussed in [177], differences in deformation mechanisms leading to BDT and THT may be explained by Wu’s percolation theory [178] and Margolina’s theory [179], respectively. Wu’s approach has taken a critical inter-particle distance or a critical matrix-ligament thickness into consideration, which represents a material constant. Margolina has, however, demonstrated that critical inter-particle distance is strongly dependent on the loading conditions (like speed, loading mode and temperature). Especially, the temperature dependence of the critical inter-particle distance shows nearly a linear behaviour. This classification is, however, irrelevant in the investigated system where the structural heterogeneity lies on nanometer scale in contrast to a particle-matrix morphology of most conventional polymer blends.

Examination of fracture surfaces allows an analysis of crack propagation phenomena. As shown in SEM micrographs of fracture surfaces in fig 6.16, the transition BDT is associated not only with a strong increase in stable crack growth but also with a principal change in crack propagation mechanism. ST2 undergoes a brittle failure after crack-tip blunting via unstable crack propagation. In the blends with 5 and 10 wt % LN4, a small amount of stable crack growth

may be observed before the unstable crack growth begins, which is visible in SEM micrographs as structures formed by coalescence of microvoids (fig 6.16a,b and 6.17a). Such a crack propagation mechanism is typical for semicrystalline polymers like HDPE [173], where the structures are in nanometer scale, as well. In a composition range 10-20 wt % LN4, as a consequence of increasing disordered morphology, a sudden change from unstable crack propagation via coalescence of microvoids to the crack propagation via shear-flow occurs (fig 6.16c and 6.17b). The individual crack growth areas (parabolic marks) are separated by clearly visible shear-lips. Crack growth via shear-flow mechanism is typical for many amorphous polymers like polycarbonate [172].

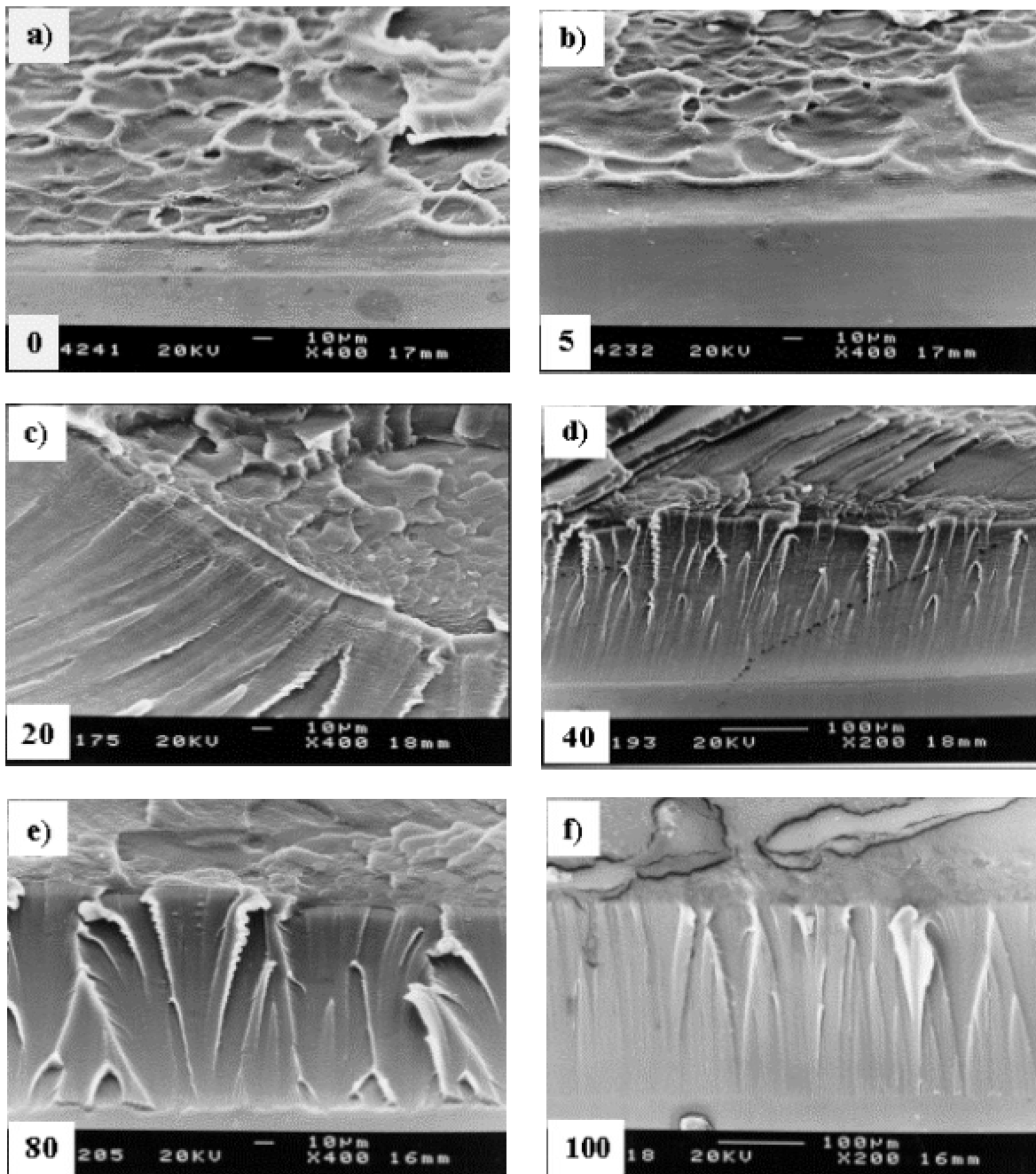


Figure 6.16: Scanning electron micrographs of fracture surfaces of ST2/LN4 blends (SENB specimens) loaded in impact test; the figures at the lower left bottom corner of each image stands for LN4 wt %.

Here, the crack becomes again sharp after blunting and propagates through the material by translation of the whole crack front [176]. This leads to the stretch zone at the end of whole fracture surface length in contrast to the stretch-zone in blends containing 5 and 10 wt % of LN4 which is formed at the end of razor-notch.

The transition in deformation mechanisms at LN4 content of 20 wt % (microvoids coalescence to shear-flow) associated with change in crack growth mode is demonstrated clearly by high magnification of SEM micrographs given in fig 6.17.

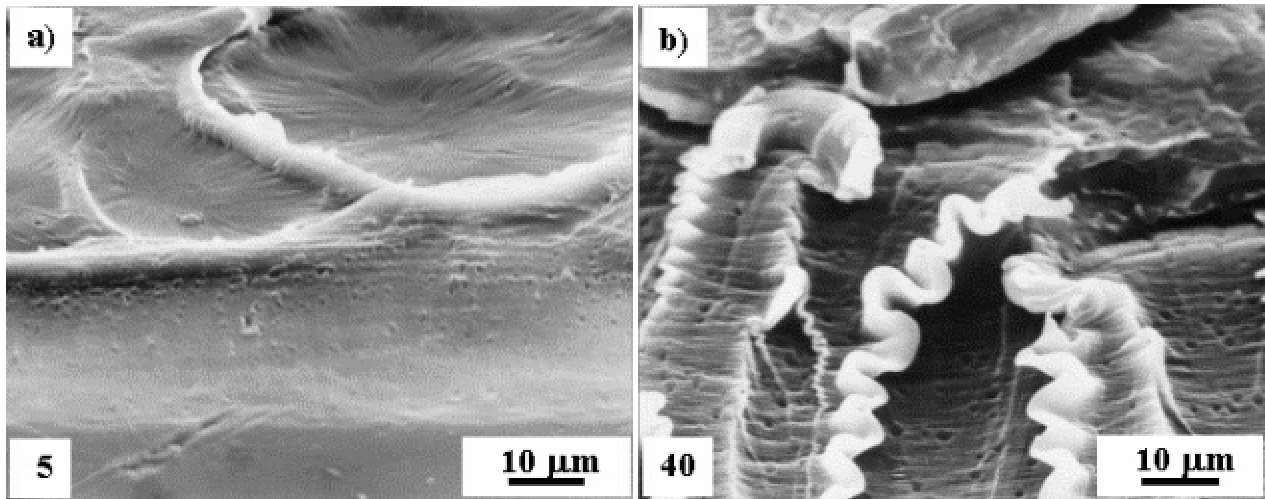


Figure 6.17: High magnification of SEM pictures of fracture surfaces of ST2/LN4 blends (SENB specimens) loaded in impact test; the figures at the lower left bottom corner of each image stands for LN4 wt %.

The size of the stretch zone can be used as a measure for plastic deformation during crack-tip blunting, which is indicated by stretch zone width (SZW) and stretch zone height (SZH) along and normal to the direction of crack propagation, respectively. The decrease of SZW in the blends with increasing LN4 content (fig. 6.16) may be attributed to the transition from the behaviour of a conventional thermoplastic material (ST2) to that of a thermoplastic elastomer (LN4) i.e., a transition from viscoelastic to entropy-elastic deformation behaviour.

In contrast to conventional polymer blends where the toughness modification is achieved through the dispersion of a soft phase in a hard matrix (macrophase separation), the investigated binary block copolymer blends represent nanometer structured materials. New mechanism of toughness modification (where the transition from a lamellar structure with a high long range order to a less ordered structure plays the central role) results in a specific morphology-toughness correlation which differs fundamentally from toughening mechanism in conventional polymer blends.

An evidence of a strong correlation between fracture toughness and structural disorder of the microphase separated domains is provided by another set of binary block copolymer blends. TEM image of injection moulded LN2-S74/20 wt % LN4-S65, given in fig 6.18a, exhibits a long range order nearly as pronounced as in the pure triblock copolymer LN2. This highly ordered

morphology results in F-f diagram presented in fig 6.18b under same set of condition as ST2/LN2 blends. In contrast to ST2/20 wt % LN4 blend, LN2/LN4 blends with identical composition shows predominantly unstable crack propagation and nearly linear elastic behaviour (compare with fig 6.11).

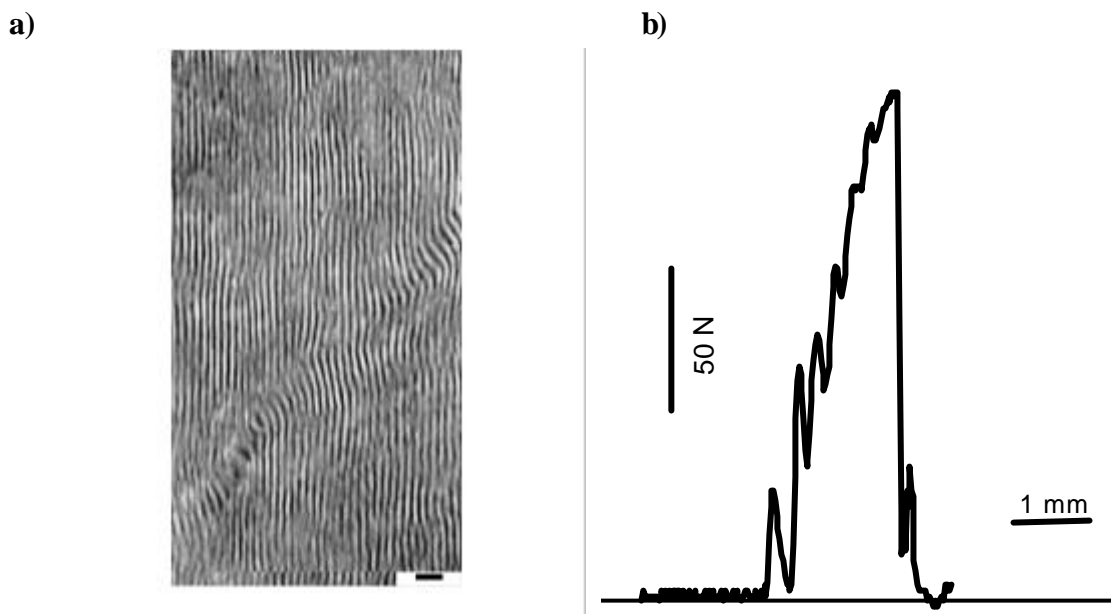


Figure 6.18: Influence of long range ordered morphology on fracture behaviour of binary block copolymer blends: a) TEM image of injection moulded LN2/20 wt % LN4 with injection direction vertical and b) corresponding F-f diagram.

6.4 Conclusions

Morphology, mechanical properties and deformation behaviour of binary blends consisting of asymmetric styrene/butadiene block copolymers are investigated. Toughness of the blends is especially characterised by the use of fracture mechanics approach. The mixtures represent a partially compatible system in which both microphase and macrophase separation of the blend components (which are themselves microphase separated) are observed.

The studied binary blends allow a balance of stiffness/toughness ratio in a wide composition range. Further, these blends provide unique combinations for preparing transparent ultra-high impact thermoplastically processable materials whose toughness appears to be favoured by structurally disordered microphase separated morphology.

The fracture behaviour of binary block copolymer blends investigated in this work is summarised in fig 6.19. A transition from brittle to tough behaviour occurs at ~ 10-20 wt % LN4, when the morphology changes from highly ordered lamellae to worm-like PS domains in a rubbery matrix. Meanwhile, the crack propagation mechanism shifts from microvoid coalescence to shear-flow. A second broad transition (tough/high impact) takes place at ~ 50-60 LN4 content as the morphology closely resembles that of pure LN4, and the rubber-like crack propagation mechanism (tearing) predominates.

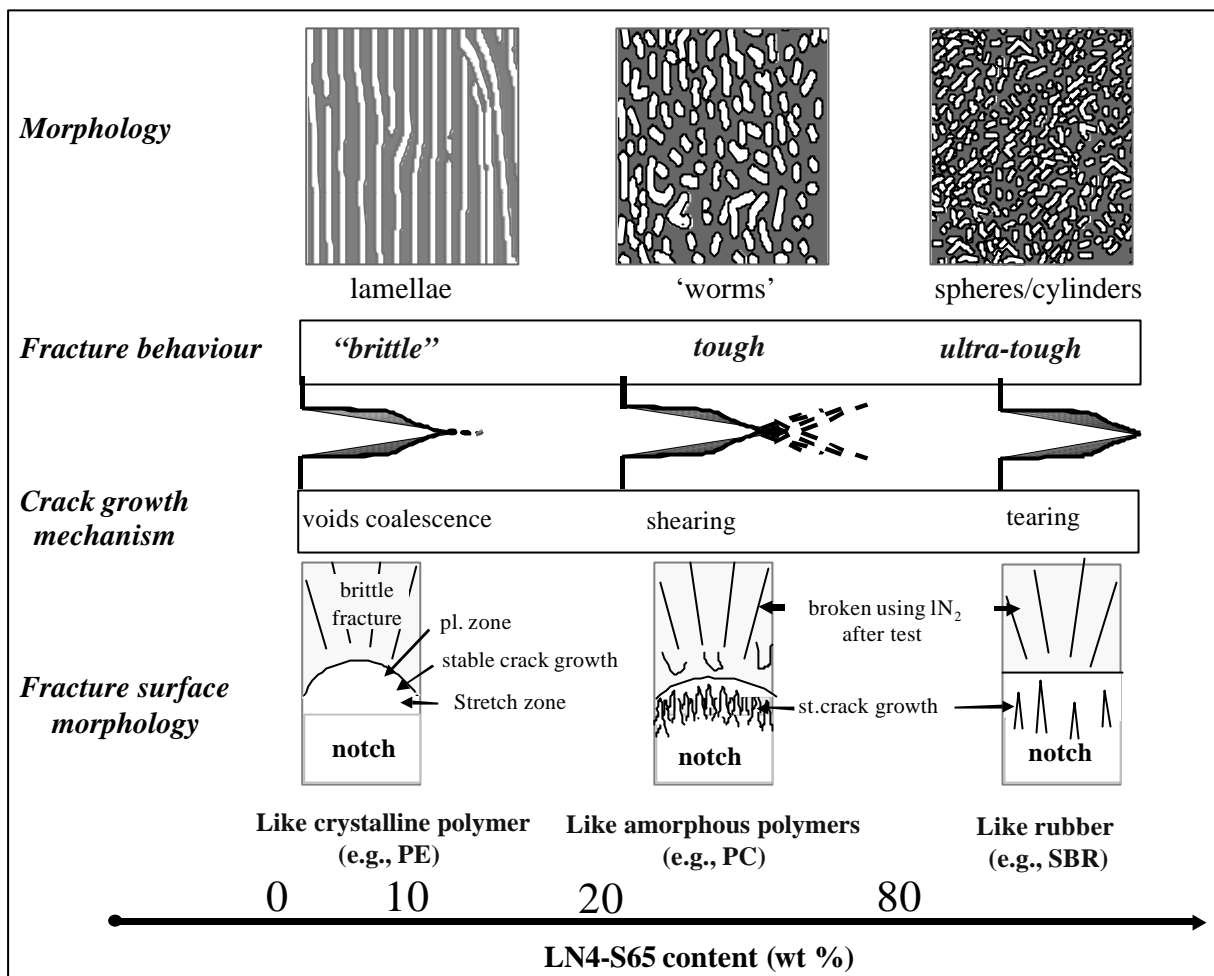


Figure 6.19: Scheme showing correlation between microphase morphology, fracture mechanism and fracture surface morphology of binary block copolymer blends.

To adequately clarify the toughness enhancement in the investigated block copolymer blends from the micromechanical standpoint, in situ microscopic deformation tests should be carried out in future.

7. SUMMARY AND PERSPECTIVES

This work deals with morphology, mechanical properties and deformation mechanisms of selected two component amorphous block copolymers (and the blends) in a narrow composition range ($\Phi_{\text{Styrene}} \sim 70$ vol %) as a function of copolymer molecular architecture. It has attempted to solve a few fundamental issues, and raised some new problems.

Summary of the Results

The major achievements can be listed as follows:

1. Molecular architecture of the asymmetric styrene/butadiene block copolymers exercises a dramatic influence on their phase behaviour, morphology formation and mechanical properties. For example, all the three kinds of classical morphologies (styrene domains in rubbery matrix, alternating styrene and butadiene layers, and butadiene domains in styrene matrix) were observed in a narrow composition range ($\Phi_{\text{Styrene}} \sim 70$ vol %) via architectural modification. This significant shift in phase behaviour has led to a drastic transition in mechanical and micromechanical behaviour. Hence, architectural modification may provide a novel route to develop block copolymers with tailored mechanical properties.
2. In a linear symmetric SBS triblock copolymer with 74 volume fraction styrene (LN1-S74), hexagonal PB cylinders in PS matrix have been observed. Depending on the constitution of the centre PB block and asymmetry of PS outer blocks, a significant shift from classical morphology is observed. Well defined lamellar morphology has been found in an asymmetric triblock copolymer (LN2-S74) with identical chemical composition as LN1-S74. At a total styrene volume fraction of 65%, morphology typical of a system close to order-disorder transition (short disordered cylinders without well-defined hexagonal symmetry) is observed in a linear block copolymer (LN4-S65) with styrene-co-butadiene (S/B) matrix.

As a consequence of modified architecture, a “two-component three-phase” morphology has been observed in an asymmetric tapered star block copolymer (ST2-S74) consisting of arms having basic SBS structure. The styrene domains found inside butadiene phase may be regarded as reinforcing fillers which enhance the toughening activity of these rubbery layers. Another neat star block copolymer ST1-S74 is found to possess a lamellae-like morphology, as well.

3. In general, the mechanical properties and underlying deformation mechanisms observed in the investigated systems can be explained on the basis of microphase separated morphologies.

Due to presence of PS matrix, the linear symmetric SBS triblock copolymer LN1-S74 containing 74 vol % polystyrene deforms by the formation of craze-like deformation zones. However, these craze-like zones are principally different from the deformation structures formed by rubber phase cavitation in classical diblock copolymers. Craze-like zones in the SBS triblock copolymer are likely to be formed via cavitation of the styrene phase which is favoured by the termination of the chain ends in the PS matrix. The deformation of block copolymers possessing alternating lamellae and PS domains in S/B matrix strongly depends on the orientation of microstructures relative to the strain direction. Typical “chevron”-morphology is observed in polygranular samples which results from the deformation of microphase structures lying perpendicular to the strain axis. Homogeneous plastic flow of PS lamellae and/or fragmentation of PS domains takes place if the structures are originally oriented parallel to the strain direction.

The block copolymer samples having alternating glassy and rubbery layer morphology (lamellae) are found to deform via homogeneous plastic flow of both glassy and rubbery layers without forming any localised deformation zones like crazes. This mechanism is termed as “thin layer yielding” and may be used as alternative toughening mechanism for brittle polymers. The homogeneous plastic flow of glassy lamellae takes place if their thickness lies in the range of 20 nm (= critical thickness D_{crit}) which is nearly the same magnitude as the thickness of craze fibrils in polystyrene homopolymer. These layers yield in the same manner as the craze fibrils in PS where the adjacent PB layers have functions analogous to that of microvoids in crazes.

The exact magnitude of D_{crit} cannot be ascertained because it may vary with the type of interface between the layers, chemical structure of the layers under consideration and the loading conditions. The results obtained so far indicate that the magnitude of D_{crit} shifts to lower values with increasing loading rate and decreasing temperature. Systematic study using model system is required to fully clarify this dependence.

4. Depending on the molecular weight of polystyrene homopolymer (hPS), both microphase and macrophase separated structures are observed blends of the star block copolymer ST2-S74 and hPS. Since the formation of equilibrium structures is strongly suppressed by

shear stress and rapid cooling process, no pronounced macrophase separation is observed in injection moulded samples.

The microphase separated blends having PS lamella thickness in the same range as the parent block copolymer, the “thin layer yielding” mechanism prevails. The macrophase separated blends having PS particles deform by yielding of lamellar matrix and voiding at the poles of these particles. In case of blends consisting of polystyrene matrix, typical fibrillated crazes are observed.

The deformation structures found in injection moulded blends consisting of star block copolymer and standard polystyrene (PS190) provide additional evidences for the “thin layer yielding” mechanism. At a PS190 content of 20 wt %, a transition from homogeneous plastic flow of lamellae to deformation localisation in the craze-like zones is observed. This transition appears when the thickness of PS lamellae approaches ca. 30 nm indicating that the magnitude of D_{crit} in styrene/butadiene block copolymers lies clearly below 30 nm.

At higher PS190 content (e.g., $\Phi_{PS190} \geq 60$ wt %), new kinds of deformation structures lying normal to the strain direction are observed which contain the characteristics of both crazes and shear bands. These structures are similar to the ‘kink bands’ noticed in lamellar diblock copolymers subjected to shear deformation. Negligibly small amount of strain of lamellae in these bands is the reason of their low elongation at break.

Under impact loading conditions, the lamellar block copolymers (which show ductile behaviour in tensile test) behave brittle. Their blends with polystyrene also show brittle behaviour. These are the indications of the loading rate dependence of the “thin layer yielding” mechanism. Similar behaviour would be expected at decreasing temperature.

In practical applications, the materials are desired which show tough behaviour both under slow and impact loading conditions. Binary blends consisting of a star block copolymer (ST2-S74) and a linear block copolymer having elastomeric properties (LN4-S65) enable a combination of stiffness and toughness in a wide composition range.

A strong increase in toughness has been observed at an LN4 content of 20 wt %. Obviously, this transition is attributable with the transition from highly ordered lamellar morphology to disordered worm-like domain-structure. The characterisation of fracture behaviour via fracture mechanics illustrates the existence of two different transitions: the first brittle/ductile transition at an LN4 content of about 10-20 wt % and the second ductile/high impact transition at 50-60 wt % LN4. A strong increase in fracture toughness observed at 20 wt % LN4 is associated with the transition in crack propagation

mechanism from unstable crack propagation via microvoids coalescence to stable crack propagation via shear-flow. The binary block copolymer blends may offer unique possibility of producing toughened, transparent and thermoplastically processable materials on the basis of nanophase separated structures.

Future Perspectives

In order to fully clarify the issues raised in the course of this study, the future works should be concentrated on the following points.

1. This study has dealt with phase behaviour and deformation mechanisms block copolymers having complex architectures in a narrow composition range. In order to establish a concrete correlation between molecular architecture, morphology and deformation mechanisms, a systematic study on model systems with well defined molecular parameters (e.g., number, composition and symmetry of arms in star block copolymers) is necessary.
2. Additional information for the description of the new mechanism “thin layer yielding” should be collected by investigating similar systems (having layer structures) with the variation of interfacial structure, temperature and loading rate.
3. Further investigations are necessary to confirm the influence of block copolymer architecture on the deformation behaviour of block copolymer/homopolymer blends.
4. The requirements for the toughness enhancement in binary block copolymer blends should be clarified by the analysis of micromechanical processes of deformation.

8. ZUSAMMENFASSUNG UND PERSPEKTIVE

Im Rahmen dieser Arbeit werden die Morphologie, die mechanischen Eigenschaften und die Deformationsmechanismen ausgewählter amorpher Styrol/Butadien-Blockcopolymerer und Abmischungen in einem engen Zusammensetzungsbereich ($\Phi_{\text{Styrol}} \sim 70$ Vol. %) in Abhängigkeit von der molekularen Architektur untersucht. Die Arbeit versucht, einige grundlegende Fragen zu beantworten und gleichzeitig einige neue Fragestellungen aufzuzeigen.

Zusammenfassung der Ergebnisse

Die wichtigsten Ergebnisse können wie folgt aufgelistet werden:

1. Die molekulare Architektur der unsymmetrischen Styrol/Butadien-Blockcopolymerer übt einen starken Einfluss auf das Phasenverhalten, die Morphologieausbildung und die mechanischen Eigenschaften aus. Alle typischen klassischen Morphologien (Styrol-Domänen in Butadien-Matrix, alternierende PS- und PB-Lamellen, PB-Domänen in PS-Matrix) der Blockcopolymerer werden im engen Zusammensetzungsbereich ($\Phi_{\text{Styrol}} \sim 70$ Vol. %) allein durch die Variation der Kettenarchitektur gefunden. Diese Tatsache hat eine erhebliche Änderung im mechanischen und mikromechanischen Verhalten zur Folge. Daraus folgt, dass die Modifikation der Architektur für die Herstellung von Blockcopolymeren mit maßgeschneiderten mechanischen Eigenschaften einen neuen Weg eröffnet.
2. Bei einem symmetrischen linearen SBS-Triblockcopolymer mit 74 % Styrolvolumenanteil (LN1-S74) werden hexagonal geordnete PB-Zylinder in der PS-Matrix beobachtet. Bedingt durch den molekularen Aufbau des PB-Mittelblocks und durch die Asymmetrie der PS-Außenblöcke wird in linearen Blockcopolymeren eine eindeutige Abweichung von der klassischen Morphologie festgestellt. Bei gleicher Zusammensetzung wie LN1-S74 wird in einem asymmetrischen Triblock (LN2-S74) eine eindeutig lamellare Morphologie gefunden.
Ein anderes lineares Blockcopolymer (LN4-S65) mit einem gesamten Styrolvolumenanteil von 65 % besitzt wegen der Anwesenheit einer Styrol-co-Butadien-(S/B)-Matrix eine Morphologie, die für ein System in der Nähe des Ordnungs-

Unordnungs-Überganges typisch ist (kurze PS-Zylinder in einer S/B-Matrix ohne ausgeprägte Fernordnung).

Aufgrund der modifizierten Architektur wird in einem asymmetrischen verschmierten Styrol/Butadien-Sternblockcopolymer (ST2-S74) mit SBS-Ästen eine „Zwei-Komponenten-Drei-Phasen-Morphologie“ gefunden. Die sich innerhalb von PB-Lamellen befindenden Styrol-Domänen wirken als „Füllstoff“ und verstärken zugleich die Zähigkeitssteigernde Wirkung der Kautschukschichten. Ein anderes Sternblockcopolymer (ST1-S74) ohne verschmierten Übergang zeigt ebenfalls eine lamellenartige Morphologie.

3. Im Allgemeinen lassen sich die in untersuchten Systemen auftretenden Deformationsmechanismen und die resultierenden mechanischen Eigenschaften über die mikrophasenseparierten Morphologien diskutieren.

Aufgrund des Vorhandenseins der PS-Matrix verformt sich ein lineares symmetrisches SBS-Triblockcopolymer mit 74 % Volumenanteil Polystyrol (LN1-S74) durch Ausbildung crazeartiger Deformationszonen. Diese crazeartigen Deformationszonen unterscheiden sich aber grundsätzlich von den in klassischen Diblockcopolymeren wegen der durch Lochbildung (Cavitation) der Kautschukphase ausgebildeten Deformationsstrukturen. Es handelt sich bei SBS-Triblockcopolymeren um eine Cavitation der Styrolphase, die möglicherweise durch Termination der Kettenenden an der PS-Matrix begünstigt wird.

Die Deformation von Blockcopolymeren mit Lamellenstruktur und PS-Domänen in Styrol-co-Butadien-Matrix ist sehr stark von der Orientierung der Morphologie relativ zur Dehnrichtung abhängig. In polygranulären Proben bildet sich eine typische „Chevron“-Morphologie heraus, die durch die Deformation der quer zur Dehnrichtung liegenden mikrophasenseparierten Morphologie zustande kommt. Homogenes plastisches Fließen der PS-Lamellen und/oder Fragmentierung der PS-Domänen findet statt, wenn sich die Strukturen ursprünglich parallel zur Deformationsrichtung orientiert haben.

Die Styrol/Butadien-Blockcopolymeren mit alternierenden Schichten (Lamellen) deformieren sich durch homogenes plastisches Fließen der Lamellen, ohne lokal begrenzte Deformationszonen zu bilden. Dieser Mechanismus wird als Dünnschichtfließen (Thin-Layer-Yielding) bezeichnet, welches als alternativer Zähigkeitssteigernder Mechanismus in spröden Polymeren angewendet werden kann. Das Homogenfließen der glasartigen Schichten findet dann statt, wenn die Schichtdicke etwa 20 nm (= kritische Schichtdicke D_{crit}) beträgt (Größenordnung wie Craze fibrillendicke im Polystyrol-Homopolymer).

Diese Schichten fließen auf ähnliche Weise wie die Crazeffibrillen in PS, wobei die benachbarten PB-Schichten eine analoge Funktion wie die Mikrovoids in Crazes besitzen. Ein exakter Wert von D_{crit} kann aber nicht festgelegt werden, weil der Wert von den Eigenschaften der Grenzschicht zwischen den Lamellen, von der chemischen Struktur der Schichten und von den Belastungsbedingungen abhängen kann. Die Ergebnisse deuten darauf hin, daß sich der Wert D_{crit} mit zunehmender Belastungsgeschwindigkeit und abnehmender Temperatur nach unten verschiebt. Systematische Untersuchungen an Modellsystemen sind notwendig, um diese Abhängigkeit vollständig aufzuklären.

4. Abhängig vom Molekulargewicht und von der Zusammensetzung werden in Blends aus dem Sternblockcopolymer ST2-S74 und dem Polystyrolhomopolymer (hPS) Morphologien mit und ohne Makrophasenseparation des zugemischten Polystyrols beobachtet. Beim Spritzgießen ist die Ausbildung einer gleichgewichtsnahen Morphologie aufgrund von Scherung und rascher Abkühlung unterdrückt; daher tritt keine ausgeprägte Makrophasentrennung auf.

Das mikrophasenseparierte Blend, das PS-Lamellen in vergleichbarer Dicke wie das reine Sternblockcopolymer besitzt, deformiert sich durch den „Thin-Layer-Yielding“-Mechanismus. Blends mit makrophasenseparierten hPS-Teilchen verformen sich durch plastisches Fließen der Lamellenmatrix und durch Hohlrumbildung an den Polen der PS-Teilchen, während in Blends mit Polystyrol-Matrix typischerweise fibrillierte Crazes im PS beobachtet werden.

Die in spritzgegossenen Blends aus Sternblockcopolymer und Standardpolystyrol (PS190) festgestellten Deformationsstrukturen liefern zusätzliche Beweise für den „Thin-Layer-Yielding“-Mechanismus. Bei einem PS190-Anteil von 20 Gew. % wird ein Übergang vom homogenen plastischen Fließen von PS-Lamellen zu lokal begrenzter crazeartiger Deformation beobachtet. Dieser Übergang erfolgt, wenn sich die Dicke der PS-Lamellen 30 nm nähert. Dies deutet wiederum darauf hin, dass die kritische Schichtdicke für Polystyrolschichten in Styrol/Butadien-Blockcopolymeren deutlich unterhalb 30 nm liegt.

Bei höherem PS190-Gehalt (z.B. $\Phi_{\text{PS190}} \geq 60$ Gew. %) werden neuartige, senkrecht zur Dehnrichtung liegende Deformationszonen beobachtet, die Merkmale von Crazes und Scherbändern aufweisen. Diese Deformationsstrukturen ähneln den bei lamellaren Diblockcopolymeren unter Scherdeformation auftretenden „Kink-Bands“. Die geringe Dehnung der Lamellen in diesen Deformationsbändern korreliert mit der kleinen Bruchdehnung der Proben.

Unter schlagartiger Beanspruchung verhalten sich die lamellaren Blockcopolymere, die beim Zugversuch duktilen Verhalten zeigen, spröde. Deren Blends mit PS verhalten sich ebenfalls spröde. Daraus kann man die Dehnratenabhängigkeit des „Thin-Layer-Yielding“-Mechanismus ableiten. Ein ähnliches Verhalten würde man bei abnehmender Temperatur erwarten.

Für die Praxis werden aber Materialien gewünscht, die sowohl bei langsamer als auch bei schlagartiger Belastung zähes Verhalten zeigen. Binäre Blends aus einem Sternblockcopolymer (ST2-S74) und einem linearen Triblockcopolymer mit elastomeren Eigenschaften (LN4-S65) ermöglichen eine Kombination aus Steifigkeit und Zähigkeit über einen breiten Zusammensetzungsbereich.

Eine sprunghafte Zunahme der Zähigkeit wurde bei einem LN4-Anteil von 20 Gew. % beobachtet. Dieser Zunahme liegt offensichtlich ein Übergang von einer hochgeordneten lamellaren Morphologie zu einer ungeordneten wurmförmigen Domänenstruktur zugrunde. Die Charakterisierung des Bruchverhaltens durch bruchmechanische Konzepte lässt zwei Übergänge erkennen: einen ersten Übergang (Spröde-Zäh-Übergang) bei einem LN4-Gehalt von 10-20 Gew. % und einen zweiten Übergang (Zäh-Hochschlagzäh-Übergang) bei einem LN4-Gehalt von 50-60 Gew. %. Die starke Zunahme der Zähigkeit bei 20 Gew. % LN4 ist verbunden mit einem prinzipiellen Wechsel im Rissausbreitungsmechanismus von dominierend instabiler Rissausbreitung durch Hohlraumkoaleszenz zu stabiler Rissausbreitung durch Scherfließen. Die binären Blockcopolymerblends könnten damit die Möglichkeit bieten, optisch transparente, thermoplastisch verarbeitbare und hochschlagzähe Werkstoffe auf der Basis von nanophasenseparierten Strukturen herzustellen.

Ausblick

Ausgehend von den im Rahmen der Arbeit erreichten Ergebnissen können folgende Vorschläge unterbreitet werden, um weitere Anhaltspunkte für Lösungen von Problemen bzw. Antworten auf noch offene Fragen zu finden:

1. Diese Arbeit hat das Phasen- und Deformationsverhalten von Blockcopolymeren mit komplexer molekularer Architektur in einem engen Zusammensetzungsbereich behandelt. Um eine vollständige Korrelation der molekularen Architektur, der Morphologie und der Deformationsmechanismen darzustellen, sind Untersuchungen an Modellsystemen mit

definiert erweiterten molekularen Parametern (z. B. Zahl, Zusammensetzung und Symmetrie der Äste in Sternblockcopolymeren) notwendig.

2. Durch die Einbeziehung weiterer Systeme sowie durch Variationen von Grenzschichtstrukturen, Temperatur und Belastungsgeschwindigkeit sollten zusätzliche Informationen zur Erklärung des neuartigen Mechanismus „Thin-Layer-Yielding“ gewonnen werden.
3. Für einen vermuteten Einfluß der Blockcopolymerarchitektur auf das Deformationsverhalten der Blockcopolymer/Homopolymer-Blends sollten durch weitere Untersuchungen neue Hinweise gesammelt werden.
4. Für die Ableitung konkreter Bedingungen für eine Zähigkeitssteigerung in binären Blockcopolymer-Blends sind neben den durchgeführten bruchmechanischen Analysen insbesondere weitere Analysen der mikromechanischen Prozesse der Deformation notwendig.

9. REFERENCES

1. G.H. Michler: (1992), *Kunststoff-Mikromechanik-Morphologie, Deformations-und Bruchmechanismen*, Carl Hanser, München.
2. I.W. Hamley: (1998), *The Physics of Block copolymers*, Oxford Science Publications, Oxford.
3. A.J. Ryan and I.W. Hamley: (1997), *Morphology of block copolymers*, In R.N Haward and R.J. Young (Eds.), *The Physics of Glassy Polymers*, chapter 10, p. 451-497, Chapman and Hall, London.
4. F.S. Bates and GH Fredrickson: (1999), *Block copolymers-Designer soft materials*, AIP Phys. Today, 2, 32-38.
5. C. Gustin: (2000), *Thermoplastische Olefinelastomere*, p. 247-269, VDI-K Jahrbuch VDI-Gesellschaft Kunststofftechnik,
6. K. Binder: (1994), *Phase transitions in polymer blends and block copolymer melts: Some recent developments*, In *Advances in Polymer Science* 112, p. 183-299, Springer Verlag, Berlin.
7. L.H. Sperling: (1992), *Introduction to Physical Polymer Science*, 2nd Edition, chapter 4, p. 122-150, Wiley-Interscience Publication, New York.
8. U. Eisele: (1990), *Introduction to Polymer Physics*, Springer Verlag, Heidelberg.
9. F.J. Balta Calleja and Z. Roslaniec (Eds.): (2000), *Block Copolymers*; Marcel-Dekker Publishers, New York.
10. E.L. Thomas and R.L. Lescanec: (1995), *Phase morphology in block copolymer systems*, In A. Keller, M. Warner and A.H. Windle (Eds.), *Self-order and Form in Polymeric Materials*, p.147-164. Chapman & Hall, London.
11. Y. Matshuhita: (1998), *Block and graft copolymers*, In T. Araki, U. Tankong and M. Shibayama (Eds.), *Structure and Properties of Multiphase Polymeric Materials*, chapter 5, p. 121-154, Marcel Dekker Inc., New York.
12. T. Hashimoto: (1998), *Order-disorder transition in block copolymers*, In G. Holden, N.R. Legge, R.P. Quirk and H.E. Schroeder (Eds.), *Thermoplastic Elastomers*, 2nd Edition, chapter 15A, p. 429-463, Hanser Publishers, Munich.
13. L. Leibler: (1980), *Theory of microphase separation in block copolymers*, *Macromolecules* 13, 1602-1617.
14. F.S. Bates and G.H. Fredrickson: (1998), *Block copolymer thermodynamics: Theory and experiment*, In G. Holden, N.R. Legge, R.P. Quirk and H.E. Schroeder (Eds.), *Thermoplastic Elastomers*, 2nd Edition, Chapter 12, p. 336-364, Hanser Publishers, Munich.
15. J.M.G. Cowie: (1982), *Carbon chain block copolymers and their relationship with solvents*, In I Goodman (Ed.), *Developments in Block Copolymers-I*, p. 1-37, Applied Science Publishers, London.
16. A.E. Woodward (Ed.), (1988), *Atlas of polymer Morphology*, Chapter 6, p. 189-215, Hanser Publishers, Munich.
17. A.J. Khandpur, S. Förster, F.S. Bates, I.W. Hamley, A.J. Ryan, W. Bras, K. Almdal and K. Mortensen: (1995), *Polyisoprene-polystyrene diblock copolymer phase diagram near the order-disorder transition*, *Macromolecules* 28, 8796-8806.
18. D.A. Hajduk, P.E. Harper, S.M. Gruner, C.C. Honeker, E.L. Thomas and L.J. Fetters: (1995), *A reevaluation of bicontinuous cubic phase in star block copolymers*, *Macromolecules* 28, 2570-2573.

19. D.A. Hajduk, P.E. Harper, S.M. Gruner, C.C. Honeker, G. Kim, E.L. Thomas and L.J. Fetters: **(1994)**, The gyroid- A new equilibrium morphology in weakly segregated diblock copolymers, *Macromolecules* 27, 4063-4075.
20. Y. Mogi, M. Nomura, H. Kotsuji, Y. Matsuhita and I. Noda: **(1994)**, Superlattice structures in morphologies of the ABC triblock copolymers, *Macromolecules* 27, 6755-6760.
21. Y. Mogi, K. Mori, Y. Matsuhita and I. Noda: **(1992)**, Tricontinuous morphology of triblock copolymer of the ABC type, *Macromolecules* 22, 5412-5415.
22. Y. Mogi, H. Kotsuzi, Y. Kaneko, K. Mori, Y. Matsuhita and I. Noda: **(1992)**, Preparation and morphology of triblock copolymers of the ABC type, *Macromolecules* 25, 5408-5411.
23. M. Shibayama, H. Hasegawa, T. Hashimoto and H. Kawai: **(1982)**, Microdomain structure of an ABC-type triblock copolymer of polystyrene-poly[(4-vinylbenzyl)dimethylamine]-polyisoprene cast from solution, *Macromolecules* 15, 274-280.
24. V. Abetz, T. Goldacker, **(2000)**, Formation of superlattices via blending of block copolymers, *Macromol. Rapid Comm.* 21, 16-34.
25. U. Breiner, U. Krappe, E.L. Thomas and R. Stadler: **(1998)**, Structural characterisation of the ‘Knitting Pattern’ in polystyrene-b-poly(ethylene-co-butylene)-b-Poly(methyl methacrylate) triblock copolymers, *Macromolecules* 31, 135-141.
26. R. Stadler, C. Auschra, J. Beckmann, U. Krappe, I. Voigt-Martin and L. Leibler: **(1995)**, Morphology and thermodynamics of Poly (A-block-B-block-C) triblock copolymers, *Macromolecules* 31, 3080-3097.
27. F. Drolet and G. H. Fredrickson: **(1999)**, Combinatorial screening of complex block copolymer assembly with self consistent field theory, *Phys. Rev. Lett.* 83, 4317-4320.
28. Y. Bohbot-Raviv and Z.-G. Wang: **(2000)**, Discovering new ordered phases of block copolymers, *Phys. Rev. Lett.*, 85, 3428-3431.
29. N. Hadjichristidis, S.Pispas, M. Pitsikalis, H. Iatrou and C. Vlahos: **(1999)**, Asymmetric star polymers: Synthesis and properties, In *Advances in Polymer Science* 142, p. 71-127, Springer Verlag, Berlin.
30. N. Hadjichristidis, H. Iatrou, S.K. Behal, J.J. Chludzinski, M.M. Disco, R.T. Garner, K. Liang, D.J. Lohse and S.T. Milner: **(1993)**, Morphology and miscibility of miktoarm styrene-diene copolymers and terpolymers, *Macromolecules* 26, 5812-5815.
31. C. Lee, S.P. Gido, Y. Poulos, N. Hadjichristidis, N.B. Tan, S.F. Trevino and J.W. Mays: **(1997)**, H-shaped double graft copolymers: Effect of molecular architecture on morphology, *J. Chem. Phys.* 107, 6460-6469.
32. C. Lee, S.P. Gido, Y. Poulos, N. Hadjichristidis, N.B. Tan, S.F. Trevino and J.W. Mays: **(1998)**, π -shaped double graft copolymers: Effect of molecular architecture on morphology. *Polymer* 39, 4631-4638.
33. M. Pitsikalis, S. Pispas, J.W. Mays and N. Hadjichristidis: **(1998)**, Nonlinear block copolymer architectures, In *Advances in Polymer Science* 135, p. 1-137, Springer Verlag, Berlin.
34. T. Hashimoto, S. Koizumi, H. Hasegawa, T. Izumitani, and S. T. Hyde: **(1992)**, Observation of “mesh” and “strut” structures in block copolymer/homopolymer mixtures, *Macromolecules* 25, 1433-1439.
35. I. Yamaoka and M. Kimura: **(1993)**, Effects of morphology on mechanical properties of SBS triblock copolymer, *Polymer* 34, 4399-4409.
36. S.T. Milner: **(1994)**, Chain architecture and asymmetry in copolymer microphases, *Macromolecules* 27, 2333-2335.

37. A.V. Dobrynin and I.Y. Erukhimovich: **(1993)**, Computer-aided comparative investigation of architecture influence on block copolymer phase diagrams, *Macromolecules* 26, 276-281.
38. G. Floudas, S. Pispas, N. Hajdichristidis, T. Pakula and I. Erukhimovich: **(1996)**, Microphase separation in star block copolymers of styrene and isoprene: Theory, experiment and simulation, *Macromolecules* 29, 4142-4154.
39. M.W. Matsen and M. Schick: **(1994)**, Microphase separation in star block copolymer melts, *Macromolecules* 27, 6761-6767.
40. A.N. Morozov and J.G.E.M. Fraaije: **(2001)**, Phase behaviour of block copolymer melts with arbitrary architecture, *J.Chem. Phys.* 114, 2452-2465.
41. K. Knoll and N. Nießner: **(1998)**, Styroflex—A new transparent styrene-butadiene copolymer with high flexibility. In Roderic P. Quirk (Ed.), *ACS Symp. Series 696, Applications of Anionic Polymerization Research*, chapter 9, 112-128.
42. K. Knoll and N. Nießner: **(1998)**, Styrolux and Styroflex-From transparent high impact polystyrene to new thermoplastic elastomers, *Macromol. Symp.* 132, 231-243.
43. R.P. Quirk and M. Morton: **(1998)**, Research on anionic triblock copolymers. In G. Holden, N.R. Legge, R.P. Quirk and H.E. Schroeder (Eds.), *Thermoplastic Elastomers, 2nd Edition*, Chapter 4, p. 71-100, Hanser Publishers, Munich.
44. J. S. Shim and J.P. Kennedy: **(1999)**, Novel thermoplastic elastomers. II. Properties of star block copolymers of PSt-b-PIB Arms emanating from cyclosiloxane cores, *J. Polym. Sci. A* 37, 815-824.
45. S. Asthana and J.P. Kennedy: **(1999)**, Star block polymers of multiple polystyrene-b-polyisobutylene arms radiating from a polydivinylbenzene core, *J. Polym. Sci. A* 37, 2235-2243.
46. J.S. Shim and J.P. Kennedy: **(2000)**, Novel Thermoplastic Elastomers. III. Synthesis, characterisation, and properties of star-block copolymers of poly(indene-b-isobutylene) arms emanating from cyclosiloxane cores, *J. Polym. Sci. A* 38, 279-290.
47. J.S. Shim, S. Asthana, N. Omura and J.P. Kennedy: **(1998)**, Novel Thermoplastic Elastomers. I. Synthesis and characterization of star-block copolymers of PSt-b-PIB arms emanating from cyclosiloxane cores, *J. Polym. Sci. A* 36, 2997-3012.
48. J.P. Kennedy: **(1998)**, Thermoplastic elastomers by carbocationic polymerisation, In G. Holden, N.R. Legge, R.P. Quirk and H.E. Schroeder (Eds.), *Thermoplastic Elastomers, 2nd Edition*, Chapter 13, p. 366-393, Hanser Publishers, Munich.
49. A.M. Mayes and M. Olvera de la Cruz: **(1989)**, Microphase separation in multiblock copolymer melts, *J. Chem. Phys.* 91, 7228-7235,
50. M. Olvera de la Cruz and I.C. Sanchez: **(1986)**, Theory of microphase separation in graft and star block copolymers, *Macromolecules* 19, 2501-2508.
51. A.M. Mayes and M. Olvera de la Cruz: **(1991)**, Concentration fluctuation effects on disorder-order transition in block copolymer melts, *J. Chem. Phys.* 95, 4670-4677.
52. K. Knoll: **(1996)**, Anionische Blockcopolymer; In *Kunststoff-Handbuch: 4. Polystyrol*, H. Gausepohl et al. (Eds.), chapter 3, p. 145-166, Hanser Verlag, München.
53. J.-J. Ma, M.K. Nestegard, B.D. Majumdar and M.M. Sheridan: **(1998)**, Asymmetric star block copolymers: Anionic synthesis, characterisation and pressure sensitive adhesive performance, *ACS Symp. Series 696*, 159-166.

54. M.W. Matsen: **(2000)**, Equilibrium behaviour of asymmetric ABA triblock copolymer melts, *J. Chem. Phys.*; 113, 5539-5544.
55. K. Gerberding, G. Heinz and W. Heckmann: **(1980)**, Blockcopolymer mit breiter Segmentmolekül-massenverteilung, *Makromol. Chem. Rapid Commun.* 1, 221-225.
56. F. Annighöfer and W. Gronski: **(1984)**, Block copolymers with broad interphase. Determination of morphological parameters and interphase width by electron microscopy and small angle X-ray scattering, *Makromol. Chem.* 185, 2213-2231.
57. F. Bühler and W. Gronski: **(1986)**, Block copolymers with controlled interphase width: Effects of interphase and composition on domain dimensions, *Makromol. Chem.* 187, 2019-2037.
58. J. Sameth, R.J. Spontak, S.D. Smith, A. Ashraf and K. Mortensen: **(1993)**, Microphase separated tapered triblock copolymers, *Journal de Physique* 3, 59-62.
59. J. Laurer, S.D. Smith, J. Sameth, K. Mortensen and R.J. Spontak: **(1997)**, Interfacial modification as route to novel bilayered morphologies in binary block copolymer/homopolymer blends, *Macromolecules* 30, 549-560.
60. S.A. Moctezuma, E.N. Martínez, R. Flores and E. Fernández-Fassnacht: **(1998)**, Tapered block copolymers of styrene and butadiene: Synthesis, structure and properties, *ACS Symp. Series* 696, 129-141.
61. S. Asai: **(1996)**, Styrene butadiene tapered block copolymers (TBC), *Polymer Preprints* 37, 706-707.
62. S.L. Aggarwal: **(1986)**, Introduction and Overview. In M. J. Folkes (Ed.), *Processing, Structure and Properties of Block Copolymers*, chapter 2, p. 125-164, Elsevier Applied Science Publishers, London.
63. P. Hodrokoukes, G. Floudas, S. Pipas and N. Hajdichristidis: **(2001)**, Microphase separation in normal and inverse tapered block copolymers of polystyrene and polyisoprene: 1. Phase state, *Macromolecules* 34, 650-657.
64. J.M. Zielinski and R.J. Spontak: **(1992)**, Thermodynamic consideration of triblock copolymers with a random middle block, *Macromolecules* 25, 5957-5964.
65. A. Aksimentiev and R. Holyst: **(1999)**, Phase behaviour of gradient copolymers, *J. Chem. Phys.* 11, 2329-2339.
66. R. Adhikari, R. Godehardt, W. Lebek, R. Weidisch, G.H. Michler and K. Knoll: **(2001)**, Correlation between morphology and mechanical properties of different styrene/butadiene block copolymers: A scanning force microscopy study, *J. Macromol. Sci. B*, in press
67. T. Hashimoto, Y. Tsukuhara, K. Tachi and H. Kawai: **(1983)**, Structure and properties of tapered block copolymers. 4. 'domain boundary mixing' and 'mixing in domain' effects on microdomain morphology and linear dynamic mechanical response, *Macromolecules* 16, 648-657.
68. G. Holden: **(2000)**, *Understanding Thermoplastic Elastomers*; p. 15-35, Carl Hanser Verlag, Munich.
69. G. Holden: **(1998)**, *Applications of Thermoplastic Elastomers*; In G. Holden, N.R. Legge, R.P. Quirk and H.E. Schroeder (Eds.), *Thermoplastic Elastomers*, 2nd Edition, Chapter 16, p. 574-601, Hanser Publishers, Munich.
70. R.G.C. Arridge and M.J. Folkes: **(1986)**, *Block copolymers and blends as composite materials*; In M. J. Folkes (Ed.), *Processing, Structure and Properties of Block Copolymers*, chapter 2, p. 125-164, Elsevier Applied Science Publishers, London.

71. H. Hashimoto, M. Fujimara, T. Hashimoto and H. Kawai: **(1981)**, Copolymer films cast from solutions. 7. Quantitative studies of solubilisation of homopolymers in spherical domains systems. *Macromolecules* 14, 844-851.
72. T. Hashimoto, T. Tanaka and H. Hasegawa: **(1990)**, Ordered structures in mixtures of block copolymer and homopolymers. 2. Effects of molecular weight of homopolymers, *Macromolecules* 23, 4378-4386.
73. S. Koizumi, H. Hasegawa and T. Hashimoto: **(1994)**, Spatial distribution of homopolymers in block copolymer microdomains as observed by a combined SANS and SAXS method, *Macromolecules* 27, 7893-7906.
74. S. Koizumi, H. Hasegawa and T. Hashimoto: **(1992)**, Ordered structure of block polymer/homopolymer mixtures. 4. Vesicle formation and macrophase separation, *Makromol. Chem. Macromol. Symp.* 62, 75-91.
75. S. Koizumi, H. Hasegawa and T. Hashimoto: **(1994)**, Ordered structure of block polymer/homopolymer mixtures. 5. Interplay of macro- and microphase transitions, *Macromolecules* 27, 6532-6540.
76. H. Hasegawa and T. Hashimoto: **(1996)**, Self assembly and morphology of block copolymer systems. In S.L. Aggarwal and S. Russo (Eds.), *Comprehensive Polymer Science*, Suppl. 2; p. 497-539, Pergamon, London.
77. K.I. Winey, E.L. Thomas and L.J. Fetters: **(1991)**, Ordered morphologies in binary blends of diblock copolymer and homopolymer and characterisation of their intermaterial dividing surfaces, *J. Chem. Phys.* 95, 9367-9375.
78. K.I. Winey, E.L. Thomas and L.J. Fetters: **(1992)**, Isothermal morphology diagrams for binary blends of diblock copolymer and homopolymer, *Macromolecules* 25, 2645-2650.
79. H. Feng, Z. Feng, H. Yuan and L. Shen: **(1994)**, Miscibility, microstructure and dynamics of blends containing block copolymer: 1. Miscibility of blends of homopolystyrene with styrene-butadiene block copolymers, *Macromolecules* 27, 7830-7834.
80. H. Feng, Z. Feng and L. Shen: **(1994)**, Miscibility, microstructure and dynamics of blends containing block copolymer: 2. Microstructure of blends of homopolystyrene with styrene-butadiene block copolymers *Macromolecules* 27, 7835-7839.
81. H. Feng, Z. Feng and L. Shen: **(1994)**, Miscibility, microstructure and dynamics of blends containing block copolymer: 3. Molecular motion in homopolystyrene and polystyrene/four-arm styrene-butadiene star block copolymer blends, *Macromolecules* 27, 7840-7842.
82. K.I. Winey, E.L. Thomas and L.J. Fetters: **(1992)**, The ordered bicontinuous double-diamond morphology in diblock copolymer/homopolymer blends, *Macromolecules* 25, 422-428.
83. M.M. Disko, K.S. Liang, S.K. Behal, R.J. Roe and K.J. Jeon: **(1993)**, Catenoid-lamellar phase in blends of styrene-butadiene diblock copolymer and homopolymer, *Macromolecules* 26, 2983-2986.
84. I. Yamaoka: **(1998)**, Effects of morphology on the toughness of styrene-butadiene-styrene triblock copolymer/methyl methacrylate-styrene copolymer blends, *Polymer* 39, 1765-1780.
85. I. Yamaoka: **(1998)**, Anisotropic behaviour of styrene-butadiene-styrene triblock copolymer/methyl methacrylate-styrene copolymer blends, *Polymer* 39, 1081-1093.
86. M. Hoffman, G. Kampf, H. Kromer and G. Pampus: **(1970)**, Kinetics of aggregation and dimensions of supramolecular structures in nanocrystalline block copolymers, *Advances in Chemistry Series* 99, 351-378.

87. M. Jiang, J.-V. Xie and T.-Y. Yu: **(1982)**, Studies on phase separation in polyblends of block copolymers, *Polymer* 23, 1557-1560.
88. G. Hadziioannou and A. Skoulios: **(1982)**, Structural studies of mixtures of styrene/isoprene two- and three-block copolymers, *Macromolecules* 15, 267-271.
89. T. Hashimoto, K. Yamasaki, S. Koizumi and H. Hasegawa: **(1993)**, Ordered structures in blends of block copolymers: 1. Miscibility criteria for lamellar block copolymers, *Macromolecules* 26, 2895-2905.
90. S. Koizumi, H. Hasegawa and T. Hashimoto: **(1994)**, Ordered Structures in blends of block copolymers: 3. Self-assembly in blends of sphere- and cylinder-forming copolymers, *Macromolecules* 27, 4371-4381.
91. T. Hashimoto, S. Koizumi and H. Hasegawa: **(1994)**, Ordered structures in blends of block copolymers: 2. Self-assembly for immiscible lamellae forming copolymers, *Macromolecules* 27, 1562-1570.
92. R. J. Spontak, J.C. Fung, M.B. Braunfeld, J.W. Sedat, D.A. Agard, L. Kane, S.D. Smith, M.M. Sato and A. Ashraf: **(1996)**, Phase behaviour of ordered Diblock Copolymer Blends: Effect of Compositional Heterogeneity, *Macromolecules* 29, 4494-4507.
93. K. Kimishima ; H. Jinnai and T. Hashimoto: **(1999)**, Control of Self-Assembled Structures in Binary Mixtures of A-B Diblock Copolymer and A-C Diblock Copolymer by Changing the Interaction between B and C Block Chains, *Macromolecules* 32, 2585-2596.
94. C.M Papadakis, K. Mortensen and D. Posselt: **(1998)**, Phase behaviour of binary blends of symmetric polystyrene-polybutadiene diblock copolymers studied using SANS, *Eur. Phys. J. B4*, 325-332.
95. C.M. Papadakis, K. Mortensen and D. Posselt: **(2000)**, Macrophase-separation in binary blends of symmetric polystyrene-polybutadiene diblock copolymers, *Macromol. Symp.* 149, 99-106.
96. R. Weidisch: **(1997)**, Einfluß des Phasenverhaltens von Poly(styrol-b-butylmethacrylat) Diblockcopolymeren auf Morphologie und Deformationsverhalten, Ph. D. Thesis, University of Halle-Wittenberg.
97. R.J. Young: **(1989)**, *Introduction to Polymer Science*, Chapman and Hall, London.
98. G. Menges: **(1990)**, *Werkstoffkunde-Kunststoffe*, 3rd Edition, Hanser Publishers, Munich.
99. M.C.M. van der Sanden and H.E.H. Meijer: **(1993)**, Ultimate toughness of amorphous polymers, *Macromol. Symp.* 75, 115-126.
100. C. Mueller, J. Kerns, T. Ebeling, S. Nazarenko, A. Hiltner and E. Baer: **(1997)**, In P. Coats (Ed.), *Polymer Process Engineering* 97, Book 681, p.137-157, The Materials Institute, The University Press, Cambridge.
101. M.C. Garcia, G.H. Michler and S. Henning: **(2001)**, Micromechanical behaviour of branched polystyrene investigated by in-situ tem and ultramicrohardness, *J. Macromol. Sci.B*, in press
102. G.H. Michler: **(1996)**, Deformation and fracture (Micromechanical mechanisms), In J.S. Salamone (Ed.), *Polymeric Materials Encyclopedia – Synthesis, Properties and Applications*, CRC Press New York.
103. G.H. Michler: **(1999)**, Micromechanics of Polymers, *J. Macromol. Sci.,-Phys. B* 38, 787-802.
104. G.H. Michler: **(2001)**, Craze formation in amorphous polymers - formation of fibrillated crazes near the glass transition temperature; In W. Grellmann and S. Seidel, (Eds.), *Deformation and Fracture Behaviour of Polymers*, p. 193-208, Springer Verlag Berlin.
105. C.B Bucknall: **(1997)**, Rubber toughening; In R.N Haward and R. J. Young (Eds.), *The Physics of Glassy Polymers*, chapter 8, p. 363-412, Chapman and Hall, London.

106. G.H. Michler and J.-U. Starke: **(1994)**, Investigations of micromechanical and failure mechanisms of toughened thermoplastics by electron microscopy; In C.K. Riew and A.J. Kinloch (Eds.), ACS Advances in Chemistry Series 252, Toughened Plastics II, 251-277.
107. H.J. Elias: **(1990)**, Makromoleküle-Band 1 Grundlagen, 5th Edition, p. 962, Edition, Hüthig & Wepf Verlag, Basel, Heidelberg, New York.
108. B.J. Dair, C.C. Honecker, D.B. Alward, A. Avgeropoulos, N. Hadjichristidis, L.J. Fetters, M.S. Capel and E.L. Thomas: **(1999)**, Mechanical properties and deformation behaviour of the double gyroid phase in unoriented thermoplastic elastomers, *Macromolecules* 32, 8145-8152.
109. B.J. Dair, A. Avgeropoulos, N. Hadjichristidis and E.L. Thomas: **(2000)**, Mechanical properties of the double gyroid phase in oriented thermoplastic elastomers, *J. Mat. Sci.* 35, 5207-5213.
110. Abschlußbericht des Innovationskolleg-Neue Polymermaterialien, Teilprojekt A 2, p. 39-52, Feb. 2000, Martin-Luther-Universität Halle-Wittenberg.
111. R. Weidisch and G.H. Michler: **(2000)**, Correlation between phase behaviour, mechanical properties and deformation mechanisms in weakly segregated block copolymers; In F.J. Balta Calleja and Z. Roslaniec (Eds.), *Block Copolymers*, p. 215-249, Marcel-Dekker Publishers, New York.
112. A.S. Argon, R.E. Cohen, O.S. Gebizlioglu and C.E. Schwier: **(1983)**, Crazeing and toughness of block copolymers and blends; In H.H. Kausch (ed.) *Advances in Polymer Science 52/53, Crazeing in Polymers*, Volume I, p. 275, Springer-Verlag, Berlin, Heidelberg.
113. C.E. Schwier, A.S. Argon and R.E. Cohen: **(1985)**, Crazeing in polystyrene-polybutadiene diblock copolymer containing cylindrical polybutadiene domains, *Polymer* 26, 1985-1993.
114. A.S. Argon and R.E. Cohen: **(1989)**, Crazeing and toughness of block copolymers and blends, In H.H. Kausch (Ed.) *Advances in Polymer Science 91/92, Crazeing in Polymers-Volume II*, p. 301-351, Springer-Verlag, Berlin, Heidelberg.
115. B. Koltisko, A. Hiltner and E. Baer: **(1986)**, Crazeing in thin films of styrene-butadiene block copolymers, *J. Polym. Sci. B* 24, 2167-2183.
116. M. Matsuo, T.T. Wang, and T.K. Kwei: **(1972)**, Crazeing of polystyrene containing two rubber balls: A model for ABS plastics, *J. Polym. Sci. A* 2, 10, 1085-1095.
117. P. Beahan, A. Thomas and M. Bevis: **(1976)**, Some observations on the micromorphology of deformed ABS and HIPS rubber-modified materials, *J. Mat. Sci.* 11, 1207-1214.
118. R. Adhikari, G.H. Michler; T.A. Huy, E.M. Ivankova, R. Godehardt and K. Knoll: Influence of molecular architecture on mechanical properties of styrene/butadiene block copolymers. I: Morphology and micromechanical behaviour, manuscript in preparation
119. R. Weidisch: **(2001)**, Habilitation Thesis: Morphologie und Deformationsverhalten von Nanometerstrukturierten Polymermaterialien: Martin-Luther University, Halle-Wittenberg, in preparation
120. T.A. Huy, R. Adhikari, G.H. Michler and H.J. Radosch: **(2001)**, Deformation mechanisms of heterogeneous polymer systems studied by spectroscopic and microscopic methods, under preparation for *Macromol. Symp.*
121. S. Sakurai, S. Aida, S. Okamoto, T. Ono, K. Imaizumi and S. Nomura: **(2001)**, Preferential orientation of lamellar microdomains by uniaxial stretching of cross-linked PS-b-PB-b-PS triblock copolymer, *Macromolecules* 34, 3672-3678.

122. M. Fujimora, T. Hashimoto and H. Kawai: **(1978)**, Structural change accompanied by plastic-to-rubber transition of SBS block copolymers, *Rubber Chem. Technol* 51, 215-224.
123. T. Hashimoto, M. Fujimora, K. Saito, H. Kawai, J. Diamant and M. Shen: **(1979)**, Strain induced plastic-to-rubber transition of a SBS copolymer and its blends with PS, In S.L. Cooper, G.M. Estes, (Eds.), *ACS Advances in Chemistry Series-Multiphase Polymers*, 257-275.
124. H. Kawai, T. Hashimoto, K. Miyoshi, H. Uno and M. Fujimora: **(1980)**, Microdomain structure and some related properties of block copolymers. II. Plastic deformation mechanisms of the glassy component in rubber-toughened plastics, *J. Macromol. Sci. B* 17, 427-472.
125. R. Seguela and J. Prud'homme: **(1981)**, Deformation mechanism of thermoplastic two-phase elastomers of lamellar morphology having a high volume fraction of rubbery microphase, *Macromolecules* 14, 197-202.
126. Y. Cohen, R.J. Albalak, B.J. Dair, M.S. Capel and E.L. Thomas: **(2000)**, Deformation of oriented lamellar block copolymer films, *Macromolecules* 33, 6502-6516.
127. E.L. Thomas, R. Albalak and Y. Cohen: **(2000)**, Proceeding of 11th International Conference on "Deformation, yield and fracture of polymers"; 10-13 April 2000, Churchill College, Cambridge, UK; p. 191-194, The Chameleon Press, Limited.
128. Y. Cohen, M. Brinkmann and E.L. Thomas: **(2001)**, Undulation, dilation, and folding of a layered block copolymer, *J. Chem. Phys.* 114, 984-992.
129. D.L. Polis, S.D. Smith, N.J. Terrill, A.J. Ryan, D.C. Morse and K.I. Winey: **(1999)**, Shear-Induced Lamellar Rotation Observed in a Diblock Copolymer by in Situ Small-Angle X-ray Scattering, *Macromolecules* 32, 4668-4676.
130. D.L. Polis and K.I. Winey: **(1998)**, Controlling kink band morphology in block copolymers: Threshold criteria and stability *Macromolecules* 31, 3617-3625.
131. R. Weidisch, M. Ensslen, G.H. Michler, M. Arnold, H. Buddhe, S. Höring and H. Fischer: **(2001)**, A novel scheme for prediction of deformation mechanisms of block copolymers based on phase behaviour, *Macromolecules* 34, 2528-2533.
132. C. Creton, E.J. Kramer and G. Hadjiioannou: **(1992)**, Craze fibril extension ratio measurements in glassy block copolymers; *Colloid & Polym. Sci.*; 270, 399-404.
133. R. Seguela and J. Prud'homme: **(1988)**, Affinity of grain deformation on mesomorphic block polymers submitted to simple elongation, *Macromolecules* 21, 635-643.
134. E. Pedemonte, G. Dondero, G. Alfonso and F. de Candia: **(1975)**, Three-block copolymers: morphologies and stress-strain properties of samples prepared under various experimental conditions, *Polymer* 16, 531-538.
135. S.G. Tarasov, D.Y. Tsvankin and Y.K. Godovskii: **(1978)**, Structural changes during deformation of oriented and isotropic butadiene-styrene block copolymers, *Vysokomol. Soedin., Ser. A* 20, 1534-1542.
136. T. Pakula, K. Saijo, H. Kawai and T. Hashimoto: **(1985)**, Deformation behaviour of SBS triblock copolymer with cylindrical morphology, *Macromolecules* 18, 1294-1302.
137. J. A. Odell and A. Keller: **(1977)**, Deformation behaviour of an SBS copolymer, *Polym. Eng. and Sci.* 17, 544-559.

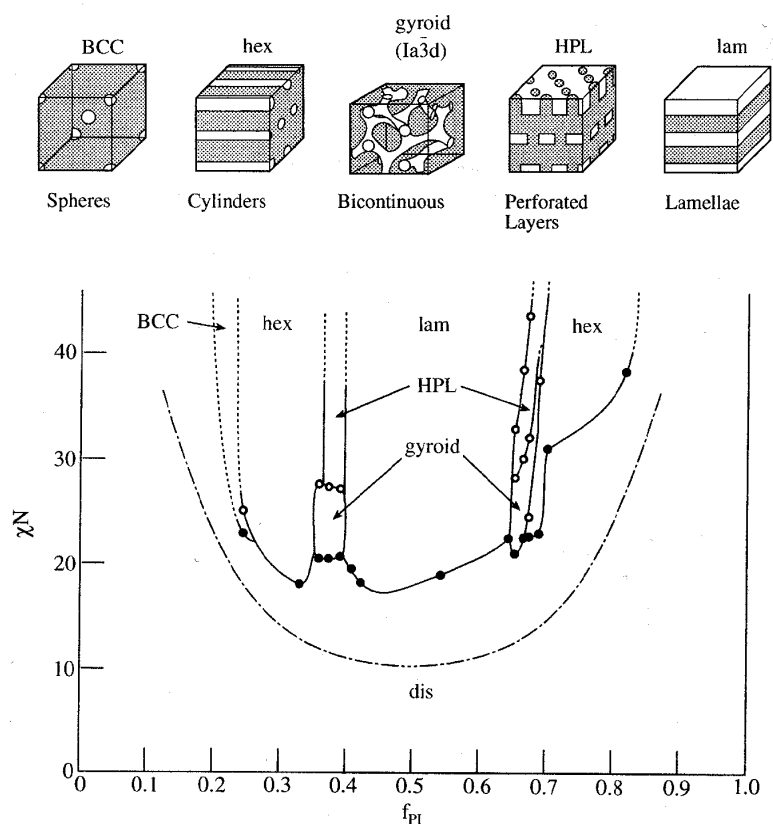
138. A. Keller and J. A. Odell: **(1985)**, The interrelation between microstructure and properties of block copolymers, In M. J. Folkes (Ed.), Processing, Structure and Properties of Block Copolymers, chapter 2, p. 29-74, Elsevier Applied Science Publishers, London.
139. J. Sakamoto, S. Sakurai, K. Doi and S. Nomura: **(1993)**, Molecular orientation of PS-b-PB-b-PS triblock copolymers with cylindrical microdomains of polystyrene, *Polymer* 34, 4837-4840.
140. S. Sakurai, J. Sakamoto, M. Shibayama and S. Nomura: **(1993)**, Effects of micro-domain structure on the molecular orientation of PS-b-PB-b-PS triblock copolymers, *Macromolecules* 26, 3351-3356.
141. C.C. Honeker: **(1997)**, Large strain deformation behaviour of oriented triblock copolymer cylinders, Ph. D. Thesis, Massachusetts institute of technology, Massachusetts.
142. C.C. Honeker, E.L. Thomas, R.J. Albalak, D.A. Hadjuk, S.M. Gruner and M.C. Capel: **(2000)**, Perpendicular Deformation of a Near-Single-Crystal Triblock Copolymer with a Cylindrical Morphology, 1. Synchrotron SAXS, *Macromolecules* 39, 9395-9406.
143. C.C. Honeker and E.L. Thomas: **(2000)**, Perpendicular Deformation of a Near-Single-Crystal Triblock Copolymer with a Cylindrical Morphology, 2. TEM, *Macromolecules* 39, 9407-9417.
144. I. Yamaoka: **(1998)**, Effects of Morphology on the Toughness of Styrene-Butadiene-Styrene Triblock Copolymer-Methyl Methacrylate-Styrene Copolymer Blends, *Polymer* 39, 1765-1778.
145. I. Yamaoka: **(1996)**, Effects of Morphology on Mechanical Properties of Styrene-Butadiene-Styrene Triblock Copolymer-Methyl Methacrylate-Styrene Copolymer Blends, *Polymer* 37, 5343-5356.
146. I. Yamaoka: **(1995)**, Toughened Polymer Blends Composed of a Ductile Styrene-Butadiene-Styrene Matrix with Brittle Methyl Methacrylate-Styrene Particles, *Polymer* 36, 3359-3368.
147. T. Kotaka, M. Tetsuhiro and K. Arai: **(1980)**, Morphology-mechanical property relationship of an SBS block copolymer and its blends with homopolymers, *J. Macromol. Sci. B* 17, 303-336.
148. Standard Draft ESIS TC4: **(1991)**, A Testing Protocol for Conducting J-Crack Growth Resistance Curve Tests on Plastics.
149. W. Grellmann, S. Seidler and W. Hesse: **(2001)**, Procedure for Determining the Crack Resistance Behaviour Using the Instrumented Impact Test. In W. Grellmann and S. Seidler (Eds.), Deformation and Fracture Behaviour of Polymers. p. 71-86, Springer Verlag, Berlin Heidelberg.
150. S. Seidler: **(1998)**, Anwendung des Risswiderstandskonzeptes zur Ermittlung strukturbezogener bruchmechanischer Werkstoffkenngrößen bei dynamischer Beanspruchung, VDI-Fortschrittberichte, Reihe 18: Mechanik/Bruchmechanik, Nr. 231, VDI-Verlag, Düsseldorf.
151. W. Grellmann and S. Seidler: **(1999)**, Possibilities and Limits of Standards and Drafts for J -Curve Determination on Polymers, In T. Winkler and A. Schubert (Eds.): Material Mechanics-Fracture, Mechanics-Micromechanics. p. 336-341, DDP Goldenberg, Dresden.
152. S. Seidler and W. Grellmann: **(1999)**, Determination of Geometry Independent J-Integral Values of Tough Polymers, *Intern. J. Fract., Lett. Fract. Micromech.* 96, L17-L21.
153. W. Grellmann, S. Seidler and R. Lach: **(2001)**, Geometrieunabhängige bruchmechanische Werkstoffkenngrößen-Voraussetzungen für die Zähigkeitsoptimierung von Kunststoffen. *Mat.-wiss. Werkstofftechnik*, in press.
154. S. Amelinckx, D. van Dyck, J. van Landuyt and G. van Tendeloo (Eds.), **(1997)**, Handbook of Microscopy-Applications in Materials Science, Solid-State Physics and Chemistry, Methods I and II, VCH Weinheim.

155. G. Odian: **(1991)**, Principles of polymerisation, 3rd Edition, Willey-Interscience, New York.
156. L.J. Fetters: **(1983)**, Synthesis and characterisation of block copolymers via anionic polymerisation, In D.J. Meier (Ed.), Block Copolymers–Science and technology, p. 17-38, Harwood Academic Publishers, London.
157. W.P. Gergen, R.G. Lutz and S. Davison: **(1998)**, Hydrogenated block copolymers in thermoplastic elastomer interpenetrating polymer networks, In G. Holden, N.R. Legge, R.P. Quirk and H.E. Schroeder (Eds.), Thermoplastic Elastomers, 2nd Edition, chapter 11, p. 297-334, Hanser Publishers, Munich.
158. S. Seiko: **(2000)**, Imaging of polymers using scanning force microscopy: From superstructures to individual molecules, Adv. in Polym. Sci., 151, p. 61-174, Springer Verlag Berlin Heidelberg.
159. S.N. Magonov, V. Elings and M.H. Whangbo: **(1997)**, Phase imaging and stiffness in tapping mode atomic force microscopy, Surf. Sci. 375, 385-391.
160. S.N. Magonov and M.G. Heaton: **(1998)**, Atomic force microscopy, Part: 6 Recent developments in AFM of polymers, American Laboratory 30, 9-15.
161. R. Godehardt, S. Rudolph, W. Lebek, S. Goerlitz, R. Adhikari, E. Allert, J. Giesemann and G.H. Michler: **(1999)**, Morphology and micromechanical behaviour of blends of ethene-1-hexene copolymers, J. Macromol. Sci. B 38, 817-836.
162. M. Langela: **(2001)**, Morphologische und rheologische Eigenschaften der Blockcopolymeren, Ph. D. Thesis, Max-Planck-Institut für Polymerforschung, Mainz, in preparation.
163. Y. Tselikas, N. Hadjichristidis, R.L. Lescanec, C.C. Honeker, M. Wohlgemuth and E.L. Thomas: **(1996)**, Architecturally-induced tricontinuous cubic morphology in compositionally symmetric miktoarm starblock copolymers, Macromolecules 29, 3390-3396.
164. Y. Zhang, and U. Wiesner: **(1995)**, Symmetric diblock copolymers under LAOS flow: entanglement effect, J. Chem. Phys. 103, 4784-4793.
165. F.S. Bates, K.A. Koppi, M. Tirrel, K. Almdal and K. Mortensen: **(1994)**, Influence of shear on the hexagonal-to-disorder transition in a diblock copolymer, Macromolecules 27, 5934-5937.
166. G.H. Michler, R. Adhikari, W. Lebek, S. Goerlitz, R. Weidisch and K. Knoll: **(2001)**, Morphology and deformation behaviour of asymmetric styrene/butadiene block copolymers, J. Appl. Polym. Sci. in press.
167. B.F. Fabis: **(2000)**, Factors influencing the morphology of immiscible polymer blends in melt processing, In D.R. Paul and C.B. Bucknall (Eds.), Polymer blends-Vol. 1: Formulation, Wiley-Interscience Publications, New York.
168. C.S. Henke and E.L. Thomas: **(1987)**, Effect of long range order on craze microstructure in deformed PS/PB block copolymers, In Proceedings of the 45th Annual meeting of the electron microscopy society of America, G.W. Bailey (Ed.), p. 524-525, San Francisco Press, San Francisco.
169. R. Adhikari, G.H. Michler, T.A. Huy and R. Godehardt: On the deformation behaviour of block copolymers with glassy cylinders, manuscript in preparation.
170. E.J. Kramer: **(1983)**, Microscopic and Molecular Fundamentals of Crazing, In H.H. Kausch (Ed.) Advances in Polymer Science 52/53 Crazing in polymers-Volume I, p. 5-56, Springer Verlag Berlin Heidelberg.
171. R. Adhikari, S. Henning, G.H. Michler, R. Lach and K. Knoll: Influence of temperature and strain rate on deformation behaviour of styrene/butadiene block copolymer, manuscript in preparation.

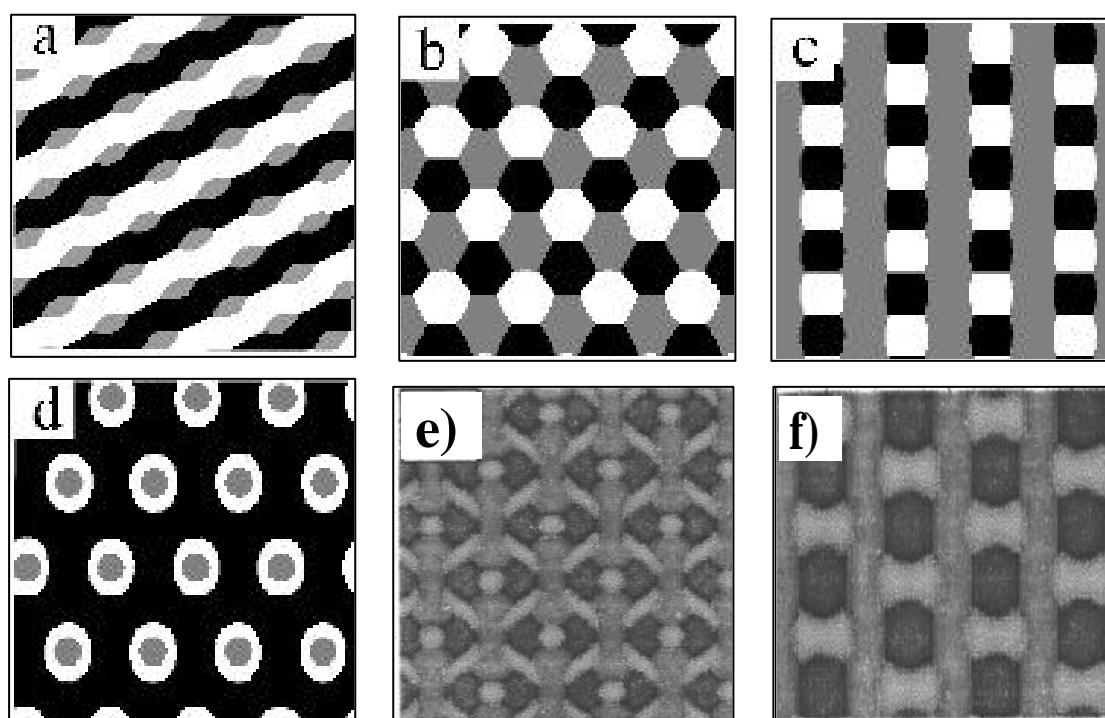
172. W. Grellmann and R. Lach: **(1997)**, Toughness and relaxation behaviour of polymethylmethacrylate, polystyrene and polycarbonate, *Appl. Macromol. Chem. Phys.* 253, 27-49.
173. H. Beerbaum and W. Grellmann: **(2000)**, The influence of morphology and structure on the crack growth of linear polyethylene, In J. G. Williams and A. Pavan (Eds.): *Fracture of Polymers, Composites and Adhesives*. P. 163-174, ESIS Publication 27, Elsevier Science Ltd., Oxford.
174. E. Ivankova, R. Adhikari, G.H. Michler, R. Weidisch and K. Knoll: **(2001)**, Investigation of micromechanical deformation mechanisms in styrene/butadiene block copolymer/polystyrene blends by means of HVEM: submitted to *Polymer*.
175. R. B. Thompson and M. W. Matsen: **(2000)**, Improving polymeric microemulsions with block copolymer polydispersity, *Phys. Rev. Lett.* 85, 670-673.
176. Y. Han, R. Lach, W. Grellmann: **(2001)**, Effects of rubber content and temperature on unstable fracture behaviour in abs materials with different particle sizes, *J. Appl. Polym. Sci.* 79, 9-20.
177. Grellmann, W., Seidler, S., Jung, K. and I. Kotter: **(2001)**, Crack-resistance behavior of polypropylene copolymers, *J. Appl. Polym. Sci.* 79, 2317-2325.
178. S. Wu: **(1985)**, Phase structure and adhesion in polymer blends: A criterion for rubber toughening, *Polymer* 26, 1855-1863.
179. A. Margolina: **(1990)**, Toughening mechanism for nylon/rubber blends: The effect of temperature, *Polym. Commun.* 31, 95-96.

APPENDICES

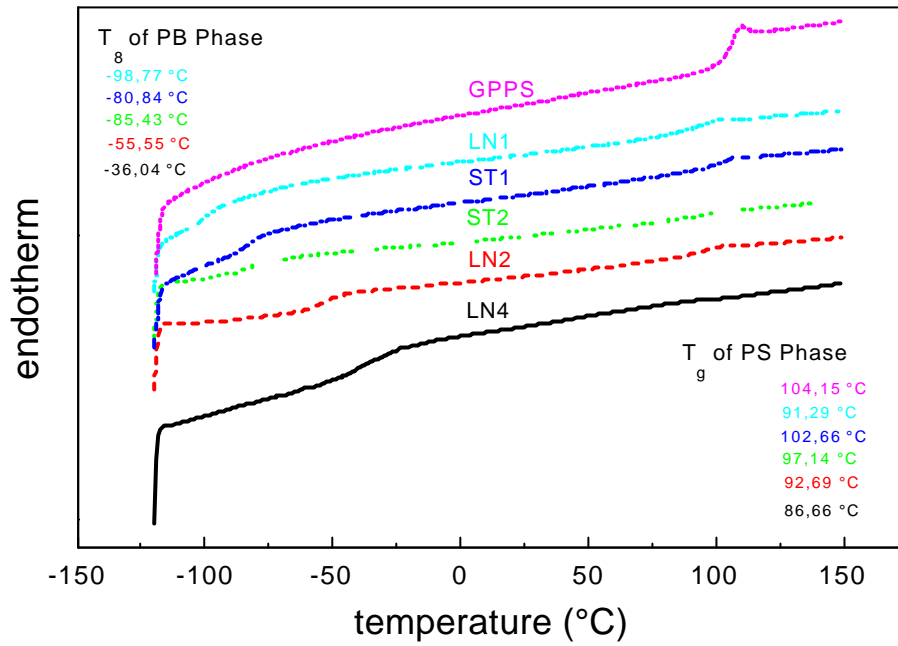
Appendix 2.1: Experimental phase diagram for PS-b-PI diblock copolymer [17]



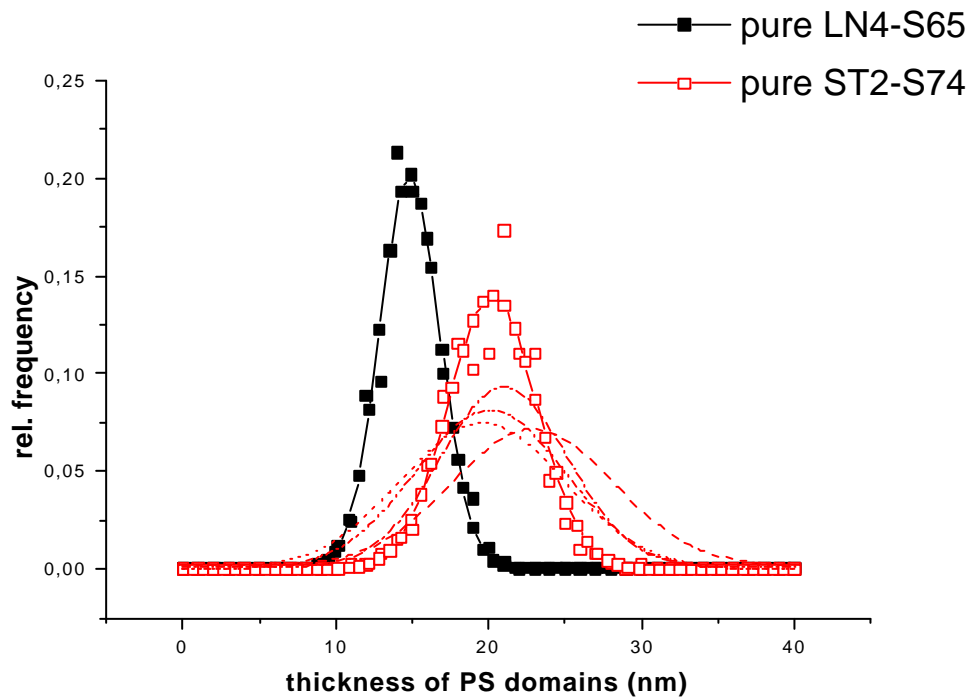
Appendix 2.2: Morphologies predicted in three-component multi-block copolymers on the basis of self consistent field theory; a-d from ref. [27] and e-f from ref. [28], a few of these morphologies are yet to be experimentally confirmed.



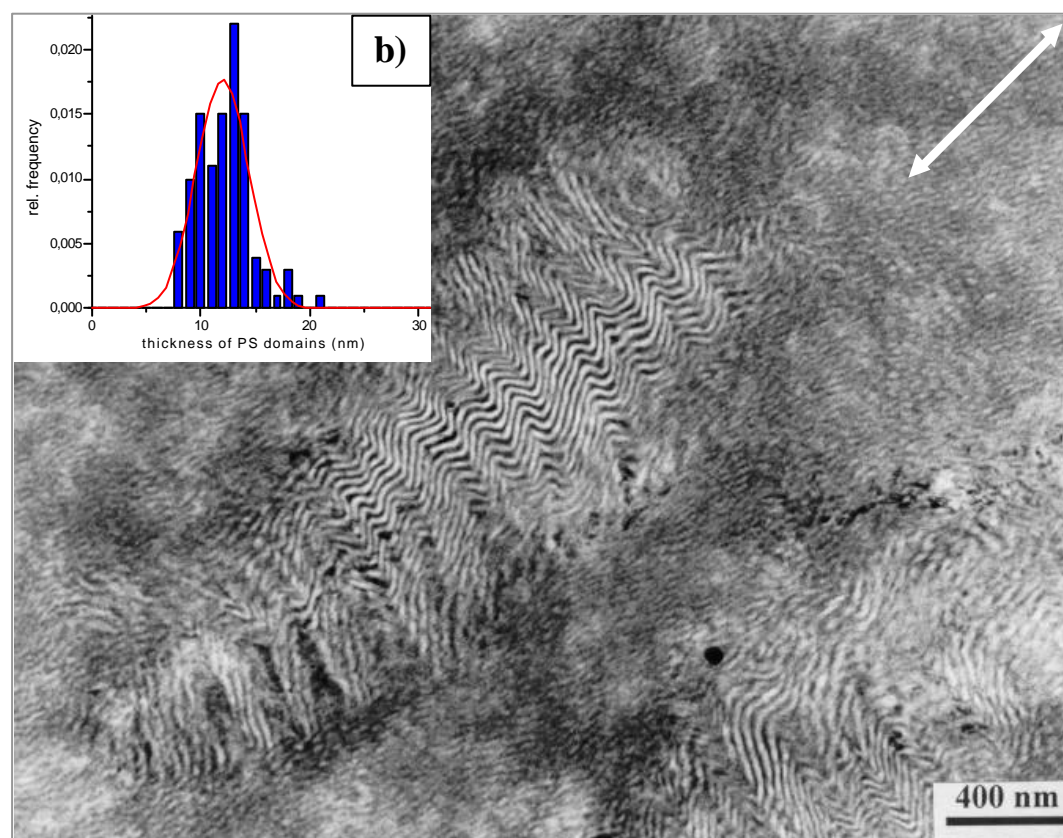
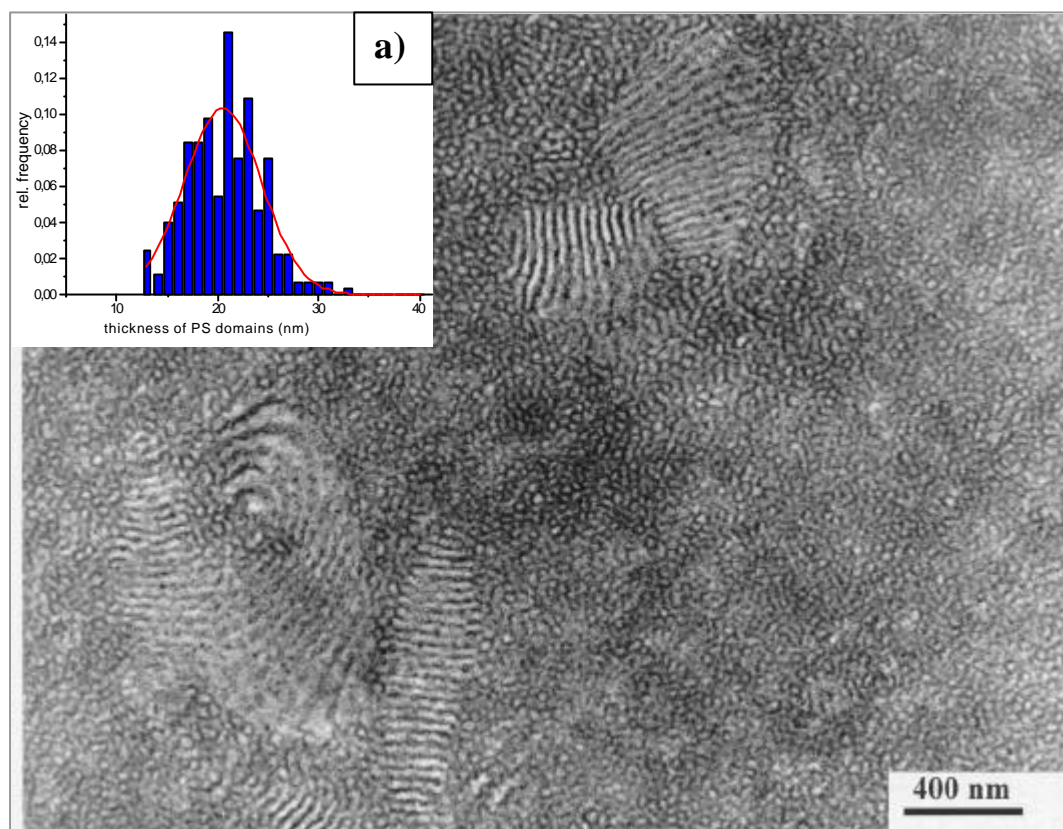
Appendix 4.1: DSC thermograms of the pure block copolymer samples listed in table 3.1



Appendix 6.1: Distribution of the thickness of PS domains fitted to Gaussian function, data points are shown only for pure block copolymers for the sake of clarity; the blends have the distribution close to that of pure star block copolymer.



Appendix 6.2: Low magnifications of TEM images showing a) Morphology and b) deformation structures in solution cast ST2/60 wt % LN4 blend; deformation direction is indicated by an arrow; distribution of the PS domains are shown in inserts.



LEBENS LAUF

PERSÖNLICHE DATEN:

Name: Rameshwar Adhikari
geboren: 03. September 1963 / Nuwakot Chokade VDC-3, Nepal
Staatsangehörigkeit: nepalesisch
Familienstand: verheiratet mit Pooja Sharma, 2 Kinder Purak & Pari
Anschrift: Geusaer Straße 88, WH 12, E-09/10
06217 Merseburg

SCHULAU SBILDUNG:

1971 - 1979 Primary School in Chokade VDC-3, Nuwakot, Nepal
1979 - 1983 Amarjyoti Secondary School, Kharanitar, Nuwakot, Nepal
Juni 1983 School Leaving Certificate (SLC)
1984 - 1986 Intermediate of Science (I. Sc.), Tri-Chandra Campus, Tribhuvan University Kathmandu

STUDIUM:

1987 - 1989 Bachelor's Degree of Science (B.Sc.), Tri-Chandra Campus, Tribhuvan University Kathmandu
1990 - 1991 Master's Degree of Science in Chemistry (M.Sc. Chem.), Central Dept. of Chemistry, Tribhuvan University, Kathmandu

BERUFSWEG:

1992 - 1997 Assistant Lecturer in Dept. of Chemistry, Tri-Chandra Campus, Tribhuvan University, Kathmandu, Tätigkeit: Lehre und Betreuung von Studenten
Mai 1995 – Juli 1996 Aufenthalt am Institut für Physikalische Chemie und Elektrochemie der Universität Karlsruhe im Rahmen des internationalen Seminars für Forschung und Lehre im Chemieingenieurwesen Technischer und Physikalischer Chemie.
Thema der Forschungsarbeit: Elektrochemische Abscheidung von Kupfer auf Gold unter Verwendung eines Atomkraftmikroskops
1997 – 1998 Lecturer in Dept. of Chemistry, Tri-Chandra Campus, Tribhuvan University, Kathmandu, Tätigkeit: Lehre und Betreuung von Studenten
seit Mai 1998 Doktorand im Institut für Werkstoffwissenschaft, FB Ingenieurwissenschaften der Martin-Luther-Universität Halle-Wittenberg
Projekt „Styrol-Butadien-Blockcopolymerere“ in Zusammenarbeit mit der BASF Aktiengesellschaft
Landesprojekt (SA) „Neue Funktionswerkstoffe auf der Grundlage schwachentmischter Blockcopolymere“
Fremdsprachen Englisch und Deutsch

Eidesstattliche Erklärung

Ich versichere hiermit an Eides statt, daß ich die vorgelegte Dissertation selbständig und nur unter Anwendung der angegebenen Literatur und Hilfsmittel angefertigt habe.

Merseburg, den 12.07.2001

Rameshwar Adhikari

Erklärung

Hiermit erkläre ich, daß ich die vorgelegte Dissertation erstmalig und an keiner anderen Fakultät eingereicht oder mich erfolglos mit einer anderen Arbeit um eine Promotion beworben habe.

Merseburg, den 12.07.2001

Rameshwar Adhikari